doi.org/10.26434/chemrxiv.12052512.v2

Harnessing powers of genomics to build molecular maps of coronavirus targets in human cells: a guide for existing drug repurposing and experimental studies identifying candidate therapeutics to mitigate the pandemic COVID-19.

Gennadi Glinsky

Submitted date: 01/04/2020 • Posted date: 03/04/2020

Citation information: Glinsky, Gennadi (2020): Harnessing powers of genomics to build molecular maps of coronavirus targets in human cells: a guide for existing drug repurposing and experimental studies identifying candidate therapeutics to mitigate the pandemic COVID-19.. ChemRxiv. Preprint. https://doi.org/10.26434/chemrxiv.12052512.v2

Coronavirus pandemic COVID-19 caused by the newly emerged SARS-CoV-2 virus is rapidly spreading around the glove and entering the most dangerous acute phase of its evolution in the United States. Recent progress in defining genetic and molecular determinants mediating the SARS-CoV-2 entry into human cells (Walls et al., 2020) should facilitate development of targeted therapeutics and efficient vaccines. Here, human genes required for SARS-CoV-2 entry into human cells, ACE2 and FURIN, were employed as baits to build genomics-guided maps of up-stream regulatory elements, their expression and functions in human body, including pathophysiologically-relevant cell types. Genes acting as repressors and activators of the ACE2 and FURIN genes were identified based on the analyses of gene silencing and overexpression experiments as well as relevant transgenic mouse models. Panels of repressors (VDR; GATA5; SFTPC; HIF1a) and activators (HMGA2; INSIG1) were then employed to identify existing drugs that manifest gene expression signatures of the potential coronavirus infection mitigation agents. Using this strategy, Vitamin D and Quercetin have been identified as putative pandemic mitigation agents. Gene expression profiles of Vitamin D and Quercetin activities and their established safety records as over-the-counter medicinal substances suggest that they may represent viable candidates for further assessment and considerations of their potential utility as coronavirus pandemic mitigation agents. Notably, gene set enrichment analyses and expression profiling experiments identify multiple drugs, smoking, and many disease conditions that appear to act as putative coronavirus infection-promoting agents. Discordant patterns of Testosterone versus Estradiol impacts on SCARS-CoV-2 targets suggest a plausible molecular explanation of the apparently higher male mortality during coronavirus pandemic. Observations reported in this contribution are intended to facilitate follow-up targeted experimental studies and, if warranted, randomized clinical trials to identify and validate therapeutically-viable interventions to combat the pandemic.

File list (2)

Harnessing powers of genomics to build molecular maps... (673.73 KiB)	view on ChemRxiv	download file
Supplemenmtal Figure S1_S13. ACE2 and FURIN genes.... (3.95 MiB)	view on ChemRxiv	download file

Harnessing powers of genomics to build molecular maps of coronavirus targets in human cells: a guide for existing drug repurposing and experimental studies identifying candidate therapeutics to mitigate the pandemic COVID-19.

Gennadi V. Glinsky[1]

[1] Institute of Engineering in Medicine

University of California, San Diego

9500 Gilman Dr. MC 0435

La Jolla, CA 92093-0435, USA

Correspondence: gglinskii@ucsd.edu

Web: http://iem.ucsd.edu/people/profiles/guennadi-v-glinskii.html

Running title: Genomics-guided mitigation maps for coronavirus pandemic

Key words: COVID-19; SARS-CoV-2 coronavirus; genomics; mitigation approaches; drugs & medicinal substances repurposing; Vitamin D; Quercetin

Abstract

Coronavirus pandemic COVID-19 caused by the newly emerged SARS-CoV-2 virus is rapidly spreading around the glove and entering the most dangerous acute phase of its evolution in the United States. Recent progress in defining genetic and molecular determinants mediating the SARS-CoV-2 entry into human cells (Walls et al., 2020) should facilitate development of targeted therapeutics and efficient vaccines. Here, human genes required for SARS-CoV-2 entry into human cells, *ACE2* and *FURIN*, were employed as baits to build genomics-guided maps of up-stream regulatory elements, their expression and functions in human body, including pathophysiologically-relevant cell types. Genes acting as repressors and activators of the *ACE2* and *FURIN* genes were identified based on the analyses of gene silencing and overexpression experiments as well as relevant transgenic mouse models. Panels of repressors (*VDR; GATA5; SFTPC; HIF1a*) and activators (*HMGA2; INSIG1*) were then employed to identify existing drugs that manifest gene expression signatures of the potential coronavirus infection mitigation agents. Using this strategy, Vitamin D and Quercetin have been identified as putative pandemic mitigation agents. Gene expression profiles of Vitamin D and Quercetin activities and their established safety records as over-the-counter medicinal substances suggest that they may represent viable candidates for further assessment and considerations of their potential utility as coronavirus pandemic mitigation agents. Notably, gene set enrichment analyses and expression profiling experiments identify multiple drugs, smoking, and many disease conditions that appear to act as putative coronavirus infection-promoting agents. Discordant patterns of Testosterone versus Estradiol impacts on SCARS-CoV-2 targets suggest a plausible molecular explanation of the apparently higher male mortality during coronavirus pandemic. Observations reported in this contribution are intended to facilitate follow-up targeted experimental studies and, if warranted, randomized clinical trials to identify and validate therapeutically-viable interventions to combat the pandemic.

Introduction

Coronavirus pandemic COVID-19 caused by the newly emerged SARS-CoV-2 virus is rapidly entering the most dangerous acute phase of its evolution in the United States. Absence of the vaccine and lack of efficient targeted therapeutic approaches emphasizes the urgent need for identification of candidate pandemic mitigation agents among existing drugs and medicinal substances.

SARS-CoV-2 virus was discovered in December 2019 and shortly thereafter it was isolated and sequenced (Zhou et al., 2020; Zhu et al., 2020). Recent analyses of the structure, function, and antigenicity of the SARS-CoV-2 spike glycoprotein revealed the key role of the *ACE2* and *FURIN* genes in facilitating the high-affinity binding of viral particles and their entry into human cells (Walls et al., 2020). The efficient invasion of host cells by the SARS-CoV-2 is further enhanced by the presence of the unexpected furin cleavage site, which is cleaved during the biosynthesis (Walls et al., 2020). This novel feature distinguishes the previously known SARS-CoV and the newly emerged SARS-CoV-2 viruses and possibly contributes to the expansion of the cellular tropism of the SARS-CoV-2 (Walls et al., 2020). The crystal structure and high-resolution cryo-electron microscopy of the SARS-CoV-2 receptor-binding domain (RBD) in complex with human ACE2 revealed specific structural features of the SARS-CoV-2 RBD that appear to enhance its binding affinity to human ACE2 (Shang et al., 2020; Yan et al., 2020). Collectively, these observations firmly established protein products of the human genes *ACE2* and *FURIN* as the high-affinity receptor (ACE2) and invasion-promoting protease (FURIN) as the principal mediators of the SARS-CoV-2 invasion into human cells.

In this contribution, genomic screens were performed employing the *ACE2* and *FURIN* genes as baits to build genomics-guided human tissues-tailored maps of up-stream regulatory elements, their expression and functions. To identify the high-priority list of potential candidate mitigation agents, the validation analyses were performed using gene silencing and

overexpression experiments as well as relevant transgenic mouse models with the emphasis on pathophysiologically-relevant cell types. Panels of repressors (*VDR; GATA5; SFTPC*) and activators (*HMGA2; INSIG1*) of the *ACE2* and *FURIN* expression were identified and then employed to identify existing drugs and medicinal substances that could be repurposed to ameliorate the outcomes of the coronavirus infection. Two of the most promising candidate mitigation agents, namely Vitamin D and Quercetin, manifest gene expression-altering activities and have established safety records as over-the-counter medicinal substances that seem sufficient for further assessment and considerations of their potential utility for amelioration of the clinical course of coronavirus pandemic. Unexpectedly, present analyses revealed discordant patterns of Testosterone versus Estradiol impacts on SCARS-CoV-2 targets with the former manifesting the potential coronavirus infection-promoting activities, which is consistent with the apparently higher male mortality across all age groups during the coronavirus pandemic.

Results and Discussion

Gene set enrichment analyses (GSEA) of genomic features associated with the *ACE2* and *FURIN* genes

One of the goals of this work was to identify human genes implicated in regulatory cross-talks affecting expression and functions of the *ACE2* and *FURIN* genes to build a model of genomic regulatory interactions potentially affecting the SCARS-CoV-2 coronavirus infection. To this end, GSEA were carried out using the *ACE2* and *FURIN* genes as baits applied to a broad spectrum of genomic databases reflecting the current state of knowledge regarding the structural, functional, regulatory, and pathophysiological features that could be statistically linked to these genes. Expression profiling experiments and GSEA revealed ubiquitous patterns of both *ACE2* and *FURIN* genes across human tissues (Supplemental Figure S1) with notable examples of high expression of the *FURIN* gene in the lung (second-ranked tissue in the GTEX database)

and testis being identified as the top-ranked *ACE2*-expressing tissue. In addition to the human lung tagged by the *ACE2* expression in the ACRHS4 Human Tissues database search, other noteworthy significantly enriched records are the Peripheral Blood Mononuclear Cells (PBMC), Natural Killer Cells and Macrophages tagged by the *FURIN* expression (Supplemental Figure S1).

GSEA of the virus perturbations' data sets among Gene Expression Omnibus (GEO) records of up-regulated genes identified the SARS-CoV challenge at 96 hrs (GSE47960) as the most significantly enriched record (Supplemental Figure S2) tagged by expression of both *ACE2* and *FURIN* in human airway epithelial cells. These observations suggest that coronavirus infection triggers the increased expression of both *ACE2* and *FURIN* genes 4 days after the initial encounter with host cells (Figure 1; Supplemental Figure S2). These findings were corroborated by the increased *FURIN* expression documented in the PBMC of patients with severe acute respiratory syndrome (Figure 1; Supplemental Figure S1; Reghunathan et al., 2005). It would be of interest to investigate whether this potentially infection-promoting effect on expression of the host genes in virus-targeted cells is mediated by the virus-induced release of the biologically-active molecules with the paracrine mode of actions such as interleukins and cytokines.

GSEA identified numerous significantly enriched records of common human disorders manifesting up-regulation of either *ACE* or *FURIN* genes (Supplemental Figure S3), which is consistent with the clinical observations that individuals with underlying health conditions are more likely to have clinically severe and lethal coronavirus infection. Similarly, exploration of the DisGeNET database of human disorders highlighted multiple disease states' records manifesting altered expression of either *ACE2* of *FURIN* genes (Supplemental Figure S3). Cigarette smoking appears to significantly increase the *ACE2* expression in human large airway

epithelial cells (Supplemental Figure S3), indicating that cigarette smoking should be considered as a potential coronavirus infection-promoting agent.

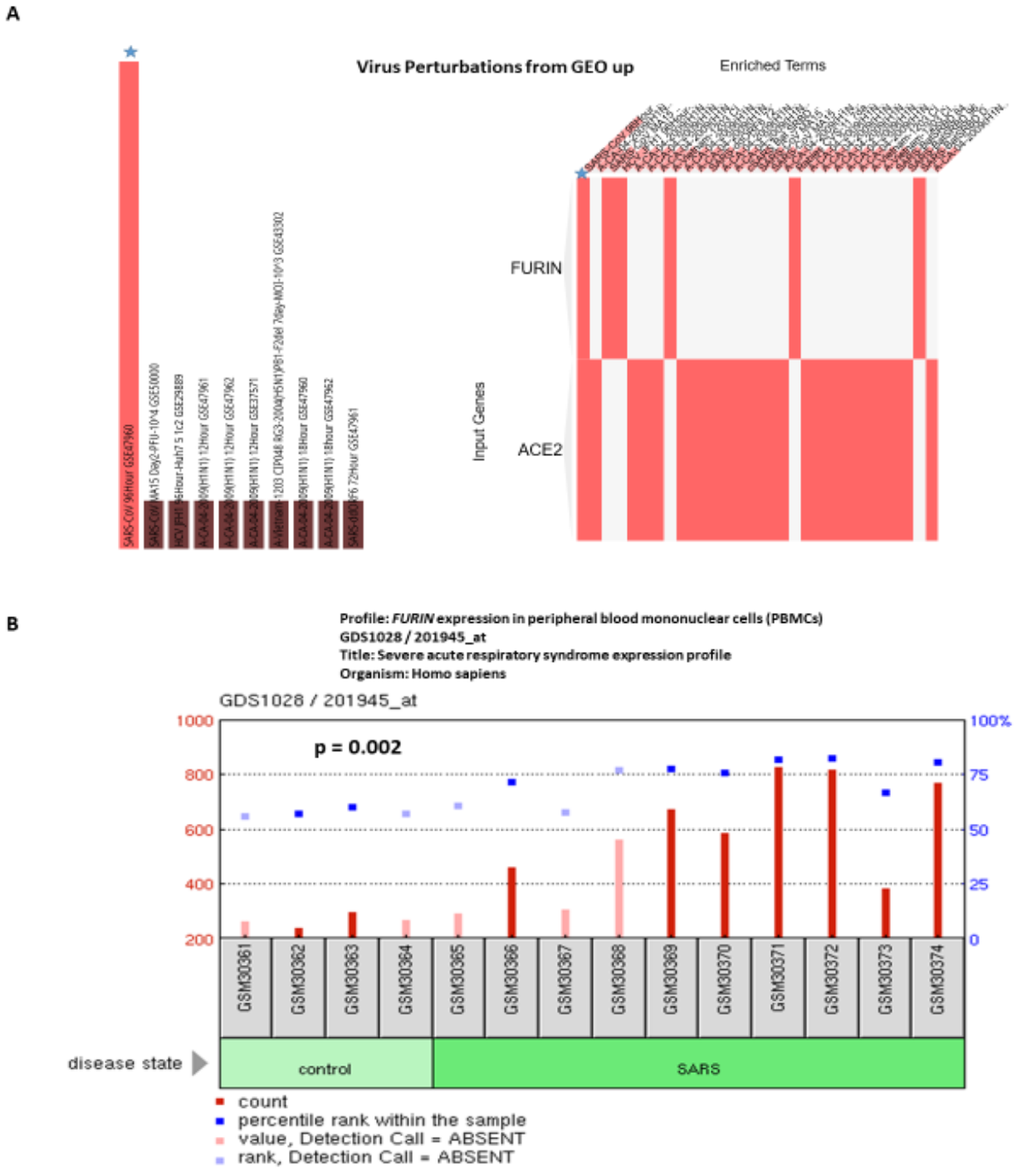

Figure 1. Effects of viral challenges on expression of the *ACE2* and *FURIN* genes.

a. Gene Set Enrichment analyses of the Virus Perturbations from GEO focused on up-regulated genes.
b. Increased *FURIN* expression in peripheral blood mononuclear cells (PBMC) of patients with Severe Acute Respiratory Syndrome (SARS).

Gene Ontology (GO) analyses revealed that *ACE2* and *FURIN* genes are associated with the largely non-overlapping records of GO Biological Processes, GO Molecular Functions, and GO Cellular Components (Supplemental Figure S4). The common significantly enriched records are Viral Life Cycle (GO Biological Process 2018); Peptidase activity (acting on L-amino acid peptides) and Endopeptidase activity (GO Molecular Function 2018); Membrane raft (GO Cellular Component 2018); Meprin A complex and Retrotrasposon nucleocapsid (Jensen Compartments).

Identifications of the enriched records of transcription factor-binding sites affecting the *ACE2* and *FURIN* expression

GSEA of the enriched records of transcription factors' binding sites (TFBS) using ENCODE TF ChIP-seq 2015 and ChEA 2016 databases revealed predominantly distinct patterns of TFBS associated with the *ACE2* and *FURIN* genes (Supplemental Figure S5). Common TFBS shared by both *ACE2* and *FURIN* genes are *FOS, JUND, EP300* (ENCODE TF ChIP-seq 2015) and *GATA1, GATA2, RUNX1, FOXA1, HNF4A* (ChIP-seq 2015). Consistent with these findings, non-overlapping profiles of significantly enriched records associated with either *ACE2* or *FURIN* genes were observed of pathways (BioPlanet 2019 database), protein-protein interactions (PPI) hub proteins (PPI Hub Proteins database), and drugs affecting *ACE2* and *FURIN* expression (Drug Signatures Database, DSigDB), indicating that regulatory mechanisms governing the expression and activities of the *ACE2* and *FURIN* genes are predominantly discordant (Supplemental Figure S5).

Next, the Gene Expression Omnibus (GEO) database was interrogated to gauge the effects on *ACE2* and *FURIN* expression of transcription factors having TFBS associated with

their promoters. There are multiple relevant GEO records reporting the activation effects of the *JNK1/c-FOS* pathway on *ACE2* and *FURIN* expression as well as the activation effects of *FURIN* depletion on expression of the *Fos, Jun, Jund,* and *Junb* genes (Supplemental Figure S5). Conversely, *c-Jun* inhibition (effect of the dominant negative *c-Jun*) nor *c-Jun* depletion (*c-Jun* knockout) has resulted in deceased expression of the *FURIN* gene (Supplemental Figure S5). The summary of these observations is reported in the Figure 2.

Similarly, there are several reports indicating that depletion of either *Hnf4a* or *Runx1* in mouse cells and RUNX1 in human cells decreases the *ACE2* and *FURIN* expression (Supplemental Figure S6). Conversely, *FURIN* depletion enhances expression of the *Runx1* and *Foxa1* genes in murine T cells (Supplemental Figure S6). In contrast, *FURIN* depletion decreases expression of the *Hnf4a* gene, while *Hnf4a* depletion decreases the *FURIN* gene expression (Supplemental Figure S6). The summary of these observations is reported in the Figure 2.

Identification of the *VDR* and *HIF1a* genes as putative repressors of the *ACE2* expression

Next GSEA of genomic databases were performed to identify the potential activators and repressors of the *ACE2* and *FURIN* genes. Analysis of the ARCHS4 transcription factors' co-expression database identified the *VDR* genes that co-expressed with both *ACE2* and *FURIN* genes in human tissues (Supplemental Figure S7). Other significantly enriched records manifest non-overlapping patterns of co-expression with either *ACE2* of *FURIN* genes. The GTEX expression profile of the *VDR* gene in human tissues revealed the ubiquitous pattern of expression and placed the *VDR* expression in human lungs in the top quartile (Supplemental Figure S7). Analysis of gene expression profiling experiments of wild type and vitamin D receptor (Vdr) knockout primary bone marrow-derived macrophages reported by Helming et al. (2005) demonstrate increased expression of the *ACE2* gene in the *VDR* knockout cells (Supplemental Figure S7) implicating the product of the *VDR* gene as the putative repressor of

the *ACE2* expression. Consistent with this hypothesis, Vitamin D appears to inhibit the *ACE2* expression in human bronchial smooth muscle cells (Supplemental Figure S7).

A

JNK1/c-FOS pathway-associated activation of the *ACE2* and *FURIN* expression may trigger the auto-regulatory negative feed-back loop of the FURIN-mediated repression of the expression of *JUN, JUNB, JUND,* and *c-FOS* genes

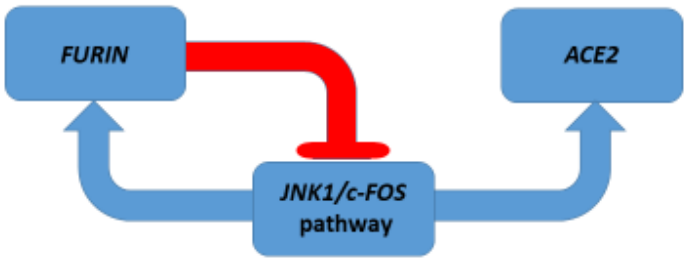

B

RUNX1 pathway-associated activation of the *ACE2* and *FURIN* expression may trigger the auto-regulatory negative feed-back loop of the *FURIN*-mediated repression of the *RUNX1* gene expression

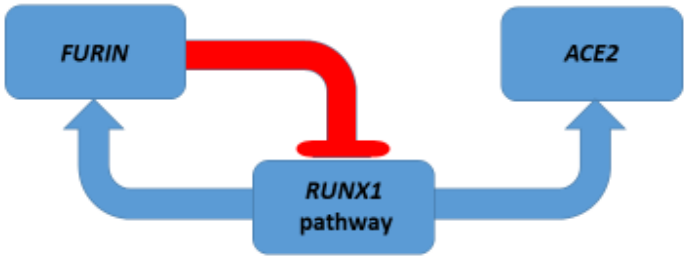

c

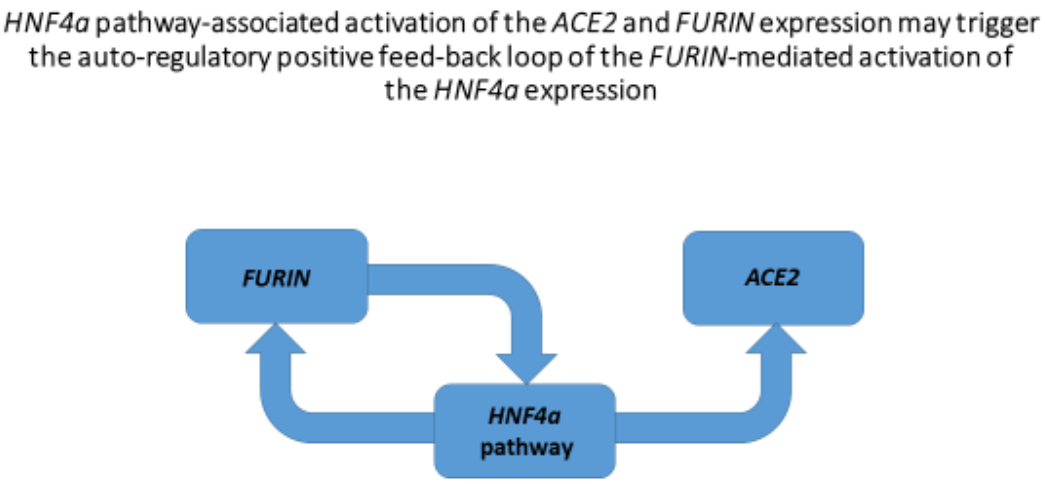

Figure 2. Pathways and genes affecting the newly emerged SARS-CoV-2 virus-related host targets.

a. *JNK1/c-FOS* pathway-associated activation of the *ACE2* and *FURIN* expression may trigger the auto-regulatory negative feed-back loop of the FURIN-mediated repression of the expression of *JUN, JUNB, JUND,* and *c-FOS* genes.

b. *RUNX1* pathway-associated activation of the *ACE2* and *FURIN* expression may trigger the auto-regulatory negative feed-back loop of the *FURIN*-mediated repression of the *RUNX1* gene expression

c. *HNF4a* pathway-associated activation of the *ACE2* and *FURIN* expression may trigger the auto-regulatory positive feed-back loop of the *FURIN*-mediated activation of the *HNF4a* expression.

Notably, examinations of direct and reciprocal effects of the *VDR* gene and Vitamin D administration on expression of the *JNK1/c-FOS* pathway genes revealed the expression profiles consistent with the potential therapeutic utility of the Vitamin D administration and activation of the *VDR* gene expression (Supplemental Figure S7). Analyses of direct and reciprocal effects of the *VDR* gene and Vitamin D administration on the *HNF4a* expression revealed that *HNF4a* depletion in human and murine cells inhibits the *VDR* gene expression, while the *Vdr* gene depletion increases the *Hnf4a* expression (Supplemental Figure S7). These

result are consistent with the hypothesis stating that Vitamin D administration and activation of the *VDR* gene expression may have mitigating effects on the coronavirus infection. The summary of these findings is reported in the Figure 3.

GSEA of the Transcription Factor's Perturbations Followed by Expression database and GEO Gene Perturbations database focused on up-regulated genes identified *HIF1a* and *POU5F1* gene products as putative repressors of the *ACE2* and *FURIN* expression (Supplemental Figure S8). These findings were corroborated by observations that *HIF1a* overexpression in human embryonic kidney cells significantly inhibits the *ACE2* expression (Supplemental Figure S8). Notably, Vitamin D significantly increases expression of the *HIF1a* gene in human bronchial smooth muscle cells (Supplemental Figure S8), suggesting that *VDR* and *HIF1A* genes may cooperate as repressors of the *ACE2* expression.

GSEA identify Estradiol and Quercetin as putative candidate coronavirus infection mitigation agents.

GSEA of the Drug Perturbations from GEO database focused on down-regulated genes identified Estradiol and Quercetin among the top significantly enriched records (Supplemental Figure S9). Estradiol appears to affect both *FURIN* and *ACE2* expression, while Quercetin seems to target the *ACE2* expression. Consistently, GSEA of the Ligand Perturbations from GEO focused on down-regulated genes identified five of Estradiol administration records (50%) among top ten significantly enriched ligand perturbations records (Supplemental Figure S9). GSEA of the Drug Perturbations from GEO database focused on up-regulated genes indicated that doxorubicin, imatinib, and bleomycin may act as potential coronavirus infection-promoting agents (data not shown). Collectively, these observations provide the initial evidence supporting the hypothesis that both Estradiol and Quercetin may function as potential candidate coronavirus infection mitigation agents.

A

JNK1/c-FOS pathway-associated activation of the *ACE2* and *FURIN* expression may trigger the auto-regulatory negative feed-back loop of the FURIN-mediated repression of the expression of *JUN, JUNB, JUND,* and *c-FOS* genes

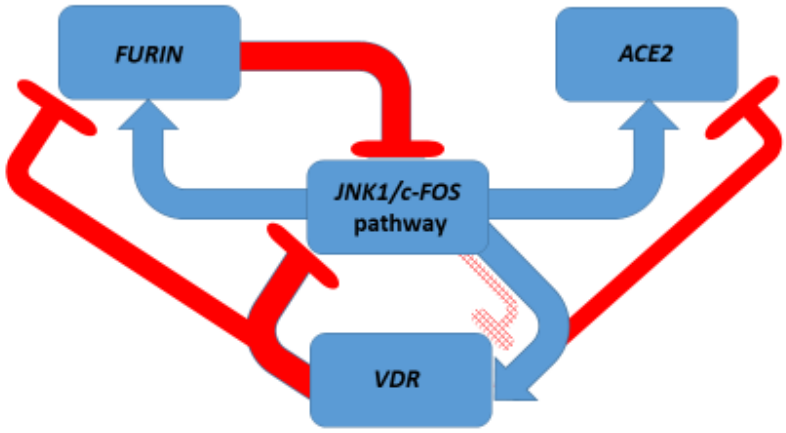

B

HNF4a pathway-associated activation of the *ACE2* and *FURIN* expression may trigger the auto-regulatory positive feed-back loop of the *FURIN*-mediated activation of the *HNF4a* expression

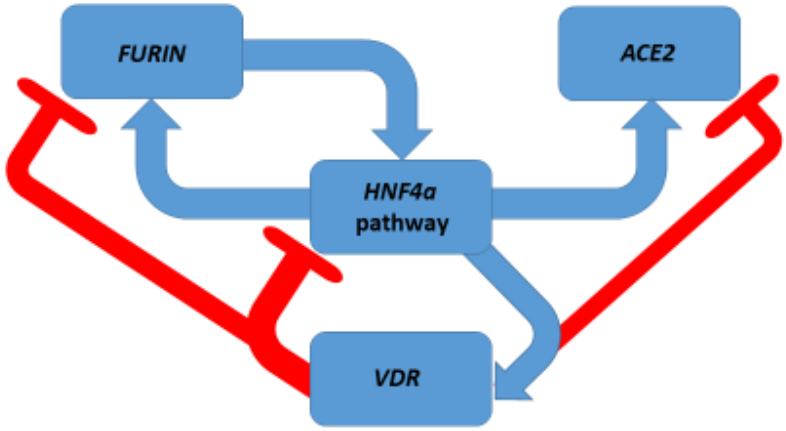

Figure 3. Effects of the *VDR* gene and Vitamin D on pathways and genes affecting the newly emerged SARS-CoV-2 virus-related host targets.

a. *JNK1/c-FOS* pathway-associated activation of the *ACE2* and *FURIN* expression may trigger the auto-regulatory negative feed-back loop of the FURIN-mediated repression of the expression of *JUN, JUNB, JUND,* and *c-FOS* genes.

b. *HNF4a* pathway-associated activation of the *ACE2* and *FURIN* expression may trigger the auto-regulatory positive feed-back loop of the *FURIN*-mediated activation of the *HNF4a* expression.

Consistent with this hypothesis, interrogation of the GEO records revealed that Quercetin appears to inhibit expression of several potential coronavirus infection-promoting genes: *c-FOS* expression in human and rat cells (Supplemental Figure S9); *Runx1* expression in rat cells (Supplemental Figure S9); *HNF4a* expression in human cells (Supplemental Figure S9). However, Quercetin administration appears to increase *c-Fos* expression in cultured rat cardiomyocytes (Supplementary Figure S9).

Confirmation of the Estradiol and Quercetin activities as potential candidate coronavirus infection mitigation agents.

Results of GSEA suggest that both Estradiol and Quercetin appear to exhibit biological activities consistent with the activity of medicinal compounds expected to mitigate the coronavirus infection. Next, manual curation of the GEO data sets has been carried out to identify further experimental evidence supporting this hypothesis. Administration of Estradiol appears to inhibit *ACE2* and/or *FURIN* expression in rat, mouse, and human cells (Supplemental Figure S10) and the effects of Estradiol seem to be mediated by the estrogen receptor beta. In agreement with the hypothesis on potential therapeutic utility of the Quercetin, administration of Quercetin has resulted in significantly decreased expression of the *ACE2* gene during differentiation of human intestinal cells (Supplemental Figure S10).

However, Estradiol administration appears to manifest the cell type-specific effects on c-FOS expression (Supplemental Figure S10). For example, it decreases the c-FOS expression in endometrium of Macaca mulatta while it increases c-FOS expression in the mouse uterus (Supplemental Figure S10). These observations indicate that any definitive conclusions regarding the potential clinical utility of identified herein potential coronavirus infection mitigating agents should be made only after appropriately designed and carefully executed preclinical studies and randomized clinical trials. In contrast to the Estradiol, which exhibit evidence of both putative coronavirus infection-mitigating actions and coronavirus infection-promoting activities,

administration of Testosterone appears to manifest more clearly-defined patterns of altered gene expression consistent with Testosterone being identified as the potential coronavirus infection-promoting agent (Supplemental Figure S11).

Potential mechanisms affecting gene expression inferred from transgenic mouse models and observed in pathophysiologically and therapeutically relevant mouse and human cells.

Taking into considerations that the effects of potential coronavirus infection mitigation agents often manifest cell type-specific patterns of gene expression changes, next the manual curation of the GEO gene expression profiles were carried out to identify the relevant host genetic targets and putative mitigation agents. These analyses identified several candidate repressors (*VDR; GATA5; SFTC; HIF1a*) and activators (*INSIG1; HMGA2*) of the *ACE2* and *FURIN* expression (Supplemental Figure S12). Notably, the effects on gene expression of the administration of either Vitamin D or Quercetin appear consistent with their definition as putative coronavirus infection mitigation agents (Supplemental Figure S12). The summary of these observations is presented in the Figure 4. The conclusion regarding the findings of cell type-specific effects on gene expression of putative coronavirus infection mitigating agents remains valid and examples of the potential negative effects of drugs on the ACE2 expression are reported in the Supplemental Figure S12). For example, the *HIF1a* expression is significantly increased in murine alveolar type I cells deficient in sterol-response element-binding proteins inhibitor Insig1 (Supplemental Figure S6). These data indicate that the *INSIG1* gene product, which appears to function as activator of the *ACE2* expression, may function as the inhibitor of the *HIF1a* expression, thus interfering with the *HIF1a*-mediated *ACE2* repression in specific cell types. Additional examples of the potential positive and negative effects on gene expression inferred from transgenic mouse models are reported in the Supplemental Figure S13.

Is Vitamin D deficiency a potential risk factor for increased disease severity in older adults and elderly individuals?

Present analyses suggest that Vitamin D and vitamin D receptor (*VDR*) are putative mitigation factors of the coronavirus infection. Conversely, the Vitamin D deficiency could be a potential aggravating factor for the clinical course of pandemic. Multiple lines of evidence suggest that Vitamin D deficiency, particularly in elderly, might be a negative factor affecting the clinical course of the pandemic. In the United States, approximately 30% of whites and 5% of African Americans have sufficient Vitamin D level (Kennel et al., 2010) and the significant increase of the prevalence of individuals with severe Vitamin D deficiency has been reported (Ginde et al., 2009a). Age-associated decline of the human skin function to produce the Vitamin D in response to the sunlight exposure is likely a contributing factor to the Vitamin D deficiency in older individuals, since it has been reported that elderly people produce 75% less of cutaneous Vitamin D3 than young individuals (Lips, 2001). A meta-analysis of randomized controlled clinical trials indicated that intake of ordinary doses of Vitamin D was associated with significant decrease in total mortality rates (Autier and Gandini, 2007). A prospective study of the 3,408 older adults in the United States demonstrated that a group at high risk of all-cause mortality could be defined by the serum 25-hydroxyvitamin D [25(OH)D] level (Ginde et al., 2009b). A significant, independent, inverse association was observed between the serum 25(OH)D level and all-cause and cardiovascular diseases (CVD) mortality (Ginde et al., 2009b). To date, the vast majority of observational studies reported inverse associations between the circulating 25(OH)D concentration and all-cause mortality in generally healthy populations (Heath et al., 2019). In generally healthy adults over 50 years old, significant inverse associations were found between low 25(OH)D levels and all-cause mortality, respiratory and cardiovascular events, as well as markers relating to hip and non-vertebral fractures (Caristia et al., 2019). Therefore, it would be important to determine whether Vitamin D deficiency may be one of the risk factors

contributing to the increased disease severity in older adults and elderly individuals during coronavirus pandemic.

Conclusion

The main motivation of this work was to identify human genes implicated in regulatory cross-talks affecting expression and functions of the *ACE2* and *FURIN* genes to build a model of genomic regulatory interactions potentially affecting the SCARS-CoV-2 coronavirus infection. A panel of genes acting as activators and/or repressor of the *ACE2* and/or *FURIN* expression then could be employed to search for existing drugs and medicinal substances that, based on their mechanisms of activities, could be defined as the candidate coronavirus infection mitigation agents. After experimental and clinical validation, these existing drugs could be utilized to ameliorate the clinical severity of the pandemic. This knowledge could also be exploited in an ongoing effort to discover novel targeted therapeutics tailored to prevent the SCARS-CoV-2 infection and block the virus entry into human cells.

One of the important findings documented herein is that identified medicinal compounds with potential coronavirus infection-mitigating effects also appear to induce cell type-specific patterns of gene expression alterations. Therefore, based on all observations reported in this contribution, it has been concluded that any definitive recommendations regarding the potential clinical utility of identified herein putative coronavirus infection mitigating agents, namely Vitamin D and Quercetin, should be made only after preclinical studies and randomized clinical trials have been appropriately designed, carefully executed, and the desired outcomes have been reached.

A

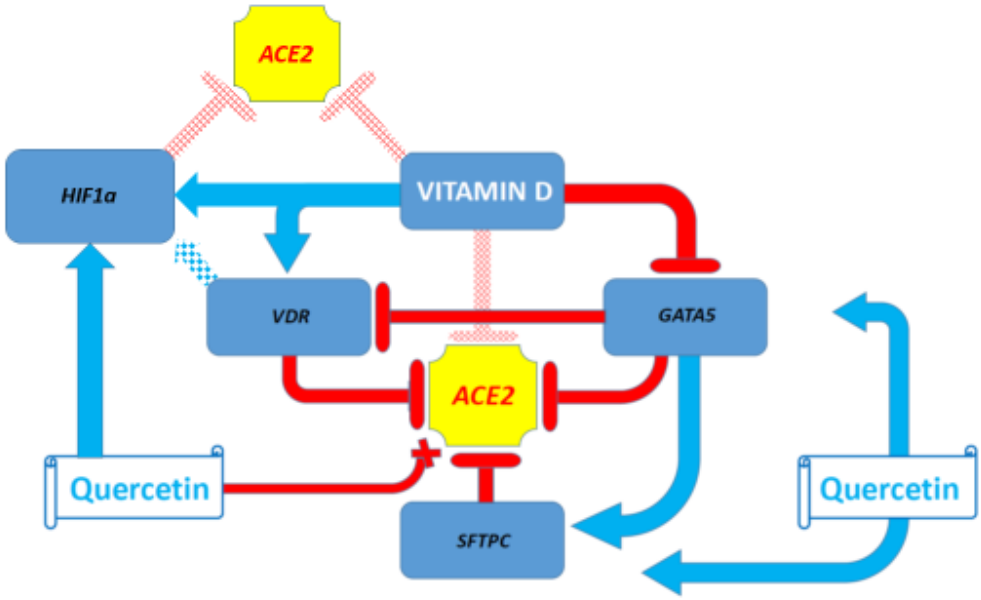
ACE2
HIF1α
VITAMIN D
VDR
GATA5
ACE2
Quercetin
SFTPC
Quercetin

B

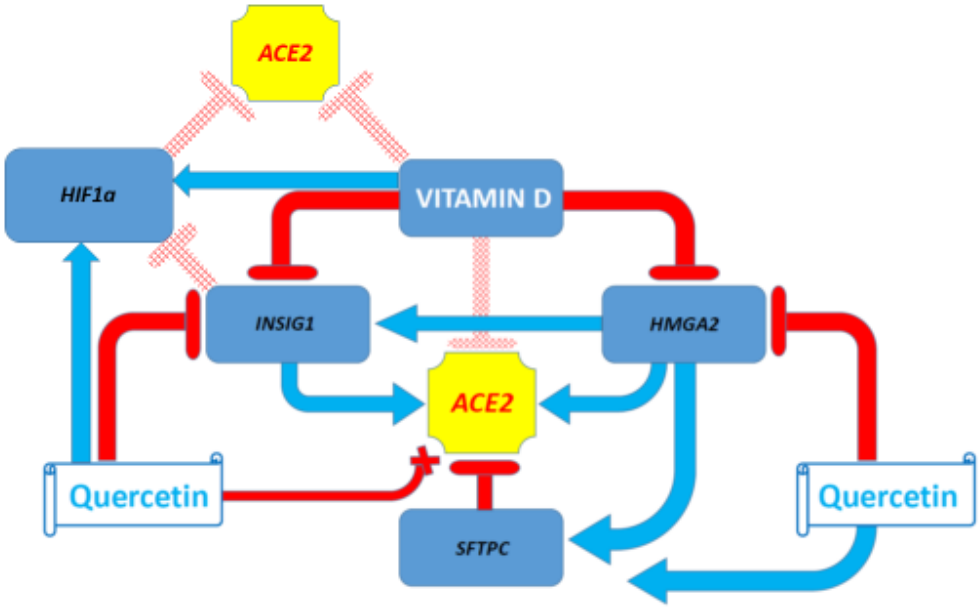
ACE2
HIF1α
VITAMIN D
INSIG1
HMGA2
ACE2
Quercetin
SFTPC
Quercetin

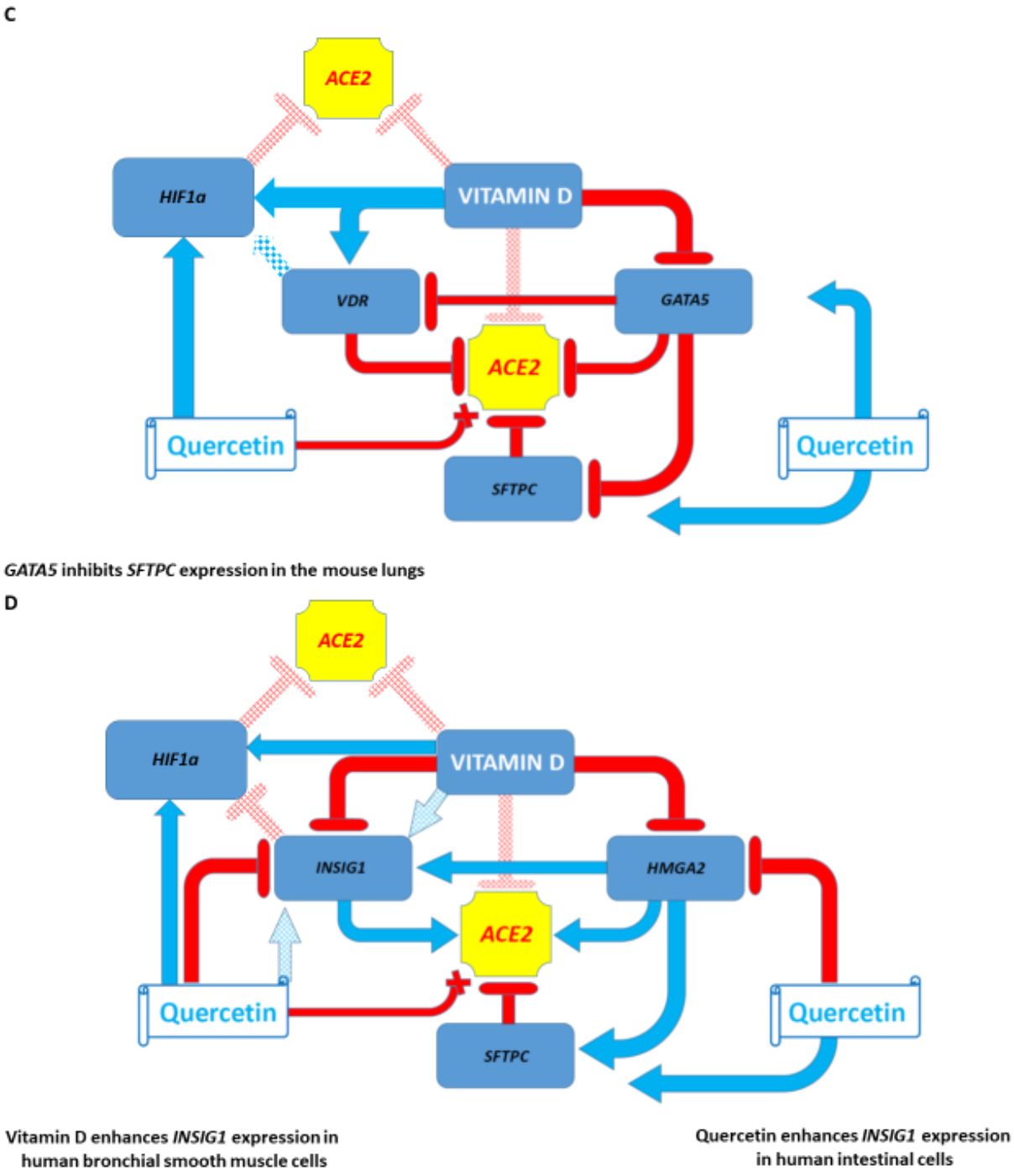

Figure 4. Effects of the *VDR* gene, Vitamin D, and Quercetin on pathways and genes affecting the newly emerged SARS-CoV-2 virus-related host targets.

a. Effects of the *VDR* gene, Vitamin D, and Quercetin on repressors of the *ACE* expression.

b. Effects of the *VDR* gene, Vitamin D, and Quercetin on activators of the *ACE* expression.

c. Effects of the *VDR* gene, Vitamin D, and Quercetin on repressors of the *ACE* expression reflecting *GATA5* inhibitory effects on *SFTPC* expression in the mouse lungs.

d. Effects of the *VDR* gene, Vitamin D, and Quercetin on activators of the ACE expression reflecting the cell type-specific effects of Vitamin D and Quercetin: Vitamin D-induced activation of the *INSIG1* expression in human bronchial smooth muscle cells and Quercetin-induced activation of the *INSIG1* expression in human intestinal cells.

Most recently, a super-computer modeling study using the world's most powerful supercomputer, SUMMIT, identified several candidate small molecule drugs which bind to either the isolated the SCARS-CoV-2 Viral S-protein at its host receptor region or to the S protein-human ACE2 interface (Smith and Smith, 2020). Interestingly, in this study Quercetin was identified among top 5 scoring ligands for viral S-protein-human ACE2 receptor interface. Thus, Quercetin appears also a potentially promising therapeutic molecule that may directly interfere with the binding of the SCARS-CoV-2 virus to human cells. Previously reported experiments demonstrated that Quercetin appears to inhibit the SARS-CoV virus entry into host cells (Yi et al., 2004). Since the SCARS-CoV-2 virus utilizes for the entry in human cells the same receptor (ACE2) and the accessory protease FURIN as the SARS-CoV coronavirus (Wells et al., 2020), these observations suggest that Quercetin may, indeed, possess antiviral activity against the SARS-CoV-2 as well.

It has been observed that administration of Testosterone appears to manifest clearly-defined patterns of altered gene expression consistent with Testosterone being identified as the potential coronavirus infection-promoting agent, particularly in some cell types that may play a role in the virus entry into human body and the respiratory system (Supplemental Figure S11). This is in contrast to Estradiol, which seems to manifest cell type-specific effects on gene expression consistent with either infection-inhibiting or infection-promoting patterns of gene expression changes. It would be of interest to determine whether this discordant effects may contribute to the apparently higher mortality among men with coronavirus infection.

Present analyses highlighted the major uncertainty regarding the outcomes of the current pandemic associated with the potential of the SCARS-CoV-2 virus for the expansion of the cellular tropism (Walls et al., 2020) based on access to genetically vulnerable host cells due to nearly ubiquitous expression of the *ACE2* and *FURIN* genes in the human body. Particularly dangerous seems noted in this contribution the potential ability of the SCARS-CoV-2 virus to infect the immune cells. Taken together with predominantly cell type-specific patterns of expression of genetic repressors and activators of the *ACE2* and *FURIN* expression it may complicate the development of universally effective therapeutics. The availability of many genetically-relevant transgenic mouse models, in particular, the *Furin* null mice, should be regarded as a considerable advantage for preclinical development of drug candidates tailored to target the coronavirus infection. Specifically, the potential therapeutic utility of the highly selective ($K_{i,}$ 600 pm) intrinsically-specific FURIN inhibitor (a1-antitrypsin Portland (a1-PDX); Jean et al., 1998) should be tested in the immediate future.

Methods

Data source and analytical protocols

All data analyzed in this study were obtained from the publicly available sources. Gene set enrichment analyses (GSEA) were carried-out using the Enrichr bioinformatics platform, which enables the interrogation of nearly 200,000 gene sets from more than 100 gene set libraries. The Enrichr API (January 2020 through March 2020 releases) (Chen et al., 2013; Kuleshov et al., 2016) was used to test genes linked to the ACE2 and FURIN genes (or other genes of interest) for significant enrichment in numerous functional categories. In all tables and plots (unless stated otherwise), in addition to the nominal p values and adjusted p values, the "combined score" calculated by Enrichr is reported, which is a product of the significance estimate and the magnitude of enrichment (combined score c = log(p) * z, where p is the

Fisher's exact test p-value and z is the z-score deviation from the expected rank). Validation of the GSEA findings were carried-out employing the computational retrievals and manual curations of the gene expression profiles of the Gene Expression Omnibus (GEO) database.

Statistical Analyses of the Publicly Available Datasets

All statistical analyses of the publicly available genomic datasets, including error rate estimates, background and technical noise measurements and filtering, feature peak calling, feature selection, assignments of genomic coordinates to the corresponding builds of the reference human genome, and data visualization, were performed exactly as reported in the original publications (Glinsky, 2015-2020; Glinsky and Barakat, 2019; Glinsky et al., 2019; Guffanti et al., 2018) and associated references linked to the corresponding data visualization tracks (http://genome.ucsc.edu/). Any modifications or new elements of statistical analyses are described in the corresponding sections of the Results. Statistical significance of the Pearson correlation coefficients was determined using GraphPad Prism version 6.00 software. Both nominal and Bonferroni adjusted p values were estimated. The statistical significance between the mean values was estimated using the Student T-test. The significance of the differences in the numbers of events between the groups was calculated using two-sided Fisher's exact and Chi-square test, and the significance of the overlap between the events was determined using the hypergeometric distribution test (Tavazoie et al., 1999).

Supplemental Information

Supplemental information includes Supplemental Figures S1-S13. Supplemental information is available upon request.

Author Contributions

This is a single author contribution. All elements of this work, including the conception of ideas, formulation, and development of concepts, execution of experiments, analysis of data, and writing of the paper, were performed by the author.

Acknowledgements

This work was made possible by the open public access policies of major grant funding agencies and international genomic databases and the willingness of many investigators worldwide to share their primary research data. This work was supported in part by the OncoScar, Inc.

References

Autier P, Gandini S. Vitamin D supplementation and total mortality: a meta-analysis of randomized controlled trials. Arch Intern Med. 2007; 167: 1730-1737.

Caristia S, Filigheddu N, Barone-Adesi F, Sarro A, Testa T, Magnani C, Aimaretti G, Faggiano F, Marzullo P. Vitamin D as a biomarker of ill health among the over-50s: A systematic review of cohort studies. Nutrients. 2019; 11. pii: E2384. doi: 10.3390/nu11102384.

Chen EY, Tan CM, Kou Y, Duan Q, Wang Z, Meirelles GV, Clark NR, Ma'ayan A. 2013. Enrichr: interactive and collaborative HTML5 gene list enrichment analysis tool. BMC Bioinformatics 14, 128. doi: 10.1186/1471-2105-14-128.

Ginde AA, Liu MC, Camargo CA Jr. Demographic differences and trends of vitamin D insufficiency in the US population, 1988-2004. Arch Intern Med. 2009a; 169: 626-632.

Ginde AA, Scragg R, Schwartz RS, Camargo CA Jr. Prospective study of serum 25-hydroxyvitamin d level, cardiovascular disease mortality, and all-cause mortality in older U.S. Adults. J Am Geriatr Soc. 2009b; 57: 1595-1603.

Glinsky GV. 2015. Transposable elements and DNA methylation create in embryonic stem cells human-specific regulatory sequences associated with distal enhancers and non-coding RNAs. Genome Biol Evol 7: 1432-1454.

Glinsky GV. 2016. Mechanistically distinct pathways of divergent regulatory DNA creation contribute to evolution of human-specific genomic regulatory networks driving phenotypic divergence of Homo sapiens. Genome Biol Evol 8:2774-88.

Glinsky GV. 2016. Activation of endogenous human stem cell-associated retroviruses (SCARs) and therapy-resistant phenotypes of malignant tumors. Cancer Lett 376:347-359.

Glinsky GV. 2016. Single cell genomics reveals activation signatures of endogenous SCAR's networks in aneuploid human embryos and clinically intractable malignant tumors. Cancer Lett 381:176-93.

Glinsky GV. 2017. Human-specific features of pluripotency regulatory networks link NANOG with fetal and adult brain development. BioRxiv. https://www.biorxiv.org/content/early/2017/06/19/022913; doi: https://doi.org/10.1101/022913.

Glinsky GV. 2018. Contribution of transposable elements and distal enhancers to evolution of human-specific features of interphase chromatin architecture in embryonic stem cells. Chromosome Res. 2018. 26: 61-84.

Glinsky G, Durruthy-Durruthy J, Wossidlo M, Grow EJ, Weirather JL, Au KF, Wysocka J, Sebastiano V. 2018. Single cell expression analysis of primate-specific retroviruses-derived HPAT lincRNAs in viable human blastocysts identifies embryonic cells co-expressing genetic markers of multiple lineages. Heliyon 4: e00667. doi: 10.1016/j.heliyon.2018.e00667. eCollection 2018 Jun. PMID: 30003161.

Glinsky GV, Barakat TS. 2019. The evolution of Great Apes has shaped the functional enhancers' landscape in human embryonic stem cells. 37:101456. PMID: 31100635. DOI: 10.1016/j.scr.2019.101456

Glinsky GV. 2020. A catalogue of 59,732 human-specific regulatory sequences reveals unique to human regulatory patterns associated with virus-interacting proteins, pluripotency and brain development. DNA and Cell Biology, 2020; 39: 126-143. doi: 10.1089/dna.2019.4988.

Guffanti G, Bartlett A, Klengel T, Klengel C, Hunter R, Glinsky G, Macciardi F. 2018. Novel bioinformatics approach identifies transcriptional profiles of lineage-specific transposable elements at distinct loci in the human dorsolateral prefrontal cortex. Mol Biol Evol. 35: 2435-2453. PMID: 30053206. PMCID: PMC6188555. DOI: 10.1093/molbev/msy143.

Heath, AK, Kim IY, Hodge AM, English DR, and Muller, DC. Vitamin D status and mortality: A systematic review of observational studies. Int. J. Environ. Res. Public Health 2019, 16, 383; doi:10.3390/ijerph16030383.

Helming L, Böse J, Ehrchen J, Schiebe S, Frahm T, Geffers R, Probst-Kepper M, Balling R, Lengeling A. 1alpha,25-Dihydroxyvitamin D3 is a potent suppressor of interferon gamma-mediated macrophage activation. Blood. 2005; 106: 4351-8.

Kennel KA, Drake MT, Hurley DL. Vitamin D deficiency in adults: when to test and how to treat. Mayo Clin Proc. 2010; 85: 752-7.

Kuleshov MV, Jones MR, Rouillard AD, Fernandez NF, Duan Q, Wang Z, Koplev S, Jenkins SL, Jagodnik KM, Lachmann A, McDermott MG, Monteiro CD, Gundersen GW, Ma'ayan A. Enrichr: a comprehensive gene set enrichment analysis web server 2016 update. Nucleic Acids Research. 2016; gkw377.

Lips P. Vitamin D deficiency and secondary hyperparathyroidism in the elderly: consequences for bone loss and fractures and therapeutic implications. Endocr Rev. 2001; 22: 477-501.

Reghunathan R, Jayapal M, Hsu LY, Chng HH, Tai D, Leung BP, Melendez AJ. Expression profile of immune response genes in patients with Severe Acute Respiratory Syndrome. BMC Immunol. 2005; 6:2.

Shang J, Ye G, Shi K, Wan Y, Luo C, Aihara H, Geng Q, Auerbach A, Li F. Structural basis of receptor recognition by SARS-CoV-2. Nature. 2020. doi: 10.1038/s41586-020-2179-y. Online ahead of print. PMID: 32225175

Smith M, Smith JC. Repurposing Therapeutics for COVID-19: Supercomputer-Based Docking to the SARS-CoV-2 Viral Spike Protein and Viral Spike Protein-Human ACE2 Interface. ChemRxiv. 2020. Preprint. https://doi.org/10.26434/chemrxiv.11871402.v3

Tavazoie, S., Hughes, J.D., Campbell, M.J., Cho, R.J., and Church, GM. Systematic determination of genetic network architecture. Nat Genet 1999; 22, 281–285.

Walls AC, Park YJ, Tortorici MA, Wall A, McGuire AT, Veesler D. Structure, function, and antigenicity of the SARS-CoV-2 spike glycoprotein. Cell. 2020. pii: S0092-8674(20)30262-2. doi: 10.1016/j.cell.2020.02.058. [Epub ahead of print]

Yi L, Li Z, Yuan K, Qu X, Chen J, Wang G, Zhang H, Luo H, Zhu L, Jiang P, Chen L, Shen Y, Luo M, Zuo G, Hu J, Duan D, Nie Y, Shi X, Wang W, Han Y, Li T, Liu Y, Ding M, Deng H, Xu X. Small molecules blocking the entry of severe acute respiratory syndrome coronavirus into host cells. J Virol. 2004; 78: 11334-9.

Yan R, Zhang Y, Li Y, Xia L, Guo Y, Zhou Q. Structural basis for the recognition of SARS-CoV-2 by full-length human ACE2. Science. 2020; 367: 1444-1448. doi: 10.1126/science.abb2762. Epub 2020 Mar 4. PMID: 32132184

Zhou, P., Yang, X.L., Wang, X.G., Hu, B., Zhang, L., Zhang, W., Si, H.R., Zhu, Y., Li, B., Huang, C.L., et al. (2020). A pneumonia outbreak associated with a new coronavirus of probable bat origin. Nature. Published online February 3, 2020. https://doi.org/10.1038/s41586-020-2012-7.

Zhu, N., Zhang, D., Wang, W., Li, X., Yang, B., Song, J., Zhao, X., Huang, B., Shi, W., Lu, R., et al. (2020). A Novel Coronavirus from Patients with Pneumonia in China, 2019. N Engl J Med. 382, 727–733.

ACE2 and FURIN

Supplemental Figure S1. Expression in human cells, tissues, and organs

RNA-Seq Expression Data from GTEx (53 Tissues, 570 Donors)

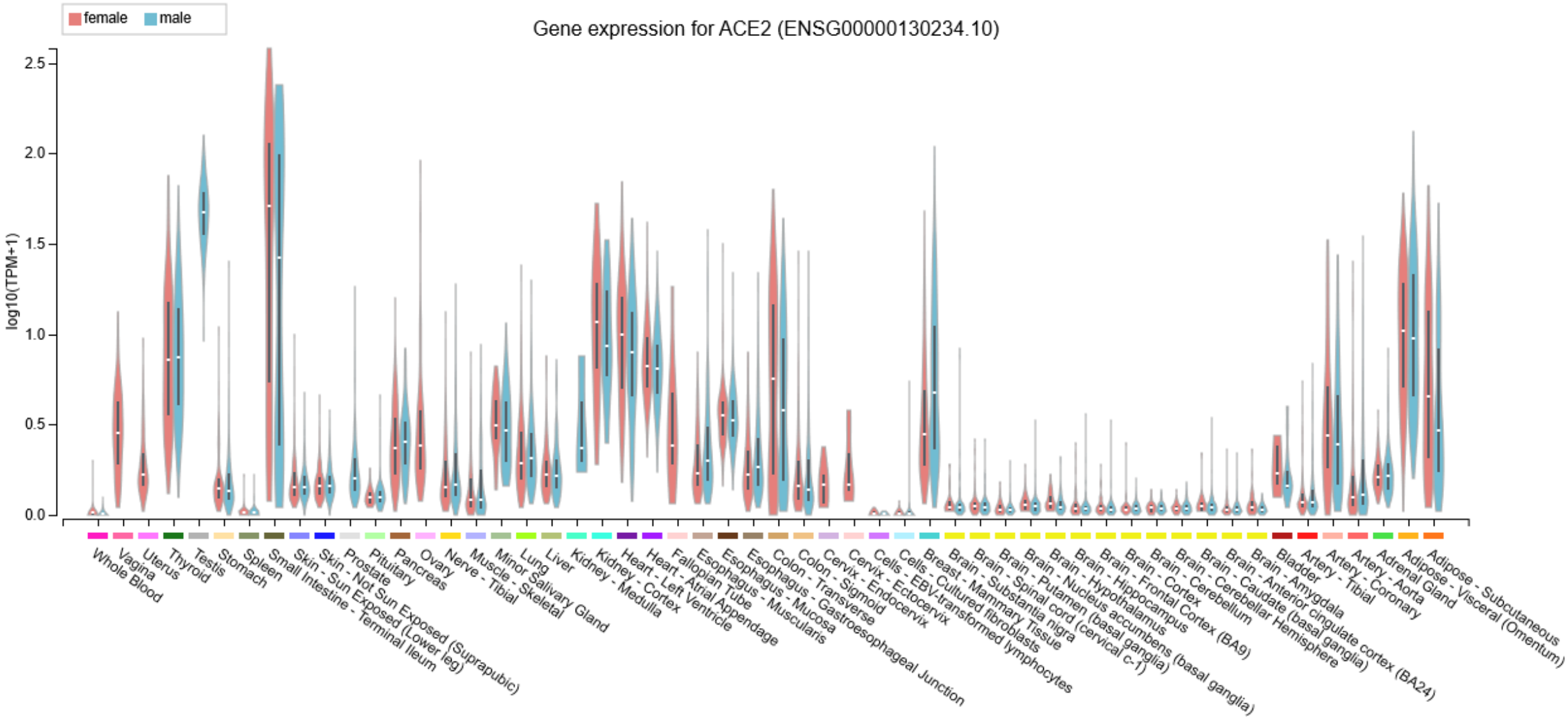

RNA-Seq Expression Data from GTEx (53 Tissues, 570 Donors)

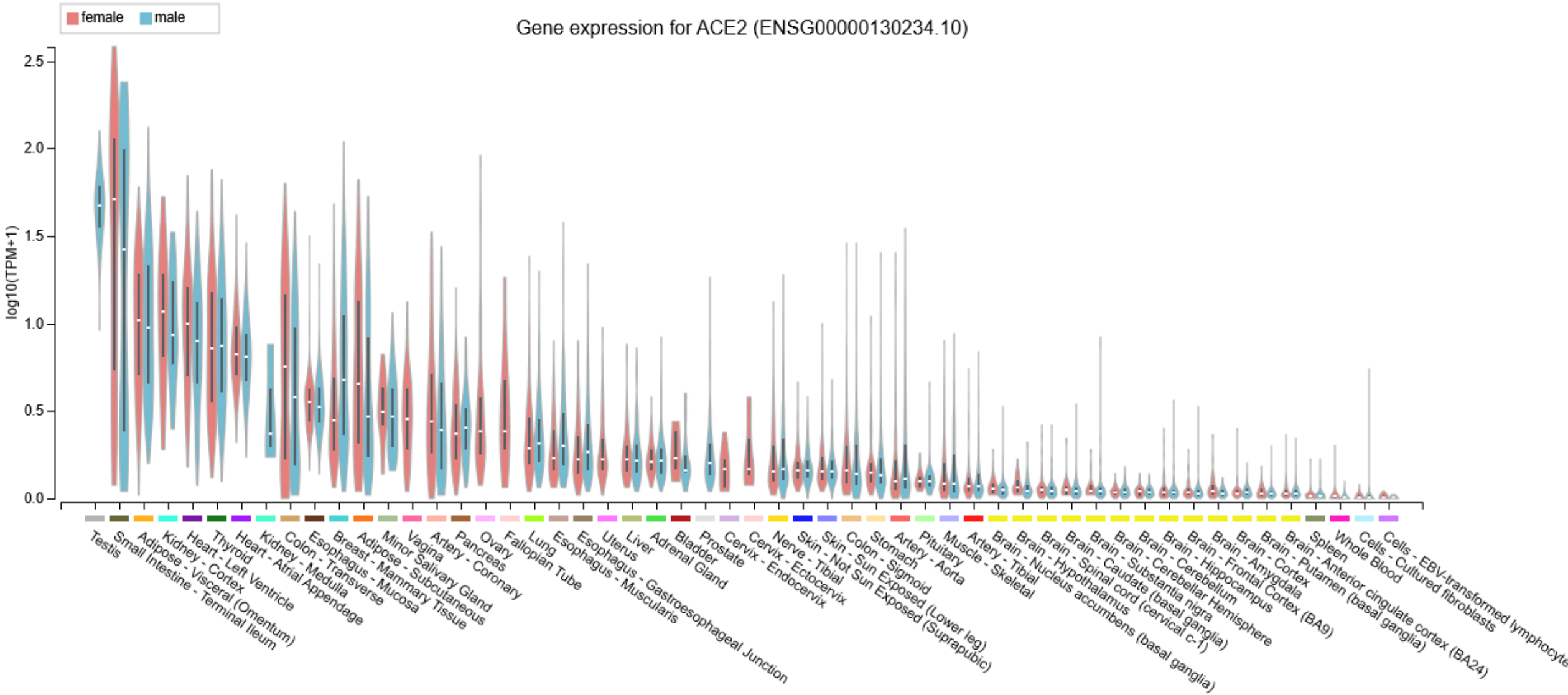

RNA-Seq Expression Data from GTEx (53 Tissues, 570 Donors)

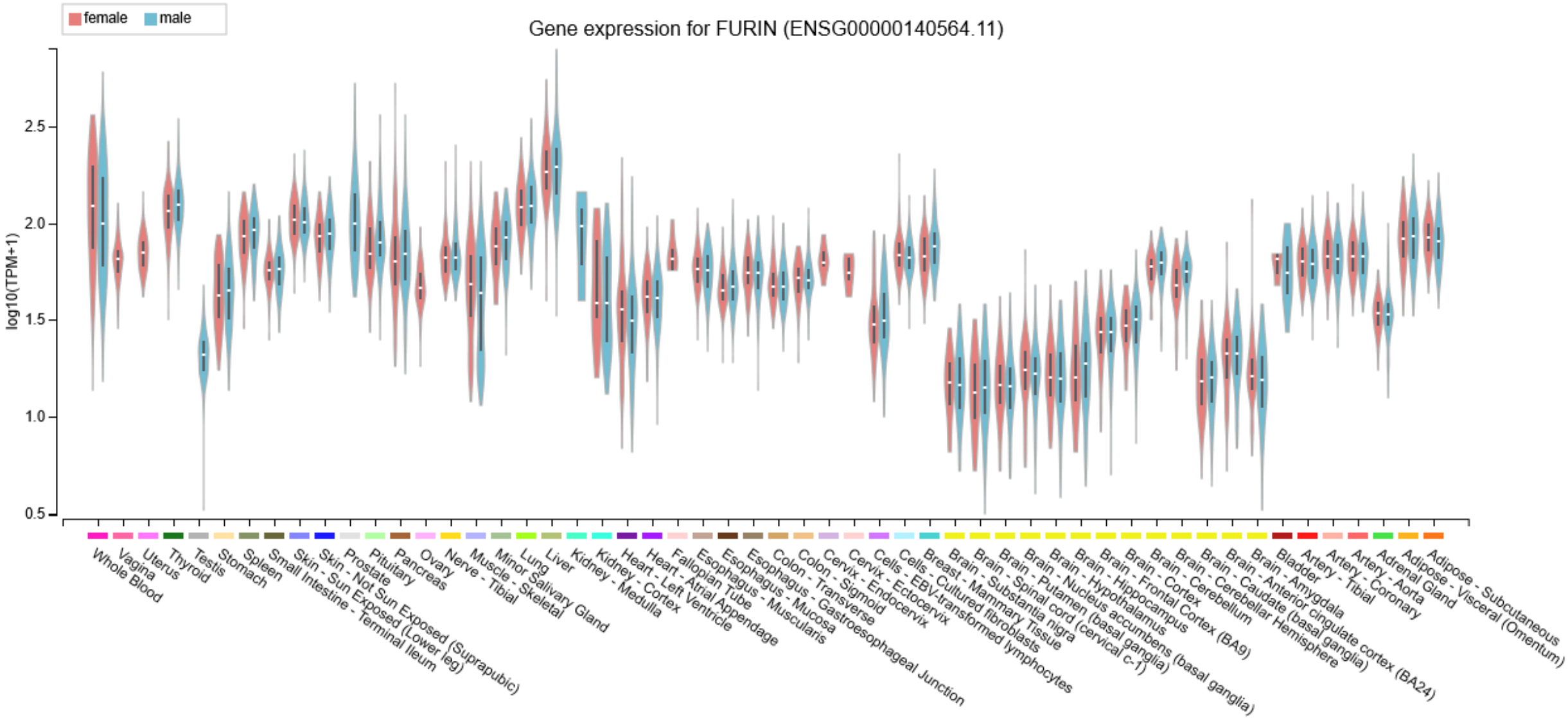

RNA-Seq Expression Data from GTEx (53 Tissues, 570 Donors)

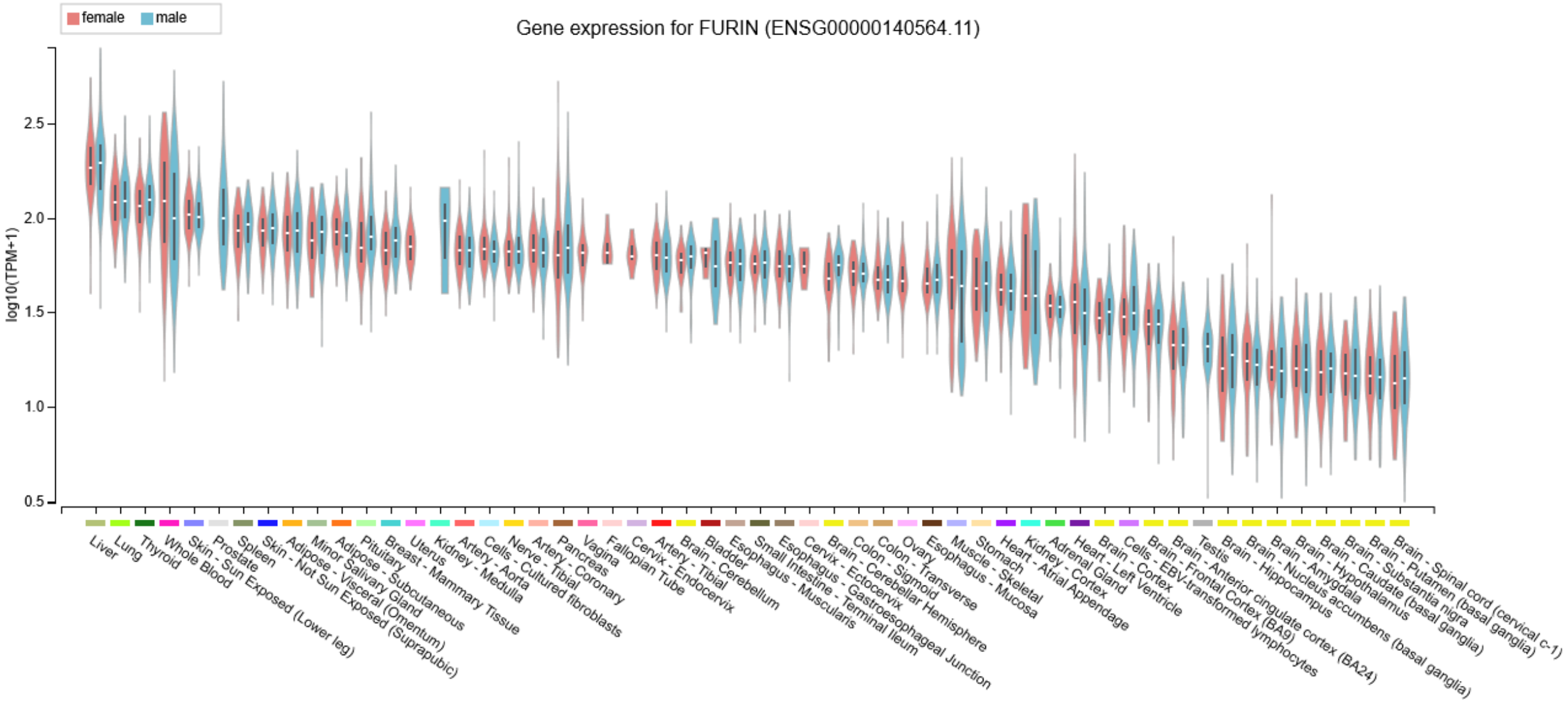

Jensen TISSUES

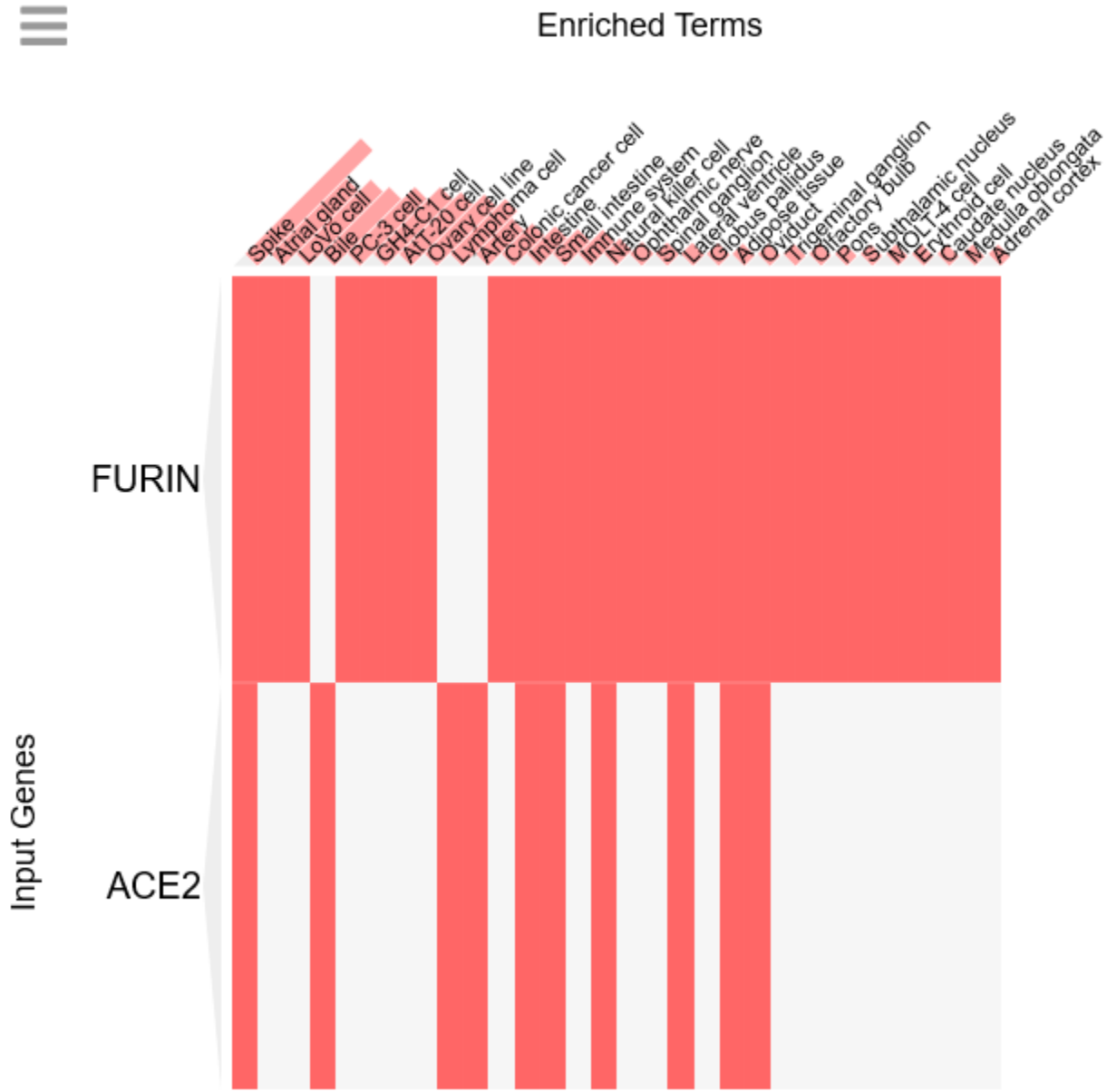

ARCHS4 Human Tissues

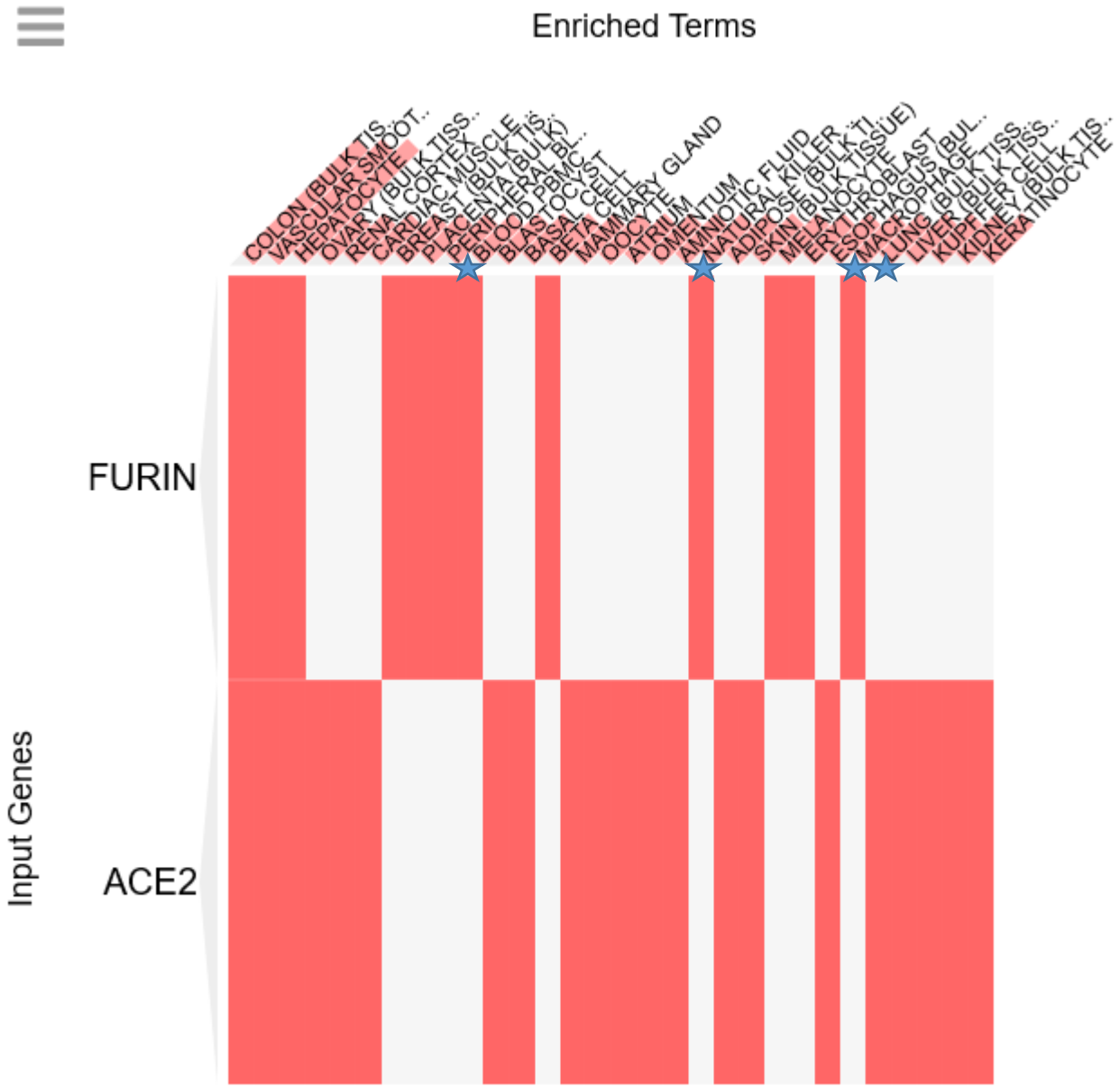

ACE2 and FURIN

Supplemental Figure S2. Effects of viral challenges on expression

Virus Perturbations from GEO up

Profile: *FURIN* expression in peripheral blood mononuclear cells (PBMCs)
GDS1028 / 201945_at
Title
Severe acute respiratory syndrome expression profile
Organism
Homo sapiens

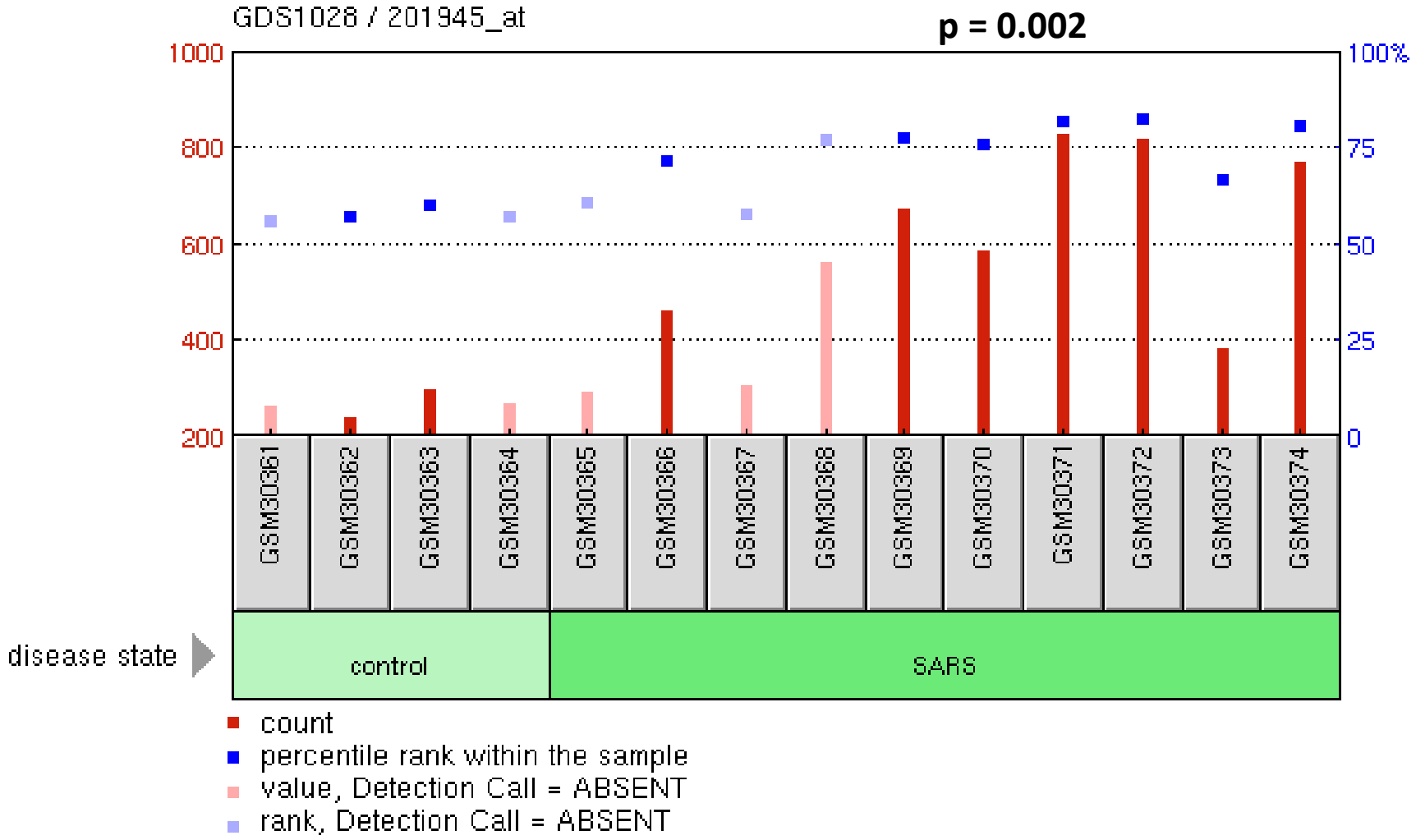

FURIN expression in peripheral blood mononuclear cells (PBMCs)

Sample	Title	Value
GSM30361	N1	264.2
GSM30362	N2	241.7
GSM30363	N3	298.1
GSM30364	N4	268.5
GSM30365	S1	295.5
GSM30366	S2	464
GSM30367	S3	**309.7**
GSM30368	S4	**564.1**
GSM30369	S5	**674.4**
GSM30370	S6	**588**
GSM30371	S7	**830.2**
GSM30372	S8	**818.8**
GSM30373	S9	**385.1**
GSM30374	S10	**771.2**

ACE2 and FURIN

Supplemental Figure S3. Effects of common human diseases on expression changes

Disease Perturbations from GEO up

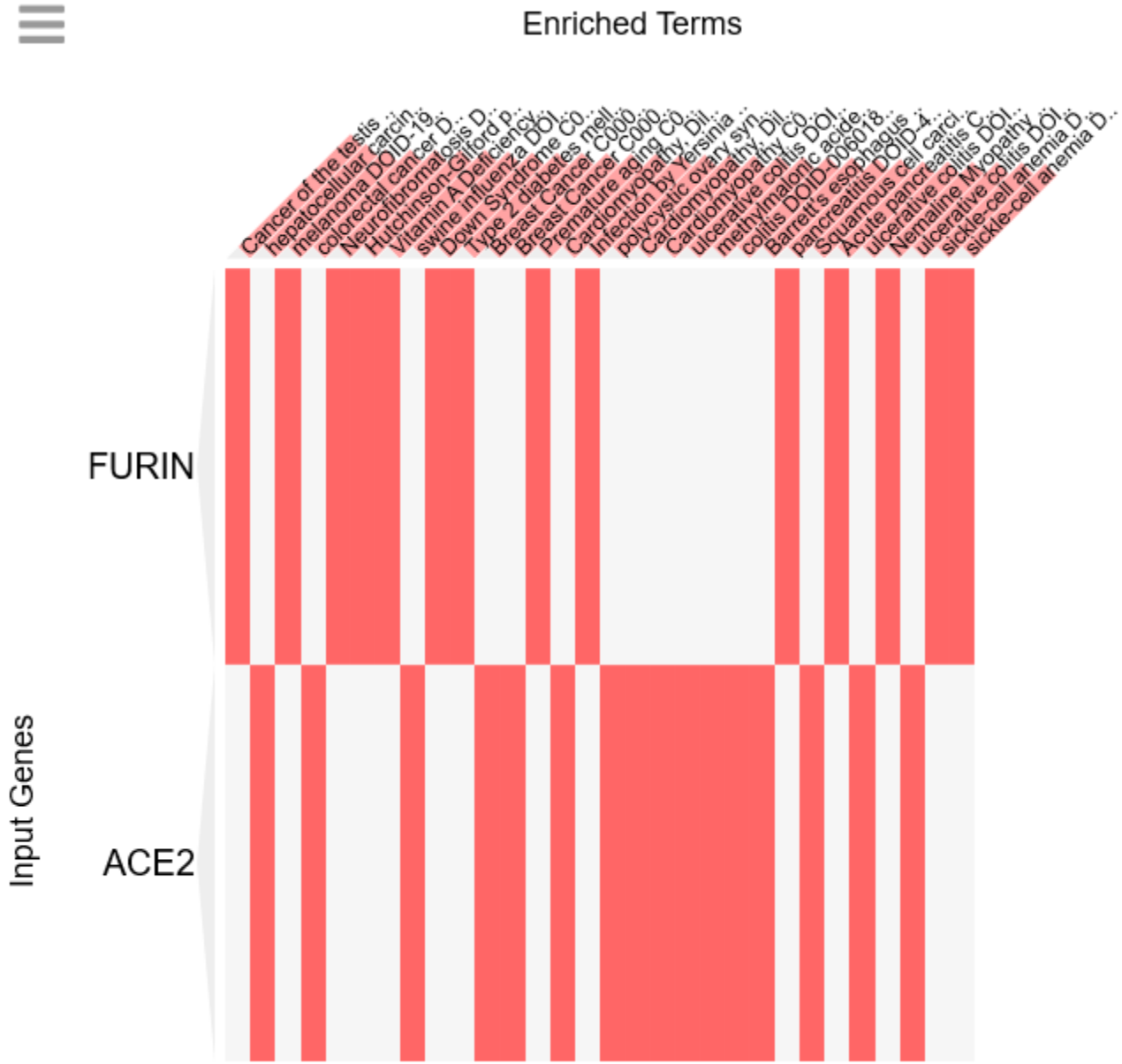

Distinct patterns of diseases associated with expression changes of the *ACE2* and *FURIN* genes

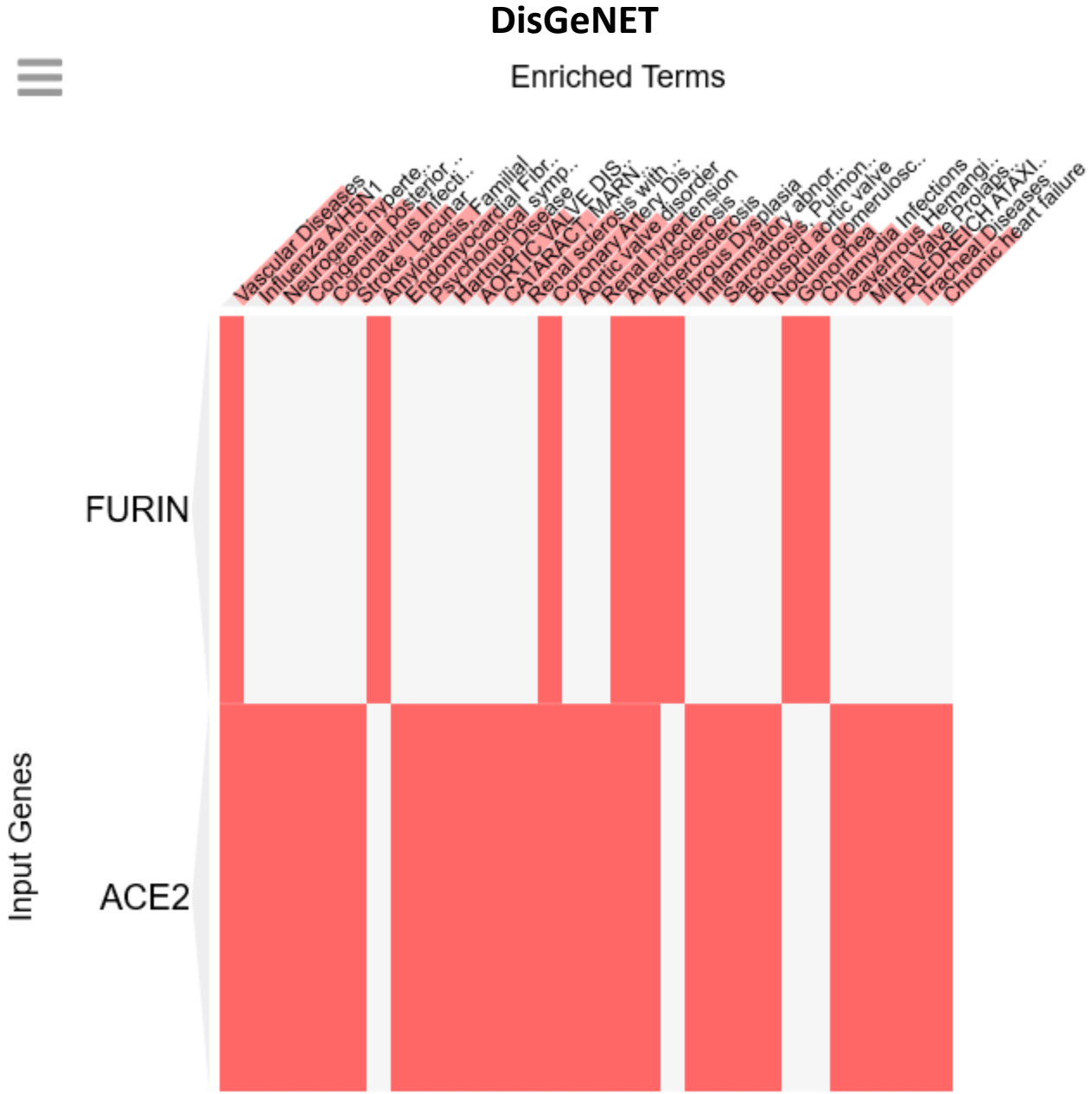

Profile: ACE2 expression
GDS2490 / 222257_s_at
Title
Large airway epithelium response to cigarette smoking (HG-133A)
Organism
Homo sapiens

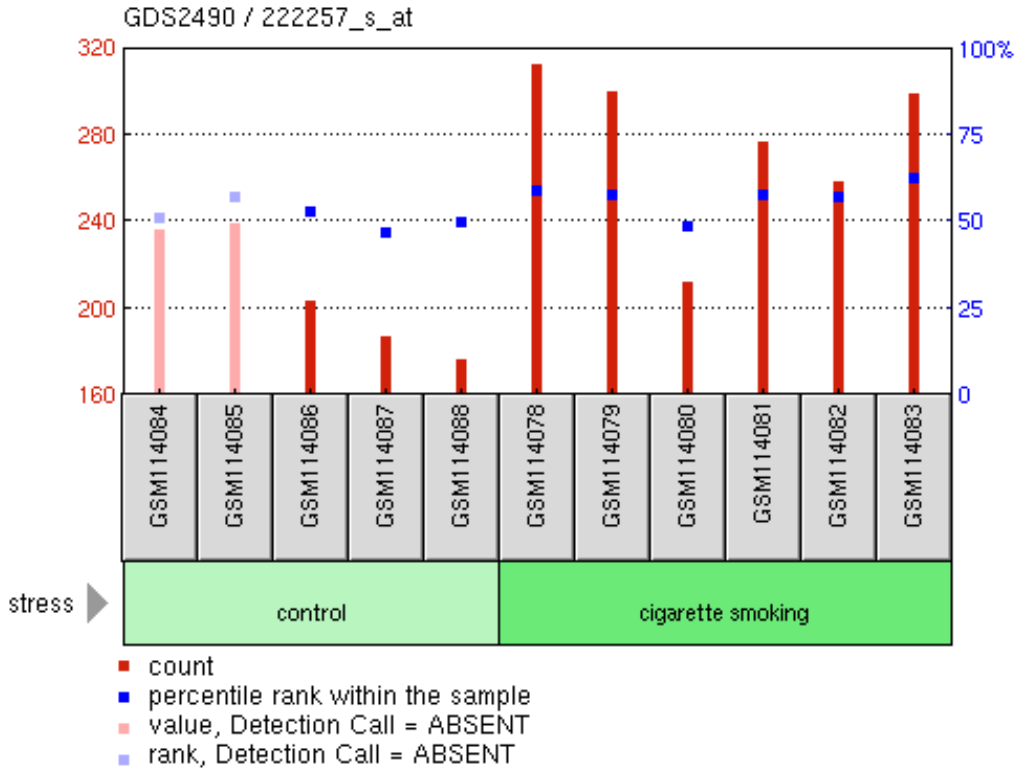

p = 0.0073

Sample	Title	Value
GSM114084	large airways, non-smoker 1, MAS5	236.4
GSM114085	large airways, non-smoker 2, MAS5	239.9
GSM114086	large airways, non-smoker 3, MAS5	203.8
GSM114087	large airways, non-smoker 4, MAS5	187.6
GSM114088	large airways, non-smoker 5, MAS5	176.5
GSM114078	large airways, smoker 1, MAS5	**313.1**
GSM114079	large airways, smoker 2, MAS5	**300.5**
GSM114080	large airways, smoker 3, MAS5	**212.8**
GSM114081	large airways, smoker 4, MAS5	**277.3**
GSM114082	large airways, smoker 5, MAS5	**258.6**
GSM114083	large airways, smoker 6, MAS5	**299.2**

ACE2 and FURIN

Supplemental Figure S4. Gene ontology (GO) analyses

GO Biological Process 2018

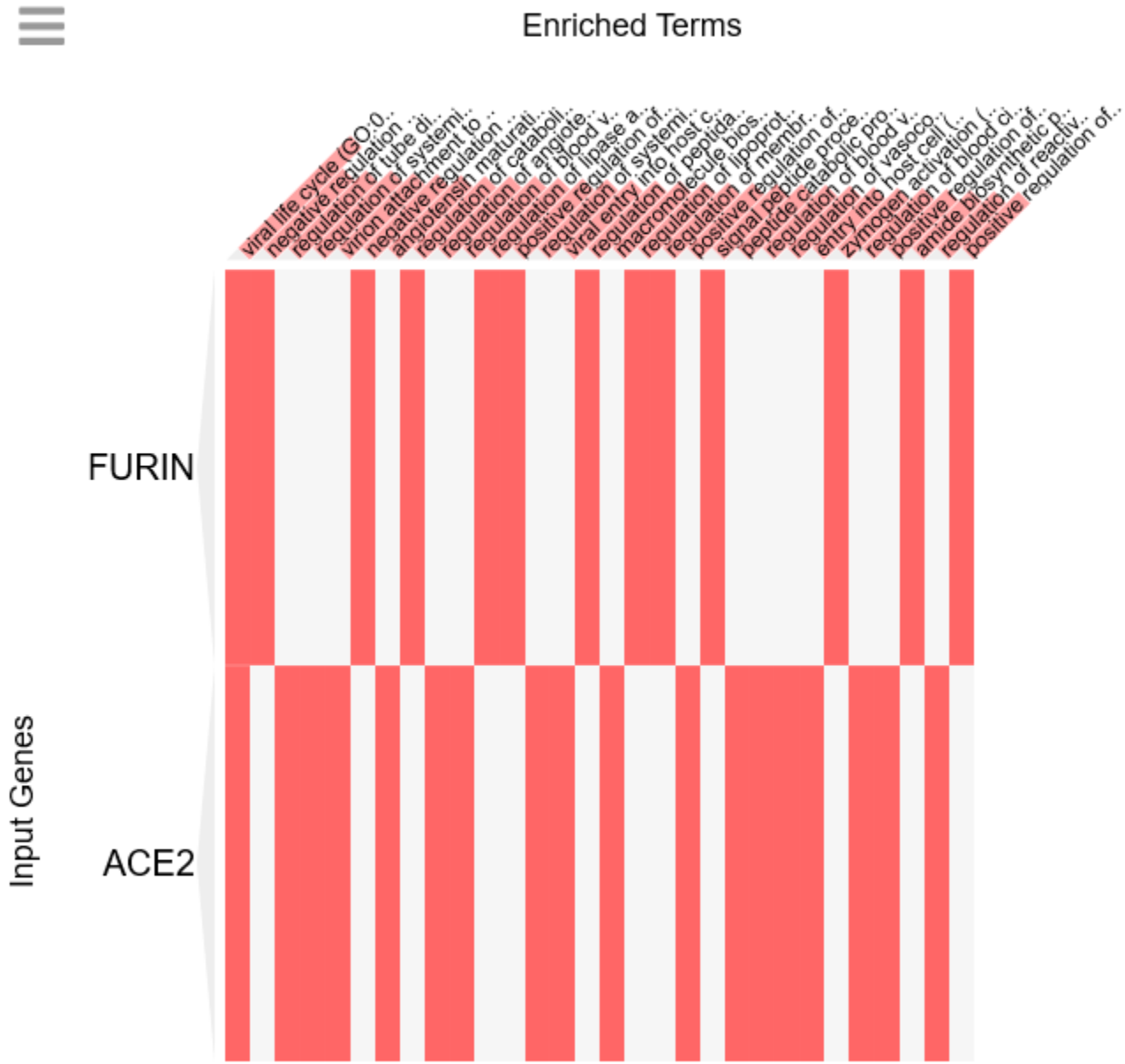

GO Molecular Function 2018

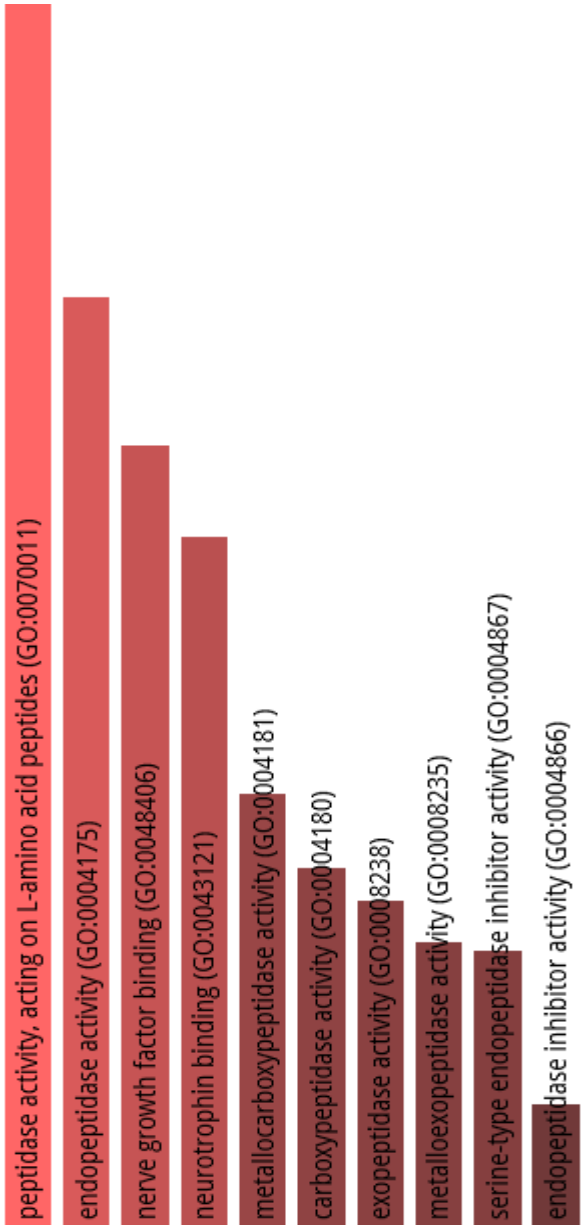

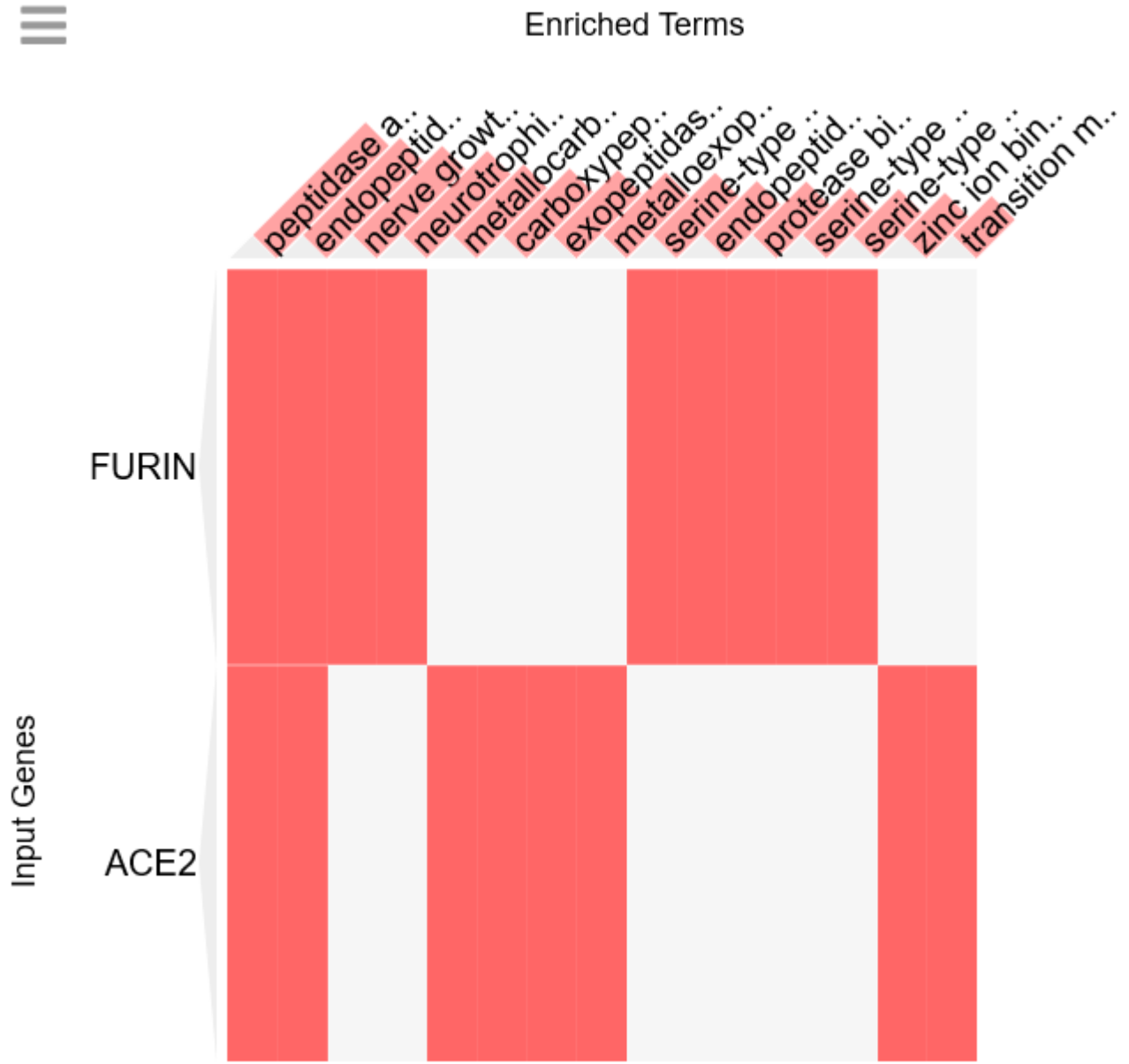

GO Cellular Component 2018

Jensen COMPARTMENTS

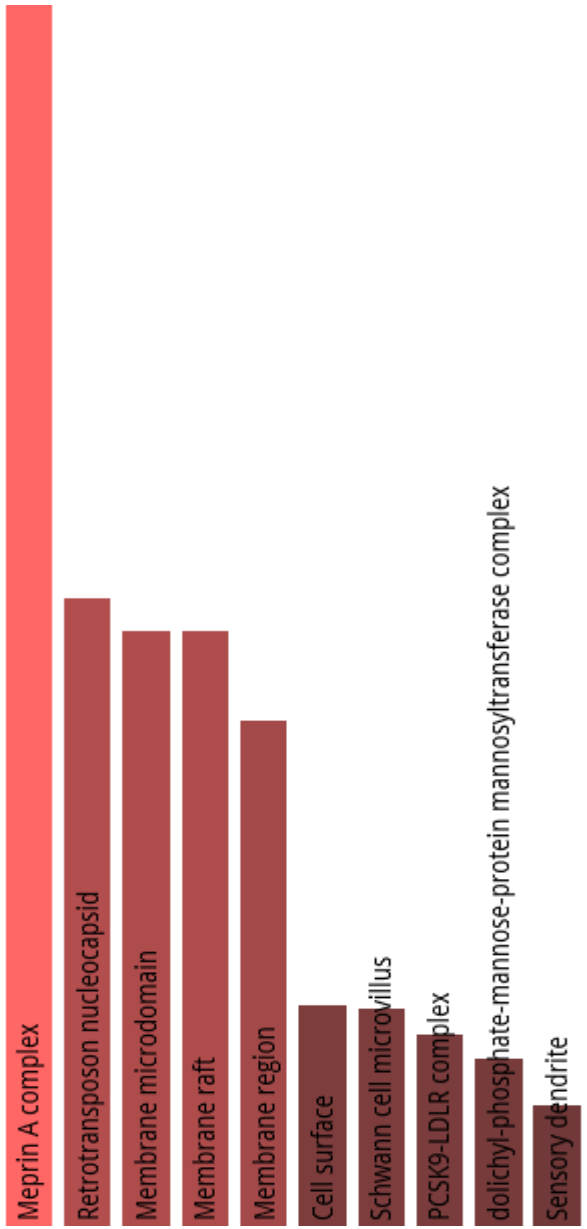

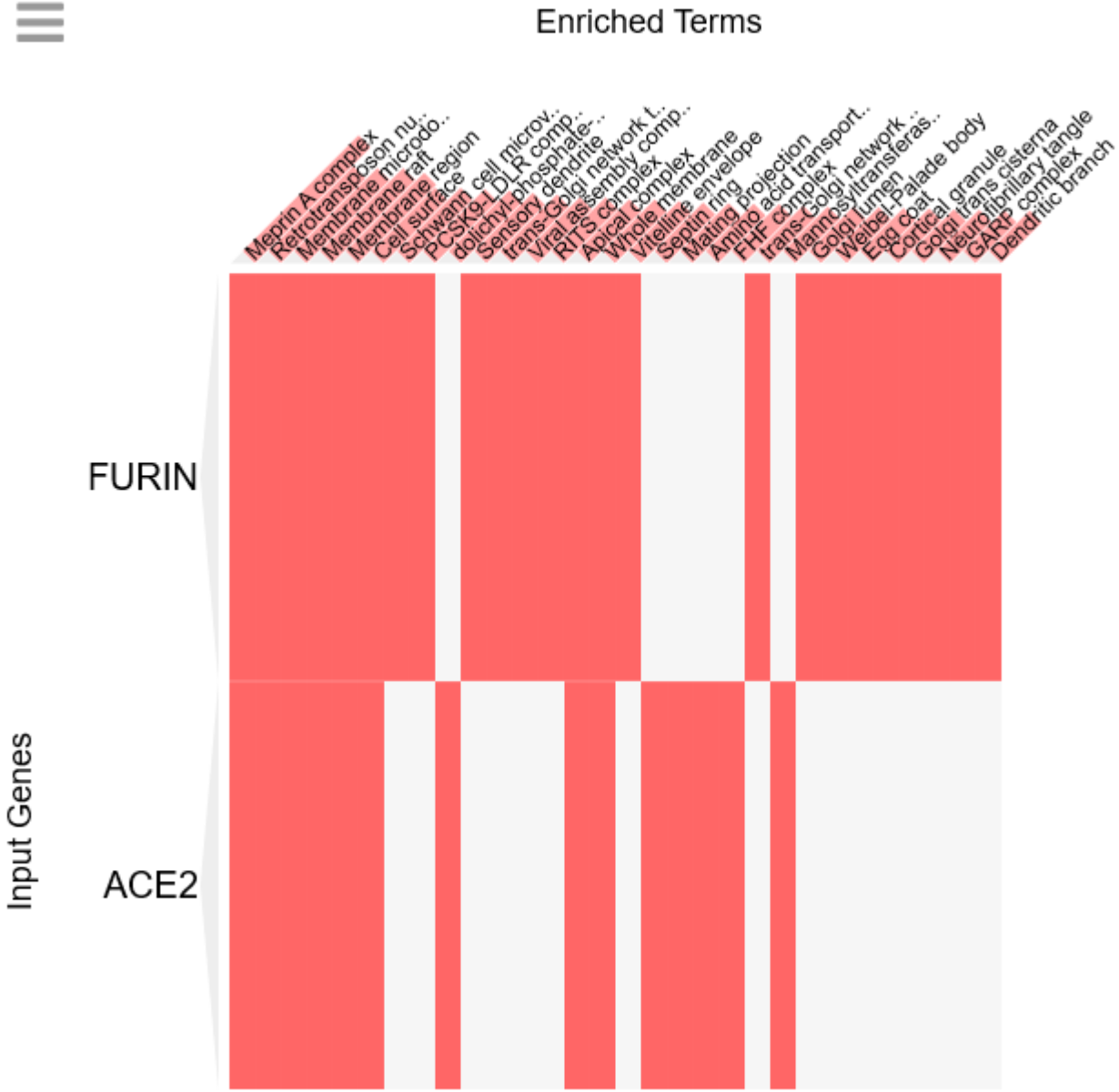

ACE2 and FURIN

Supplemental Figure S5. Potential mechanisms affecting gene expression: identifications of the enriched records of transcription factor-binding sites

Predominantly distinct transcription factors make-up chromatin of the ACE2 and FURIN genes

ENCODE TF ChIP-seq 2015

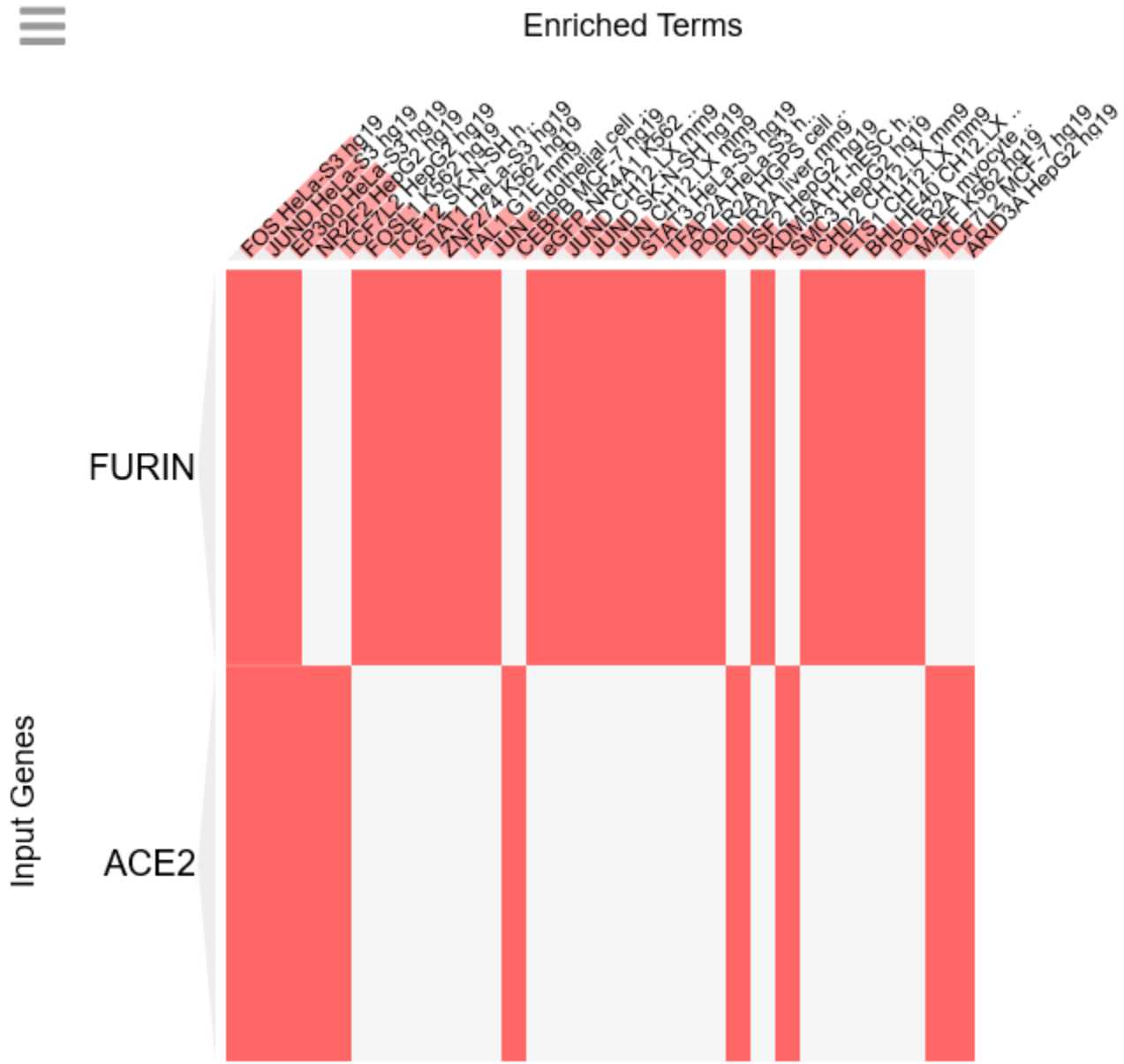

ACE2 and FURIN

Supplemental Figure S5-1. Potential mechanisms affecting gene expression: identifications of the enriched records of pathways, protein-protein interactions (PPI) hub proteins, and drugs affecting *ACE2* and *FURIN* expression

Distinct patterns of pathways associated with the *ACE2* and *FURIN* genes

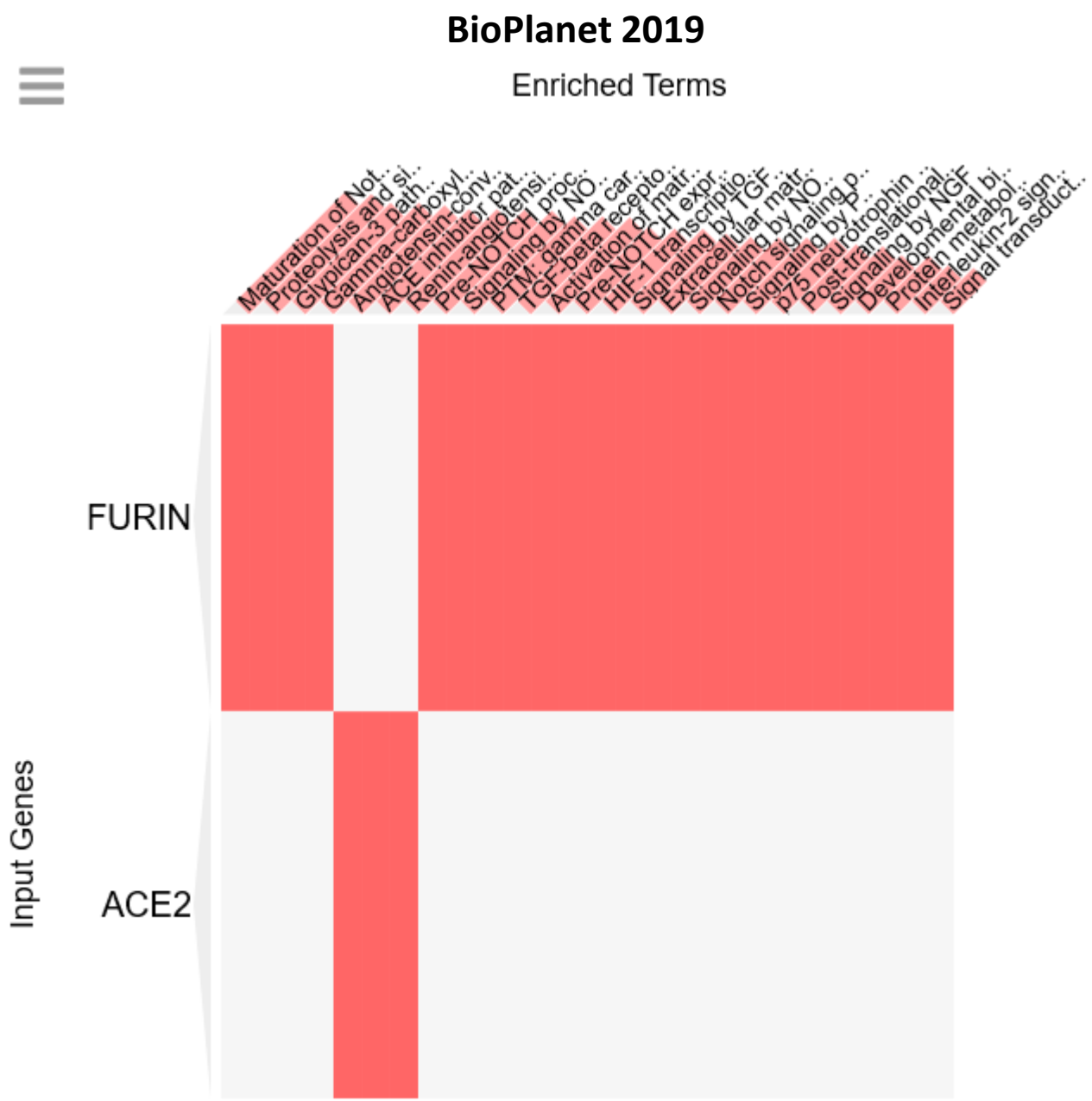

Distinct patterns of protein-protein interactions' (PPI) hub proteins associated with the *ACE2* and *FURIN* gene products

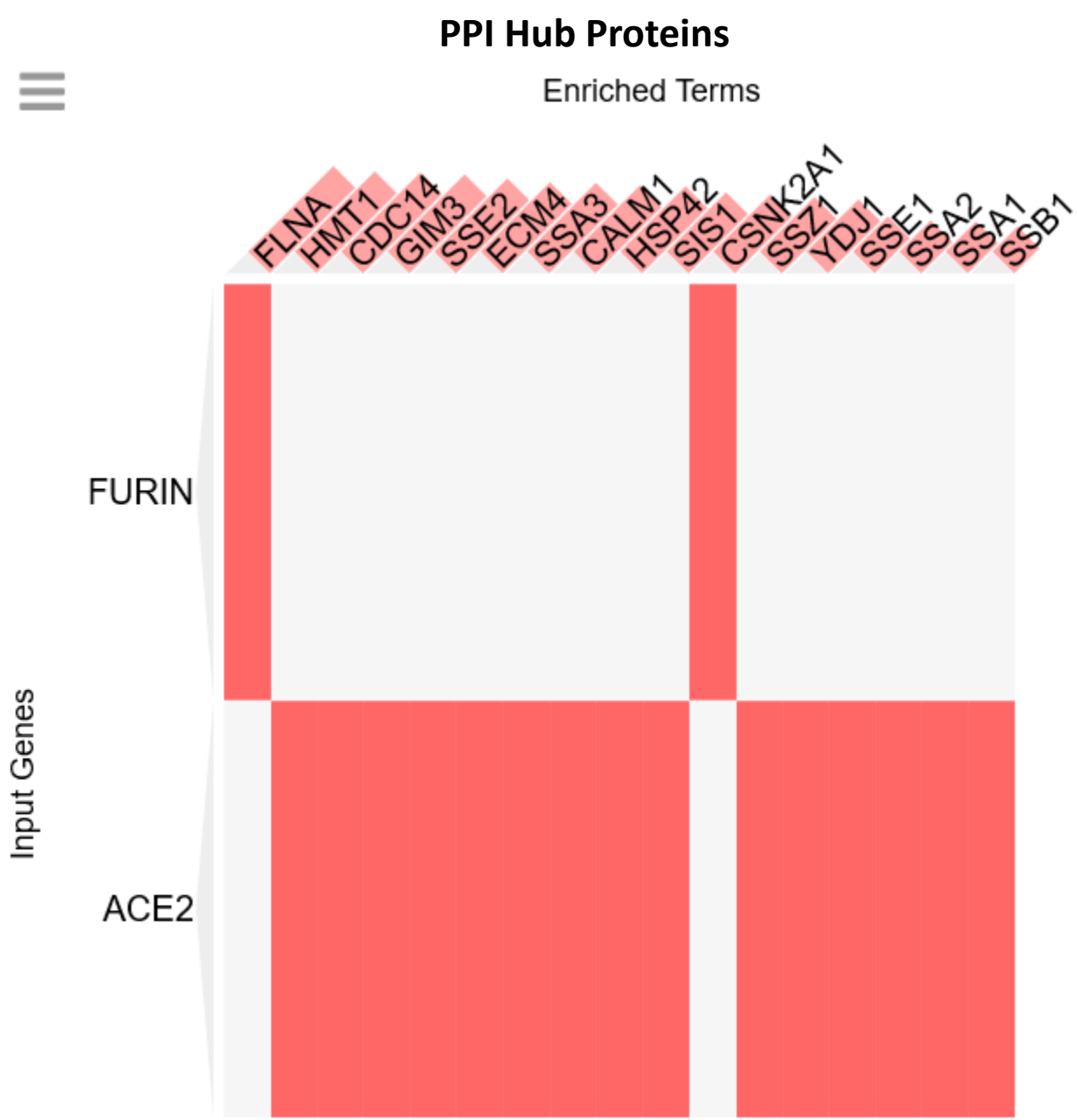

Distinct patterns of drugs affecting expression of the *ACE2* and *FURIN* genes

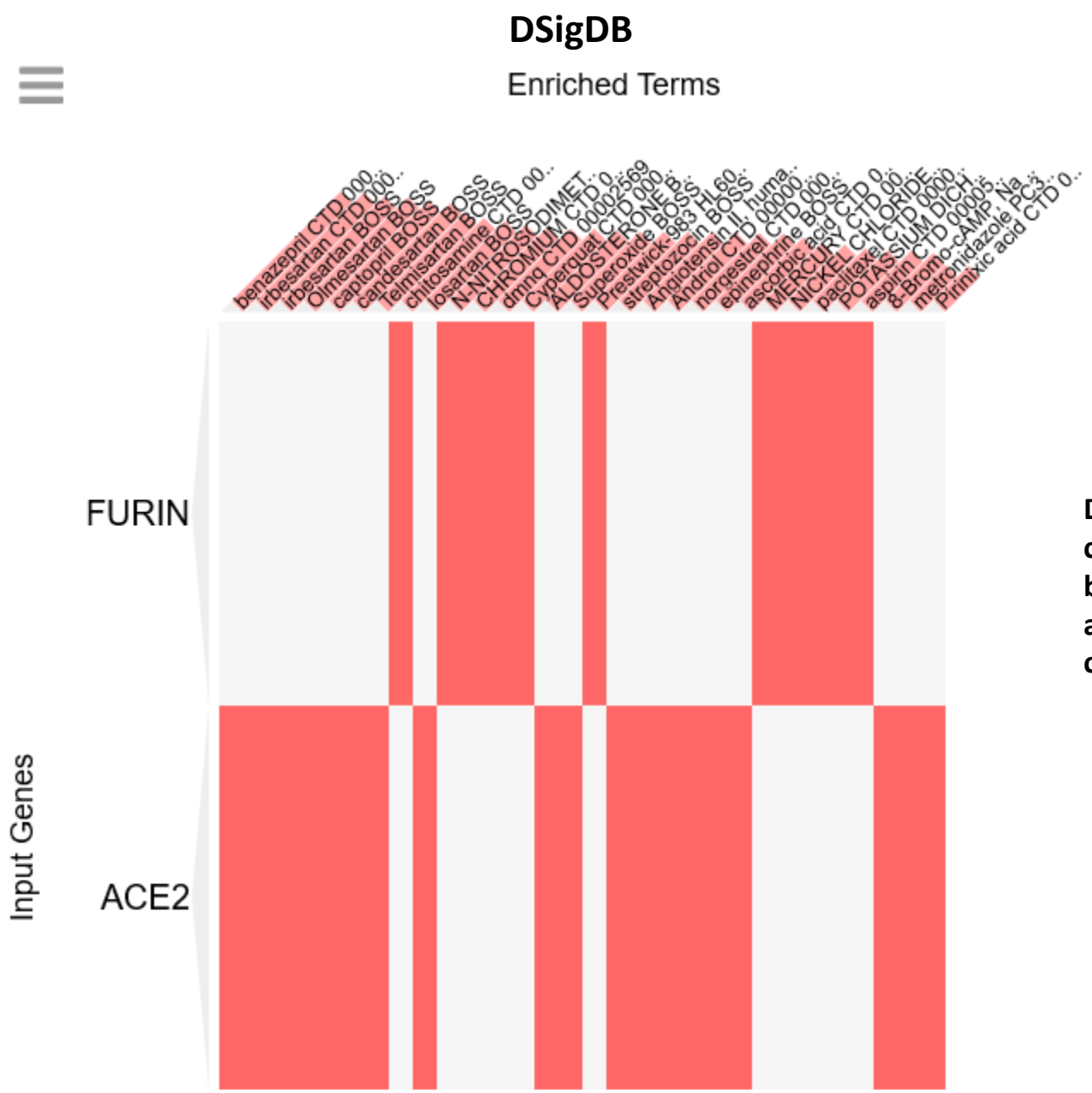

Drug Signatures Database contains drug/gene associations based on quantitative inhibition and drug-induced gene expression changes

ACE2 and FURIN

Supplemental Figure S5-2. Potential mechanisms affecting gene expression: identifications of the enriched records of transcription factor-binding sites that affect expression of target genes

Profile: *ACE2* expression
GDS3001 / 1425103_at
Title
c-Jun N-terminal kinase 1 depletion effect on livers of diet-induced obese animals
Organism
Mus musculus

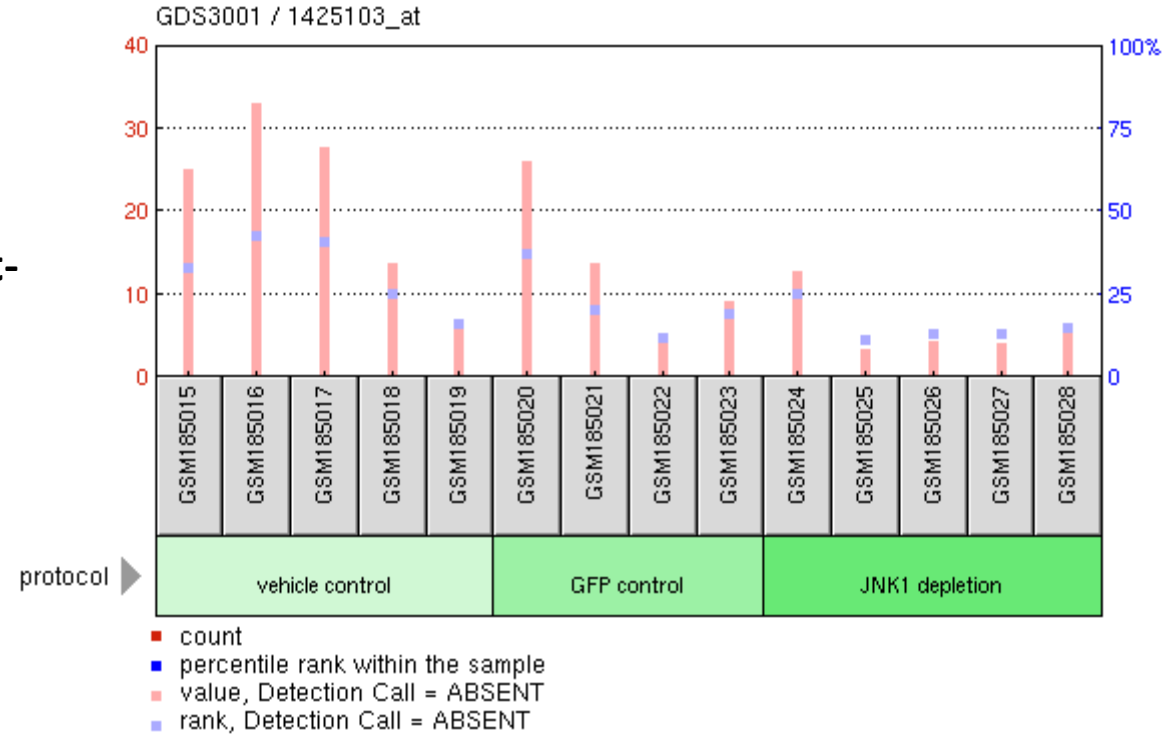

JNK1 depletion is associated with decreased expression of the *ACE2* gene

Sample	Title	Value
GSM185015	DIO Vehicle 1	25.1364
GSM185016	DIO Vehicle 2	33.1885
GSM185017	DIO Vehicle 3	27.7494
GSM185018	DIO Vehicle 4	13.9459
GSM185019	DIO Vehicle 5	6.24653
GSM185020	GFP Adv-shRNA 1	26.1209
GSM185021	GFP Adv-shRNA 2	13.8813
GSM185022	GFP Adv-shRNA 3	4.77496
GSM185023	GFP Adv-shRNA 5	9.28534
GSM185024	Jnk1 Adv-shRNA 1	12.9219
GSM185025	Jnk1 Adv-shRNA 2	3.46532
GSM185026	Jnk1 Adv-shRNA 3	4.42602
GSM185027	Jnk1 Adv-shRNA 4	4.17173
GSM185028	Jnk1 Adv-shRNA 5	5.42079

Profile: *ACE2* expression
GDS4878 / 10603066
Title
c-Jun N-terminal kinase-1 deletion effect on bile duct ligation model of liver fibrosis: time course
Organism
Mus musculus

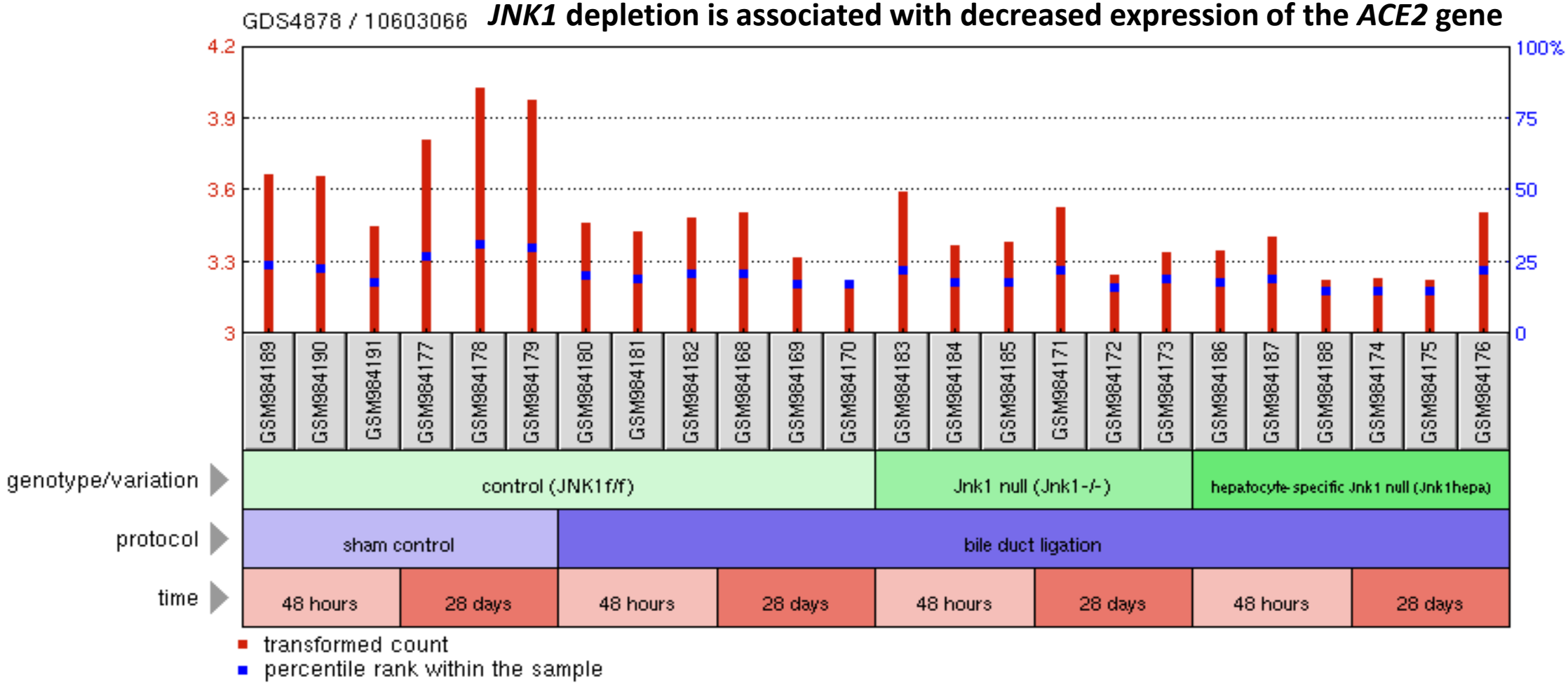

Profile: *ACE2* expression
GDS4878 / 10603066
Title: c-Jun N-terminal kinase-1 deletion effect on bile duct ligation model of liver fibrosis: time course
Organism: Mus musculus

JNK1 depletion is associated with decreased expression of the *ACE2* gene

Sample	Title	Value
GSM984189	Con sham 48h rep1	3.66522
GSM984190	Con sham 48h rep2	3.65818
GSM984191	Con sham 48h rep3	3.45112
GSM984177	Con sham 28d rep1	3.8128
GSM984178	Con sham 28d rep2	4.03119
GSM984179	Con sham 28d rep3	3.98185
GSM984180	Con BDL 48h rep1	3.46406
GSM984181	Con BDL 48h rep2	3.42924
GSM984182	Con BDL 48h rep3	3.48658
GSM984168	Con BDL 28d rep1	3.50685
GSM984169	Con BDL 28d rep2	3.32075
GSM984170	Con BDL 28d rep3	3.22149
GSM984183	JNK1KO BDL 48h rep1	3.59926
GSM984184	JNK1KO BDL 48h rep2	3.37132
GSM984185	JNK1KO BDL 48h rep3	3.38383
GSM984171	JNK1KO BDL 28d rep1	3.5343
GSM984172	JNK1KO BDL 28d rep2	3.24978
GSM984173	JNK1KO BDL 28d rep3	3.34012
GSM984186	JNK1dhepa BDL 48h rep1	3.34704
GSM984187	JNK1dhepa BDL 48h rep2	3.40698
GSM984188	JNK1dhepa BDL 48h rep3	3.22586
GSM984174	JNK1dhepa BDL 28d rep1	3.23559
GSM984175	JNK1dhepa BDL 28d rep2	3.23042
GSM984176	JNK1dhepa BDL 28d rep3	3.51026

Profile: *Fos* expression
GDS3512 / 1423100_at
Title
Furin deficiency effect on T-cells
Organism
Mus musculus

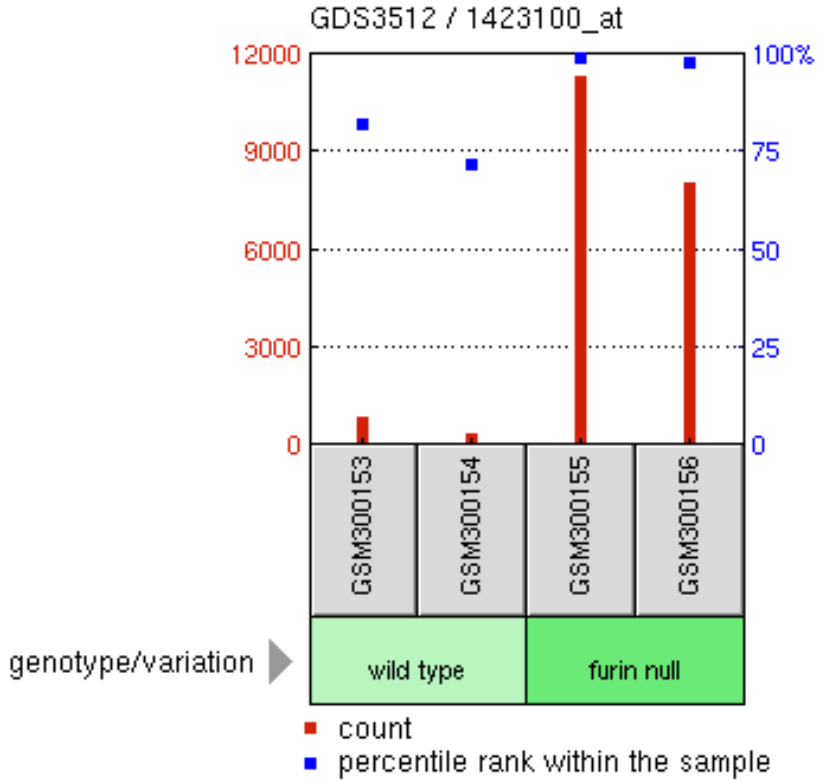

***Furin* depletion is associated with increased *Fos* expression**

Sample	Title	Value
GSM300153	Naive_Furin_Wild-type_1	873.5
GSM300154	Naive_Furin_Wild-type_2	374.2
GSM300155	Naive_Furin_Knockout_1	11333.5
GSM300156	Naive_Furin_Knockout_2	8045.2

Profile: *Jun* expression
GDS3512 / 1417409_at
Title
Furin deficiency effect on T-cells
Organism
Mus musculus

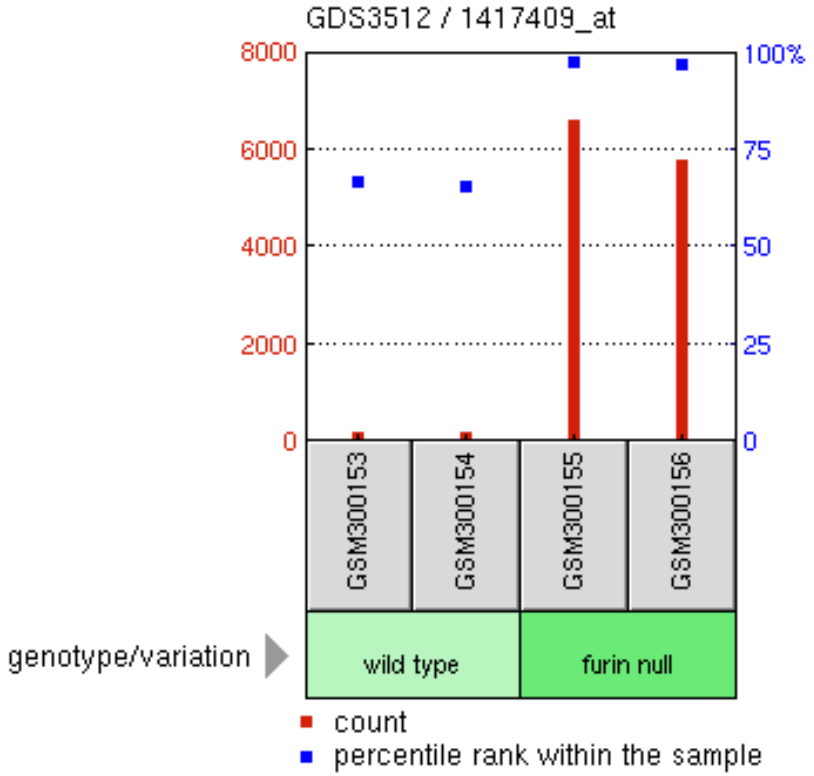

***Furin* depletion is associated with increased *Jun* expression**

Sample	Title	Value
GSM300153	Naive_Furin_Wild-type_1	232.7
GSM300154	Naive_Furin_Wild-type_2	238.9
GSM300155	Naive_Furin_Knockout_1	6631.6
GSM300156	Naive_Furin_Knockout_2	5795

Profile: *Jund* expression
GDS3512 / 1440265_at
Title
Furin deficiency effect on T-cells
Organism
Mus musculus

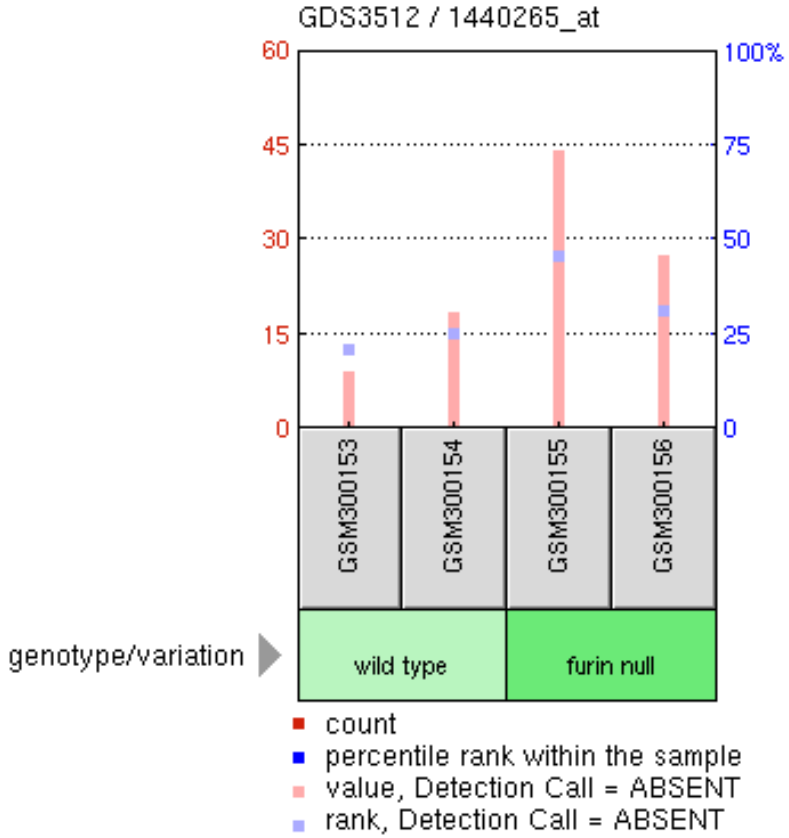

***Furin* depletion is associated with increased *Jund* expression**

Sample	Title	Value
GSM300153	Naive_Furin_Wild-type_1	9.2
GSM300154	Naive_Furin_Wild-type_2	18.5
GSM300155	Naive_Furin_Knockout_1	44.3
GSM300156	Naive_Furin_Knockout_2	27.6

Profile: *Junb* expression
GDS3512 / 1415899_at
Title
Furin deficiency effect on T-cells
Organism
Mus musculus

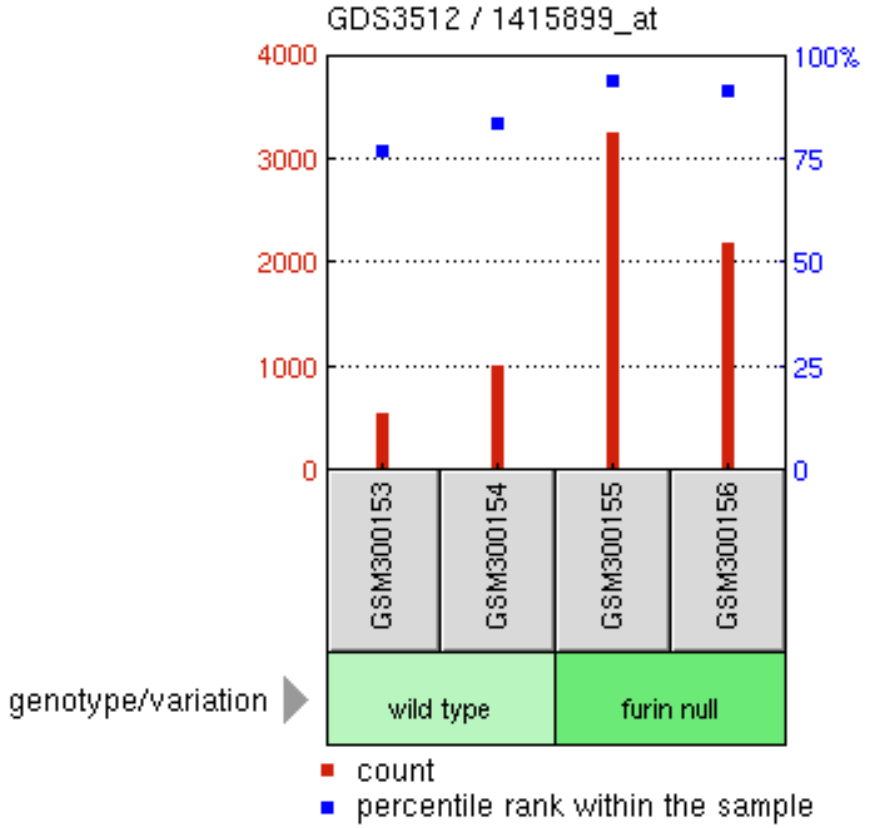

***Furin* depletion is associated with increased *Junb* expression**

Sample	Title	Value
GSM300153	Naive_Furin_Wild-type_1	556
GSM300154	Naive_Furin_Wild-type_2	1032.5
GSM300155	Naive_Furin_Knockout_1	3257.8
GSM300156	Naive_Furin_Knockout_2	2203.1

Profile: *FURIN* expression
GDS2766 / 1418518_at
Title
Dominant negative cJun effect on apolipoprotein E deficient livers
Organism
Mus musculus

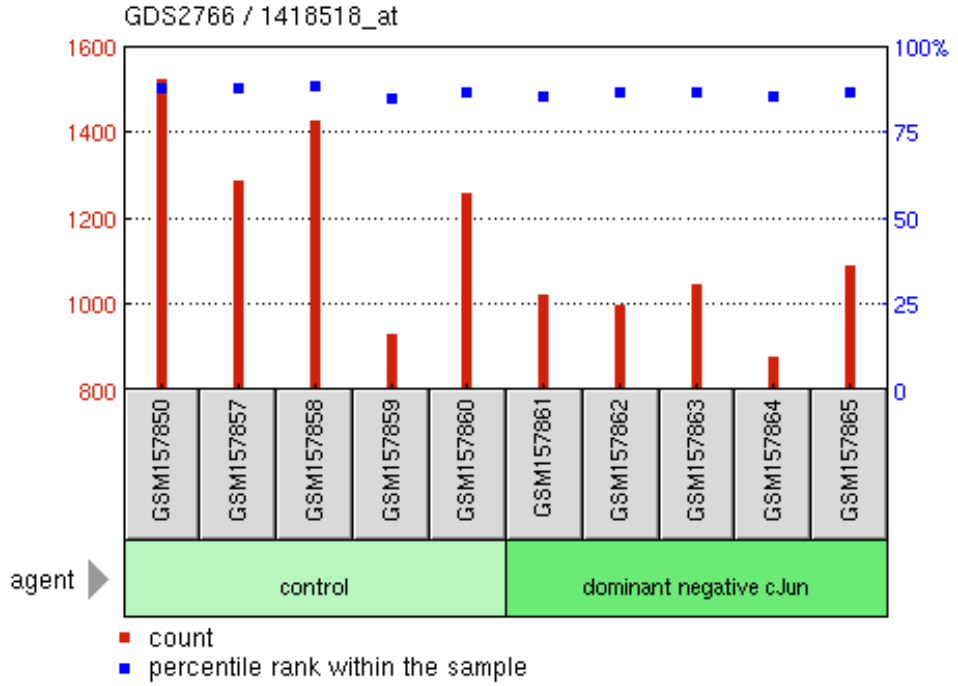

cJun inhibition is associated with decreased *Furin* expression

Sample	Title	Value
GSM157850	Control VZ11	1526.31
GSM157857	Control VZ12	1290.04
GSM157858	Control VZ13	1426.9
GSM157859	Control VZ14	932.365
GSM157860	Control VZ15	1259.69
GSM157861	Dominant negative cJun VZ16	1026.16
GSM157862	Dominant negative cJun VZ17	1002.07
GSM157863	Dominant negative cJun VZ18	1049.73
GSM157864	Dominant negative cJun VZ19	879.625
GSM157865	Dominant negative cJun VZ20	1093.33

Profile: *FURIN* expression
GDS4205 / 10564960
Title
Transcription factor c-JUN knockout effect on B lymphoid cells
Organism
Mus musculus

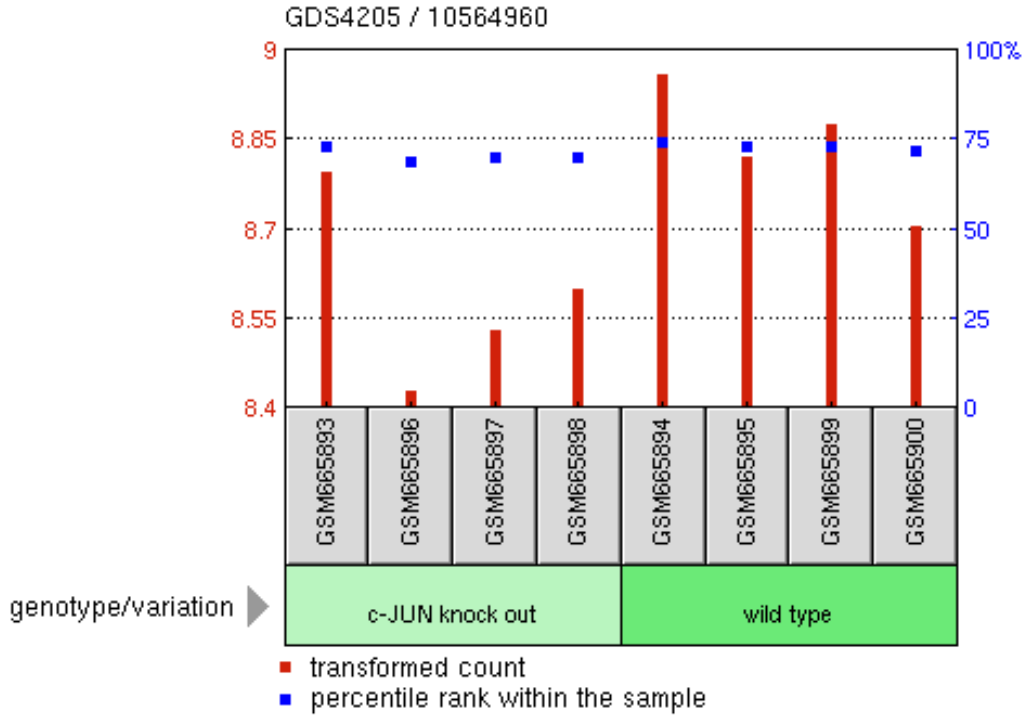

cJun depletion is associated with decreased *Furin* expression

Sample	Title	Value
GSM665893	RO35	8.79585
GSM665896	RO38	8.42939
GSM665897	D1	8.53367
GSM665898	D6	8.60035
GSM665894	RO36	8.96016
GSM665895	RO37	8.82158
GSM665899	F2	8.87409
GSM665900	F4	8.70635

Profile: *FURIN* expression
GDS1621 / X55660_at
Title
c-Jun N-terminal kinase pathway activation and suppression effect on aortic vascular smooth muscle cells
Organism
Rattus norvegicus

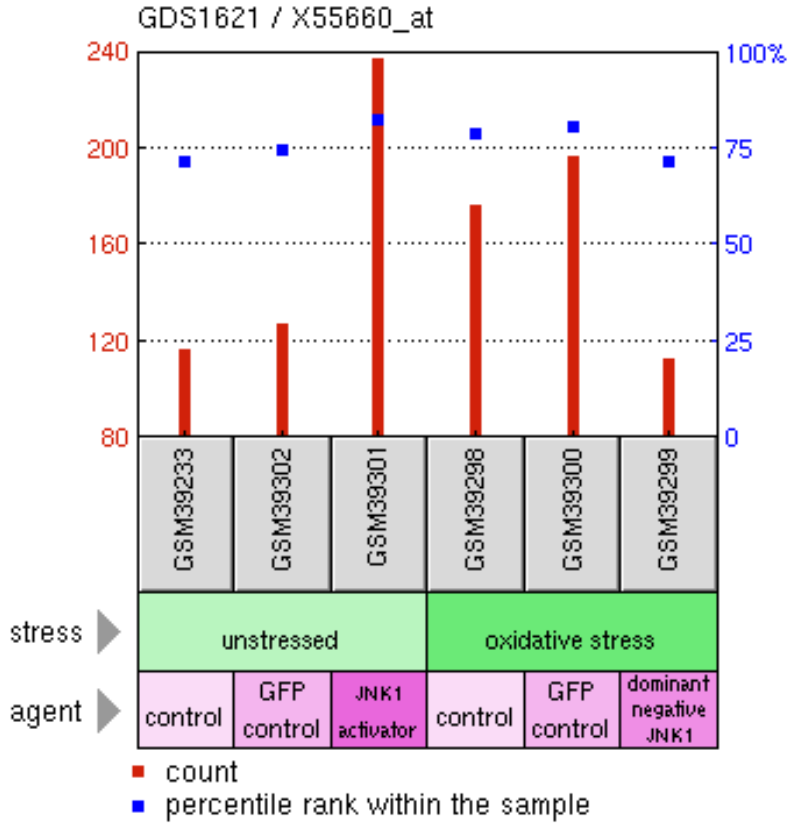

***JNK1 pathway* inhibition is associated with decreased *Furin* expression, while *JNK1* activation is associated with increased *Furin* expression**

Sample	Title	Value
GSM39233	rVSMC_control	116.8
GSM39302	rVSMC_nEGFP	128.1
GSM39301	rVSMC_MKK7ED+JNK1WT	**237.3**
GSM39298	rVSMC_H2O2	177.2
GSM39300	rVSMC_H2O2+nEGFP	197.2
GSM39299	rVSMC_H2O2+APF	**113.2**

JNK1/c-FOS pathway-associated activation of the *ACE2* and *FURIN* expression may trigger the auto-regulatory negative feed-back loop of the FURIN-mediated repression of the expression of *JUN, JUNB, JUND,* and *c-FOS* genes

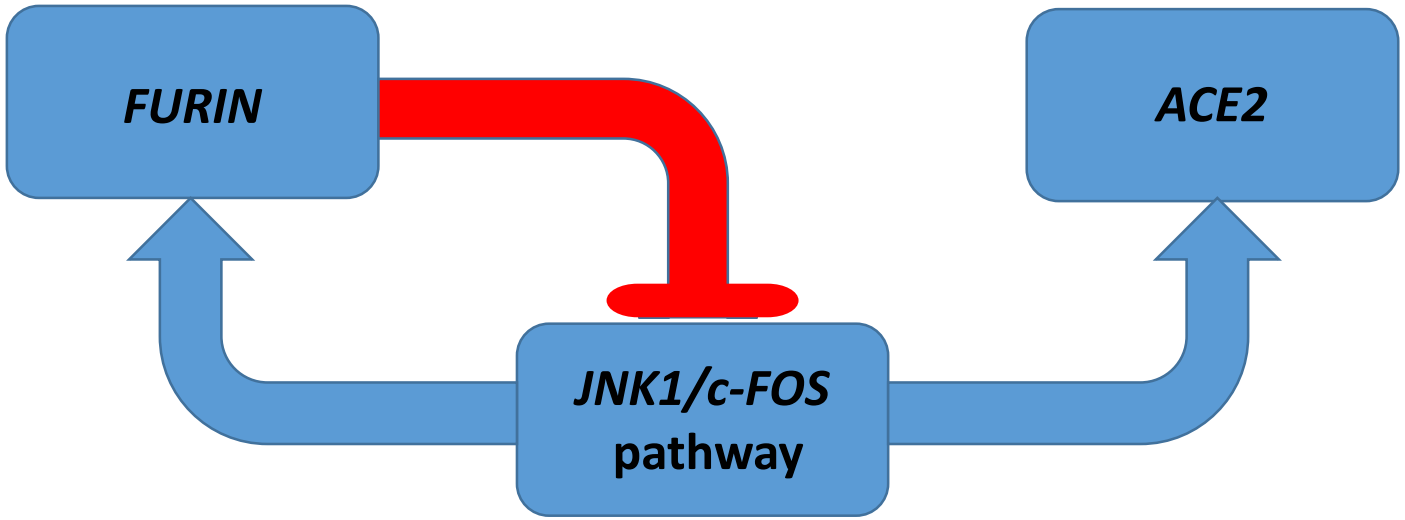

ACE2 and FURIN

Supplemental Figure S6. Potential mechanisms affecting gene expression: identifications of the enriched records of transcription factor-binding sites

Predominantly distinct transcription factors make-up chromatin of the ACE2 and FURIN genes

ChEA 2016

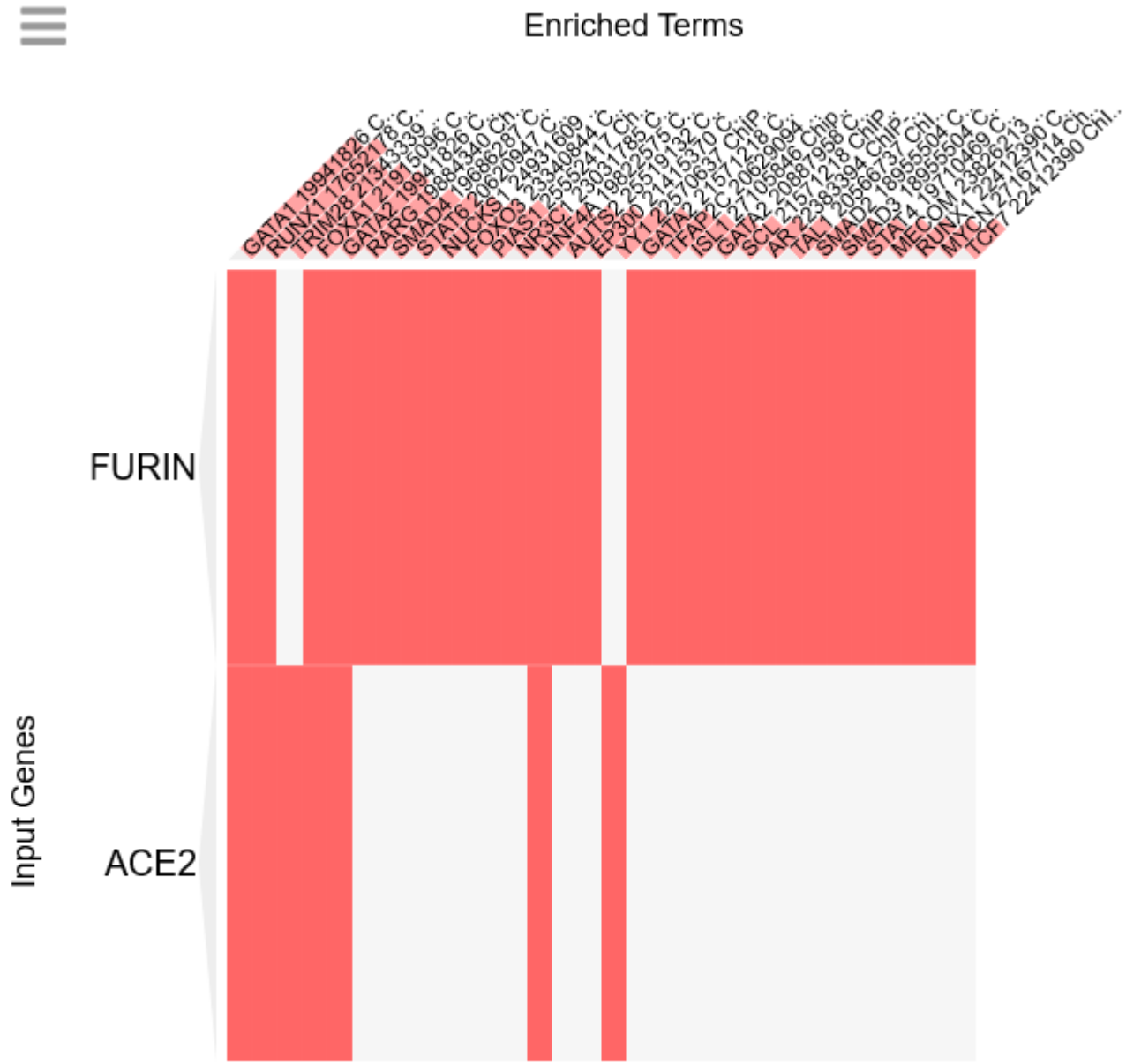

ACE2 and FURIN

Supplemental Figure S6-1. Potential mechanisms affecting gene expression: identifications of the enriched records of transcription factor-binding sites that affect expression of target genes

Profile: *ACE2* expression
GDS1916 / 1425103_at
Title
Hepatocyte nuclear factor 4 alpha knockout effect on the embryonic liver
Organism
Mus musculus

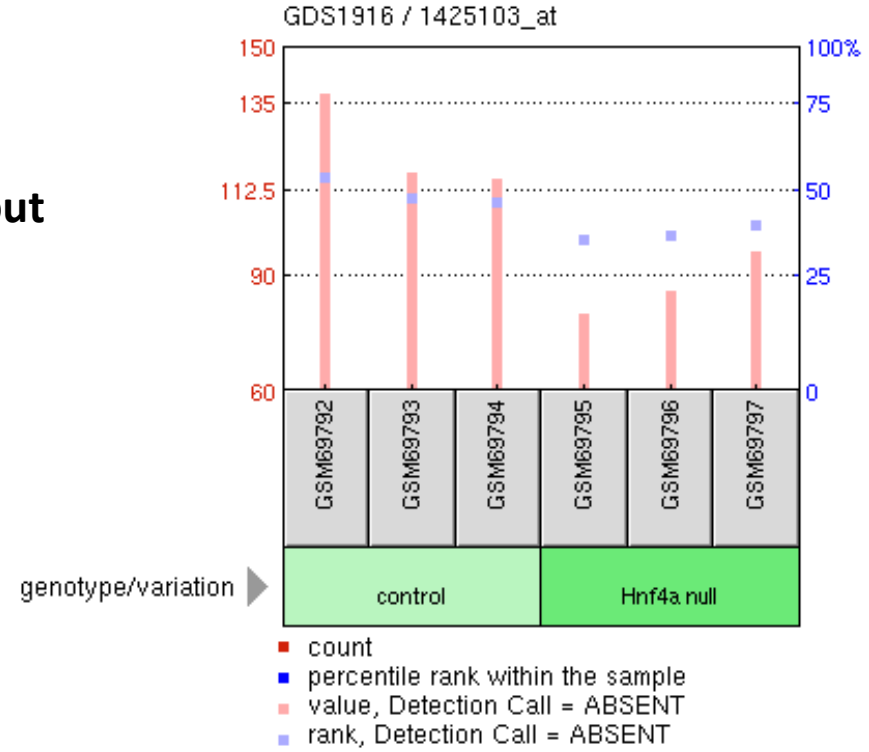

Hnf4a deficiency decreases *ACE2* expression in mouse cells

Sample	Title	Value
GSM69792	HNF4 Control_8	137.683
GSM69793	HNF4 Control_1192	117.056
GSM69794	HNF4 Control_1193	115.675
GSM69795	HNF4 Null_61	**80.4453**
GSM69796	HNF4 Null_1191	**86.1111**
GSM69797	HNF4 Null_1195	**96.6528**

Profile: *ACE2* expression
GDS5284 / 1425102_a_at
Title
Hepatocyte nuclear factor 4 alpha deficiency effect on the colon
Organism
Mus musculus

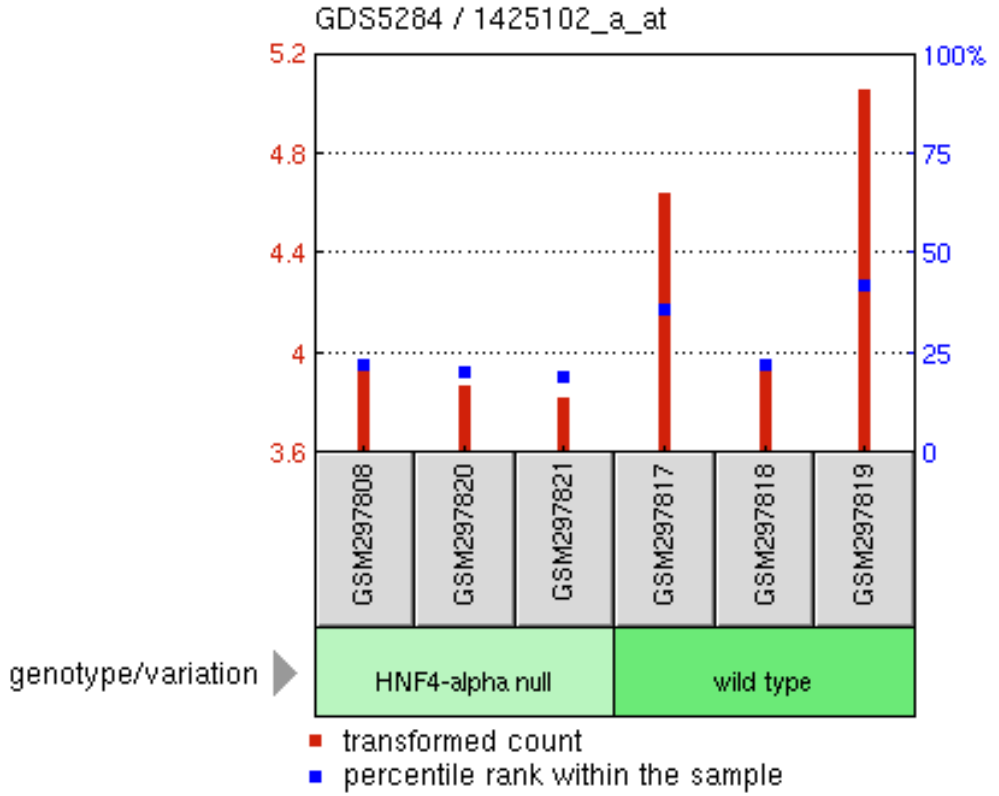

***Hnf4a* deficiency decreases *ACE2* expression in mouse cells**

Sample	Title	Value
GSM297808	mouse colon_hnf4mutant_rep1	3.94799
GSM297820	mouse colon_hnf4mutant_rep2	3.87791
GSM297821	mouse colon_hnf4mutant_rep3	3.82229
GSM297817	mouse colon_hnf4control_rep1	4.64383
GSM297818	mouse colon_hnf4control_rep2	3.9605
GSM297819	mouse colon_hnf4control_rep3	5.05635

Profile: *Hnf4a* expression
GDS3512 / 1427001_s_at
Title
Furin deficiency effect on T-cells
Organism
Mus musculus

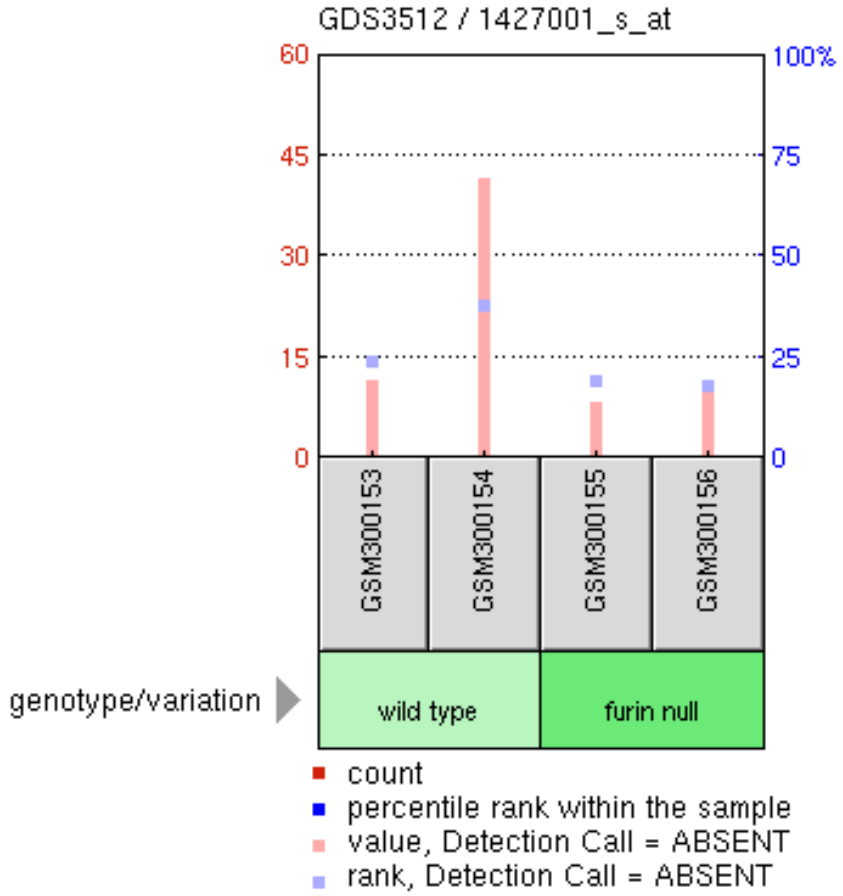

***Furin* deficiency decreases *Hnf4a* expression in murine T-cells**

Sample	Title	Value
GSM300153	Naive_Furin_Wild-type_1	11.6
GSM300154	Naive_Furin_Wild-type_2	41.8
GSM300155	Naive_Furin_Knockout_1	**8.4**
GSM300156	Naive_Furin_Knockout_2	**9.8**

Profile: *Furin* expression
GDS1916 / 1418518_at
Title
Hepatocyte nuclear factor 4 alpha knockout effect on the embryonic liver
Organism
Mus musculus

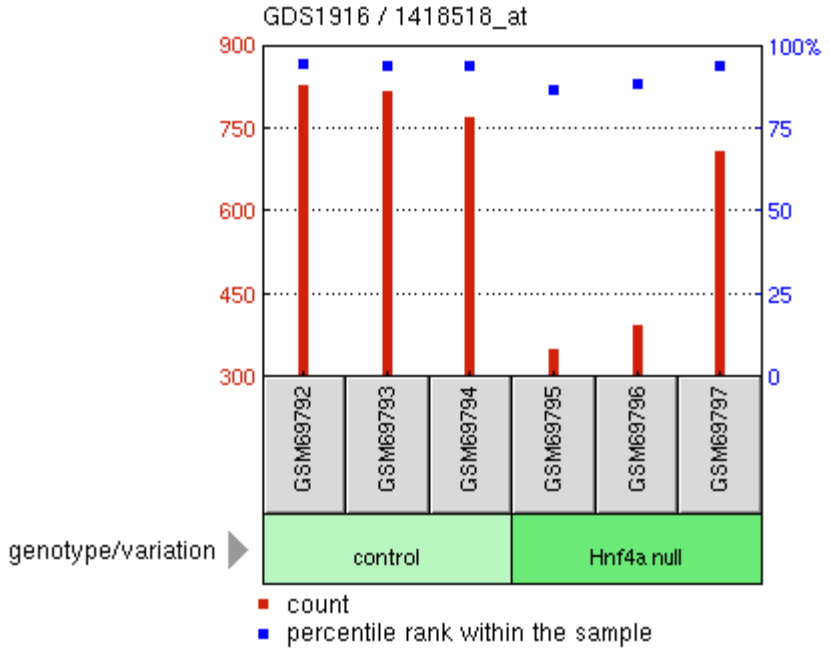

Hnf4a deficiency decreases *Furin* expression in murine cells

Sample	Title	Value
GSM69792	HNF4 Control_8	828.42
GSM69793	HNF4 Control_1192	820.313
GSM69794	HNF4 Control_1193	772.082
GSM69795	HNF4 Null_61	354.031
GSM69796	HNF4 Null_1191	396.723
GSM69797	HNF4 Null_1195	708.976

HNF4a pathway-associated activation of the *ACE2* and *FURIN* expression may trigger the auto-regulatory positive feed-back loop of the *FURIN*-mediated activation of the *HNF4a* expression

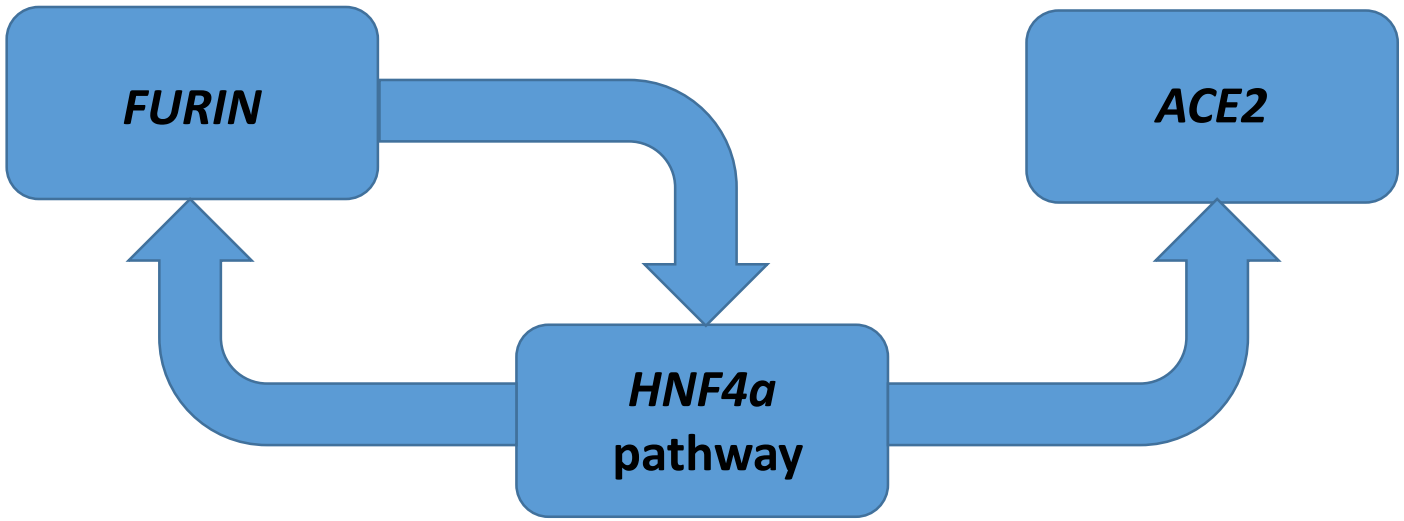

Profile: *ACE2* expression
GDS4441 / 1425103_at
Title
Runt homology domain expression effect on hematopoietic stem cells
Organism
Mus musculus

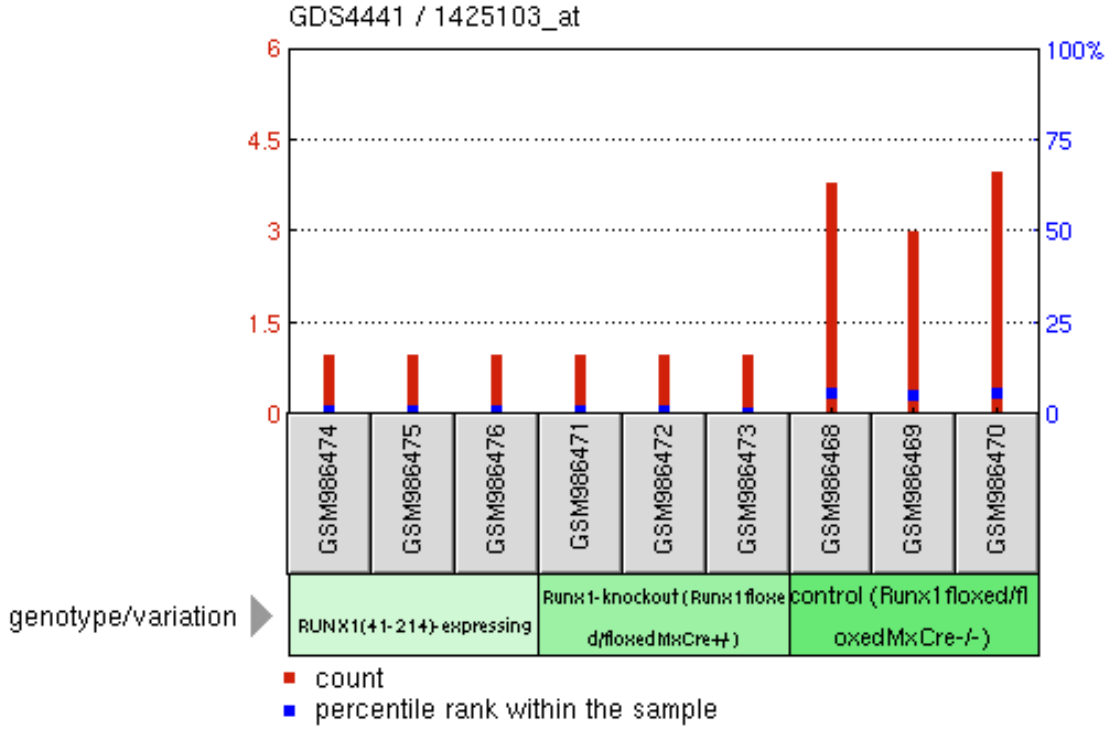

Runx1 deficiency decreases *ACE2* expression in mouse cells

Sample	Title	Value
GSM986474	RUNX1(41-214), biological replicate 1	1
GSM986475	RUNX1(41-214), biological replicate 2	1
GSM986476	RUNX1(41-214), biological replicate 3	1
GSM986471	Runx1KO, biological replicate 1	1
GSM986472	Runx1KO, biological replicate 2	1
GSM986473	Runx1KO, biological replicate 3	1
GSM986468	Control, biological replicate 1	3.83
GSM986469	Control, biological replicate 2	3
GSM986470	Control, biological replicate 3	4

Profile: *FURIN* expression
GDS5606 / 7986092
Title
Androgen effect on runt-related transcription factor 1-deficient prostate cancer cell line
Organism
Homo sapiens

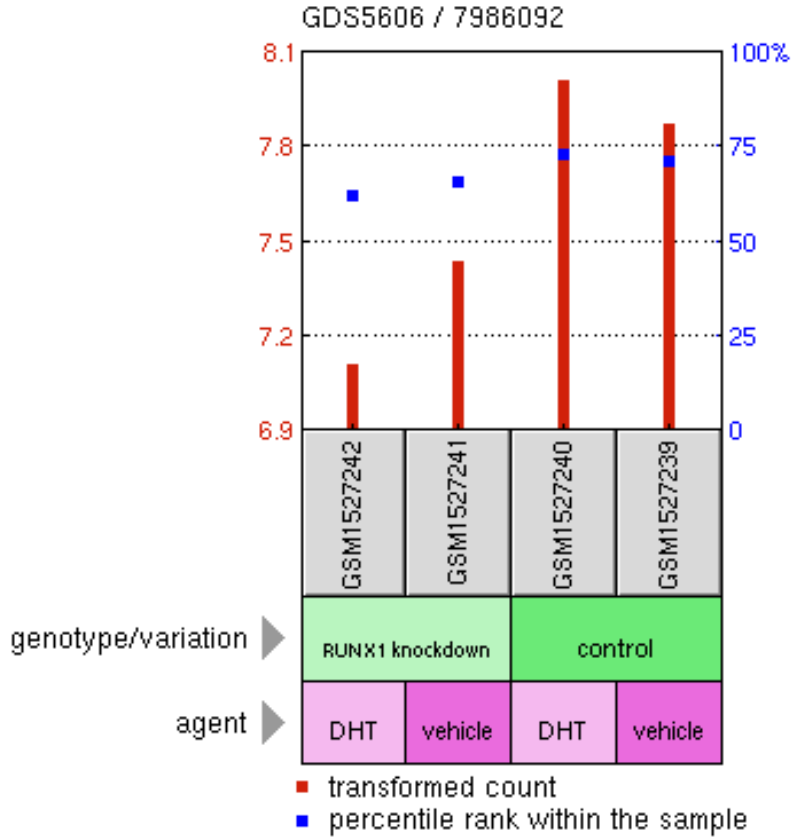

RUNX1 deficiency decreases *FURIN* expression in human cells

Sample	Title	Value
GSM1527242	LNCaP_siRUNX1_DHT	**7.11175**
GSM1527241	LNCaP_siRUNX1_Veh	**7.43782**
GSM1527240	LNCaP_siControl_DHT	8.00649
GSM1527239	LNCaP_siControl_Veh	7.87368

Profile: *Runx1* expression
GDS3512 / 1427847_at
Title
Furin deficiency effect on T-cells
Organism
Mus musculus

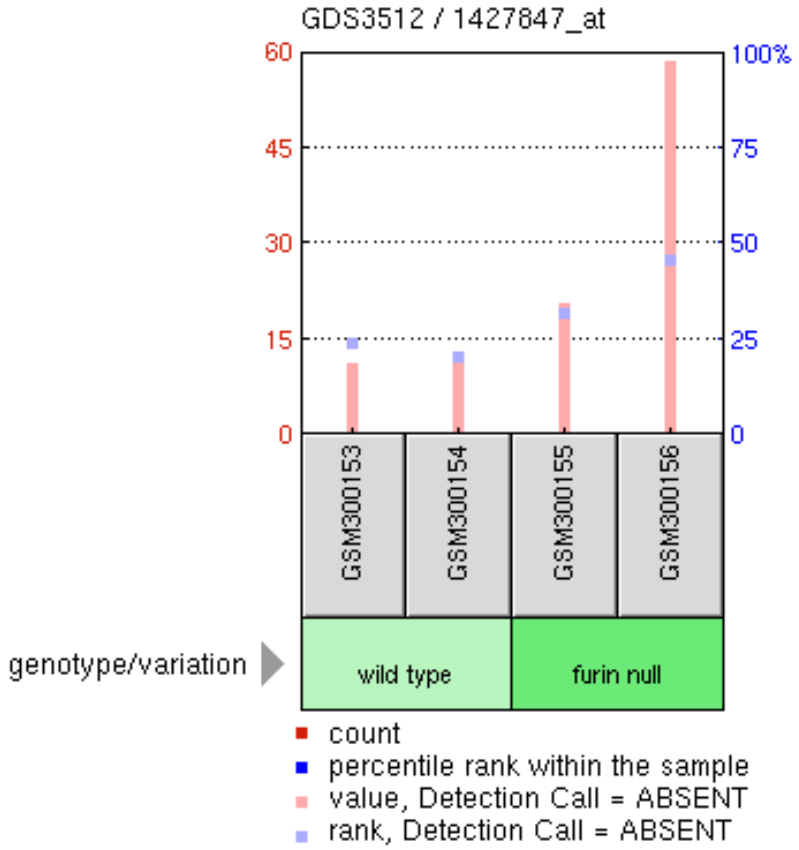

Furin deficiency enhances *Runx1* expression in murine T-cells

Sample	Title	Value
GSM300153	Naive_Furin_Wild-type_1	11.5
GSM300154	Naive_Furin_Wild-type_2	12.5
GSM300155	Naive_Furin_Knockout_1	**20.9**
GSM300156	Naive_Furin_Knockout_2	**58.7**

Profile: *Foxa1* expression
GDS3512 / 1418496_at
Title
Furin deficiency effect on T-cells
Organism
Mus musculus

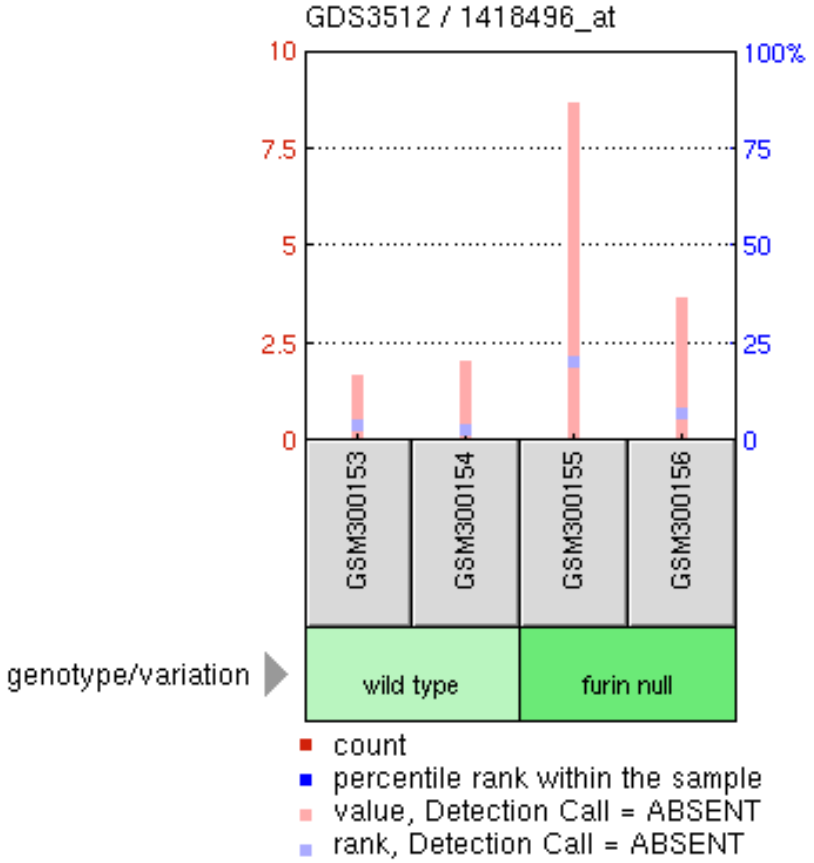

Furin deficiency enhances *Foxa1* expression in murine T-cells

Sample	Title	Value
GSM300153	Naive_Furin_Wild-type_1	1.7
GSM300154	Naive_Furin_Wild-type_2	2.1
GSM300155	Naive_Furin_Knockout_1	**8.7**
GSM300156	Naive_Furin_Knockout_2	**3.7**

RUNX1 pathway-associated activation of the *ACE2* and *FURIN* expression may trigger the auto-regulatory negative feed-back loop of the *FURIN*-mediated repression of the *RUNX1* gene expression

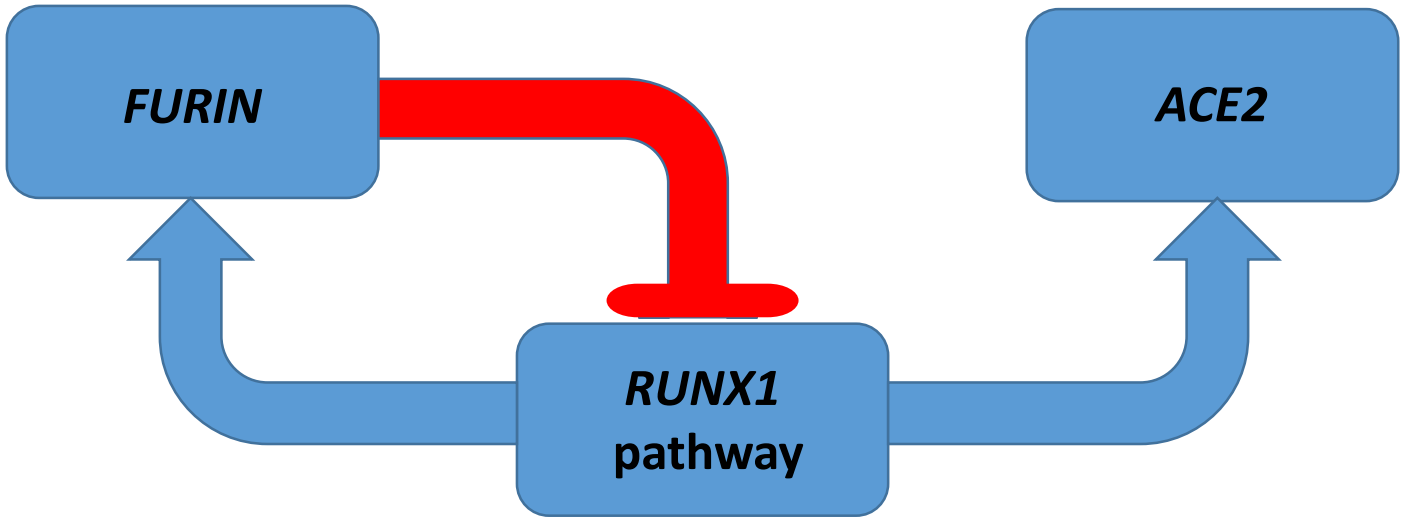

ACE2 and FURIN

Supplemental Figure S7. Potential mechanisms affecting gene expression: Putative inhibitory role of the *VDR* gene and Vitamin D

ARCHS4 TFs Co-expression

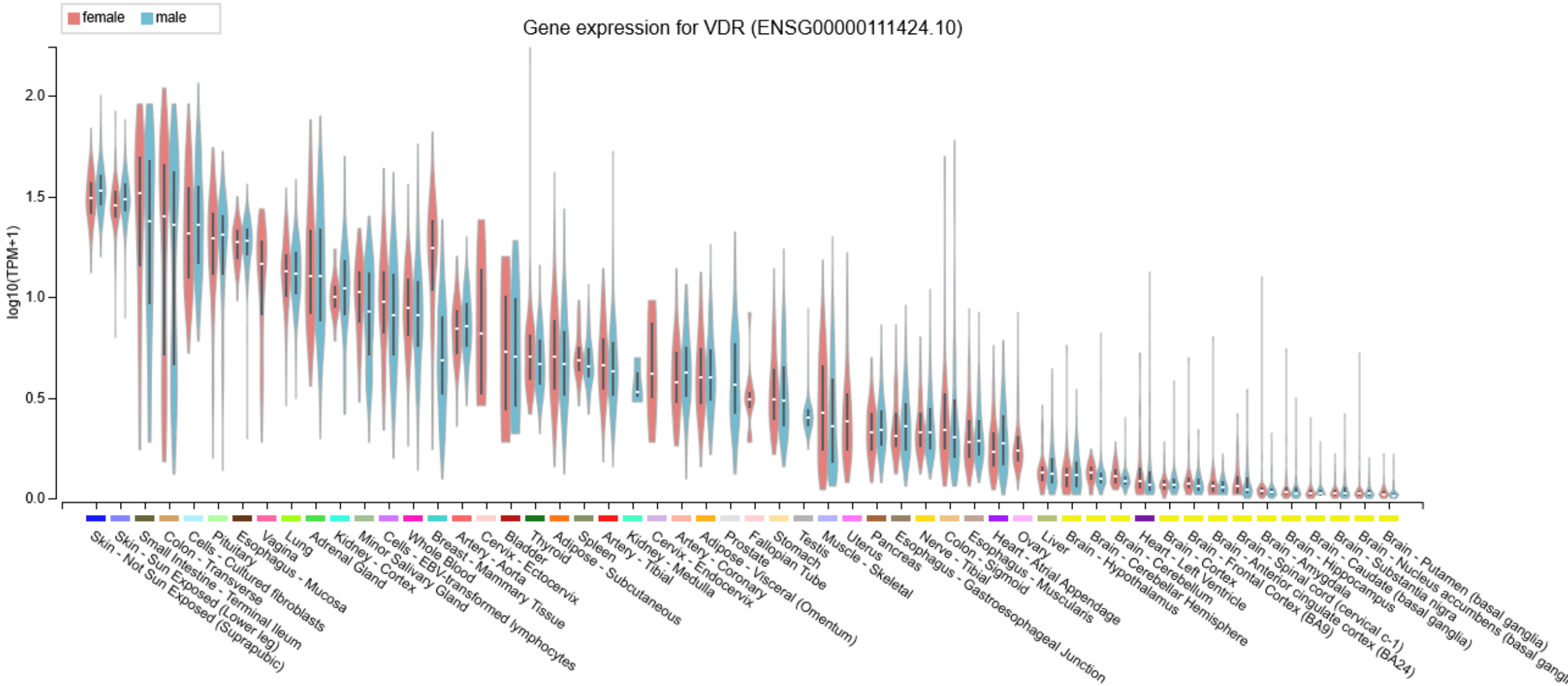
female
male
Gene expression for VDR (ENSG00000111424.10)
log10(TPM+1)
2.0
1.5
1.0
0.5
0.0
Skin - Not Sun Exposed (Suprapubic)
Skin - Sun Exposed (Lower leg)
Small Intestine - Terminal Ileum
Colon - Transverse
Cells - Cultured fibroblasts
Pituitary
Esophagus - Mucosa
Vagina
Lung
Adrenal Gland
Kidney - Cortex
Minor Salivary Gland
Cells - EBV-transformed lymphocytes
Whole Blood
Breast - Mammary Tissue
Artery - Aorta
Cervix - Ectocervix
Bladder
Thyroid
Adipose - Subcutaneous
Spleen
Artery - Tibial
Kidney - Medulla
Cervix - Endocervix
Artery - Coronary
Adipose - Visceral (Omentum)
Prostate
Fallopian Tube
Stomach
Testis
Muscle - Skeletal
Uterus
Pancreas
Esophagus - Gastroesophageal Junction
Nerve - Tibial
Colon - Sigmoid
Esophagus - Muscularis
Heart - Atrial Appendage
Ovary
Liver
Brain - Hypothalamus
Brain - Cerebellar Hemisphere
Brain - Cerebellum
Heart - Left Ventricle
Brain - Cortex
Brain - Frontal Cortex (BA9)
Brain - Anterior cingulate cortex (BA24)
Brain - Spinal cord (cervical c-1)
Brain - Amygdala
Brain - Hippocampus
Brain - Caudate (basal ganglia)
Brain - Substantia nigra
Brain - Nucleus accumbens (basal ganglia)
Brain - Putamen (basal ganglia)

ACE2 and FURIN

Supplemental Figure S7-1. Potential mechanisms affecting gene expression: Putative inhibitory role of the *VDR* gene and Vitamin D revealed by gene expression profiles in the GEO data sets

Profile: *ACE2* expression
GDS1389 / 1425103_at
Title
1alpha,25-dihydroxyvitamin D3 suppressive effect on IFN-gamma activated macrophages
Organism
Mus musculus

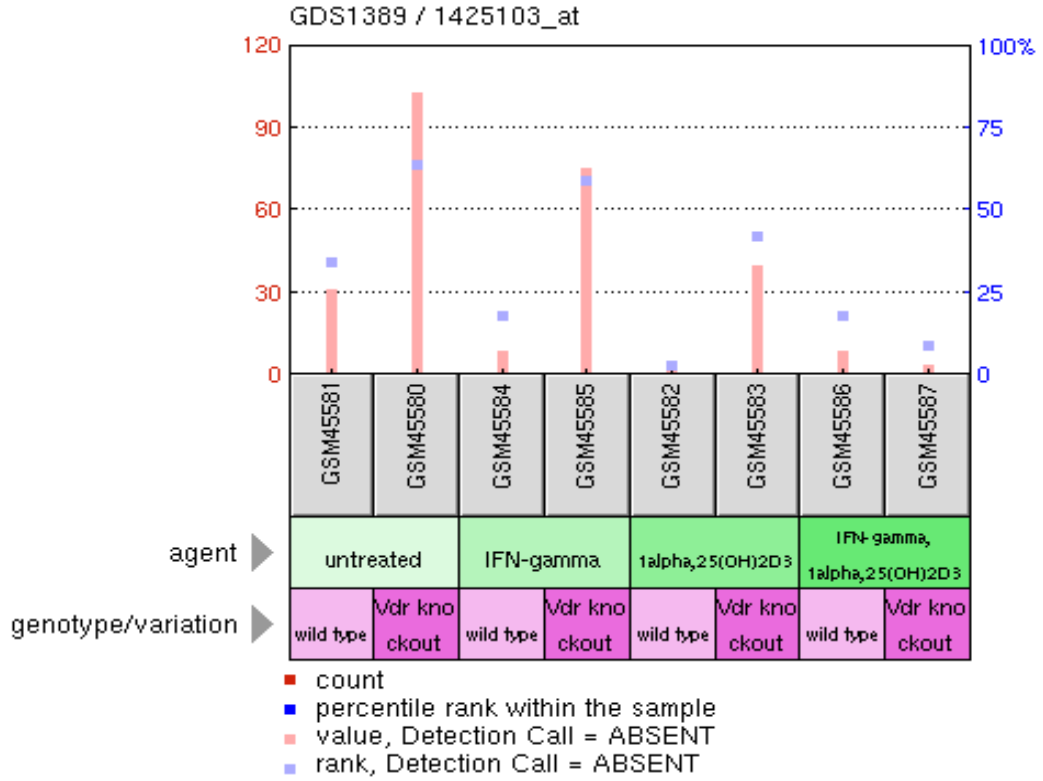

VDR depletion increases *ACE2* expression

Sample	Title	Value
GSM45581	0-WT	31.4
GSM45580	0-KO	**102.7**
GSM45584	IFN-WT	9.1
GSM45585	IFN-KO	**75.7**
GSM45582	Vit-WT	3.8
GSM45583	Vit-KO	**40.2**
GSM45586	IFN/Vit-WT	9
GSM45587	IFN/Vit-KO	4.1

VDR: a candidate inhibitor of the *ACE2* expression

GEO profile	GDS1389 / 1452138_a_at	GDS1389 / 1452138_a_at	GDS1389 / 1425103_at	GDS1389 / 1425103_at
Sample	GSM45581	GSM45580	GSM45581	GSM45580
Genotype	VDR-WT	VDR-KO	VDR-WT	VDR-KO
Expression value	27.4	59.8	31.4	102.7

GEO Profile: *ACE2* expression
GDS1389 / 1425103_at & 1452138_a_at
Title
1alpha,25-dihydroxyvitamin D3 suppressive effect on IFN-gamma activated macrophages
Organism
Mus musculus

Profile: *ACE2* expression
GDS2628 / 219962_at
Title
Vitamin D effect on bronchial smooth muscle cells
Organism
Homo sapiens

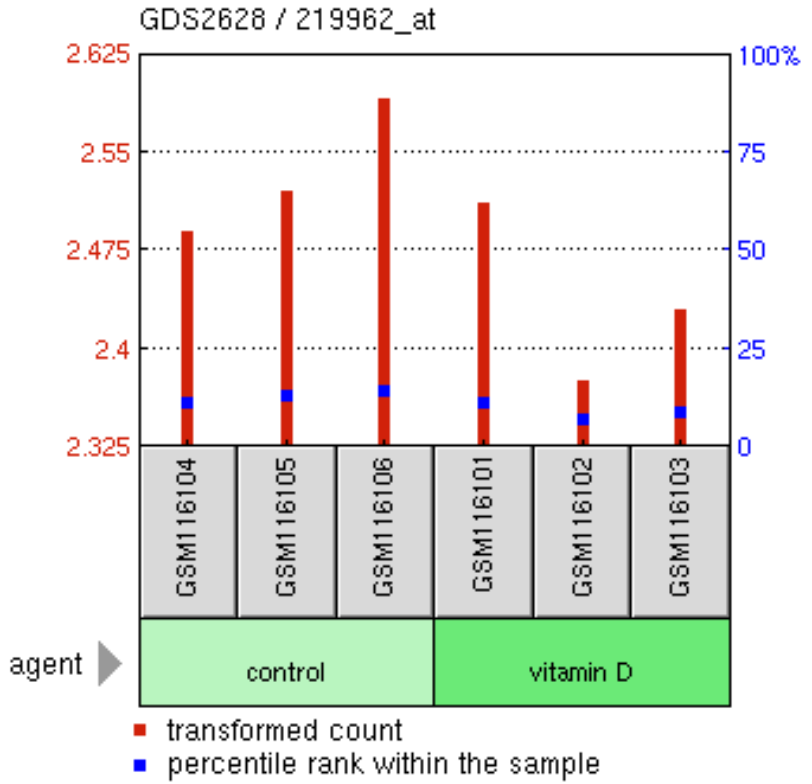

p = 0.064

Vitamin D effect on *ACE2* expression

Sample	Title	Value
GSM116104	hBSMC_control_rep1	2.49036
GSM116105	hBSMC_control_rep2	2.52156
GSM116106	hBSMC_control_rep3	2.59211
GSM116101	hBSMC_vitamin D_rep1	2.51261
GSM116102	hBSMC_vitamin D_rep2	2.37673
GSM116103	hBSMC_vitamin D_rep3	2.43005

Direct and reciprocal effects of the *VDR* gene and Vitamin D administration on expression of the *JNK1/c-FOS* pathway genes

Profile: *VDR* expression
GDS1621 / J04147_at
Title
c-Jun N-terminal kinase pathway activation and suppression effect on aortic vascular smooth muscle cells
Organism
Rattus norvegicus

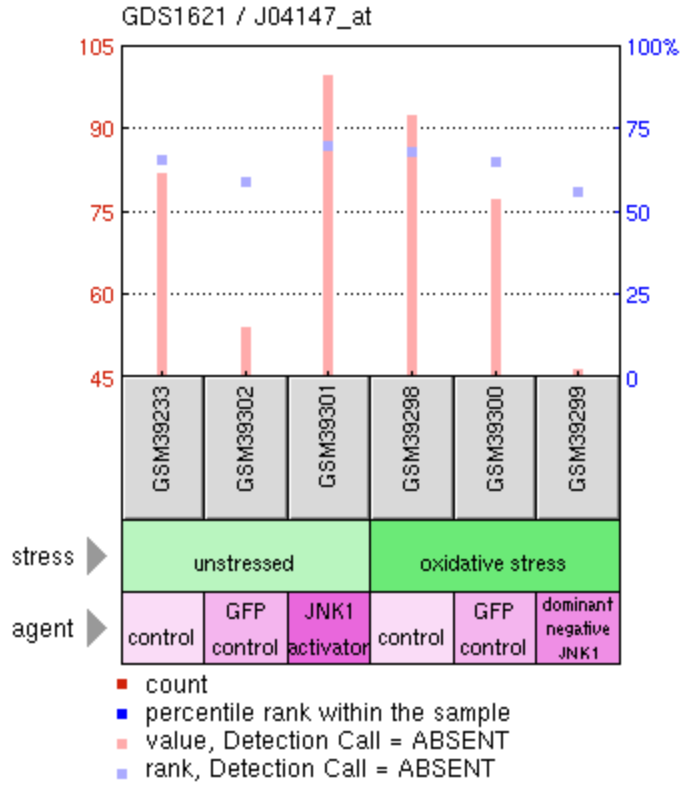

***JNK1 pathway* inhibition is associated with decreased *VDR* expression, while *JNK1* activation is associated with increased *VDR* expression**

Sample	Title	Value
GSM39233	rVSMC_control	82
GSM39302	rVSMC_nEGFP	54.3
GSM39301	rVSMC_MKK7ED+JNK1WT	99.8
GSM39298	rVSMC_H2O2	92.7
GSM39300	rVSMC_H2O2+nEGFP	77.3
GSM39299	rVSMC_H2O2+APF	45.7

Profile: *c-JUN* expression
GDS2628 / 201464_x_at
Title
Vitamin D effect on bronchial smooth muscle cells
Organism
Homo sapiens

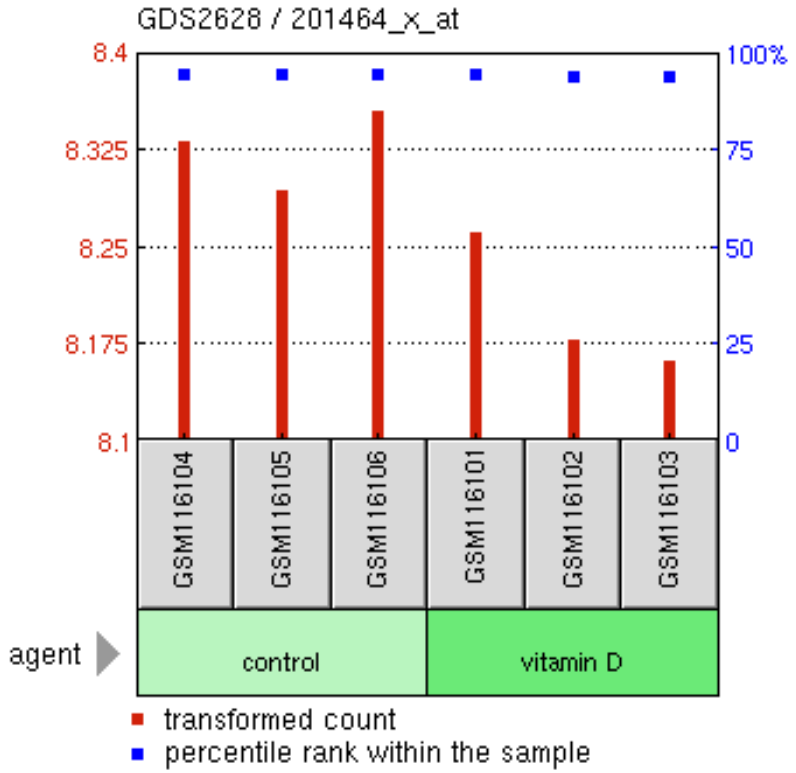

Vitamin D inhibits *c-JUN* expression

Sample	Title	Value
GSM116104	hBSMC_control_rep1	8.33308
GSM116105	hBSMC_control_rep2	8.29401
GSM116106	hBSMC_control_rep3	8.35545
GSM116101	hBSMC_vitamin D_rep1	8.26197
GSM116102	hBSMC_vitamin D_rep2	8.17801
GSM116103	hBSMC_vitamin D_rep3	8.16188

Profile: *c-FOS* expression
GDS2628 / 209189_at
Title
Vitamin D effect on bronchial smooth muscle cells
Organism
Homo sapiens

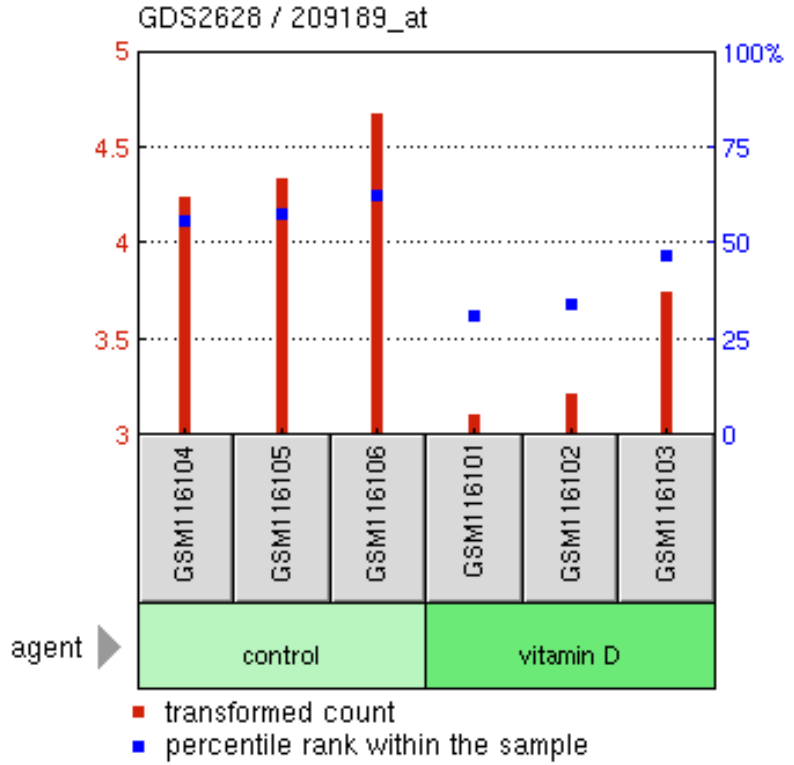

Vitamin D inhibits *c-FOS* expression

Sample	Title	Value
GSM116104	hBSMC_control_rep1	4.24348
GSM116105	hBSMC_control_rep2	4.34194
GSM116106	hBSMC_control_rep3	4.67701
GSM116101	hBSMC_vitamin D_rep1	3.11013
GSM116102	hBSMC_vitamin D_rep2	3.21701
GSM116103	hBSMC_vitamin D_rep3	3.75394

Profile: *VDR* expression
GDS766 / 99964_at
Title
Osteoclastogenesis regulation by c-Fos and Nfat
Organism
Mus musculus

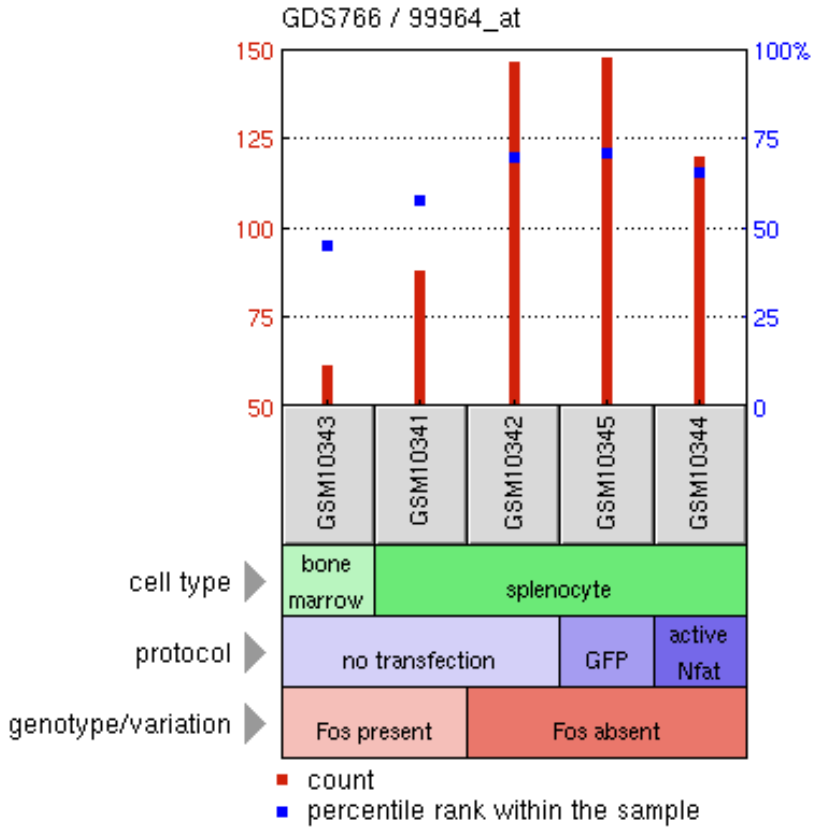

c-Fos inhibits *Vdr* expression

Sample	Title	Value
GSM10343	Fos+/+ bone-marrow	61.7
GSM10341	Fos+/+ splenocytes	88
GSM10342	Fos-/- splenocytes	146.8
GSM10345	Fos-/- splenocytes expressing GFP	147.6
GSM10344	Fos-/- splenocytes expressing deltaNFAT	120.3

JNK1/c-FOS pathway-associated activation of the *ACE2* and *FURIN* expression may trigger the auto-regulatory negative feed-back loop of the FURIN-mediated repression of the expression of *JUN, JUNB, JUND,* and *c-FOS* genes

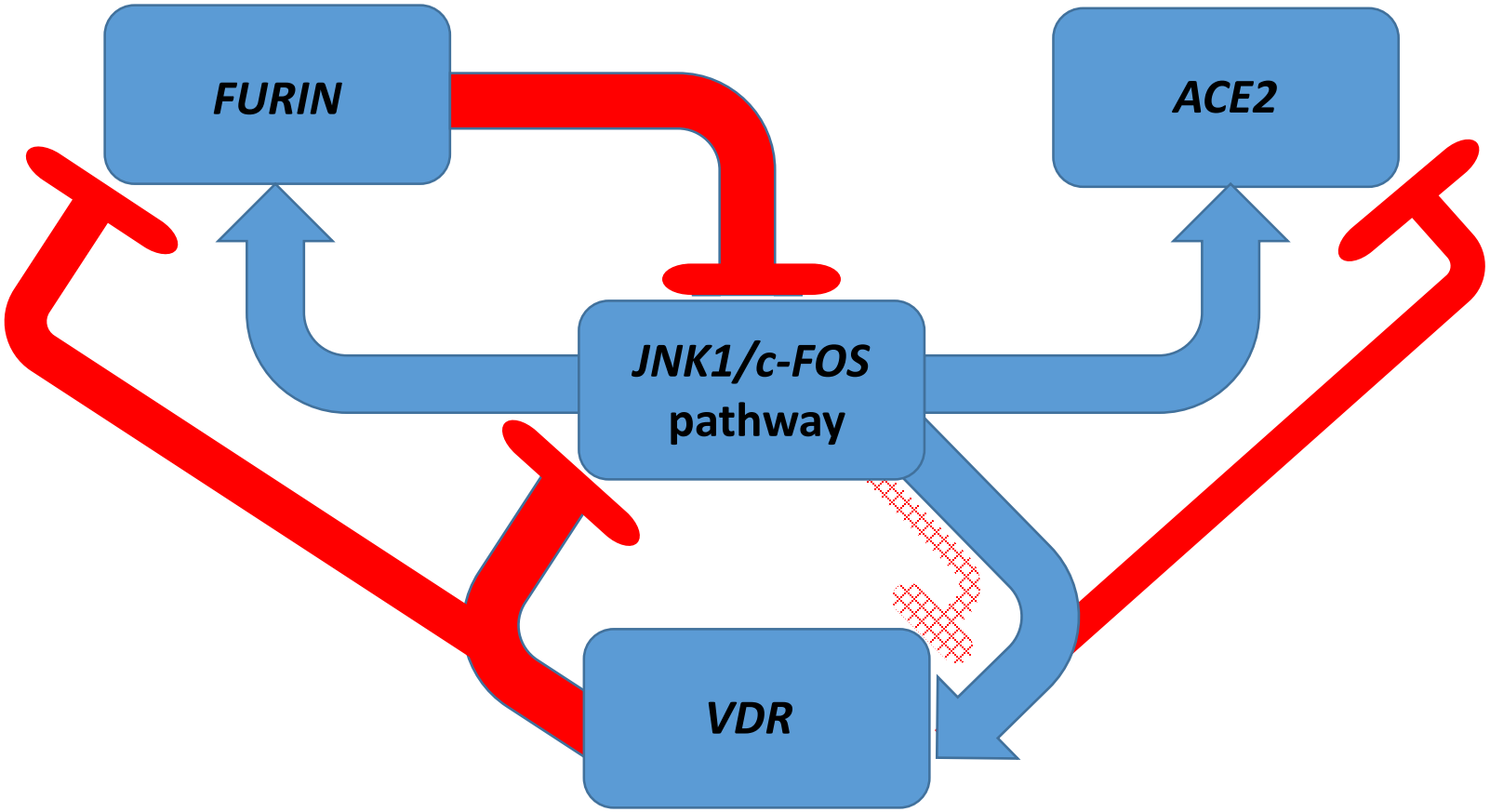

Direct and reciprocal effects of the *VDR* gene and Vitamin D administration on expression of the *HF4a* gene

Profile: *VDR* expression
GDS4798 / 213692_s_at
Title
Hepatocyte nuclear factor 4 alpha depletion effect on hepatocellular carcinoma cell line
Organism
Homo sapiens

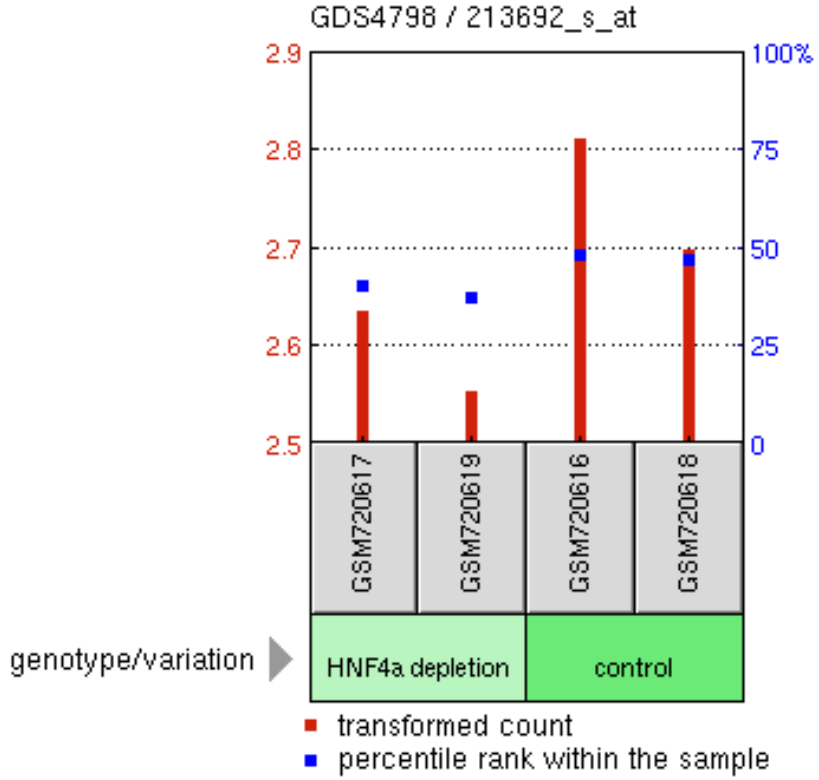

HNF4a depletion inhibits *VDR* expression

Sample	Title	Value
GSM720617	HepG2 cells, HNF4a RNAi treated, rep1	2.63638
GSM720619	HepG2 cells, HNF4a RNAi treated, rep2	2.5545
GSM720616	HepG2 cells, control, rep1	2.81268
GSM720618	HepG2 cells, control, rep2	2.69839

Profile: *VDR* expression
GDS5284 / 1418175_at
Title
Hepatocyte nuclear factor 4 alpha deficiency effect on the colon
Organism
Mus musculus

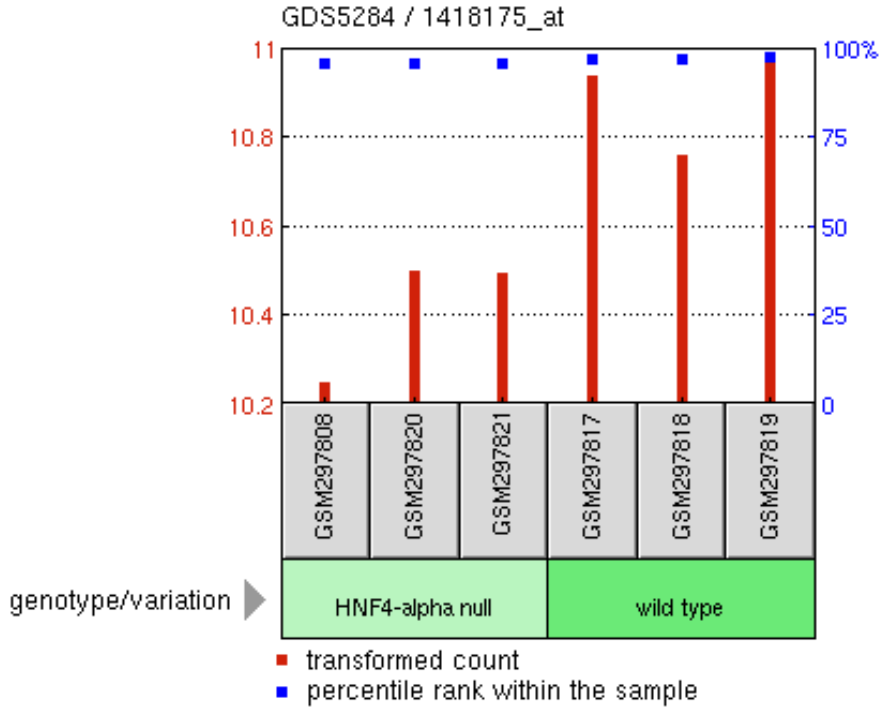

HNF4a depletion inhibits *VDR* expression

Sample	Title	Value
GSM297808	mouse colon_hnf4mutant_rep1	10.2483
GSM297820	mouse colon_hnf4mutant_rep2	10.4994
GSM297821	mouse colon_hnf4mutant_rep3	10.4987
GSM297817	mouse colon_hnf4control_rep1	10.9398
GSM297818	mouse colon_hnf4control_rep2	10.7599
GSM297819	mouse colon_hnf4control_rep3	10.9741

Profile: *HNF4a* expression
GDS1389 / 1450447_at
Title
1alpha,25-dihydroxyvitamin D3 suppressive effect on IFN-gamma activated macrophages
Organism
Mus musculus

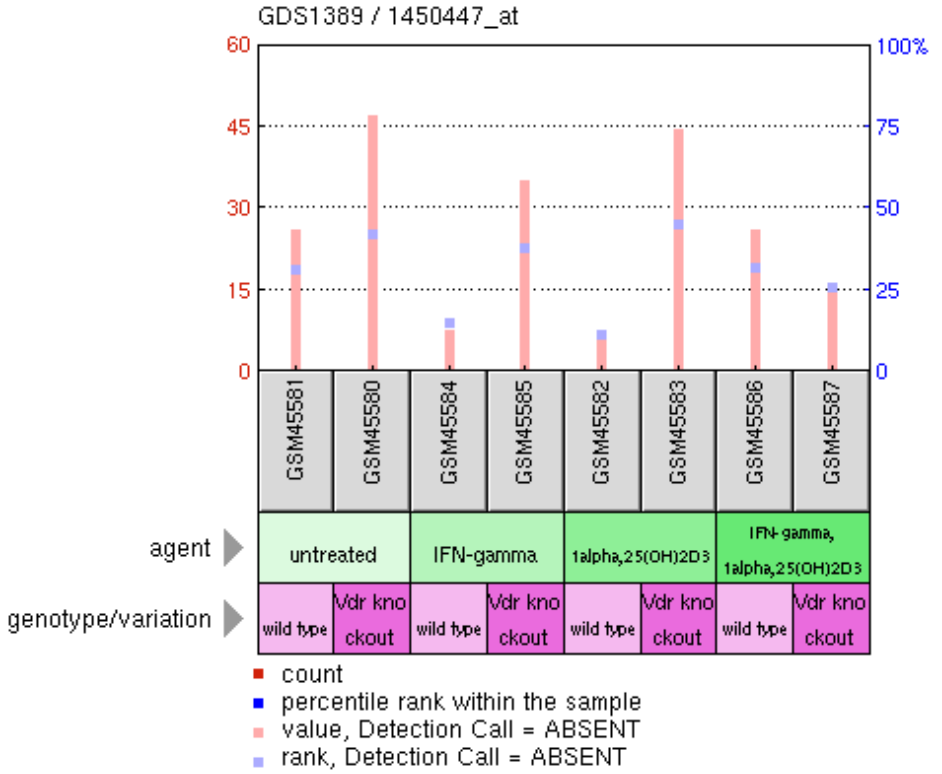

VDR depletion increases *HNF4a* expression

Sample	Title	Value
GSM45581	0-WT	26.1
GSM45580	0-KO	47.2
GSM45584	IFN-WT	7.8
GSM45585	IFN-KO	35.4
GSM45582	Vit-WT	6.9
GSM45583	Vit-KO	44.6
GSM45586	IFN/Vit-WT	26.2
GSM45587	IFN/Vit-KO	15.1

HNF4a pathway-associated activation of the *ACE2* and *FURIN* expression may trigger the auto-regulatory positive feed-back loop of the *FURIN*-mediated activation of the *HNF4a* expression

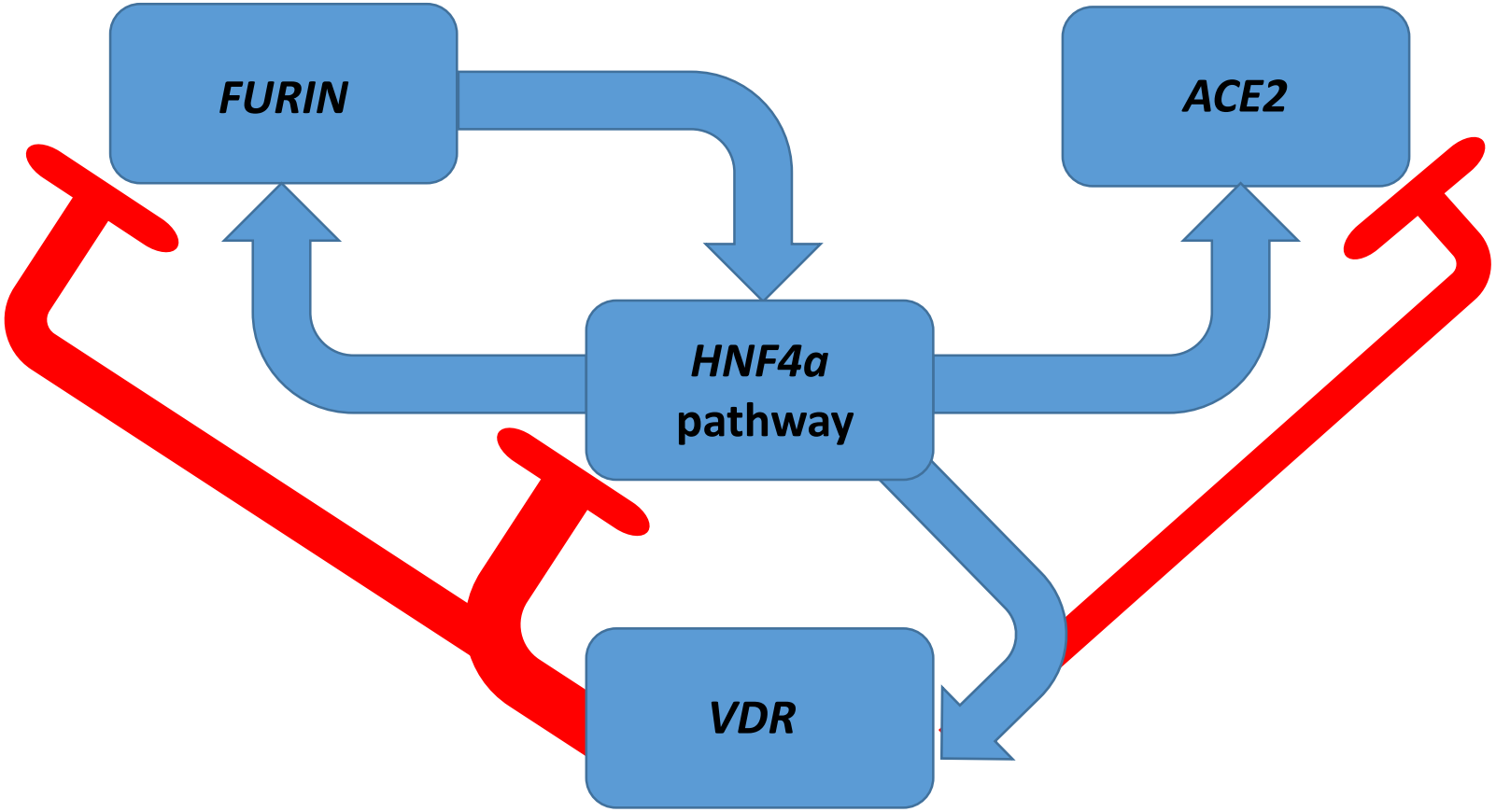

ACE2 and FURIN

Supplemental Figure S8. Potential mechanisms affecting gene expression: *HIF1A* gene product as potential repressor of the *ACE2* expression

Predominantly distinct transcription factors affect expression of the ACE2 and FURIN genes

TF Perturbations Followed by Expression

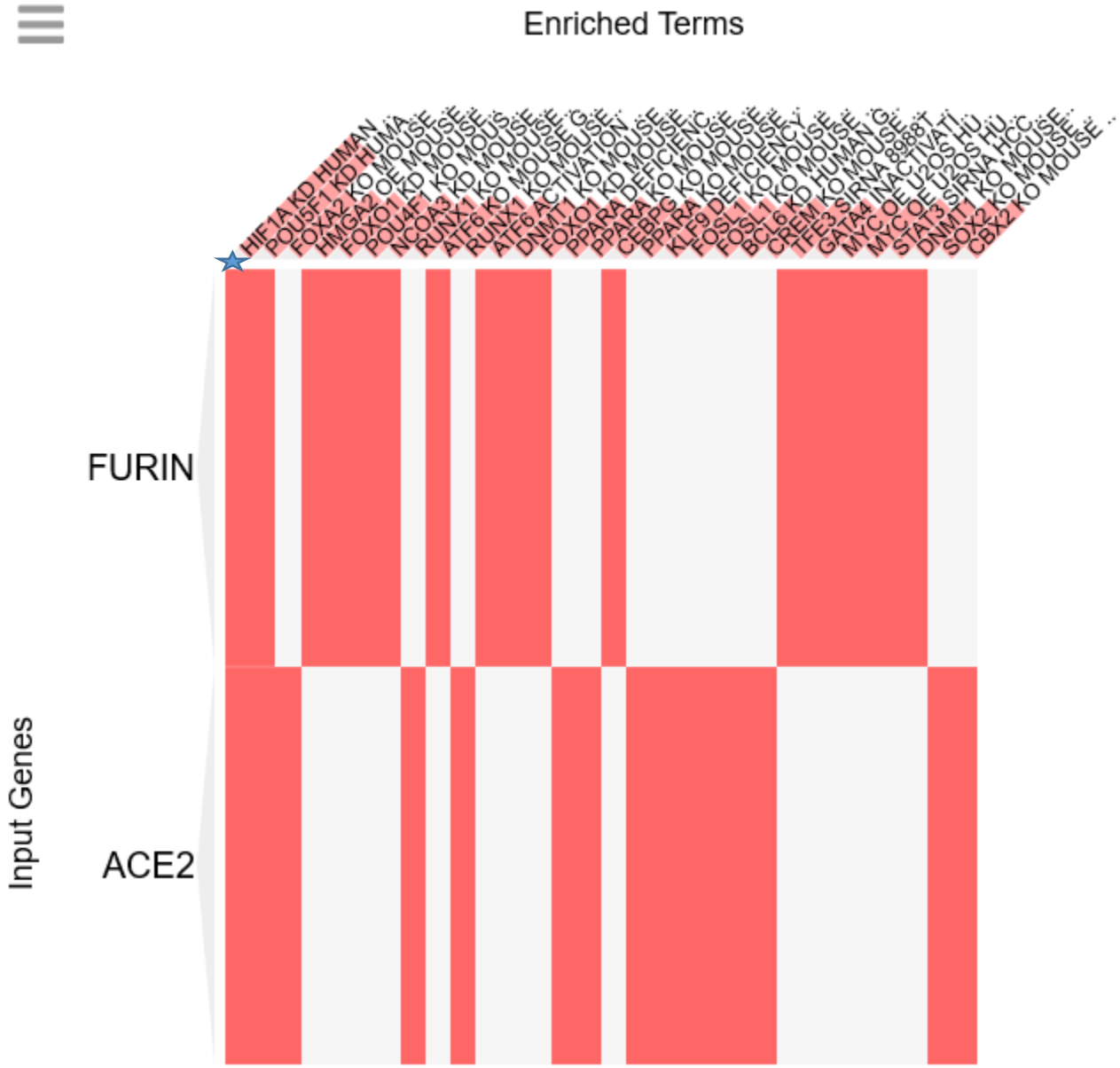

HIF1A and POU5F1: candidate inhibitors of the *ACE2* and *FURIN* expression

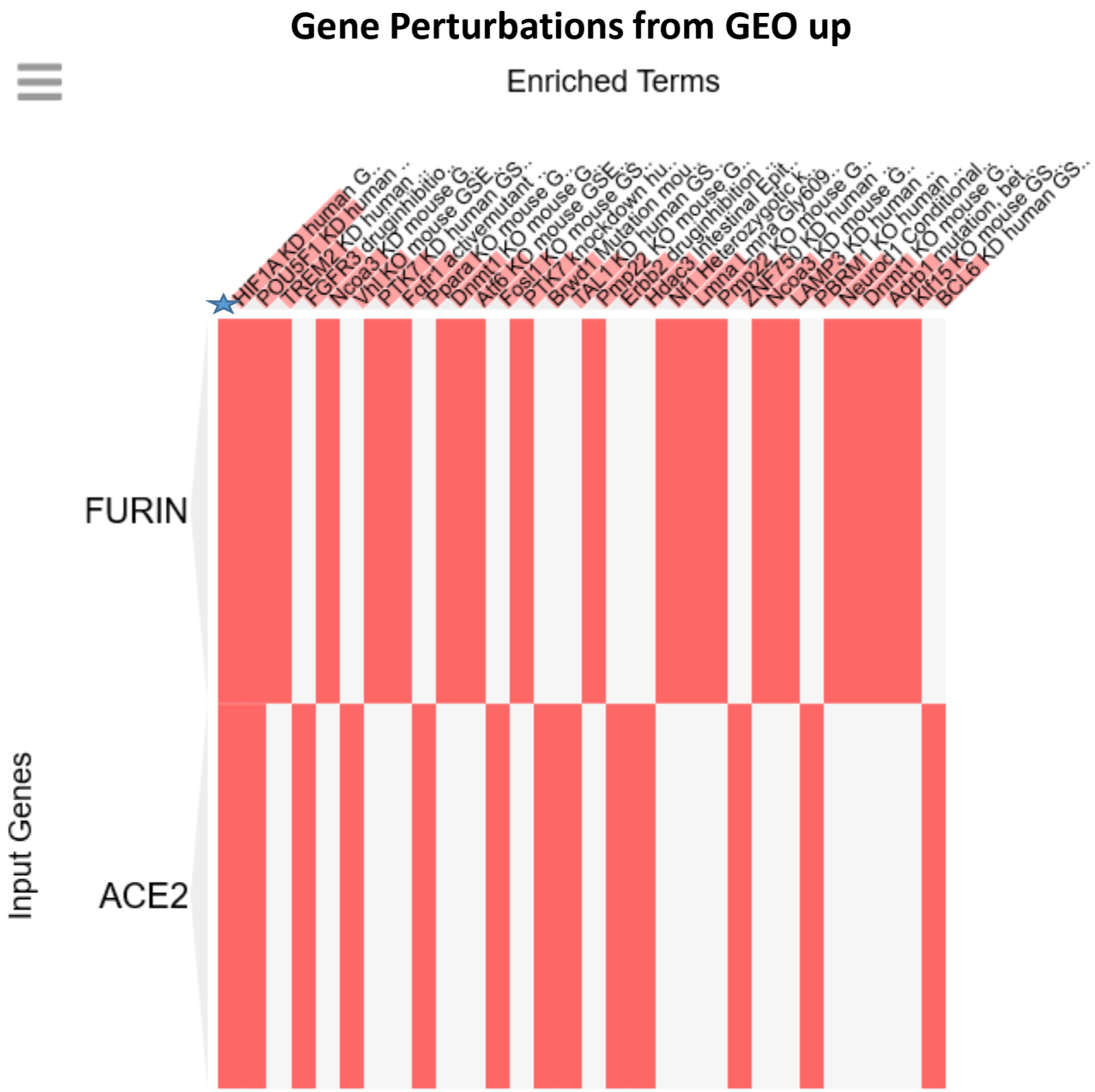

Profile: *ACE2* expression
GDS2018 / 1181882_1
Title
Hypoxia-inducible factors-1 and -2 overexpression effect on embryonic kidney cells
Organism
Homo sapiens

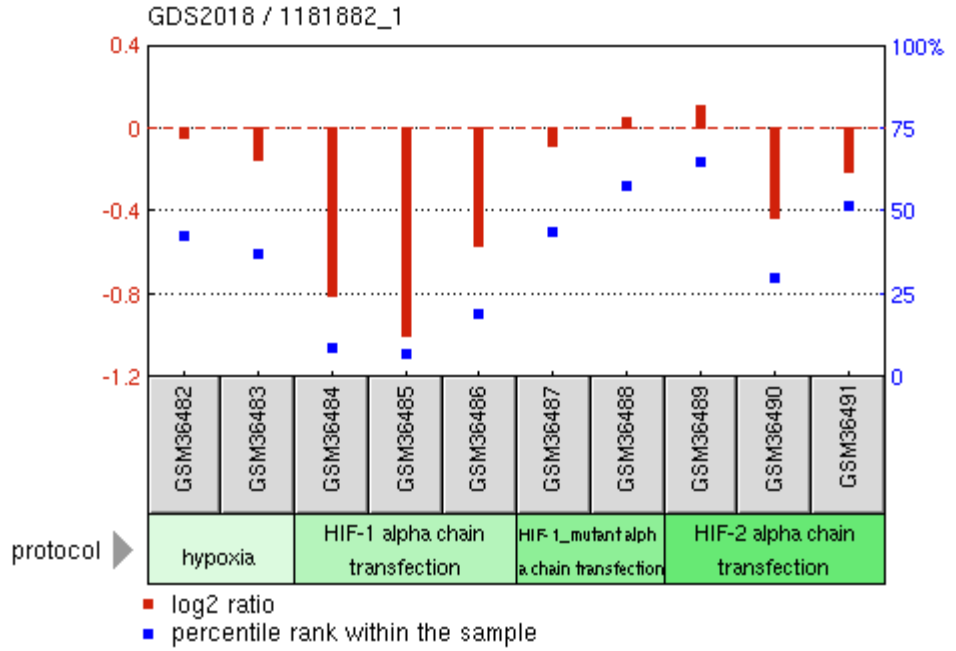

HIF1a inhibits the ACE2 expression

Sample	Title	Value
GSM36482	Nor:Hypo rep 1	-0.062
GSM36483	Nor:Hypo rep 2	-0.161
GSM36484	Nor:HIF1a rep 1	**-0.821**
GSM36485	Nor:HIF1a rep 2	**-1.013**
GSM36486	Nor:HIF1a rep 3	**-0.575**
GSM36487	Nor:HIF1amut rep 1	-0.098
GSM36488	Nor:HIF1amut rep 2	0.061
GSM36489	Nor:HIF2a rep 1	**0.115**
GSM36490	Nor:HIF2a rep 2	**-0.44**
GSM36491	Nor:HIF2a rep 3	**-0.222**

p = 0.011

p = 0.007

p = 0.021

Profile: *HIF1a* expression
GDS2628 / 200989_at
Title
Vitamin D effect on bronchial smooth muscle cells
Organism
Homo sapiens

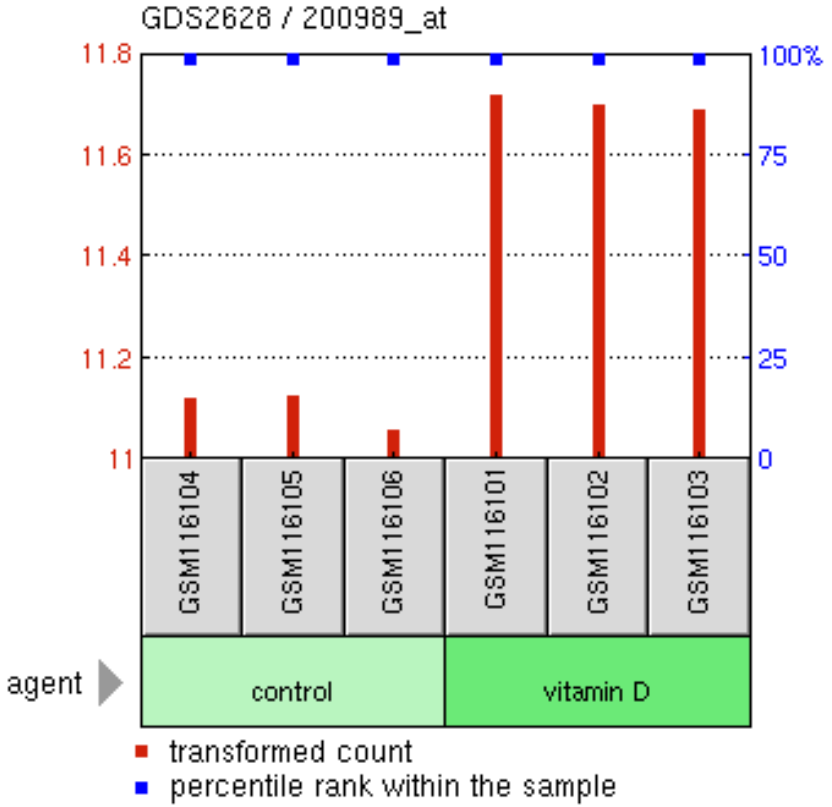

p = 0.0002

Vitamin D enhances the *HIF1a* expression

Sample	Title	Value
GSM116104	hBSMC_control_rep1	11.1243
GSM116105	hBSMC_control_rep2	11.1271
GSM116106	hBSMC_control_rep3	11.0608
GSM116101	hBSMC_vitamin D_rep1	**11.7223**
GSM116102	hBSMC_vitamin D_rep2	**11.7034**
GSM116103	hBSMC_vitamin D_rep3	**11.6893**

Supplemental Figure S9. GSEA identify Estradiol and Quercetin as potential candidate coronavirus infection mitigation agents

Distinct patterns of drugs down-regulating expression of the *ACE2* and *FURIN* genes:

Estradiol and Quercetin emerged as promising candidate coronavirus infection mitigation agents

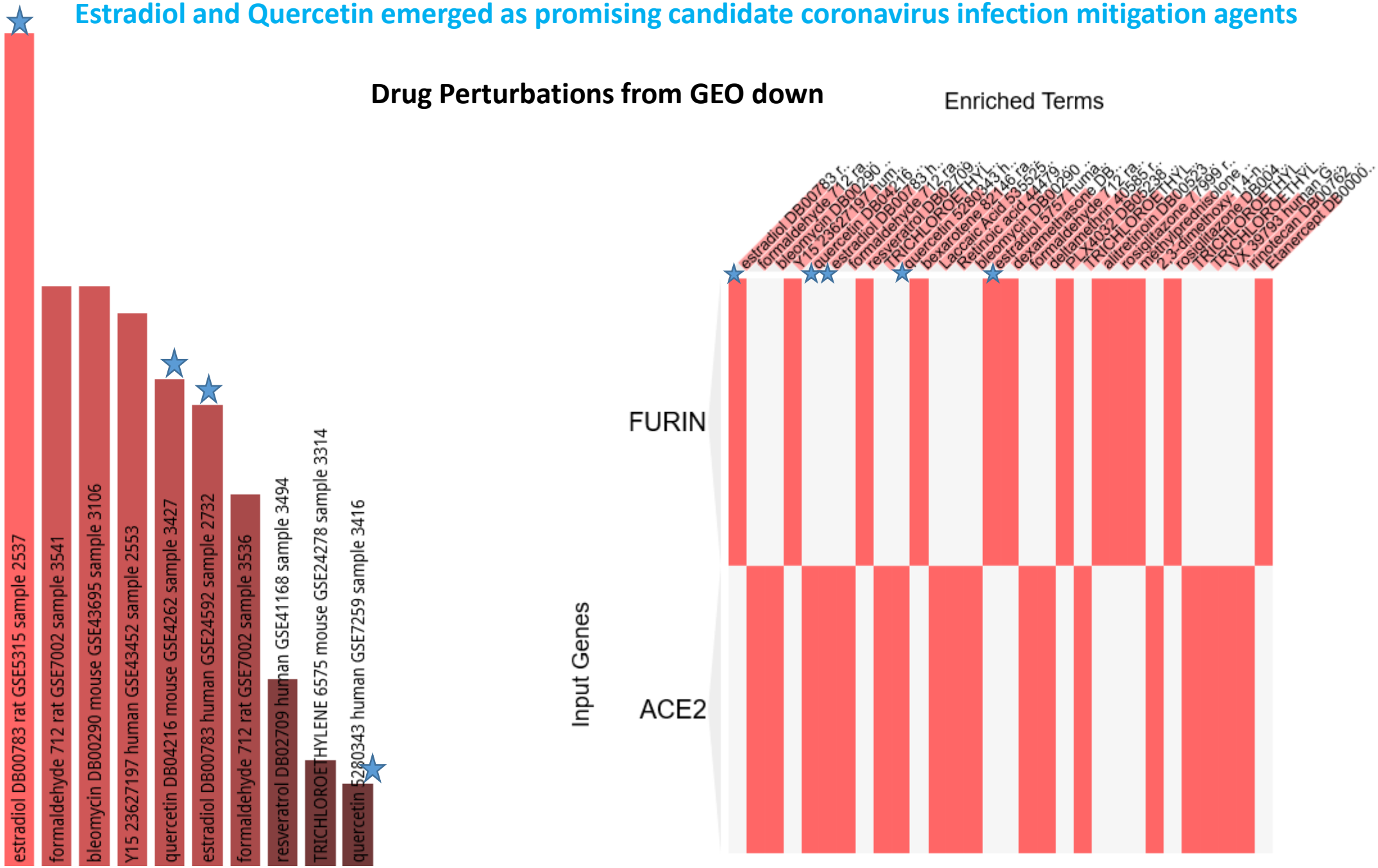

Distinct patterns of ligands down-regulating expression of the *ACE2* and *FURIN* genes

Ligand Perturbations from GEO down

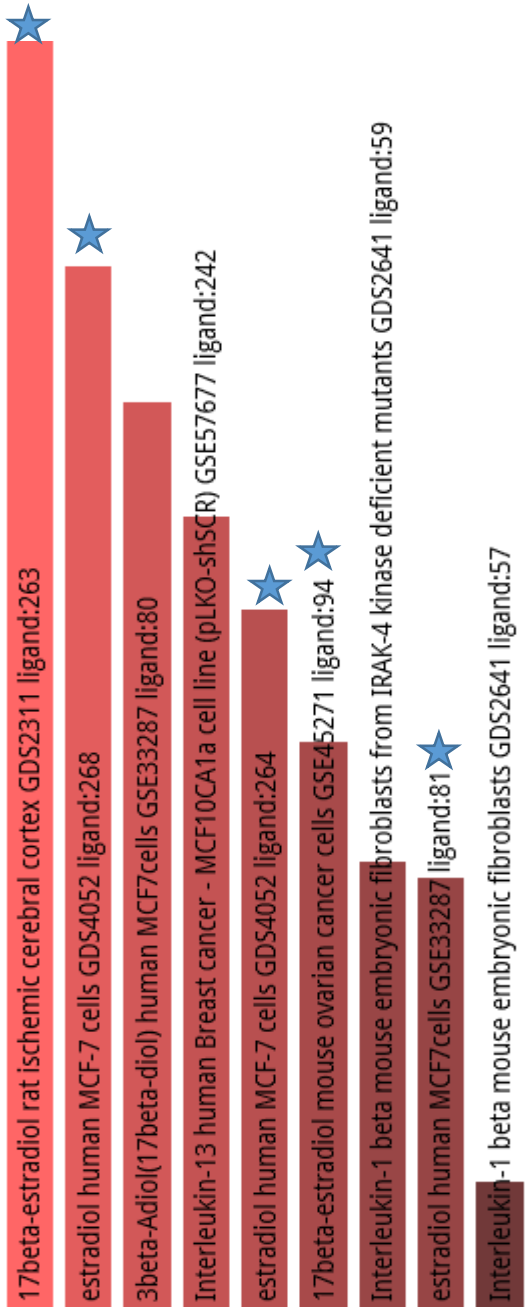

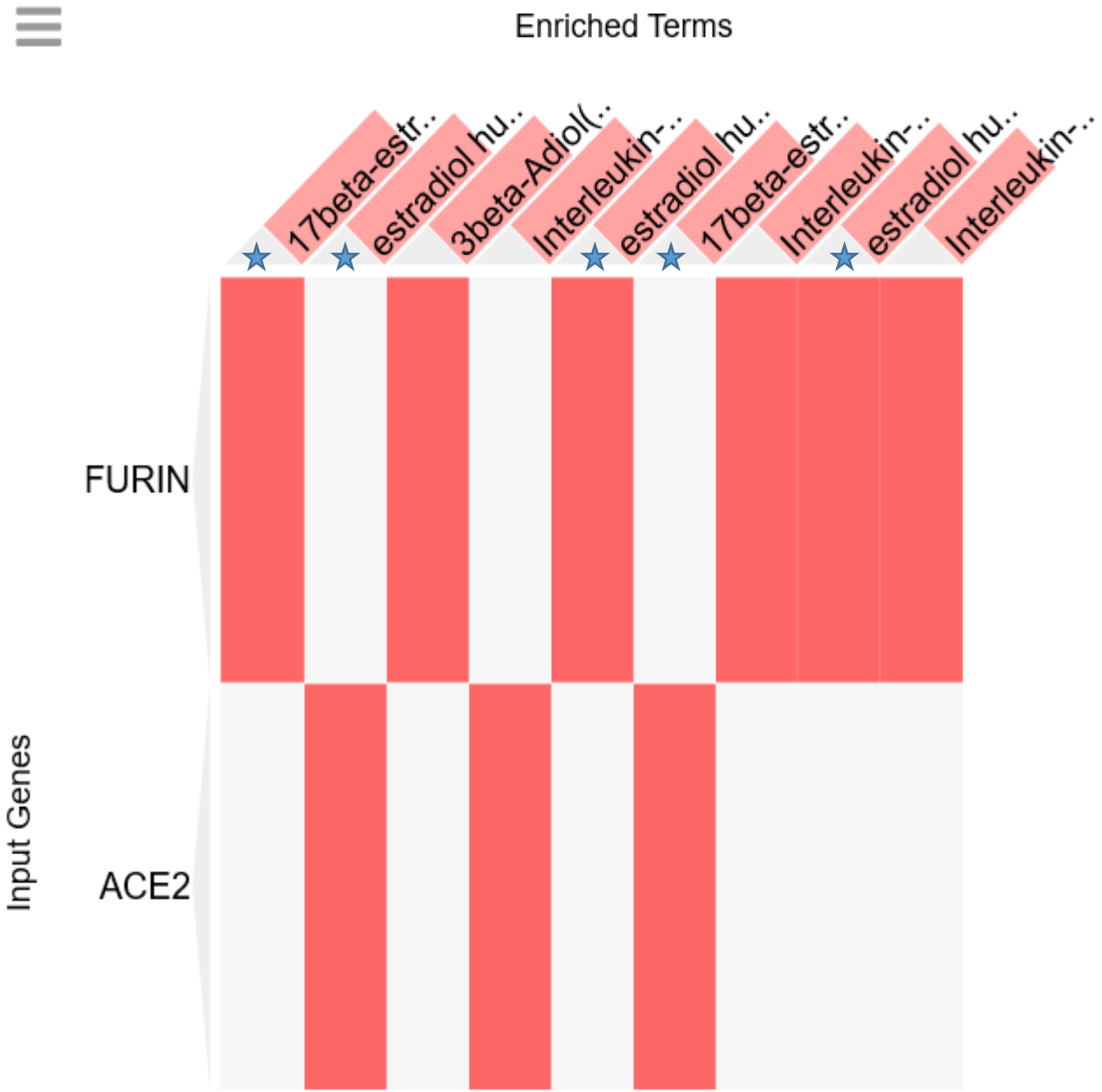

Profile: *c-FOS* expression
GDS3133 / 1375043_at
Title
Quercetin effect on the colonic mucosa
Organism
Rattus norvegicus

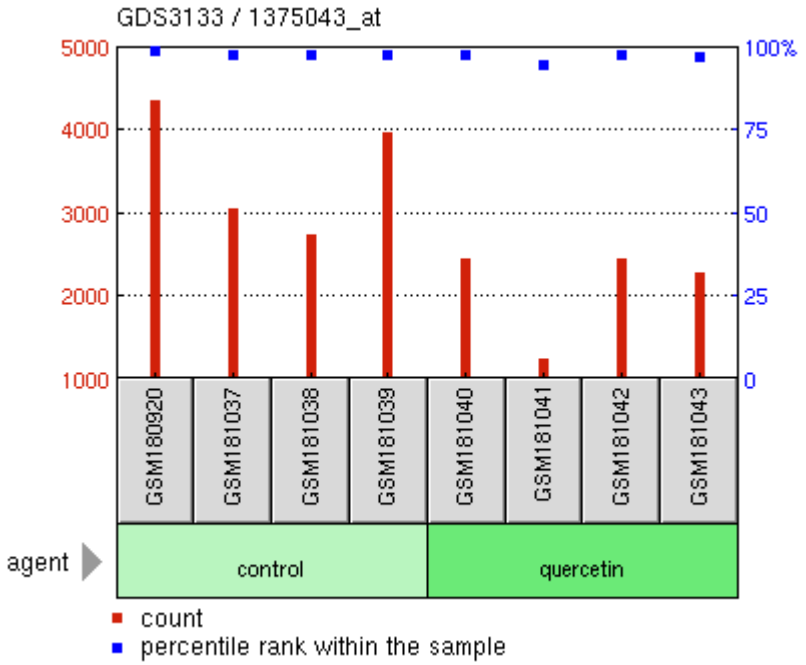

Quercetin inhibits *c-Fos* expression

Sample	Title	Value
GSM180920	Control, sample 1	4352.72
GSM181037	Control, sample 2	3050.22
GSM181038	Control, sample 3	2743.92
GSM181039	Control, sample 4	3972.13
GSM181040	Quercetin, sample 1	2451.67
GSM181041	Quercetin, sample 2	1258.62
GSM181042	Quercetin, sample 3	2468.64
GSM181043	Quercetin, sample 4	2279.08

Profile: *c-FOS* expression
GDS3032 / 209189_at
Title
Quercetin effect on intestinal cell differentiation in vitro: time course
Organism
Homo sapiens

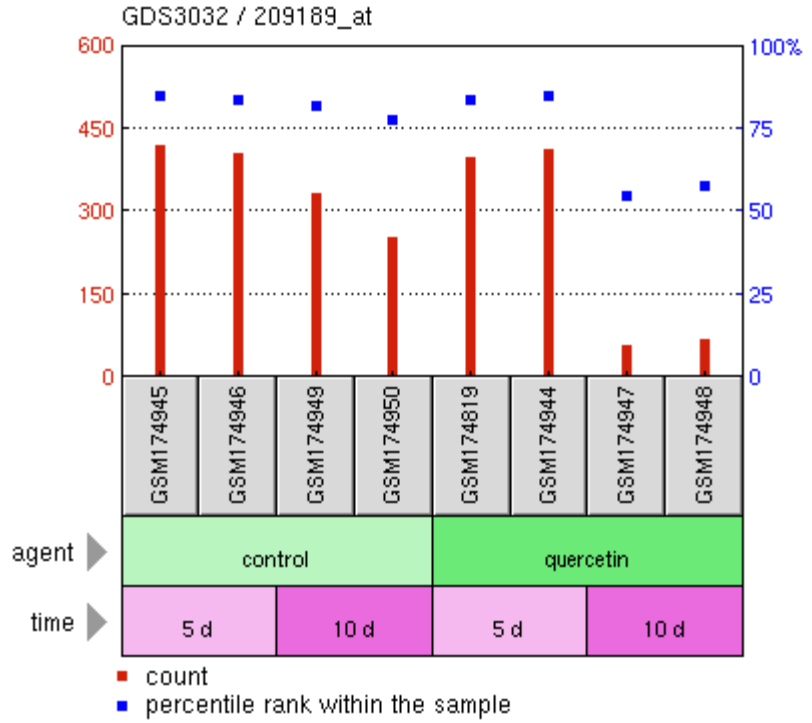

Quercetin inhibits *c-Fos* expression

Sample	Title	Value
GSM174945	Control day 05 sample 1	420.956
GSM174946	Control day 05 sample 2	404.99
GSM174949	Control day 10 sample 1	332.662
GSM174950	Control day 10 sample 2	256.542
GSM174819	Quercetin day 05 sample 1	399.894
GSM174944	Quercetin day 05 sample 2	413.261
GSM174947	Quercetin day 10 sample 1	60.5856
GSM174948	Quercetin day 10 sample 2	71.7716

Profile: *c-FOS* expression
GDS3032 / 218881_s_at
Title
Quercetin effect on intestinal cell differentiation in vitro: time course
Organism
Homo sapiens

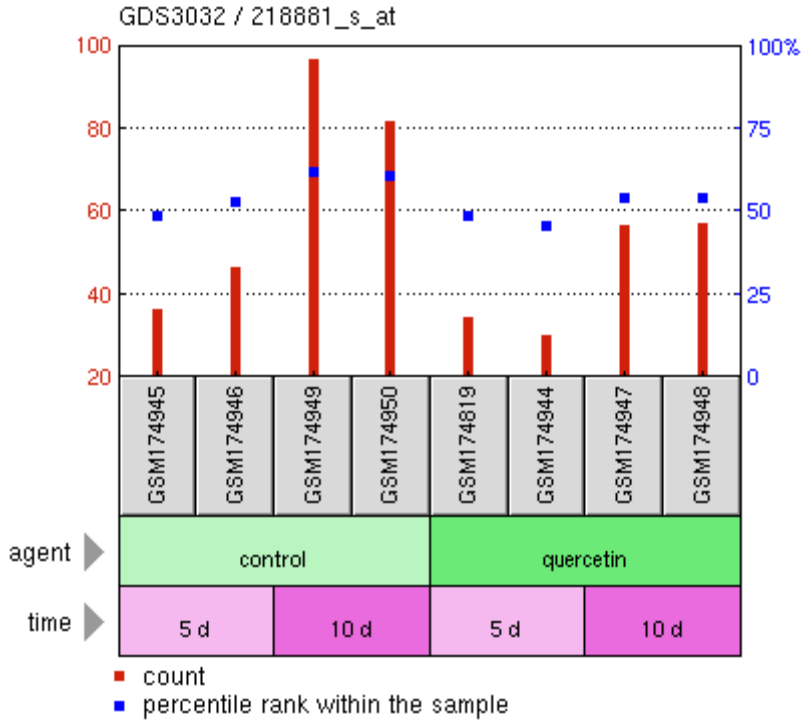

Quercetin inhibits *c-Fos* expression

Sample	Title	Value
GSM174945	Control day 05 sample 1	36.7758
GSM174946	Control day 05 sample 2	46.8416
GSM174949	Control day 10 sample 1	96.6905
GSM174950	Control day 10 sample 2	81.9045
GSM174819	Quercetin day 05 sample 1	34.7583
GSM174944	Quercetin day 05 sample 2	30.5511
GSM174947	Quercetin day 10 sample 1	56.9884
GSM174948	Quercetin day 10 sample 2	57.2094

Profile: *Runx1* expression
GDS3133 / 1368914_at
Title
Quercetin effect on the colonic mucosa
Organism
Rattus norvegicus

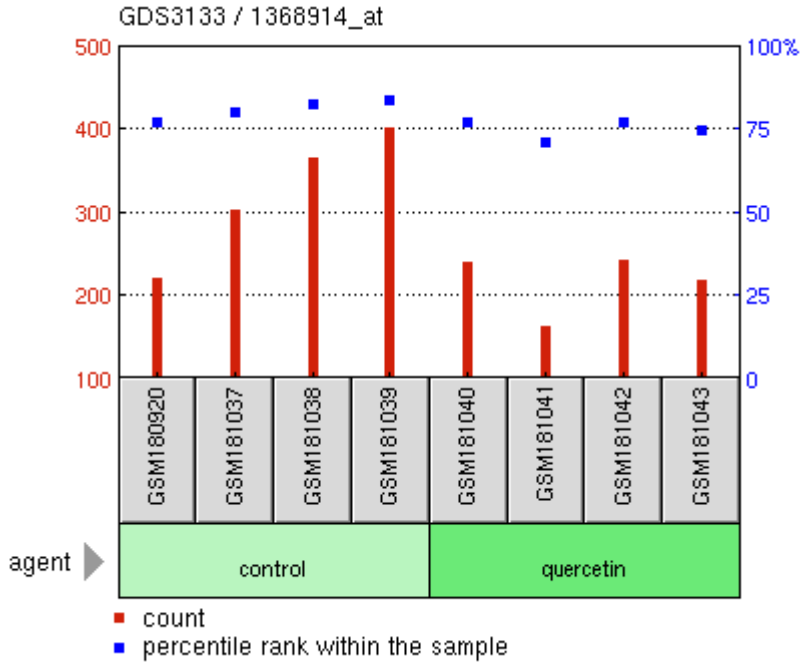

Quercetin inhibits *Runx1* expression

Sample	Title	Value
GSM180920	Control, sample 1	222.664
GSM181037	Control, sample 2	302.432
GSM181038	Control, sample 3	366.811
GSM181039	Control, sample 4	402.875
GSM181040	Quercetin, sample 1	241.637
GSM181041	Quercetin, sample 2	163.728
GSM181042	Quercetin, sample 3	243.316
GSM181043	Quercetin, sample 4	218.646

Profile: *Runxt1* expression
GDS3676 / 205528_s_at
Title
Quercetin effect on CD14+ monocyte
Organism
Homo sapiens

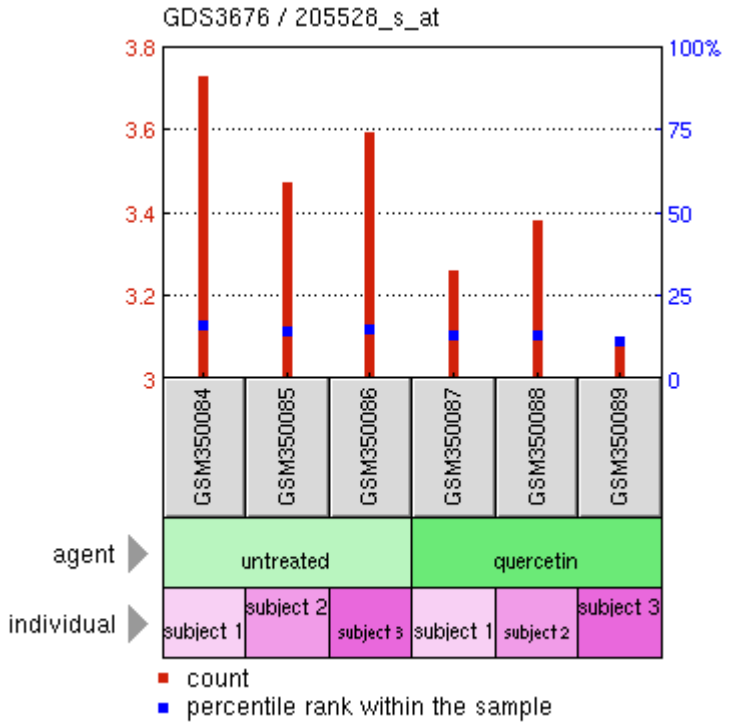

Quercetin inhibits *Runxt1* expression

Sample	Title	Value
GSM350084	CD14+ at baseline, biological replicate 1	3.72993
GSM350085	CD14+ at baseline, biological replicate 2	3.47495
GSM350086	CD14+ at baseline, biological replicate 3	3.59744
GSM350087	CD14+ after 2 wk quercetin supplementation, biological replicate 1	3.2641
GSM350088	CD14+ after 2 wk quercetin supplementation, biological replicate 2	3.38173
GSM350089	CD14+ after 2 wk quercetin supplementation, biological replicate 3	3.10117

RUNXT1, RUNX1 translocation partner 1

Profile: *HNF4a* expression
GDS3032 / 216889_s_at
Title
Quercetin effect on intestinal cell differentiation in vitro: time course
Organism
Homo sapiens

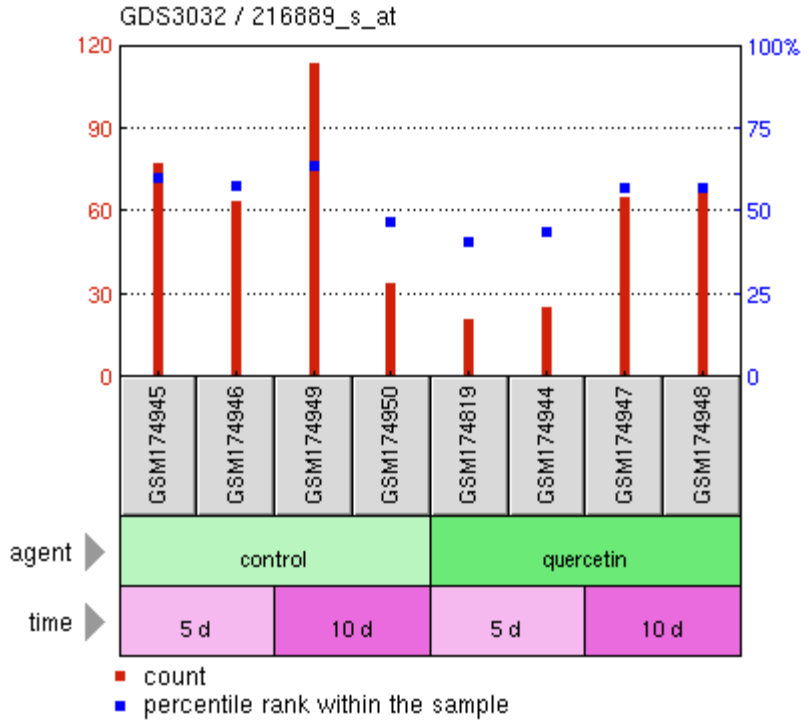

Quercetin inhibits *HNF4a* expression

Sample	Title	Value
GSM174945	Control day 05 sample 1	**77.6175**
GSM174946	Control day 05 sample 2	**63.792**
GSM174949	Control day 10 sample 1	113.821
GSM174950	Control day 10 sample 2	34.1332
GSM174819	Quercetin day 05 sample 1	**21.0188**
GSM174944	Quercetin day 05 sample 2	**25.7496**
GSM174947	Quercetin day 10 sample 1	65.2834
GSM174948	Quercetin day 10 sample 2	69.9663

Profile: *c-FOS* expression
GDS2708 / 8494
Title
Quercetin effect on cultured cardiomyocytes: time course
Organism
Rattus norvegicus

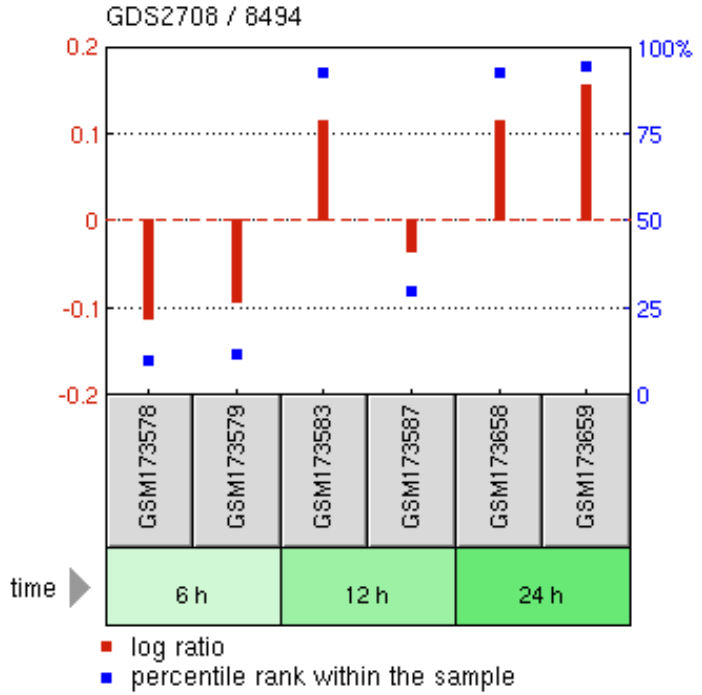

Quercetin increases *c-Fos* expression

Sample	Title	Value
GSM173578	Quercetin treated cardiomyocytes for 6 hours (Q6-A).	-0.114041
GSM173579	Quercetin treated cardiomyocytes for 6 hours (Q6-B).	-0.0962766
GSM173583	Quercetin treated cardiomyocytes for 12 hours (Q12-A).	0.118043
GSM173587	Quercetin treated cardiomyocytes for 12 hours (Q12-B).	-0.0368638
GSM173658	Quercetin treated cardiomyocytes for 24 hours (Q24-A).	0.118043
GSM173659	Quercetin treated cardiomyocytes for 24 hours (Q24-B).	0.15779

Supplemental Figure S10. Confirmation of the Estradiol and Quercetin activities as potential candidate coronavirus infection mitigation agents

Estradiol effect on *FURIN* expression in the rat ischemic brain

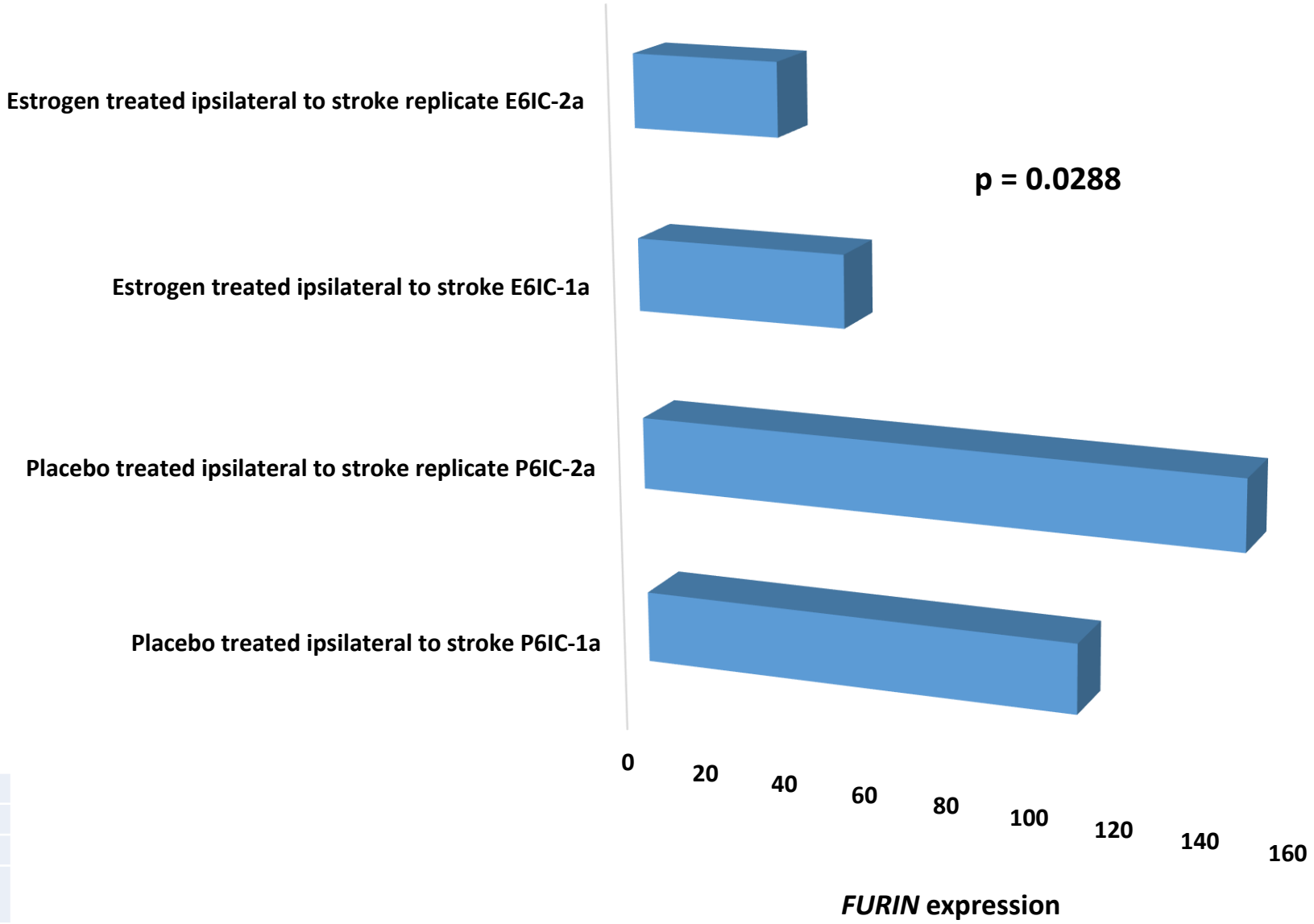

GEO Profile
GDS2311 / X55660_at
Title
Estradiol effect on the ischemic brain
Organism
Rattus norvegicus

Ethynyl estradiol effects on *ACE2* expression in mouse uterus

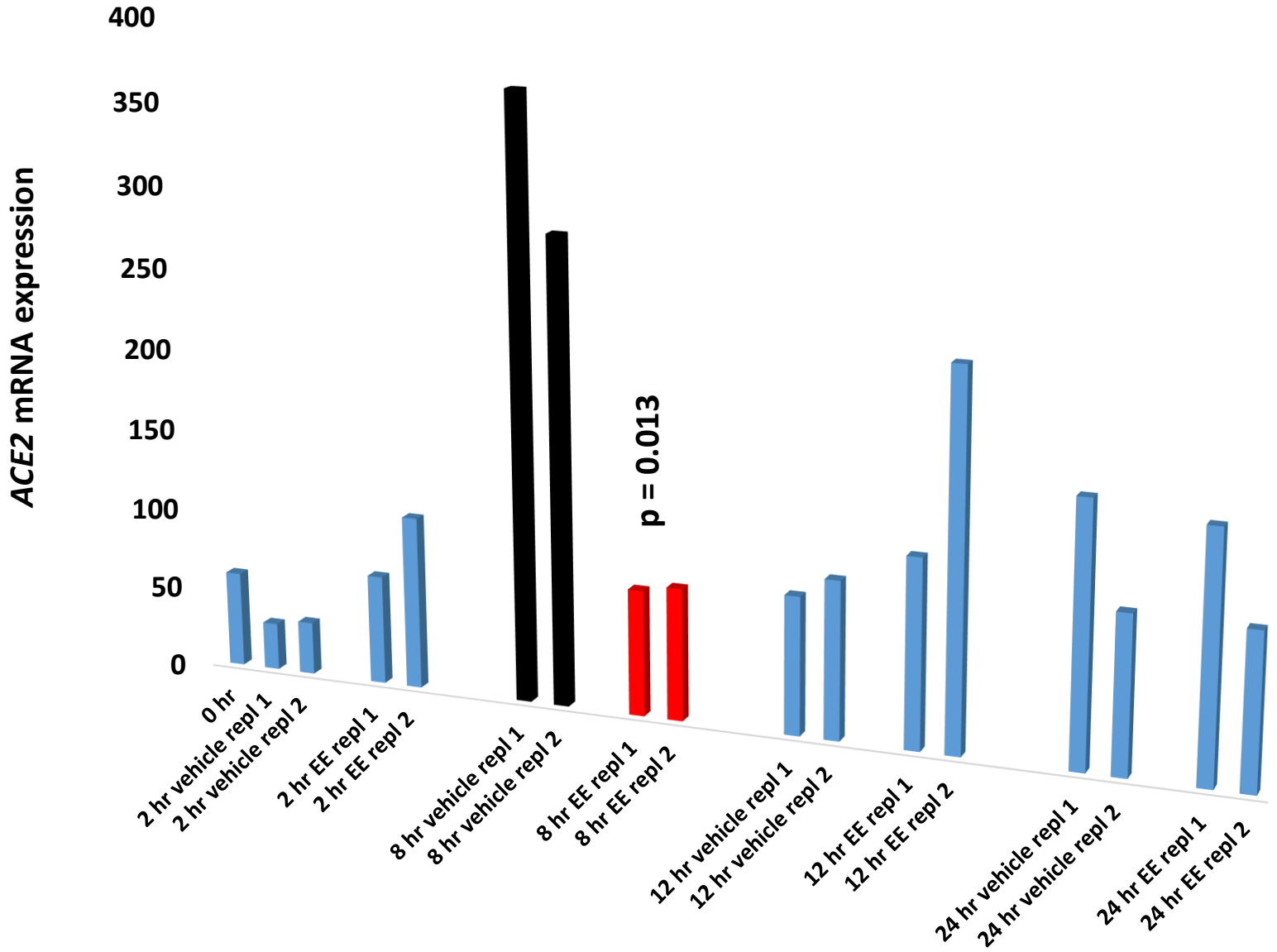

GEO Profile
GDS285 / AA690434_at
Title
Ethynyl estradiol estrogen effect in uterus
Organism
Mus musculus

Effects of estradiol and tamoxifen on *FURIN* expression mediated by the estrogen receptor beta

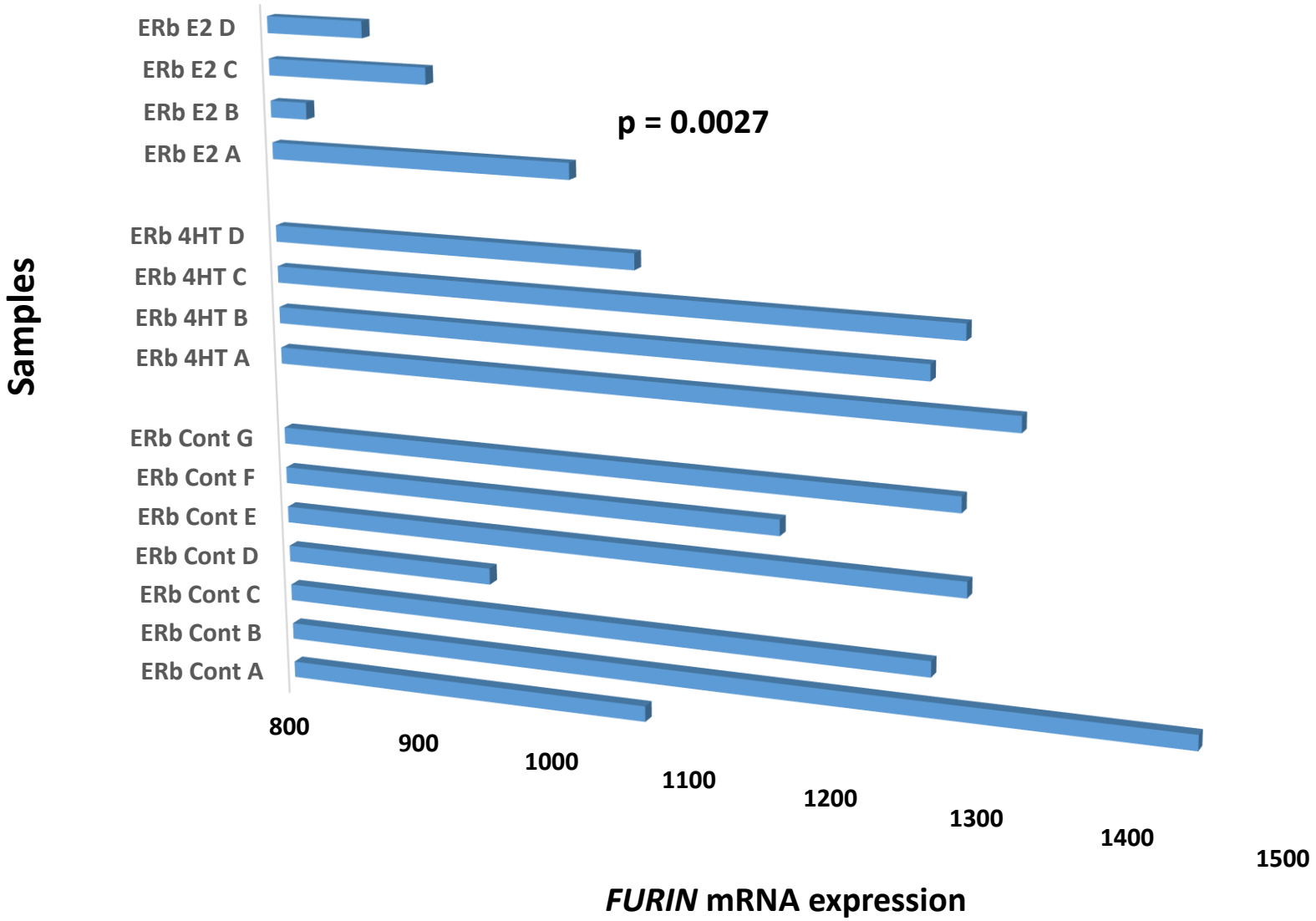

GEO Profile
GDS1094 / 201945_at
Title
Estrogen receptor alpha/beta heterodimer action in response to estrogen and tamoxifen
Organism
Homo sapiens

Effects of estradiol and tamoxifen on ACE2 expression mediated by the estrogen receptor beta

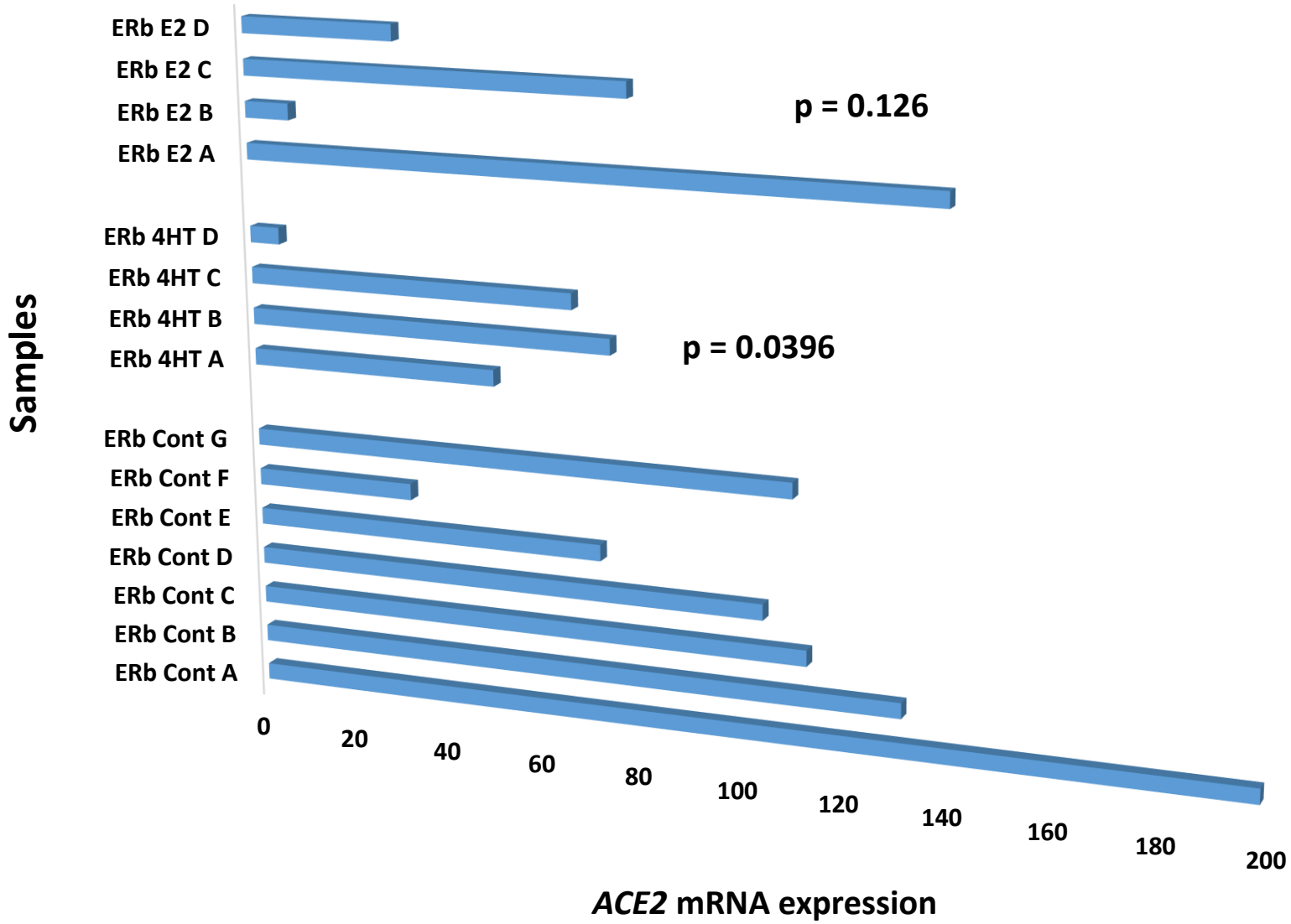

GEO Profile
GDS1094 / 219962_at
Title
Estrogen receptor alpha/beta heterodimer action in response to estrogen and tamoxifen
Organism
Homo sapiens

Profile: ACE2 expression
GDS3032 / 222257_s_at
Title
Quercetin effect on intestinal cell differentiation in vitro: time course
Organism
Homo sapiens

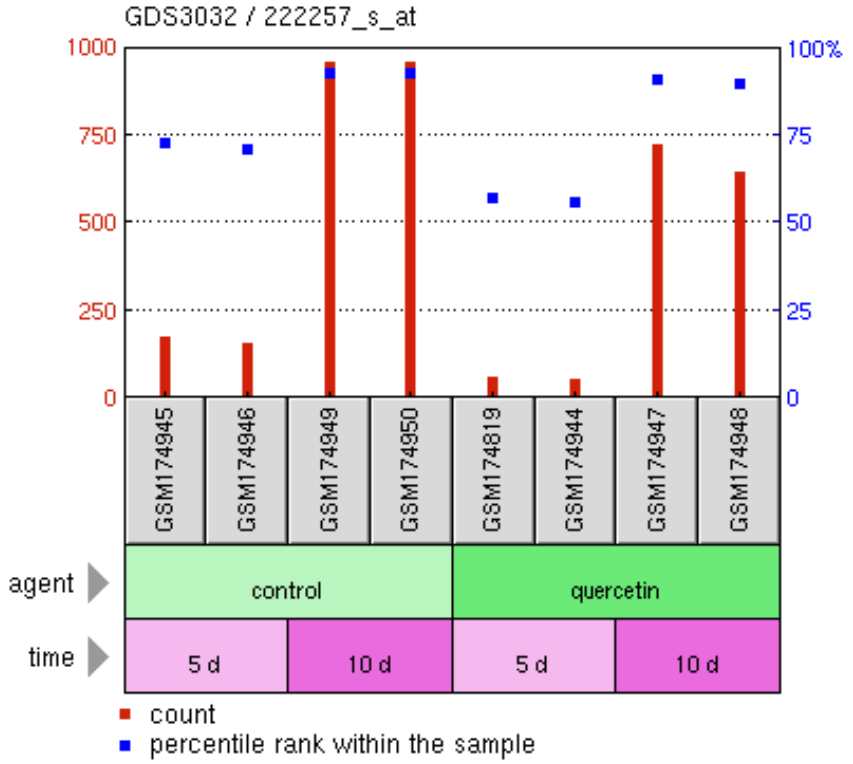

Day 5
p = 0.004

Day 10
p = 0.009

Quercetin inhibits the *ACE2* expression

Sample	Title	Value
GSM174945	Control day 05 sample 1	176.763
GSM174946	Control day 05 sample 2	157.459
GSM174949	Control day 10 sample 1	962.644
GSM174950	Control day 10 sample 2	959.364
GSM174819	Quercetin day 05 sample 1	60.6977
GSM174944	Quercetin day 05 sample 2	59.0821
GSM174947	Quercetin day 10 sample 1	725.488
GSM174948	Quercetin day 10 sample 2	649.304

Profile: ACE2 expression
GDS3032 / 219962_at
Title
Quercetin effect on intestinal cell differentiation in vitro: time course
Organism
Homo sapiens

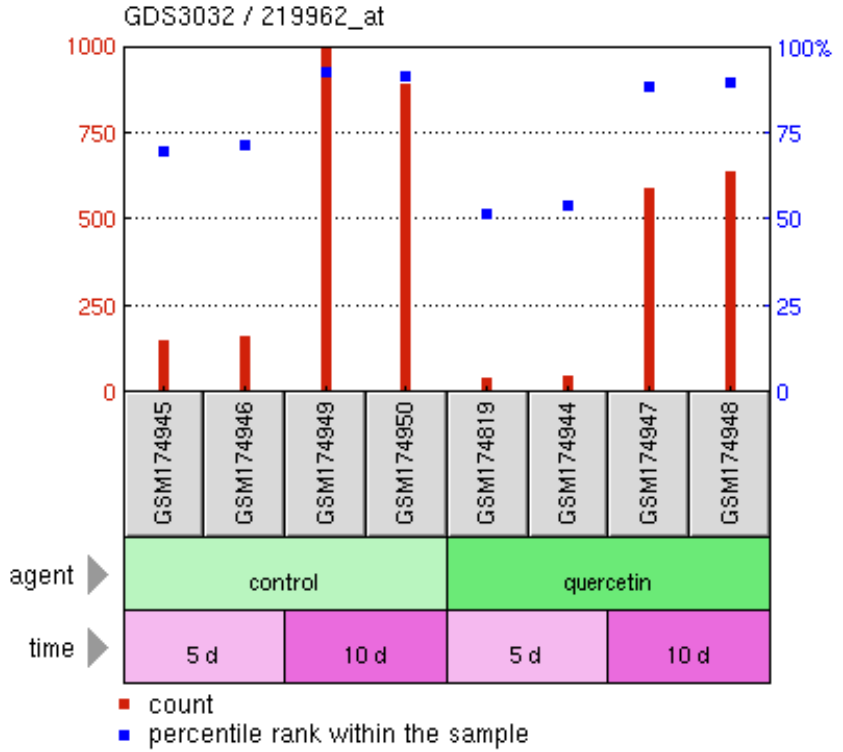

Day 5
p = 0.001

Day 10
p = 0.014

Quercetin inhibits the *ACE2* expression

Sample	Title	Value
GSM174945	Control day 05 sample 1	152.856
GSM174946	Control day 05 sample 2	163.228
GSM174949	Control day 10 sample 1	995.184
GSM174950	Control day 10 sample 2	895.468
GSM174819	Quercetin day 05 sample 1	43.9228
GSM174944	Quercetin day 05 sample 2	49.8735
GSM174947	Quercetin day 10 sample 1	595.486
GSM174948	Quercetin day 10 sample 2	642.974

Profile: *c-FOS* expression
GDS5278 / MmugDNA.38565.1.S1_at
Title
Endometrium response to tamoxifen and low dose estradiol combination therapy
Organism: Macaca mulatta

Estradiol inhibits the *c-FOS* expression

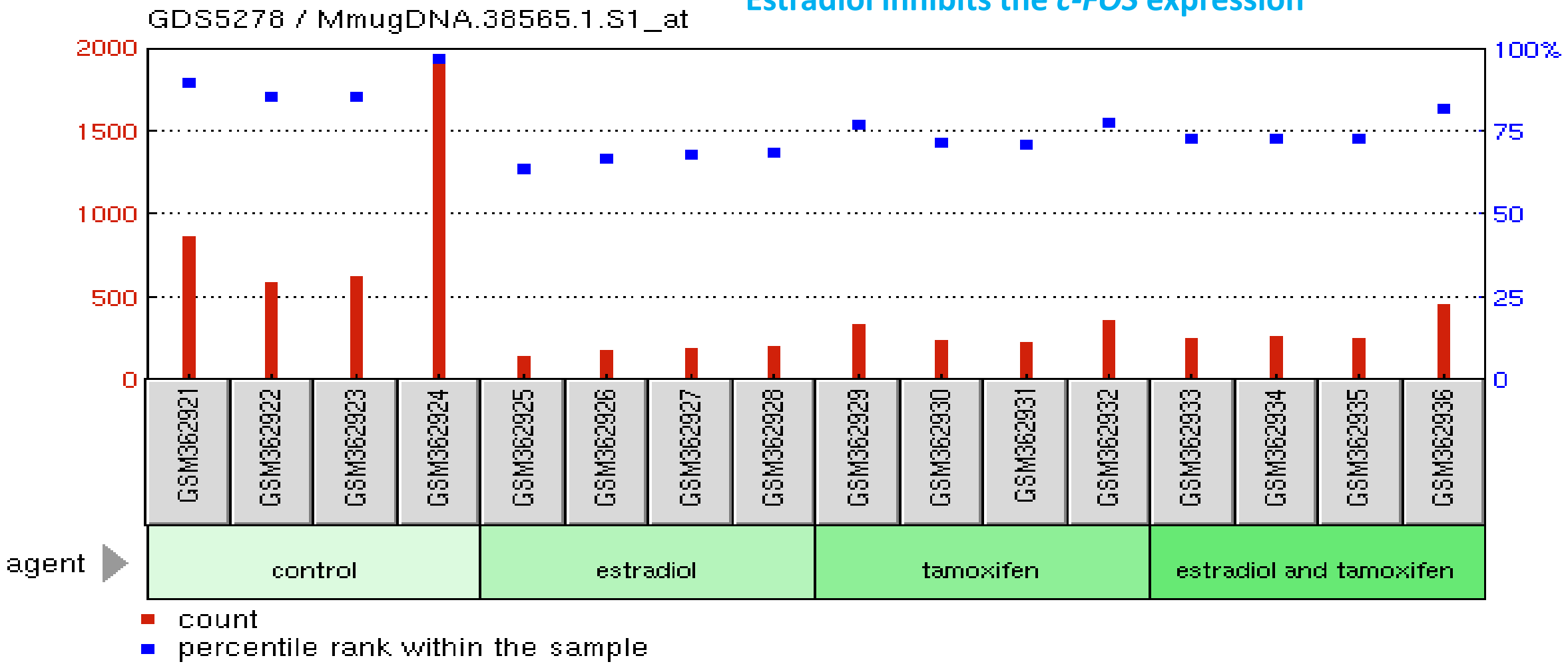

Profile: *c-FOS* expression
GDS5278 / MmugDNA.38565.1.S1_at
Title
Endometrium response to tamoxifen and low dose estradiol combination therapy
Organism: Macaca mulatta

Estradiol inhibits the *c-FOS* expression

Sample	Title	Value
GSM362921	Control 1	**868.444**
GSM362922	Control 2	**596.312**
GSM362923	Control 3	**633.478**
GSM362924	Control 4	**1956.61**
GSM362925	Estradiol 1	147.047
GSM362926	Estradiol 2	183.666
GSM362927	Estradiol 3	194.779
GSM362928	Estradiol 4	212.397
GSM362929	Tamoxifen 1	347.062
GSM362930	Tamoxifen 2	241.809
GSM362931	Tamoxifen 3	238.437
GSM362932	Tamoxifen 4	363.108
GSM362933	Estradiol and Tamoxifen 1	255.806
GSM362934	Estradiol and Tamoxifen 2	272.225
GSM362935	Estradiol and Tamoxifen 3	264.55
GSM362936	Estradiol and Tamoxifen 4	459.833

Profile: *c-FOS* expression
GDS982 / 160901_at
Title
Uterine response to physiologic, plant-derived, and synthetic estrogen
Organism: Mus musculus

Estradiol increases the *c-FOS* expression

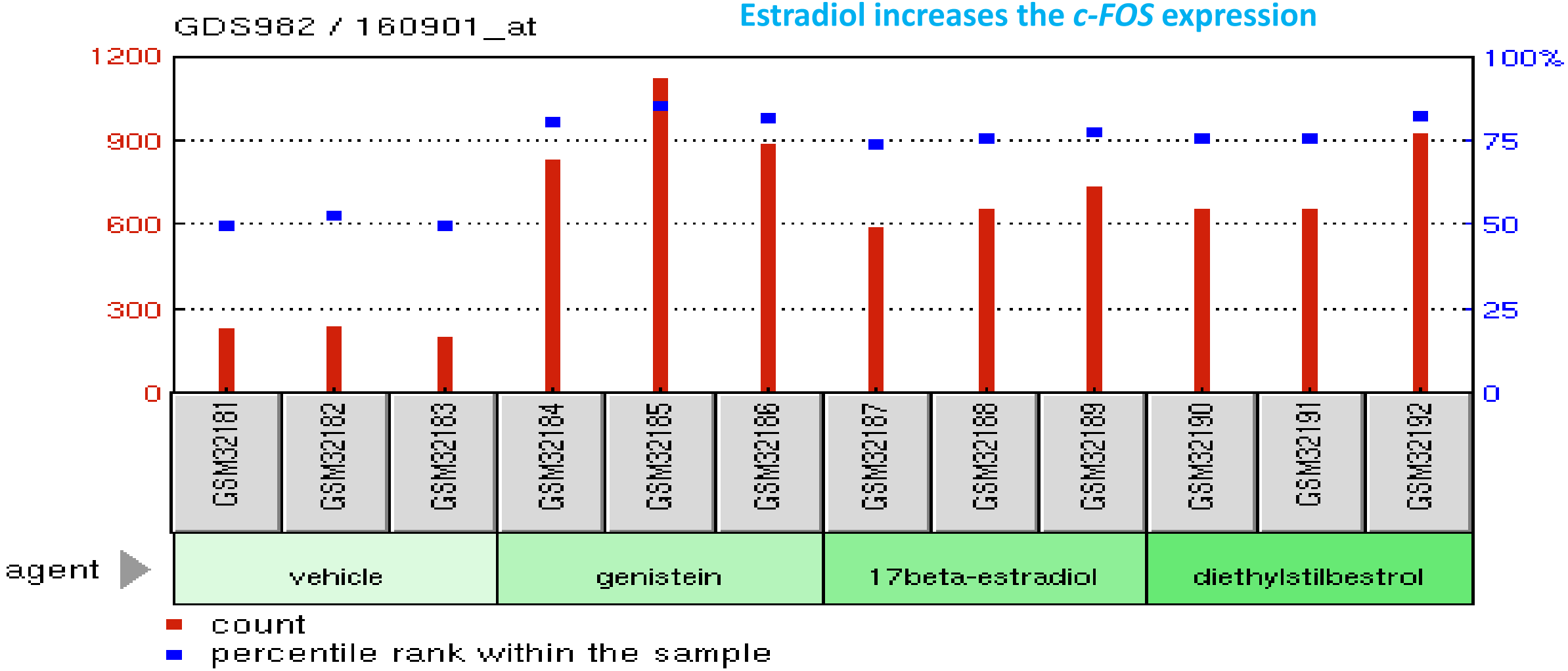

Profile: *c-FOS* expression
GDS982 / 160901_at
Title
Uterine response to physiologic, plant-derived, and synthetic estrogen
Organism
Mus musculus

Estradiol increases the *c-FOS* expression

Sample	Title	Value
GSM32181	AO C1	**236.8**
GSM32182	AO C2	**239.8**
GSM32183	AO C3	**208.6**
GSM32184	GEN G1	834.7
GSM32185	GEN G2	1122.6
GSM32186	GEN G3	892.9
GSM32187	E2 E1	599.6
GSM32188	E2 E2	660.6
GSM32189	E2 E3	740.3
GSM32190	DES D1	659.8
GSM32191	DES D2	663.9
GSM32192	DES D3	928.8

Supplemental Figure S11. Testosterone effects on gene expression

An overview of the potential coronavirus-infection promoting activities

Profile: *ACE2* expression
GDS2920 / 222257_s_at
Title
Testosterone effect on skeletal muscles of HIV-infected males experiencing weight loss
Organism
Homo sapiens

Testosterone increases *ACE2* expression

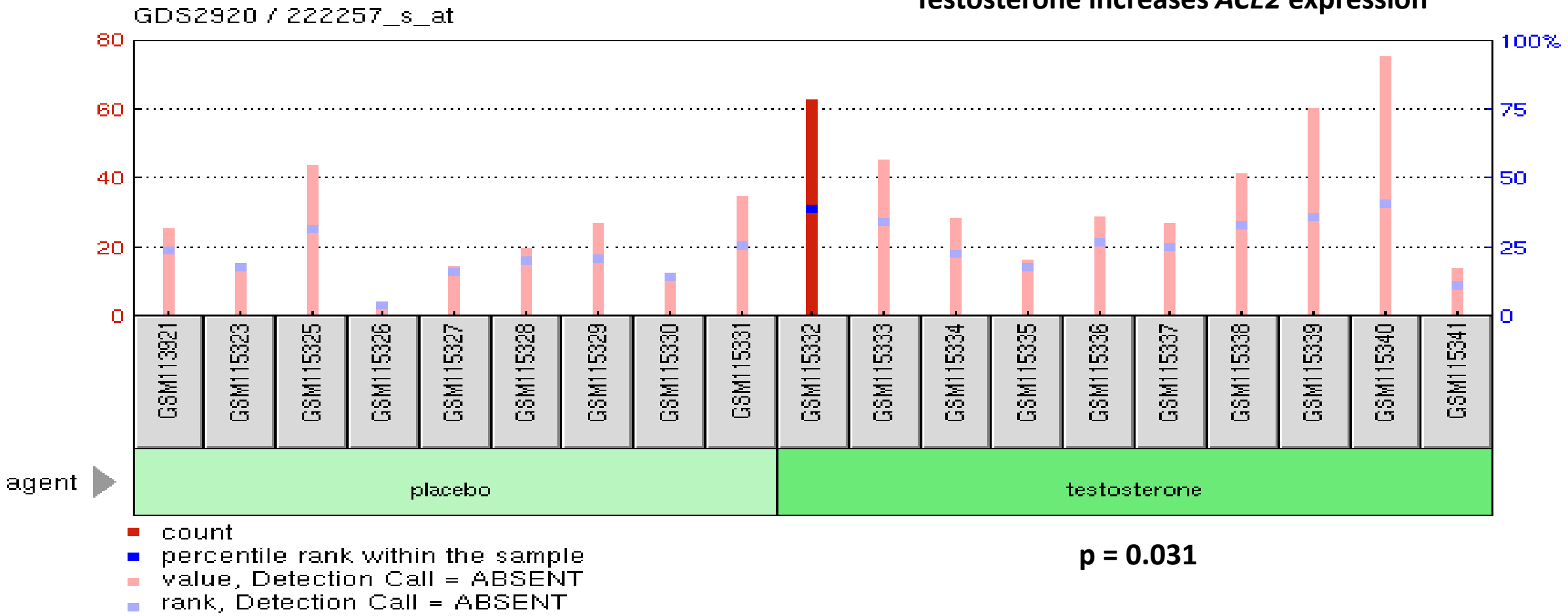

p = 0.031

Profile: *ACE2* expression
GDS2920 / 222257_s_at
Title
Testosterone effect on skeletal muscles of HIV-infected males experiencing weight loss
Organism
Homo sapiens

Testosterone increases *ACE2* expression

Sample	Title	Value
GSM113921	Placebo treated, HIV-1 positive male, day 14 (1)	25.8
GSM115323	Placebo treated, HIV-1 positive male, day 14 (2)	14.3
GSM115325	Placebo treated, HIV-1 positive male, day 14 (3)	44.3
GSM115326	Placebo treated, HIV-1 positive male, day 14 (4)	3.1
GSM115327	Placebo treated, HIV-1 positive male, day 14 (5)	14.8
GSM115328	Placebo treated, HIV-1 positive male, day 14 (6)	20.2
GSM115329	Placebo treated, HIV-1 positive male, day 14 (7)	27
GSM115330	Placebo treated, HIV-1 positive male, day 14 (8)	11.7
GSM115331	Placebo treated, HIV-1 positive male, day 14 (9)	34.9
GSM115332	Testosterone treated, HIV-1 positive male, day 14 (1)	63.1
GSM115333	Testosterone treated, HIV-1 positive male, day 14 (2)	45.6
GSM115334	Testosterone treated, HIV-1 positive male, day 14 (3)	28.8
GSM115335	Testosterone treated, HIV-1 positive male, day 14 (4)	16.8
GSM115336	Testosterone treated, HIV-1 positive male, day 14 (5)	29.2
GSM115337	Testosterone treated, HIV-1 positive male, day 14 (6)	27.3
GSM115338	Testosterone treated, HIV-1 positive male, day 14 (7)	41.7
GSM115339	Testosterone treated, HIV-1 positive male, day 14 (8)	60.3
GSM115340	Testosterone treated, HIV-1 positive male, day 14 (9)	75.5
GSM115341	Testosterone treated, HIV-1 positive male, day 14 (10)	14.1

p = 0.031

Profile: *ACE2* expression
GDS1361 / 1598
Title
Testosterone effect on meibomian gland
Organism
Mus musculus

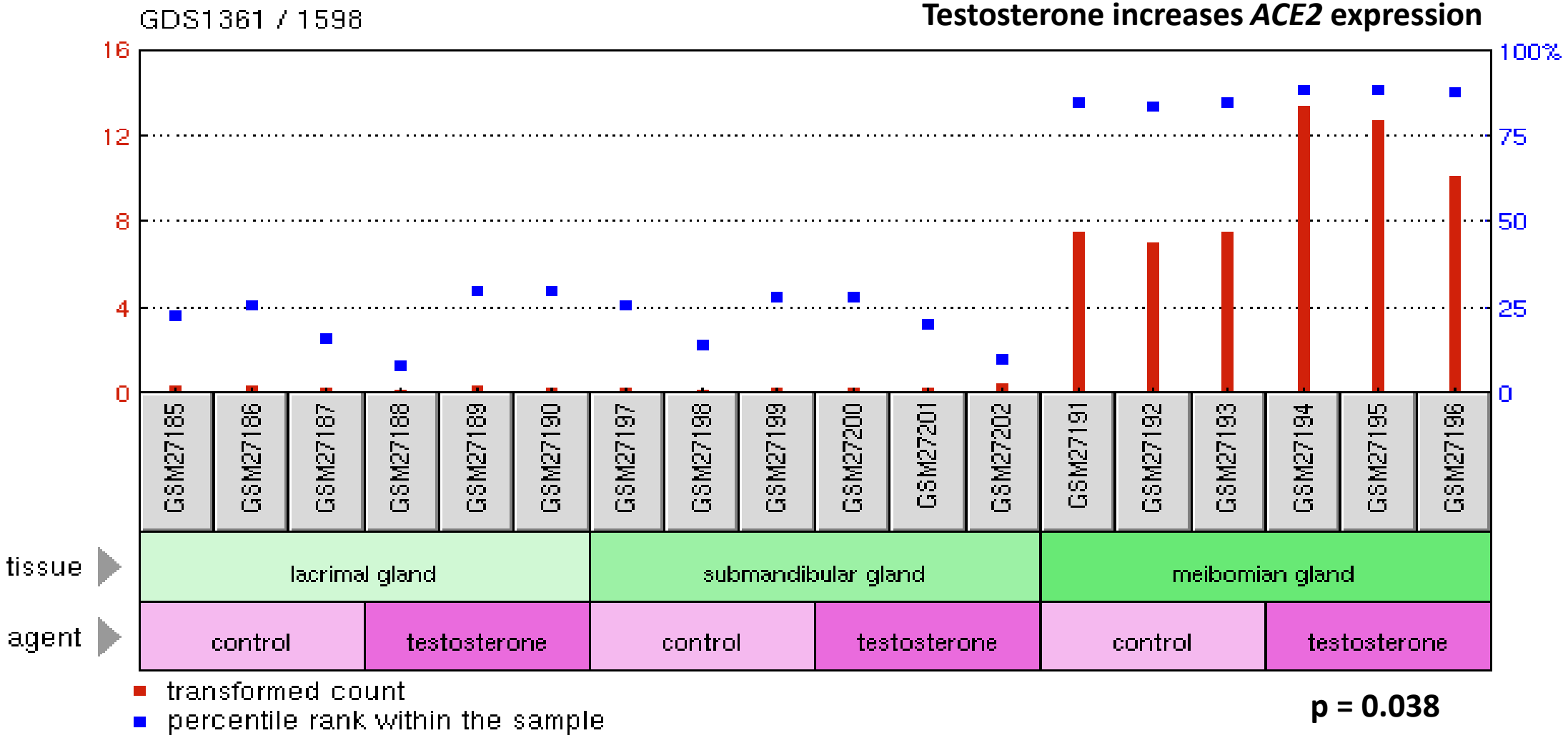

p = 0.038

Profile: *ACE2* expression
GDS1361 / 1598
Title
Testosterone effect on meibomian gland
Organism
Mus musculus

Testosterone increases *ACE2* expression

Sample	Title	Value	
GSM27185	Male Placebo-Treated Lacrimal Gland Sample A	0.432225	
GSM27186	Male Placebo-Treated Lacrimal Gland Sample B	0.457711	
GSM27187	Male Placeo-Treated Lacrimal Gland Sample C	0.359507	
GSM27188	Male Testosterone-Treated Lacrimal Gland Sample A	0.276599	
GSM27189	Male Testosterone-Treated Lacrimal Gland Sample B	0.425166	
GSM27190	Male Testosterone-Treated Lacrimal Gland Sample C	0.367615	
GSM27197	Male Placebo-Treated Submandibular Gland Sample A	0.343573	
GSM27198	Male Placebo-Treated Submandibular Gland Sample B	0.271271	
GSM27199	Male Placebo-Treated Submandibular Gland Sample C	0.384337	
GSM27200	Male Testosterone-Treated Submandibular Gland Sample A	0.365324	
GSM27201	Male Testosterone-Treated Submandibular Gland Sample B	0.308682	
GSM27202	Male Testosterone-Treated Submandibular Gland Sample C	0.205059	
GSM27191	Male Placebo-Treated Meibomian Gland Sample A	7.61018	
GSM27192	Male Placebo-Treated Meibomian Gland Sample B	7.08807	**p = 0.038**
GSM27193	Male Placebo-Treated Meibomian Gland Sample C	7.54525	
GSM27194	Male Testosterone-Treated Meibomian Gland Sample A		13.4706
GSM27195	Male Testosterone-Treated Meibomian Gland Sample B		12.7558
GSM27196	Male Testosterone-Treated Meibomian Gland Sample C		10.1925

Profile: *ACE2* expression

GDS1832 / 1598

Title

Testosterone effect on female lacrimal, meibomian, and submandibular glands

Organism

Mus musculus

Testosterone increases *ACE2* expression

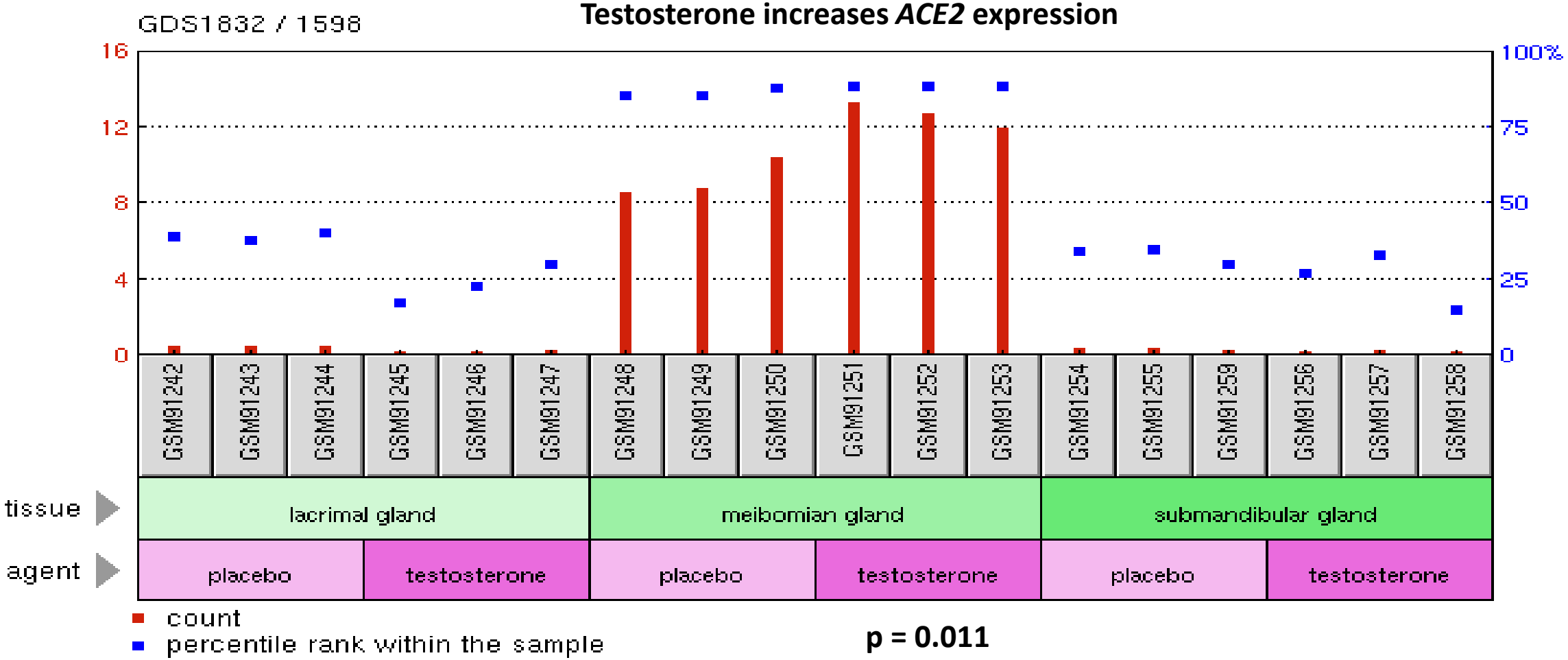

p = 0.011

Profile: *ACE2* expression
GDS1832 / 1598
Title
Testosterone effect on female lacrimal, meibomian, and submandibular glands
Organism
Mus musculus

Testosterone increases *ACE2* expression

Sample	Title	Value	
GSM91242	Female Placebo-Treated Lacrimal Gland Sample A	0.560279	
GSM91243	Female Placebo-Treated Lacrimal Gland Sample B	0.522894	**p = 0.024**
GSM91244	Female Placebo-Treated Lacrimal Gland Sample C	0.566438	
GSM91245	Female Testosterone-Treated Lacrimal Gland Sample A		**0.23071**
GSM91246	Female Testosterone-Treated Lacrimal Gland Sample B		**0.275703**
GSM91247	Female Testosterone-Treated Lacrimal Gland Sample C		**0.385156**
GSM91248	Female Placebo-Treated Meibomian Gland Sample A	**8.58739**	
GSM91249	Female Placebo-Treated Meibomian Gland Sample B	**8.79653**	
GSM91250	Female Placebo-Treated Meibomian Gland Sample C	**10.4129**	
GSM91251	Female Testosterone-Treated Meibomian Gland Sample A	**13.3238**	
GSM91252	Female Testosterone-Treated Meibomian Gland Sample B	**12.7645**	**p = 0.011**
GSM91253	Female Testosterone-Treated Meibomian Gland Sample C	**11.962**	
GSM91254	Female Placebo-Treated Submandibular Gland Sample B	0.398068	
GSM91255	Female Placebo-Treated Submandibular Gland Sample C	0.403039	
GSM91259	Female Placebo-Treated Submandibular Gland Sample A	0.35605	
GSM91256	Female Testosterone-Treated Submandibular Gland Sample A	0.238247	
GSM91257	Female Testosterone-Treated Submandibular Gland Sample B	0.365064	p = 0.130
GSM91258	Female Testosterone-Treated Submandibular Gland Sample C	0.206147	

Profile: *FURIN* expression
GDS1833 / 100515_at
Title
Testosterone effect on the female submandibular gland
Organism
Mus musculus

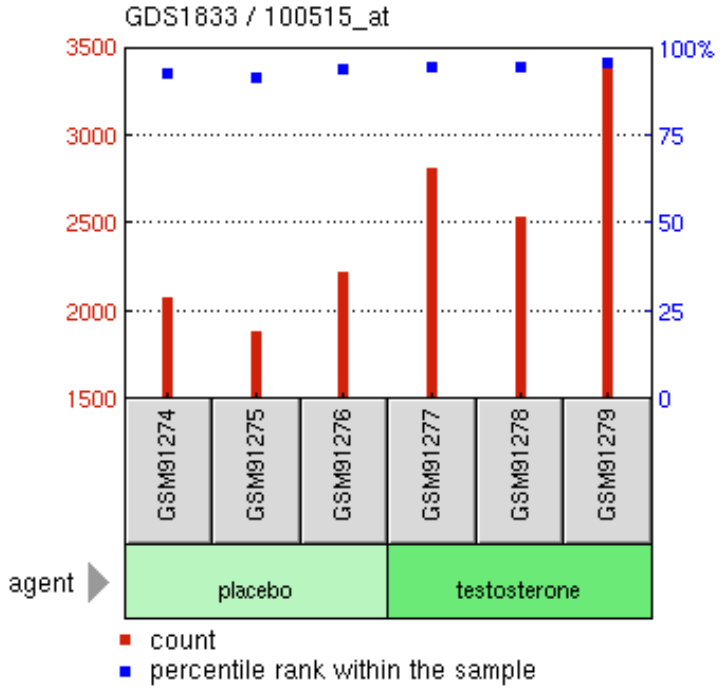

Testosterone increases *FURIN* expression

Sample	Title	Value
GSM91274	Female Placebo-Treated Submandibular Gland Sample A Technical Replicate	2087.8
GSM91275	Female Placebo-Treated Submandibular Gland Sample B Technical Replicate	1888.3 **p = 0.035**
GSM91276	Female Placebo-Treated Submandibular Gland Sample C Technical Replicate	2230.6
GSM91277	Female Testosterone-Treated Submandibular Gland Sample A Technical Replicate	**2822.9**
GSM91278	Female Testosterone-Treated Submandibular Gland Sample B Technical Replicate	**2536.3**
GSM91279	Female Testosterone-Treated Submandibular Gland Sample C Technical Replicate	**3392.9**

Profile: *FURIN* expression
GDS2562 / 100515_at
Title
Prostate response to castration and subsequent hormone replacement
Organism: Mus musculus

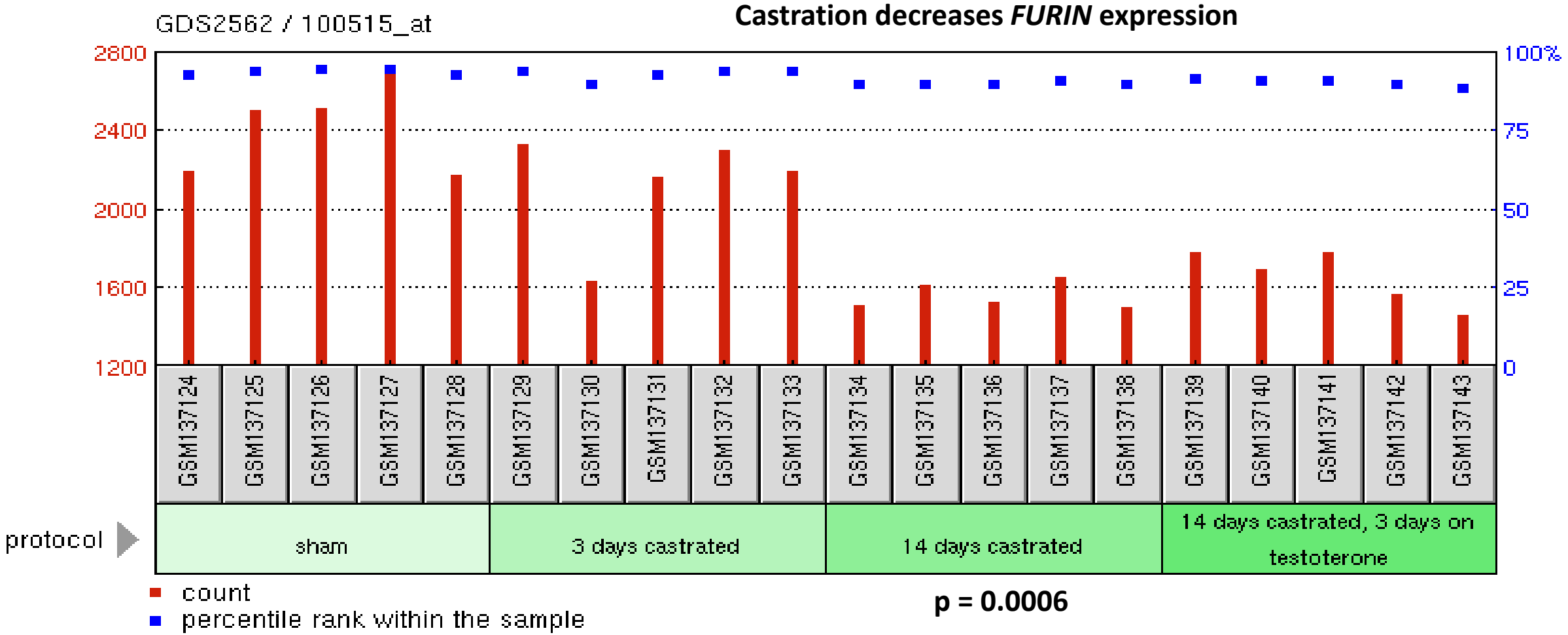

p = 0.0006

Profile: *FURIN* expression
GDS2562 / 100515_at
Title
Prostate response to castration and subsequent hormone replacement
Organism: Mus musculus

Castration decreases *FURIN* expression

Sample	Title	Value
GSM137124	PRB3660 (MG-U74A)	2201.3
GSM137125	PRB3661 (MG-U74A)	2506.4
GSM137126	PRB3662 (MG-U74A)	2519.5
GSM137127	PRB3663 (MG-U74A)	2710.3
GSM137128	PRB3664 (MG-U74A)	2173.5
GSM137129	PRB3665 (MG-U74A)	**2332.6**
GSM137130	PRB3666 (MG-U74A)	**1636.1**
GSM137131	PRB3667 (MG-U74A)	**2167.8**
GSM137132	PRB3668 (MG-U74A)	**2305.2**
GSM137133	PRB3669 (MG-U74A)	**2193.6**
GSM137134	PRB3698 (MG-U74A)	**1510.4**
GSM137135	PRB3699 (MG-U74A)	**1619.7**
GSM137136	PRB3700 (MG-U74A)	**p = 0.0006** **1532.1**
GSM137137	PRB3701 (MG-U74A)	**1654.5**
GSM137138	PRB3702 (MG-U74A)	**1502.6**
GSM137139	PRB3708 (MG-U74A)	1787.8
GSM137140	PRB3709 (MG-U74A)	1695.8
GSM137141	PRB3710 (MG-U74A)	1787.3
GSM137142	PRB3711 (MG-U74A)	1575.8
GSM137143	PRB3712 (MG-U74A)	1467.6

Profile: *FURIN* expression
GDS1361 / 5982
Title
Testosterone effect on meibomian gland
Organism
Mus musculus

Testosterone increases *FURIN* expression

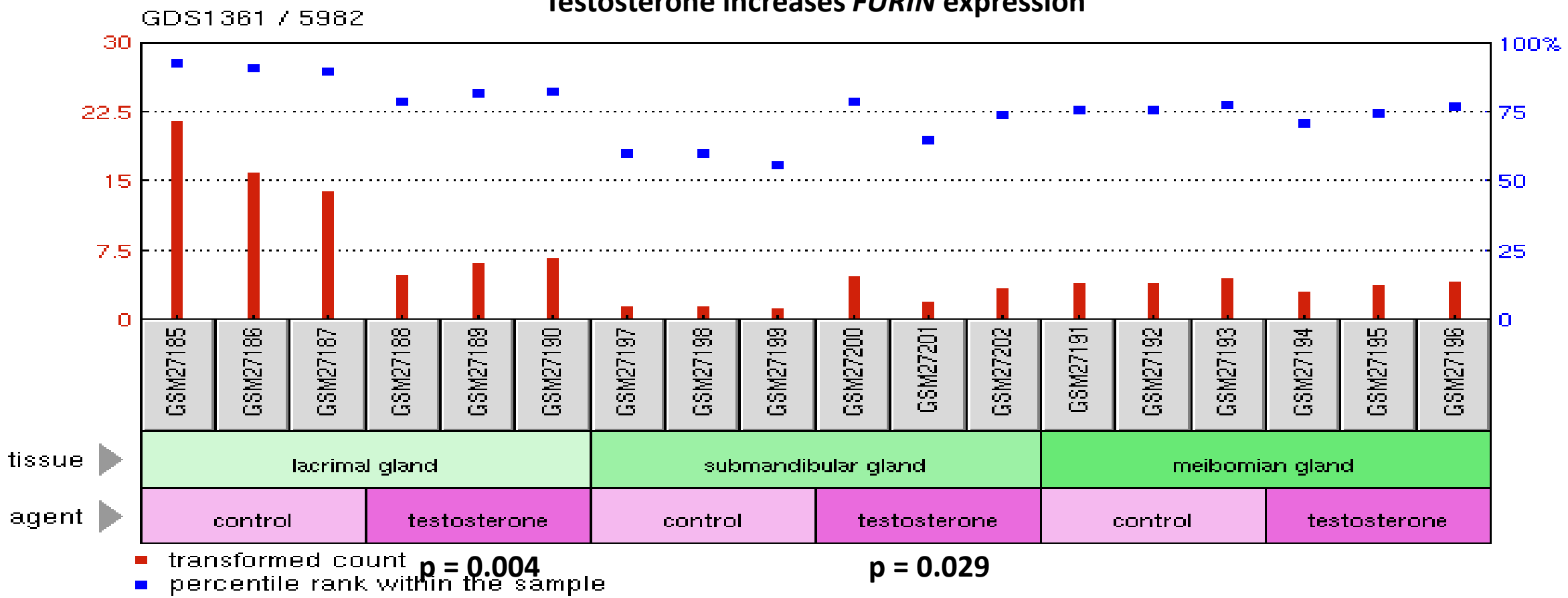

p = 0.004

p = 0.029

Profile: *FURIN* expression
GDS1361 / 5982
Title
Testosterone effect on meibomian gland
Organism
Mus musculus

Testosterone increases *FURIN* expression

Sample	Title	Value
GSM27185	Male Placebo-Treated Lacrimal Gland Sample A	21.6254
GSM27186	Male Placebo-Treated Lacrimal Gland Sample B	15.916
GSM27187	Male Placeo-Treated Lacrimal Gland Sample C	14.0492
GSM27188	Male Testosterone-Treated Lacrimal Gland Sample A	**5.04977**
GSM27189	Male Testosterone-Treated Lacrimal Gland Sample B	**6.27436**
GSM27190	Male Testosterone-Treated Lacrimal Gland Sample C	**6.81647**
GSM27197	Male Placebo-Treated Submandibular Gland Sample A	**1.62319**
GSM27198	Male Placebo-Treated Submandibular Gland Sample B	**1.54446**
GSM27199	Male Placebo-Treated Submandibular Gland Sample C	**1.27973**
GSM27200	Male Testosterone-Treated Submandibular Gland Sample A	**4.75181**
GSM27201	Male Testosterone-Treated Submandibular Gland Sample B	**2.12511**
GSM27202	Male Testosterone-Treated Submandibular Gland Sample C	**3.60242**
GSM27191	Male Placebo-Treated Meibomian Gland Sample A	4.08816
GSM27192	Male Placebo-Treated Meibomian Gland Sample B	4.09734
GSM27193	Male Placebo-Treated Meibomian Gland Sample C	4.58029
GSM27194	Male Testosterone-Treated Meibomian Gland Sample A	3.08708
GSM27195	Male Testosterone-Treated Meibomian Gland Sample B	3.88995
GSM27196	Male Testosterone-Treated Meibomian Gland Sample C	4.22759

p = 0.004

p = 0.029

Profile: *HMGA2* expression
GDS5301 / 1450780_PM_s_at
Title
Androgen deprivation effect on CD4 T-cells
Organism
Mus musculus

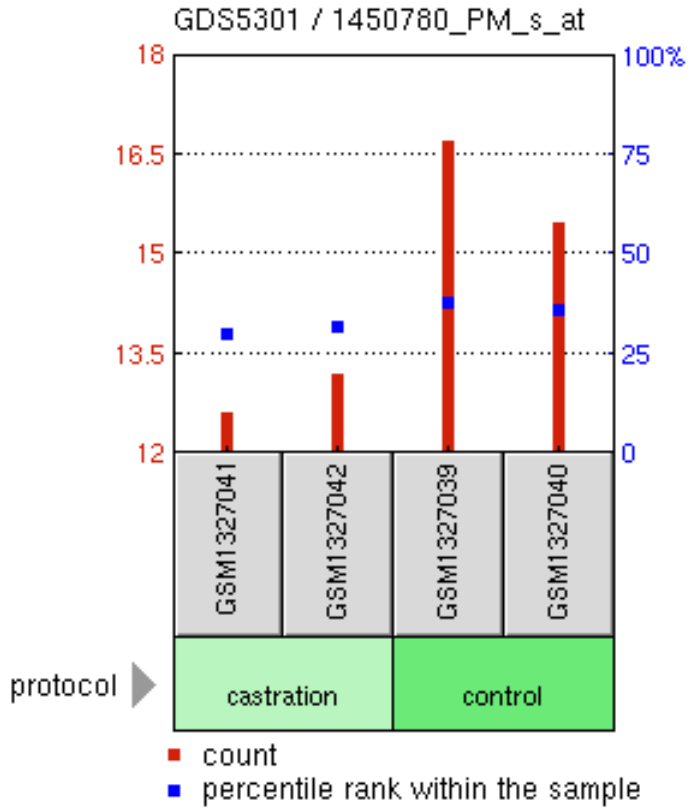

p = 0.021

Castration decreases *HMGA2* expression

Sample	Title	Value
GSM1327041	Cast_1	**12.6312**
GSM1327042	Cast_2	**13.2155**
GSM1327039	Sham_1	16.7133
GSM1327040	Sham_2	15.4878

Profile: *INSIG1* expression
GDS5301 / 1454671_PM_at
Title
Androgen deprivation effect on CD4 T-cells
Organism
Mus musculus

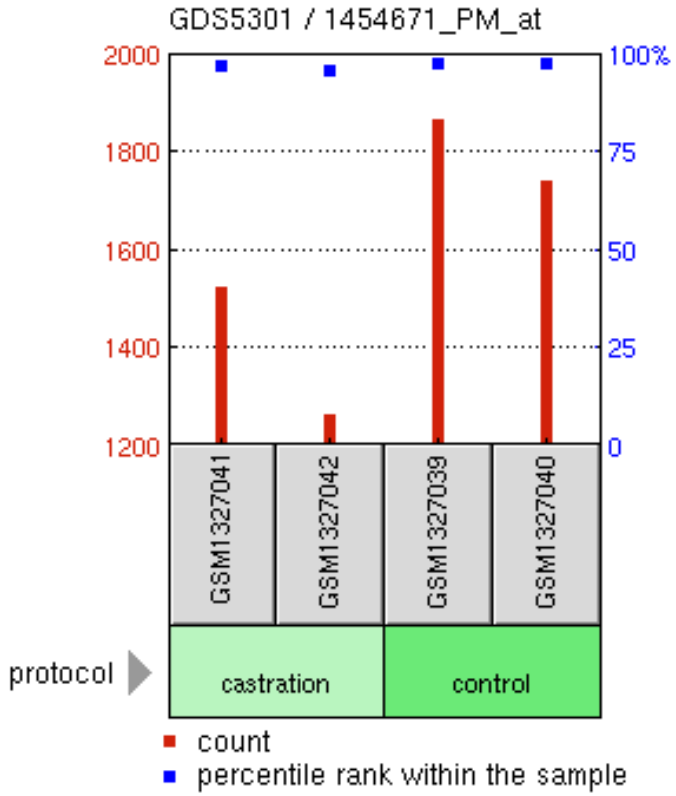

p = 0.053

Castration decreases *INSIG1* expression

Sample	Title	Value
GSM1327041	Cast_1	**1525.05**
GSM1327042	Cast_2	**1265.23**
GSM1327039	Sham_1	1866.04
GSM1327040	Sham_2	1741.1

Profile: *GATA5* expression
GDS1361 / 3834
Title
Testosterone effect on meibomian gland
Organism
Mus musculus

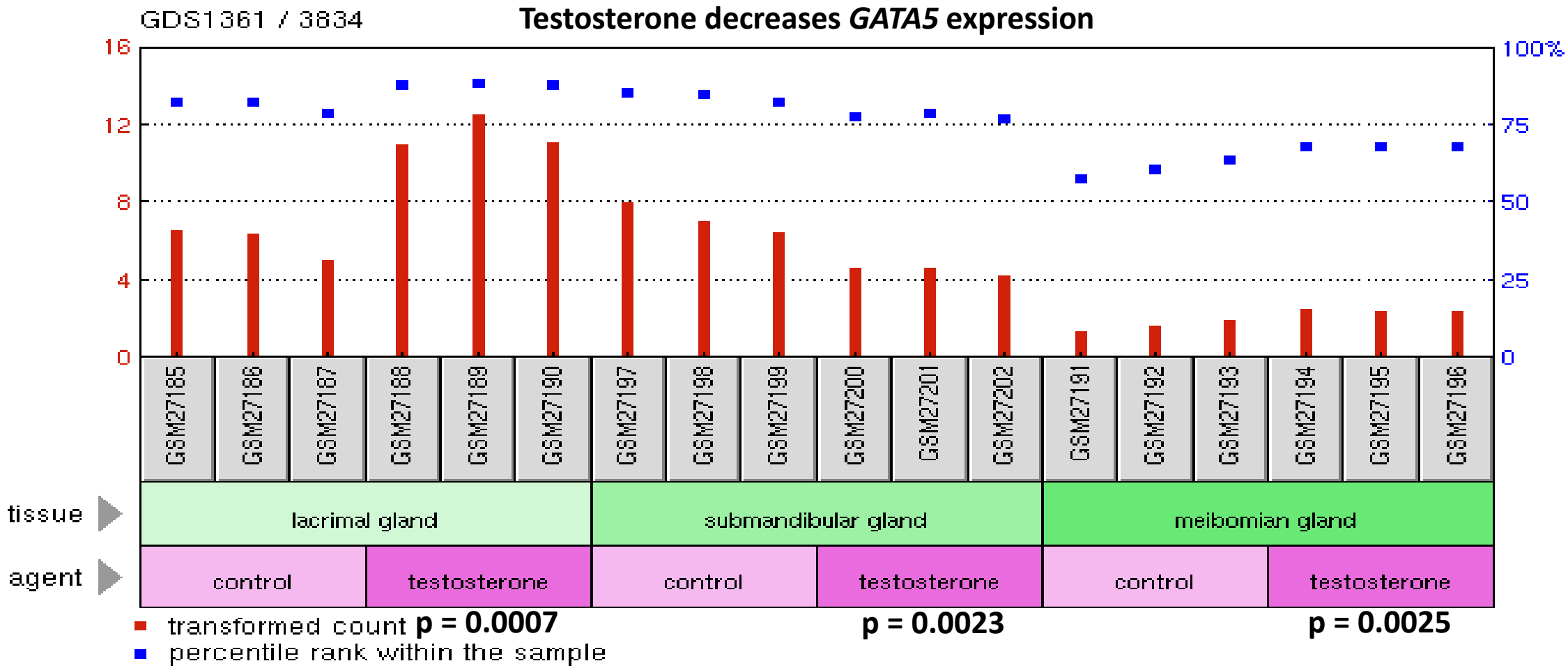

Profile: *GATA5* expression
GDS1361 / 3834
Title
Testosterone effect on meibomian gland
Organism
Mus musculus

Testosterone decreases *GATA5* expression

Sample	Title	Value	
GSM27185	Male Placebo-Treated Lacrimal Gland Sample A	6.64621	
GSM27186	Male Placebo-Treated Lacrimal Gland Sample B	6.45423	**p = 0.0007**
GSM27187	Male Placeo-Treated Lacrimal Gland Sample C	5.10327	
GSM27188	Male Testosterone-Treated Lacrimal Gland Sample A	**10.9893**	
GSM27189	Male Testosterone-Treated Lacrimal Gland Sample B	**12.5373**	
GSM27190	Male Testosterone-Treated Lacrimal Gland Sample C	**11.1312**	
GSM27197	Male Placebo-Treated Submandibular Gland Sample A	**8.00934**	
GSM27198	Male Placebo-Treated Submandibular Gland Sample B	**7.04778**	**p = 0.0023**
GSM27199	Male Placebo-Treated Submandibular Gland Sample C	**6.52222**	
GSM27200	Male Testosterone-Treated Submandibular Gland Sample A	**4.71727**	
GSM27201	Male Testosterone-Treated Submandibular Gland Sample B	**4.67808**	
GSM27202	Male Testosterone-Treated Submandibular Gland Sample C	**4.25649**	
GSM27191	Male Placebo-Treated Meibomian Gland Sample A	1.42448	
GSM27192	Male Placebo-Treated Meibomian Gland Sample B	1.65382	**p = 0.0025**
GSM27193	Male Placebo-Treated Meibomian Gland Sample C	1.92874	
GSM27194	Male Testosterone-Treated Meibomian Gland Sample A	**2.54996**	
GSM27195	Male Testosterone-Treated Meibomian Gland Sample B	**2.49176**	
GSM27196	Male Testosterone-Treated Meibomian Gland Sample C	**2.45951**	

ACE2 and FURIN

Supplemental Figure S12. Potential mechanisms affecting gene expression inferred from

transgenic mouse models and observed in pathophysiologically & therapeutically relevant mouse and human cells:

A knowledge path toward potential therapy-enhancing interventions

Profile: ACE2 expression
GDS4584 / 1425103_at
Title
Alveolar type I cells deficient in sterol-response element-binding proteins inhibitor Insig1/2
Organism
Mus musculus

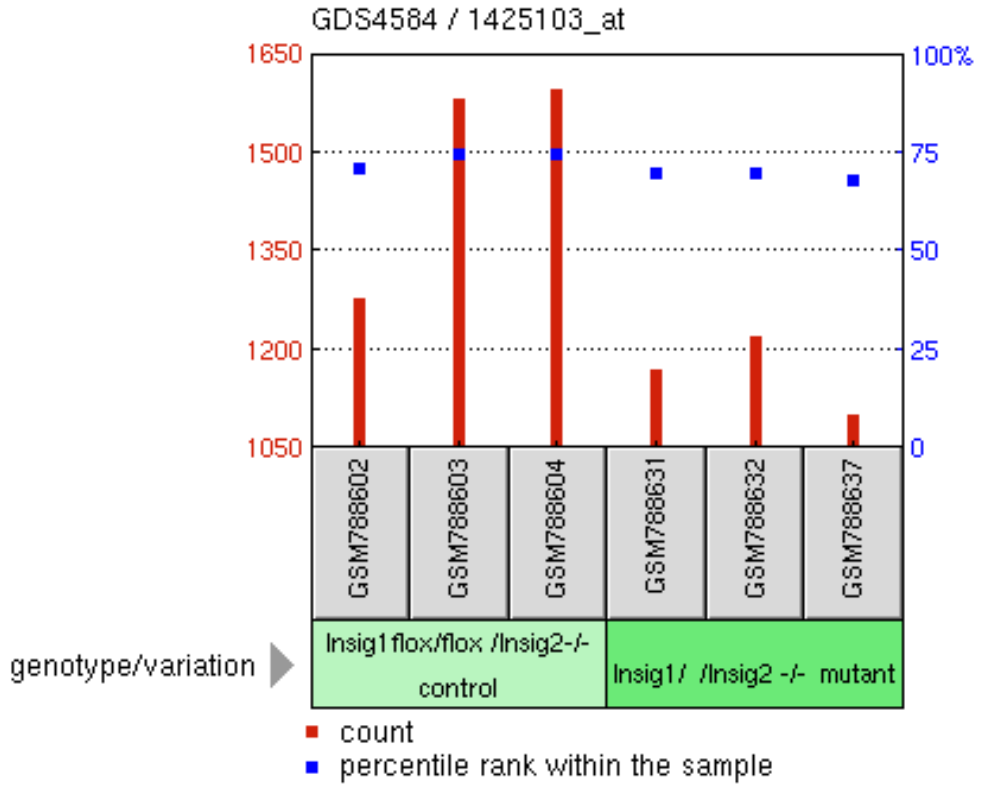

p = 0.021

Insig1: a candidate activator of the *ACE2* expression

Sample	Title	Value
GSM788602	Insig1 flox/flox /Insig2 -/- InsigKO_C1	1279.8
GSM788603	Insig1 flox/flox /Insig2 -/- InsigKO_C2	1584.9
GSM788604	Insig1 flox/flox /Insig2 -/- InsigKO_C3	1596
GSM788631	Insig1 Δ/Δ /Insig2 -/- InsigKO_E1	1169.8
GSM788632	Insig1 Δ/Δ /Insig2 -/- InsigKO_E2	1223
GSM788637	Insig1 Δ/Δ /Insig2 -/- InsigKO_E3	1102.8

Profile: ACE2 expression
GDS4584 / 1452138_a_at
Title
Alveolar type I cells deficient in sterol-response element-binding proteins inhibitor Insig1/2
Organism
Mus musculus

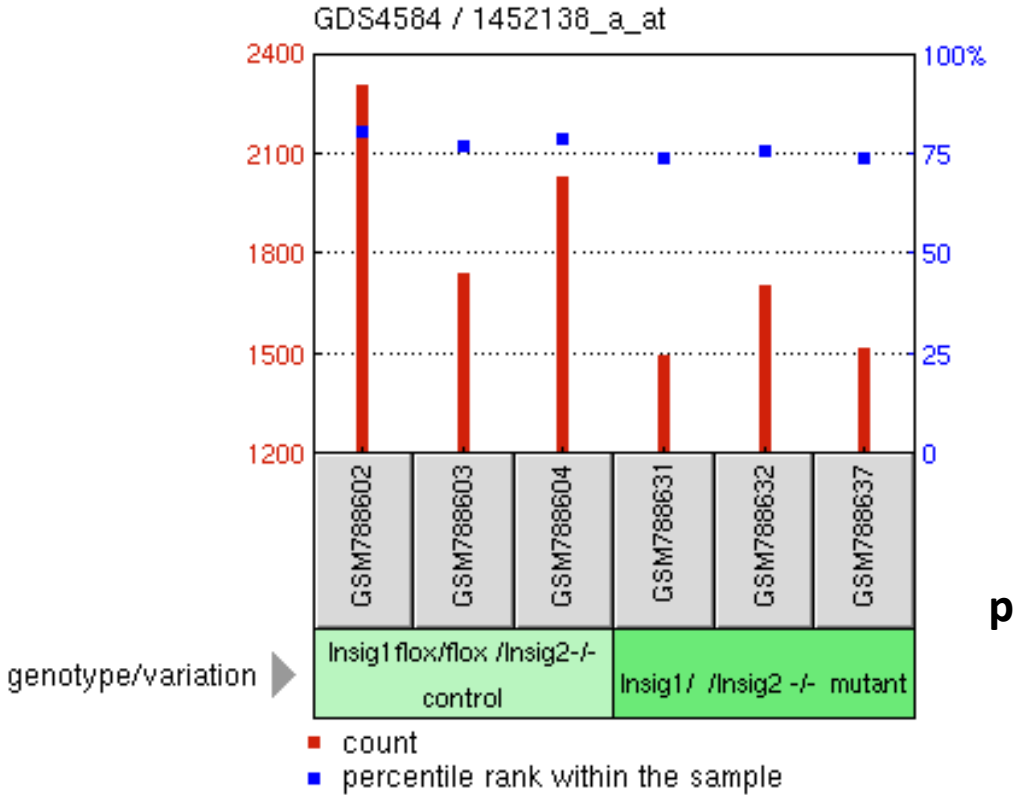

p = 0.031

Insig1: a candidate activator of the *ACE2* expression

Sample	Title	Value
GSM788602	Insig1 flox/flox /Insig2 -/- InsigKO_C1	2309.1
GSM788603	Insig1 flox/flox /Insig2 -/- InsigKO_C2	1742.5
GSM788604	Insig1 flox/flox /Insig2 -/- InsigKO_C3	2032.3
GSM788631	Insig1 Δ/Δ /Insig2 -/- InsigKO_E1	1496.5
GSM788632	Insig1 Δ/Δ /Insig2 -/- InsigKO_E2	1706.9
GSM788637	Insig1 Δ/Δ /Insig2 -/- InsigKO_E3	1518.6

Profile: *INSIG1* expression
GDS3676 / 201625_s_at
Title
Quercetin effect on CD14+ monocyte
Organism
Homo sapiens

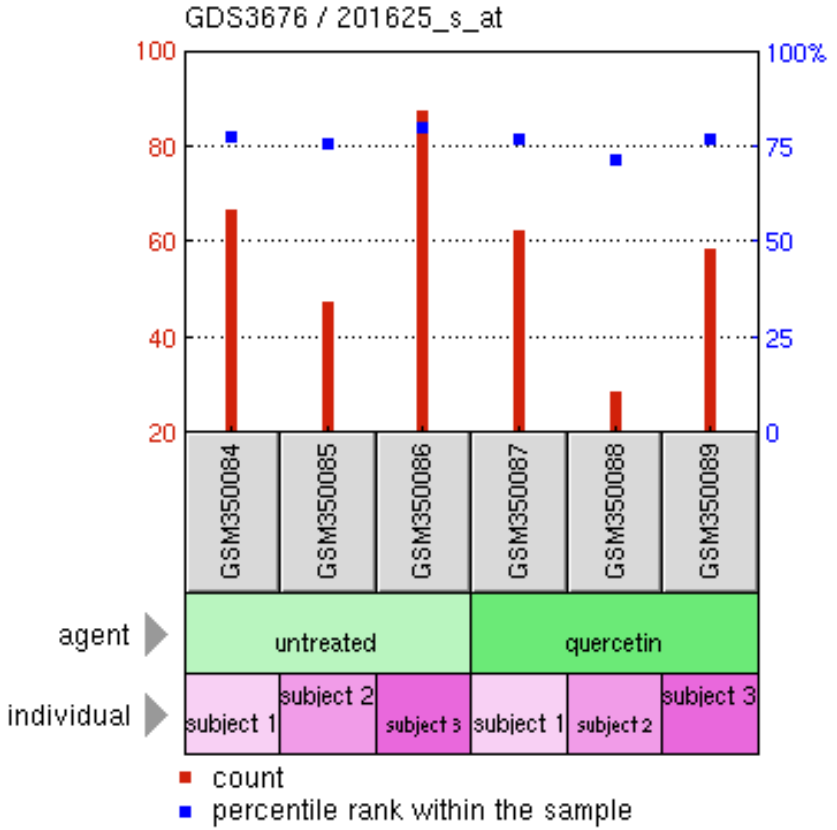

Quercetin inhibits the *INSIG1* expression

Sample	Title	Value	Percent changes
GSM350084	CD14+ at baseline, biological replicate 1	**66.9724**	
GSM350085	CD14+ at baseline, biological replicate 2	**47.9219**	
GSM350086	CD14+ at baseline, biological replicate 3	**87.5973**	
GSM350087	CD14+ after 2 wk quercetin supplementation, biological replicate 1	**62.5927**	**- 7%**
GSM350088	CD14+ after 2 wk quercetin supplementation, biological replicate 2	**28.8386**	**- 40%**
GSM350089	CD14+ after 2 wk quercetin supplementation, biological replicate 3	**58.8768**	**- 33%**

Profile: *HIF1a* expression
GDS4584 / 1427418_a_at
Title
Alveolar type I cells deficient in sterol-response element-binding proteins inhibitor Insig1/2
Organism
Mus musculus

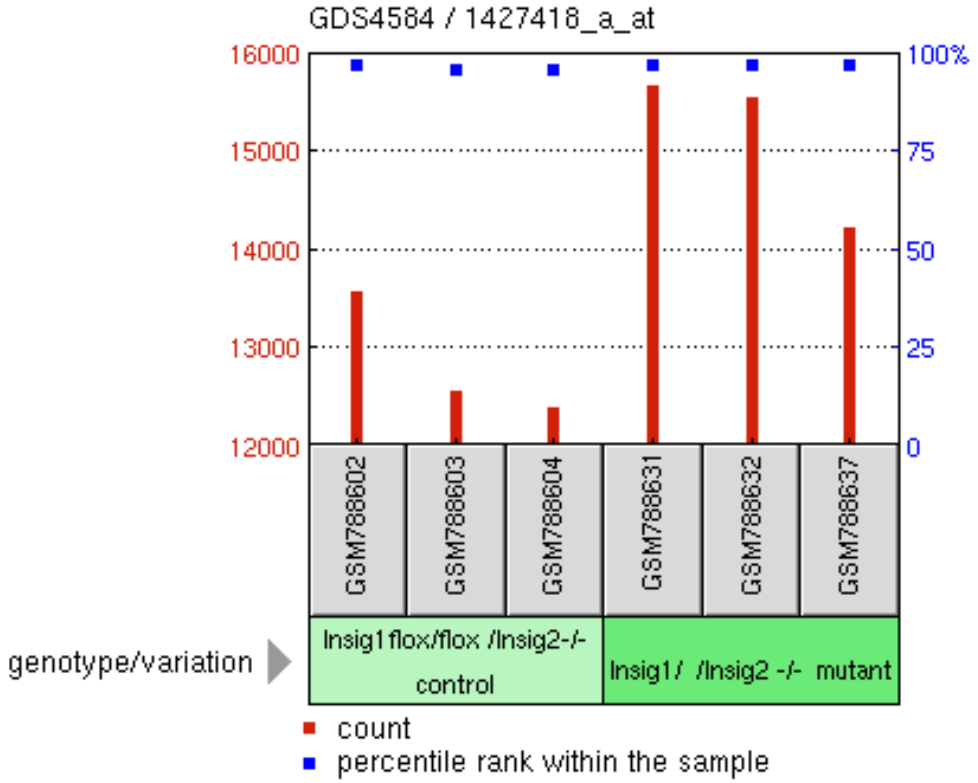

p = 0.018

Insig1: a candidate repressor of the *HIF1a* expression

Sample	Title	Value
GSM788602	Insig1 flox/flox /Insig2 -/- InsigKO_C1	13581.9
GSM788603	Insig1 flox/flox /Insig2 -/- InsigKO_C2	12568
GSM788604	Insig1 flox/flox /Insig2 -/- InsigKO_C3	12390.1
GSM788631	Insig1 Δ/Δ /Insig2 -/- InsigKO_E1	**15685.4**
GSM788632	Insig1 Δ/Δ /Insig2 -/- InsigKO_E2	**15544.2**
GSM788637	Insig1 Δ/Δ /Insig2 -/- InsigKO_E3	**14222.5**

Profile: *HIF1a* expression
GDS3676 / 200989_at
Title
Quercetin effect on CD14+ monocyte
Organism
Homo sapiens

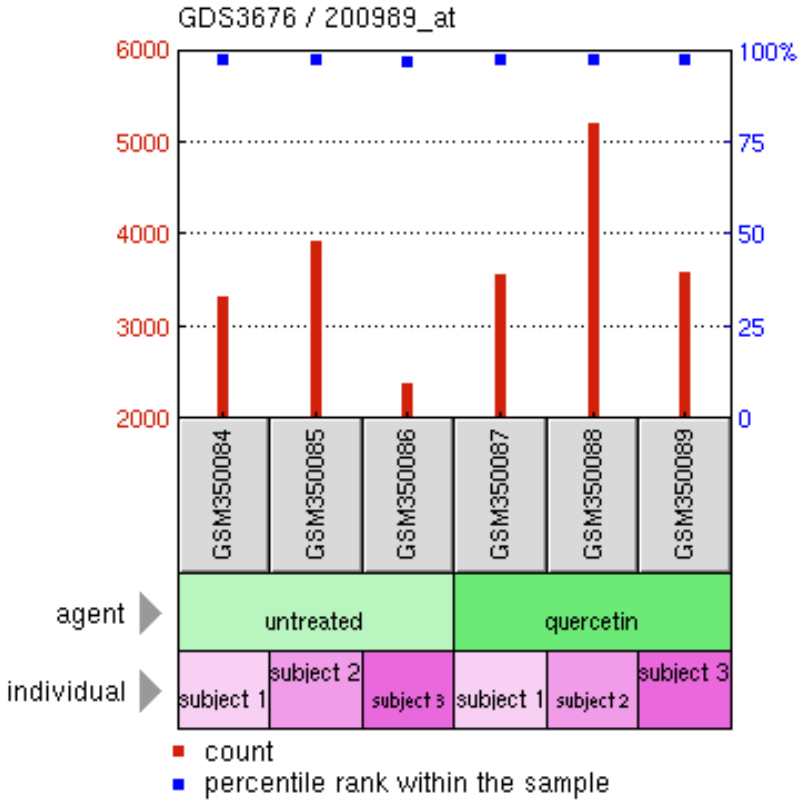

Quercetin activates the *HIF1a* expression

Sample	Title	Value
GSM350084	CD14+ at baseline, biological replicate 1	**3338.47**
GSM350085	CD14+ at baseline, biological replicate 2	**3929.88**
GSM350086	CD14+ at baseline, biological replicate 3	**2388.45**
GSM350087	CD14+ after 2 wk quercetin supplementation, biological replicate 1	**3577.94 (+ 7.2%)**
GSM350088	CD14+ after 2 wk quercetin supplementation, biological replicate 2	**5206.25 (+32.5%)**
GSM350089	CD14+ after 2 wk quercetin supplementation, biological replicate 3	**3604.21 (+50.9%)**

Profile: *HIF1A* expression
GDS3032 / 200989_at
Title
Quercetin effect on intestinal cell differentiation in vitro: time course
Organism
Homo sapiens

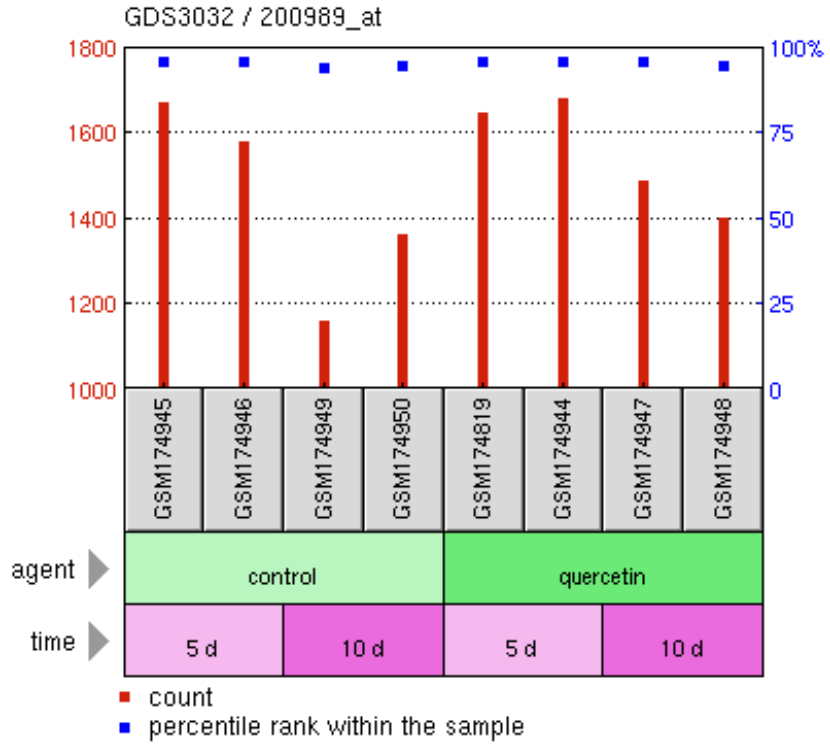

Quercetin ameliorates decline of the *HIF1a* expression

Sample	Title	Value	
GSM174945	Control day 05 sample 1	1673.78	**1628**
GSM174946	Control day 05 sample 2	1582.51	
GSM174949	Control day 10 sample 1	**1163.29**	**1264 (-22.4%)**
GSM174950	Control day 10 sample 2	**1364.98**	
GSM174819	Quercetin day 05 sample 1	1646.59	**1663**
GSM174944	Quercetin day 05 sample 2	1680.64	
GSM174947	Quercetin day 10 sample 1	1491.23	**1447 (-13.0%)**
GSM174948	Quercetin day 10 sample 2	1403.56	

Profile: ACE2
GDS4876 / 1425103_at
Title
Pulmonary surfactant protein-C deficiency effect on alveolar type II epithelial cell
Organism
Mus musculus

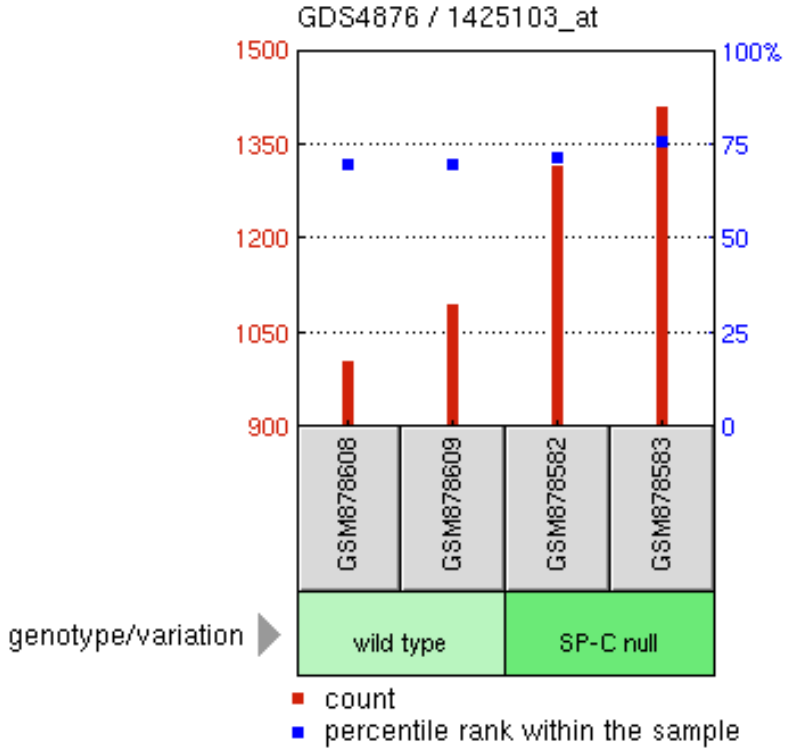

p = 0.021

SP-C (SFTPC): a candidate inhibitor of the *ACE2* expression

Sample	Title	Value
GSM878608	Wild-type Type II 1_8_9_04	1006
GSM878609	Wild-type Type II 9_27_04	1097.9
GSM878582	KO SPC Type II 9_27_04	1317.1
GSM878583	KO SPC Type II 2_8_9_04	1413.2

Profile: FURIN expression
GDS4876 / 1418518_at
Title
Pulmonary surfactant protein-C deficiency effect on alveolar type II epithelial cell
Organism
Mus musculus

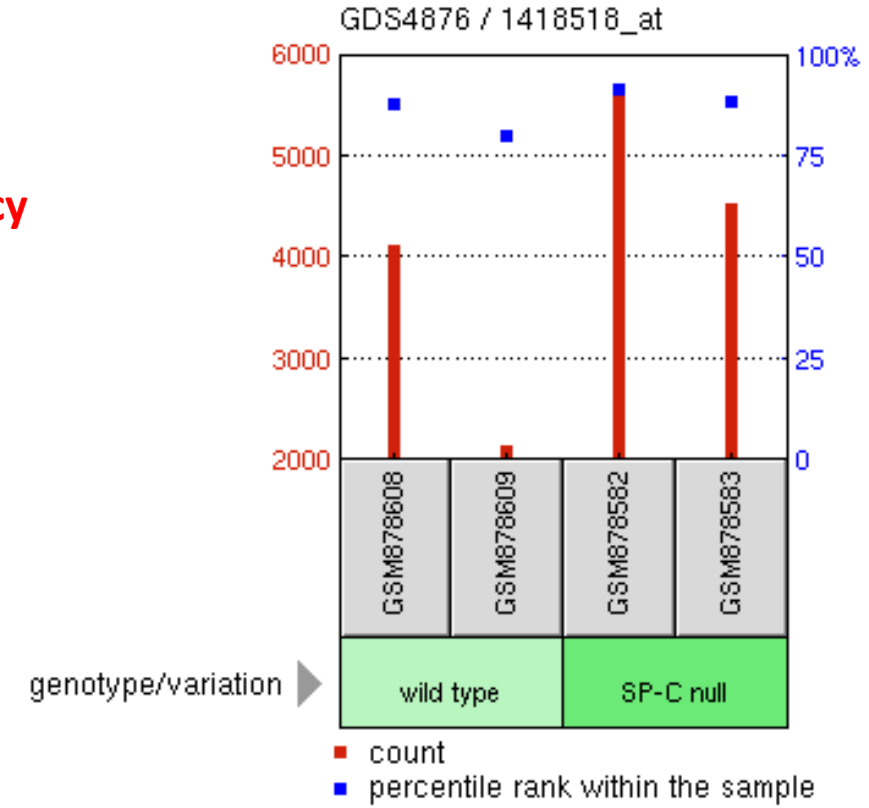

p = 0.114

SP-C (SFTPC): a candidate inhibitor of the *FURIN* expression

Sample	Title	Value
GSM878608	Wild-type Type II 1_8_9_04	4141.2
GSM878609	Wild-type Type II 9_27_04	2156.1
GSM878582	KO SPC Type II 9_27_04	5733
GSM878583	KO SPC Type II 2_8_9_04	4537.4

Profile: SP-C (SFTPC) expression
GDS3032 / 214387_x_at
Title
Quercetin effect on intestinal cell differentiation in vitro: time course
Organism
Homo sapiens

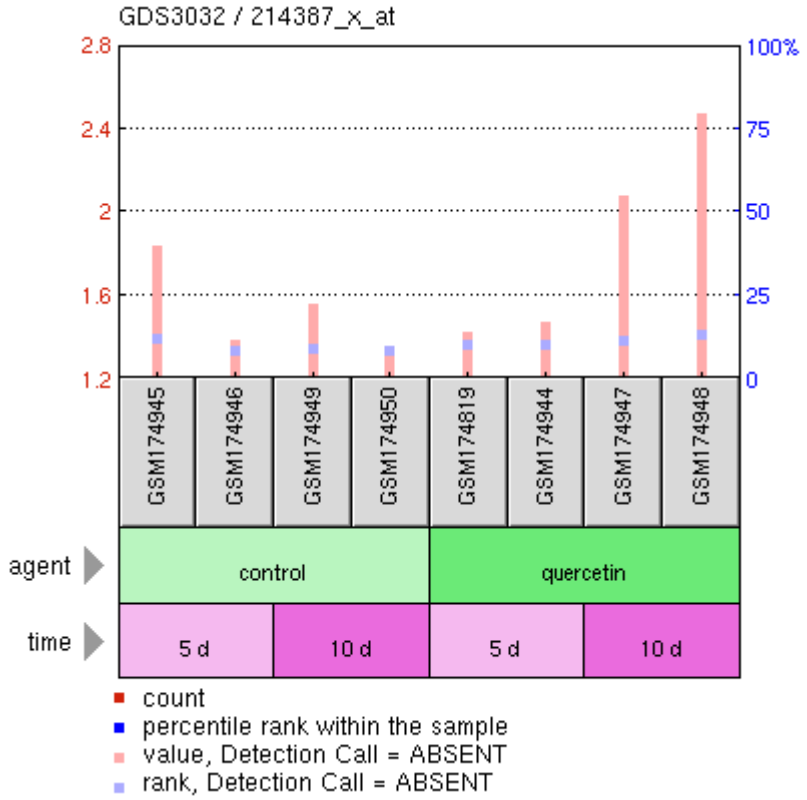

10 days
p = 0.033

Quercetin enhances the *SP-1 (SFTPC)* expression

Sample	Title	Value
GSM174945	Control day 05 sample 1	1.84127
GSM174946	Control day 05 sample 2	1.38638
GSM174949	Control day 10 sample 1	1.56441
GSM174950	Control day 10 sample 2	1.35256
GSM174819	Quercetin day 05 sample 1	1.42897
GSM174944	Quercetin day 05 sample 2	1.47099
GSM174947	Quercetin day 10 sample 1	2.08499
GSM174948	Quercetin day 10 sample 2	2.47973

Profile: SP-C (SFTPC) expression
GDS3676 / 38691_s_at
Title
Quercetin effect on CD14+ monocyte
Organism
Homo sapiens

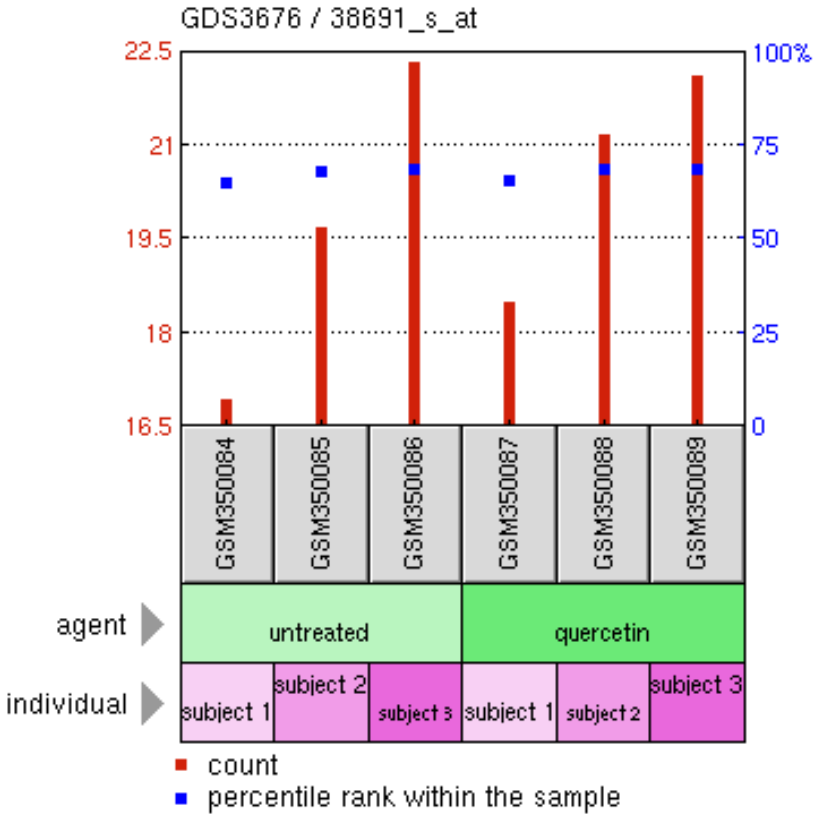

Quercetin enhances the *SP-1 (SFTPC)* expression

Sample	Title	Value
GSM350084	CD14+ at baseline, biological replicate 1	**16.9619**
GSM350085	CD14+ at baseline, biological replicate 2	**19.6833**
GSM350086	CD14+ at baseline, biological replicate 3	**22.3292**
GSM350087	CD14+ after 2 wk quercetin supplementation, biological replicate 1	**18.5089**
GSM350088	CD14+ after 2 wk quercetin supplementation, biological replicate 2	**21.1853**
GSM350089	CD14+ after 2 wk quercetin supplementation, biological replicate 3	**22.11**

Profile: ACE2 expression
GDS5048 / 10603066
Title
High Mobility Group AT-hook Protein 2 deficiency effect on the embryonic lung
Organism
Mus musculus

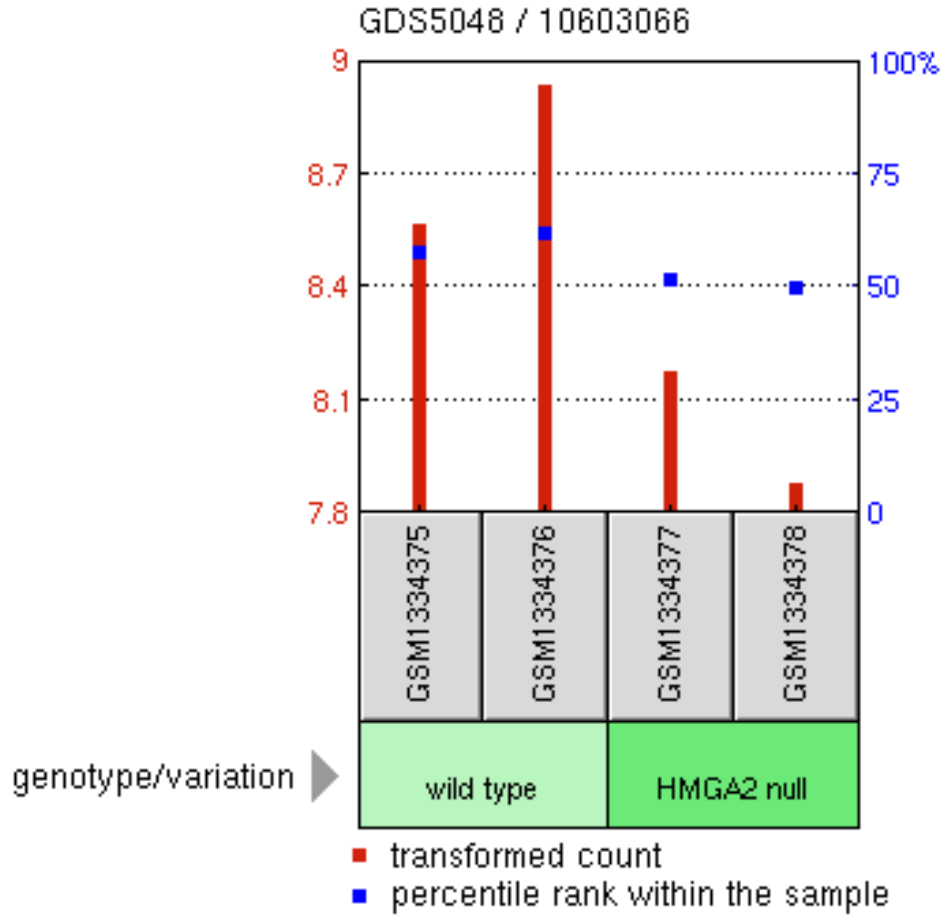

p = 0.046

HMGA2: a candidate activator of the *ACE2* expression

Sample	Title	Value
GSM1334375	E18.5 lung WT1, biological rep1	8.57131
GSM1334376	E18.5 lung WT1, biological rep2	8.93831
GSM1334377	E18.5 lung KO1, biological rep1	8.18208
GSM1334378	E18.5 lung KO2, biological rep2	7.87966

Profile: *INSIG1* expression
GDS5048 / 10520362
Title
High Mobility Group AT-hook Protein 2 deficiency effect on the embryonic lung
Organism
Mus musculus

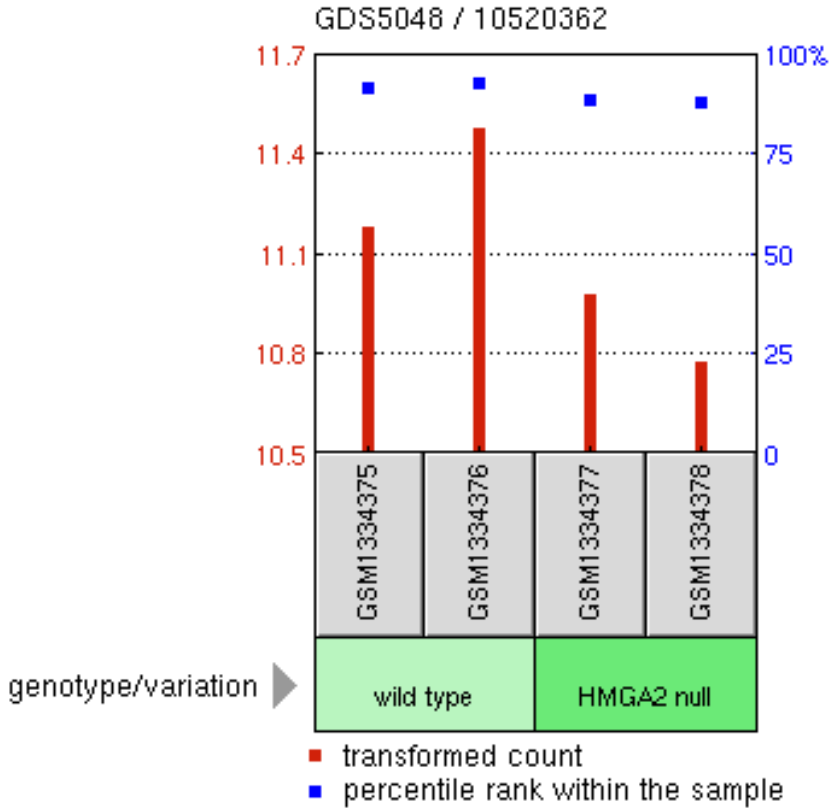

p = 0.062

HMGA2: a candidate activator of the *INSIG1* expression

Sample	Title	Value
GSM1334375	E18.5 lung WT1, biological rep1	11.1863
GSM1334376	E18.5 lung WT1, biological rep2	11.4769
GSM1334377	E18.5 lung KO1, biological rep1	10.9789
GSM1334378	E18.5 lung KO2, biological rep2	10.7801

Profile: *SFTPC* expression
GDS5048 / 10421387
Title
High Mobility Group AT-hook Protein 2 deficiency effect on the embryonic lung
Organism
Mus musculus

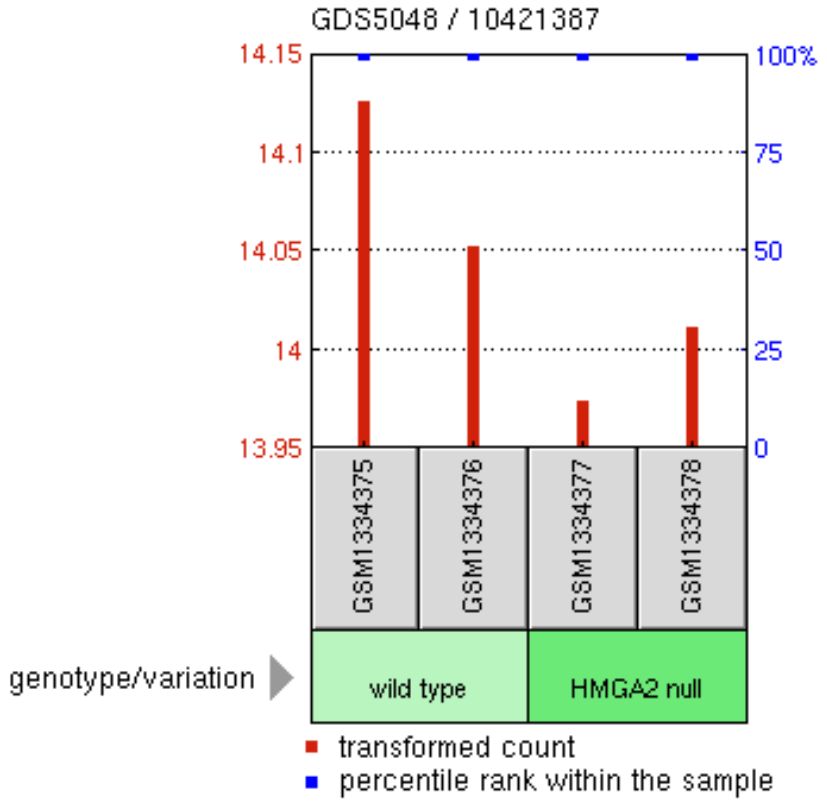

p = 0.073

HMGA2: a candidate activator of the *SFTPC* expression

Sample	Title	Value
GSM1334375	E18.5 lung WT1, biological rep1	14.1269
GSM1334376	E18.5 lung WT1, biological rep2	14.0528
GSM1334377	E18.5 lung KO1, biological rep1	13.975
GSM1334378	E18.5 lung KO2, biological rep2	14.0121

Profile: HMGA2 expression
GDS3676 / 1561633_at
Title
Quercetin effect on CD14+ monocyte
Organism
Homo sapiens

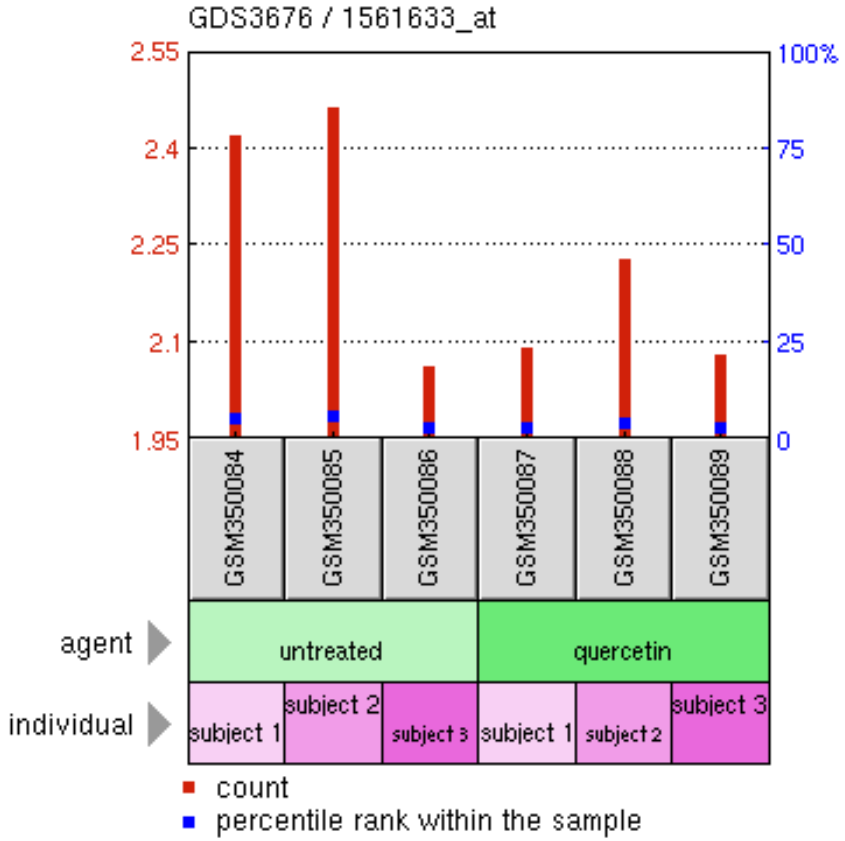

Quercetin inhibits the *HMGA2* expression

Sample	Title	Value
GSM350084	CD14+ at baseline, biological replicate 1	**2.4219**
GSM350085	CD14+ at baseline, biological replicate 2	**2.46504**
GSM350086	CD14+ at baseline, biological replicate 3	**2.06307**
GSM350087	CD14+ after 2 wk quercetin supplementation, biological replicate 1	**2.09436**
GSM350088	CD14+ after 2 wk quercetin supplementation, biological replicate 2	**2.22984**
GSM350089	CD14+ after 2 wk quercetin supplementation, biological replicate 3	**2.0814**

Profile: HMGA2 expression
GDS3032 / 208025_s_at
Title
Quercetin effect on intestinal cell differentiation in vitro: time course
Organism
Homo sapiens

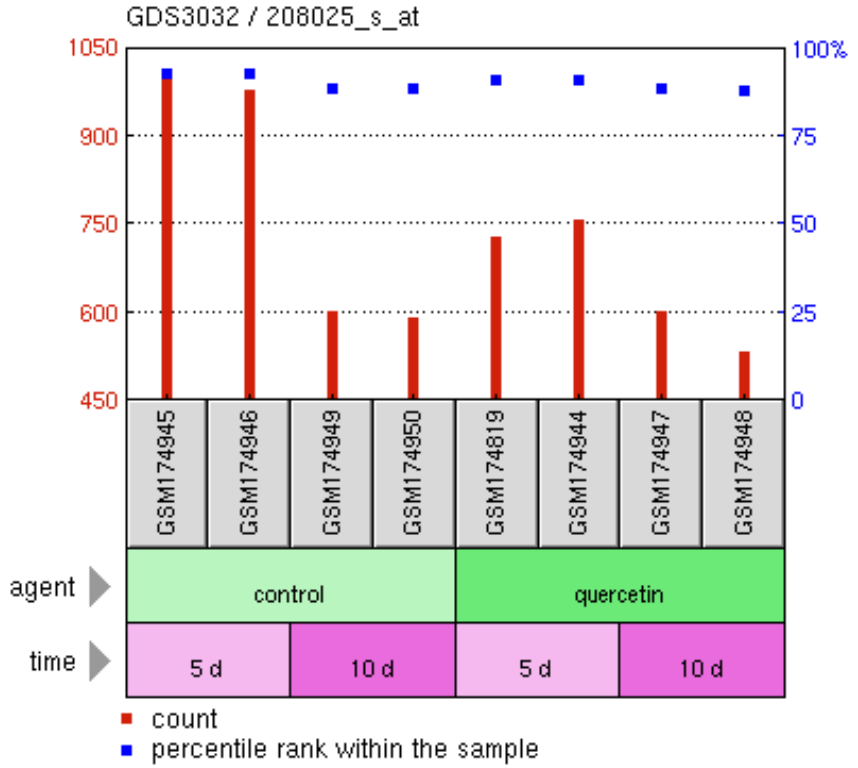

5 days
p = 0.004

Quercetin inhibits the *HMGA2* expression

Sample	Title	Value
GSM174945	Control day 05 sample 1	1015.28
GSM174946	Control day 05 sample 2	977.764
GSM174949	Control day 10 sample 1	601.884
GSM174950	Control day 10 sample 2	591.613
GSM174819	Quercetin day 05 sample 1	729.032
GSM174944	Quercetin day 05 sample 2	758.127
GSM174947	Quercetin day 10 sample 1	602.964
GSM174948	Quercetin day 10 sample 2	535.877

Profile: HMGA2 expression
GDS2708 / 14220
Title
Quercetin effect on cultured cardiomyocytes: time course
Organism
Rattus norvegicus

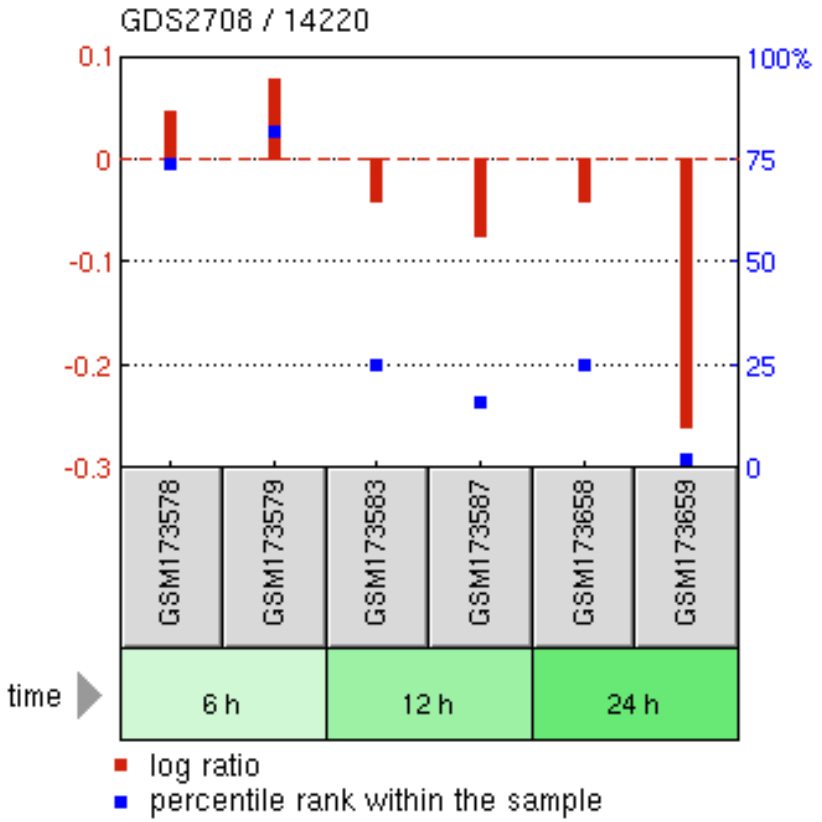

p = 0.017

Quercetin inhibits the *HMGA2* expression

Sample	Title	Value
GSM173578	Quercetin treated cardiomyocytes for 6 hours (Q6-A).	0.0475828
GSM173579	Quercetin treated cardiomyocytes for 6 hours (Q6-B).	0.0794489
GSM173583	Quercetin treated cardiomyocytes for 12 hours (Q12-A).	-0.0439453
GSM173587	Quercetin treated cardiomyocytes for 12 hours (Q12-B).	-0.078307
GSM173658	Quercetin treated cardiomyocytes for 24 hours (Q24-A).	-0.0439453
GSM173659	Quercetin treated cardiomyocytes for 24 hours (Q24-B).	-0.262591

Profile: *HMGA2* expression
GDS2628 / 1559891_at
Title
Vitamin D effect on bronchial smooth muscle cells
Organism
Homo sapiens

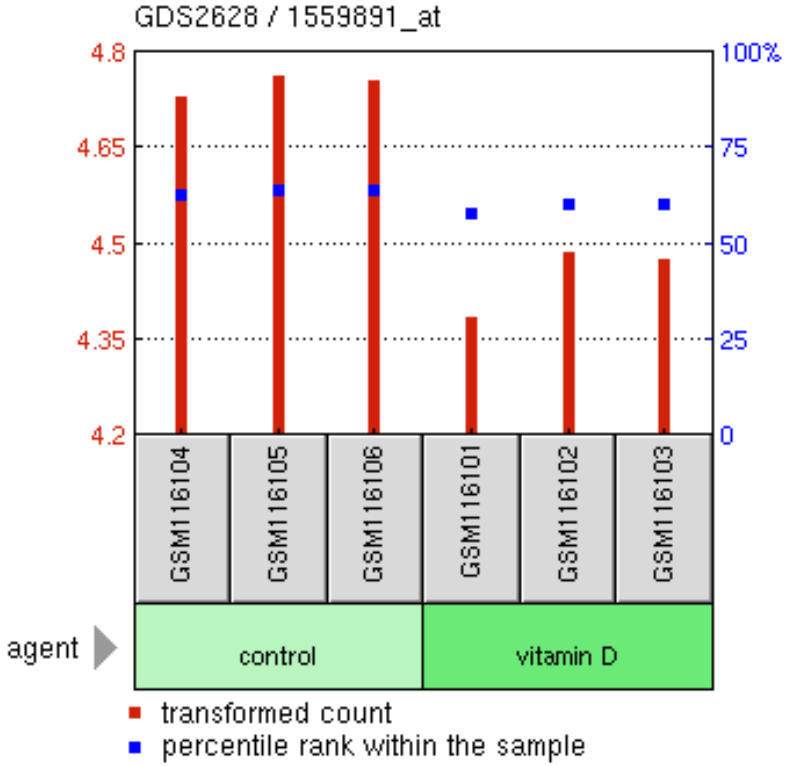

p = 0.0005

Vitamin D inhibits the *HMGA2* expression

Sample	Title	Value
GSM116104	hBSMC_control_rep1	4.73008
GSM116105	hBSMC_control_rep2	4.7629
GSM116106	hBSMC_control_rep3	4.75495
GSM116101	hBSMC_vitamin D_rep1	4.38522
GSM116102	hBSMC_vitamin D_rep2	4.48749
GSM116103	hBSMC_vitamin D_rep3	4.47664

Profile: *HMGA2* expression
GDS2628 / 208025_s_at
Title
Vitamin D effect on bronchial smooth muscle cells
Organism
Homo sapiens

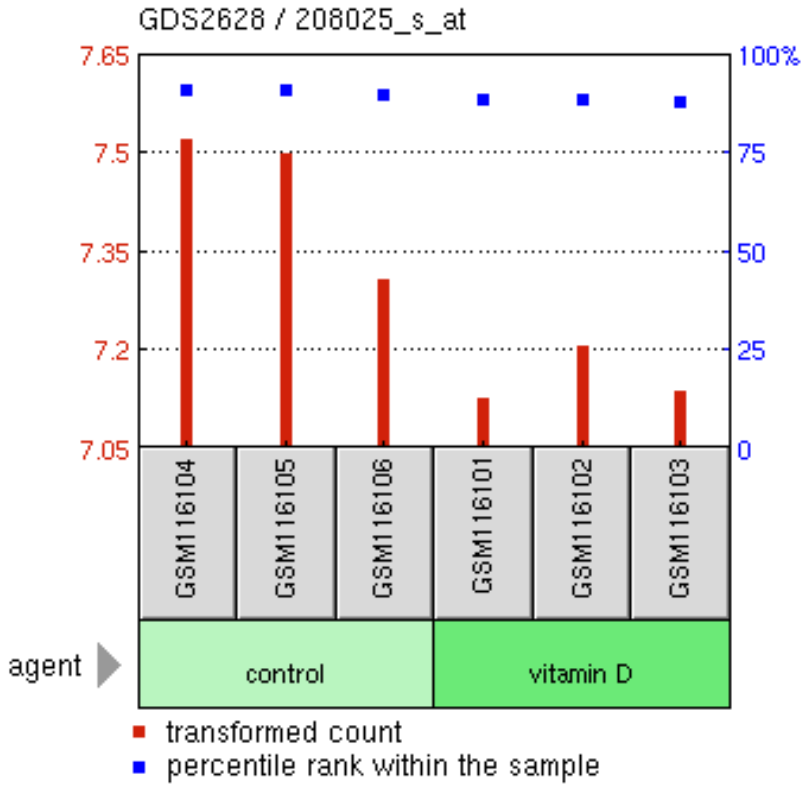

p = 0.008

Vitamin D inhibits the *HMGA2* expression

Sample	Title	Value
GSM116104	hBSMC_control_rep1	7.52243
GSM116105	hBSMC_control_rep2	7.50027
GSM116106	hBSMC_control_rep3	7.3098
GSM116101	hBSMC_vitamin D_rep1	7.12949
GSM116102	hBSMC_vitamin D_rep2	7.20614
GSM116103	hBSMC_vitamin D_rep3	7.13995

Profile: ACE2 expression
GDS4809 / 1425103_at
Title
Gata5 deficiency effect on the lung
Organism
Mus musculus

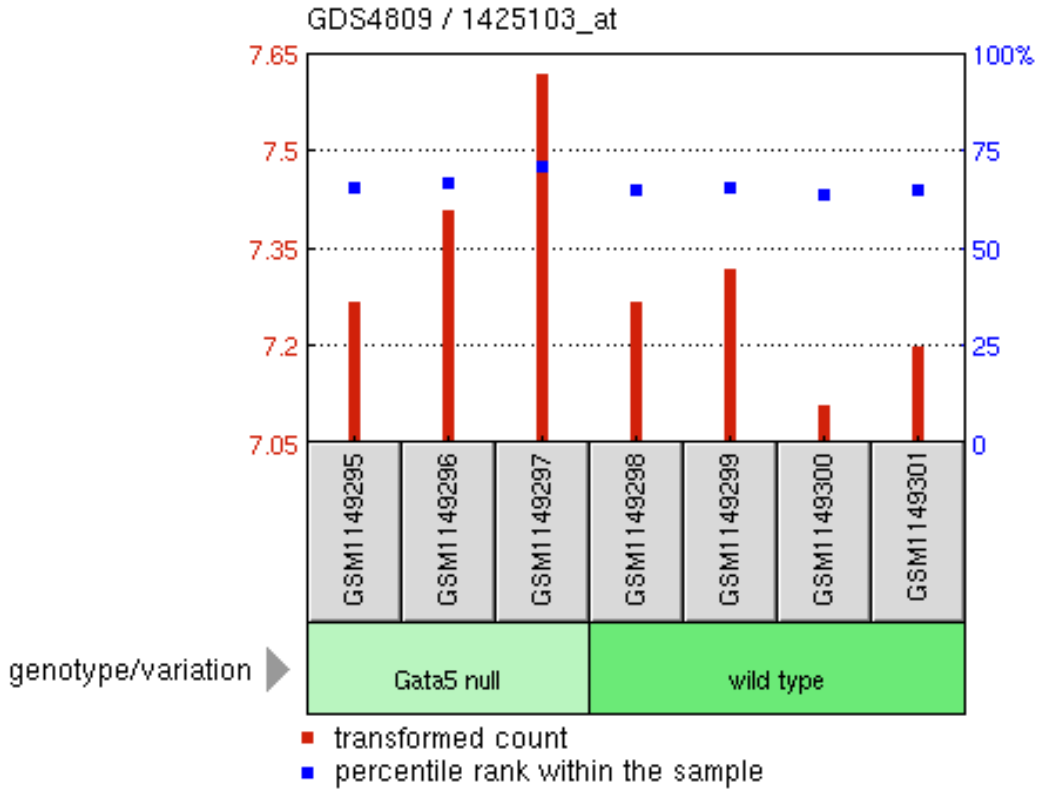

p = 0.0467

GATA5: a candidate inhibitor of the *ACE2* expression

Sample	Title	Value
GSM1149295	KO618	7.27
GSM1149296	KO621	7.41
GSM1149297	KO624	7.62
GSM1149298	WT619	7.27
GSM1149299	WT623	7.32
GSM1149300	WT648	7.11
GSM1149301	WT659	7.2

Profile: *VDR* expression
GDS4809 / 1418176_at
Title
Gata5 deficiency effect on the lung
Organism
Mus musculus

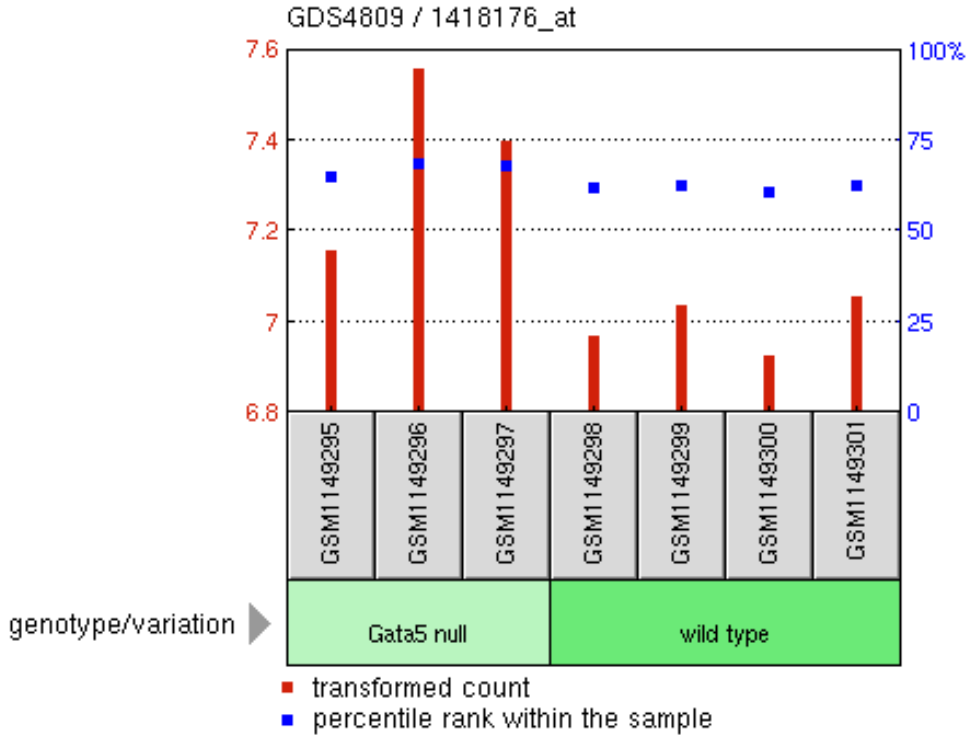

p = 0.008

GATA5: a candidate inhibitor of the *VDR* expression

Sample	Title	Value
GSM1149295	KO618	7.16
GSM1149296	KO621	7.56
GSM1149297	KO624	7.4
GSM1149298	WT619	6.97
GSM1149299	WT623	7.04
GSM1149300	WT648	6.93
GSM1149301	WT659	7.06

Profile: *SFTPC* expression
GDS4809 / 1418639_at
Title
Gata5 deficiency effect on the lung
Organism
Mus musculus

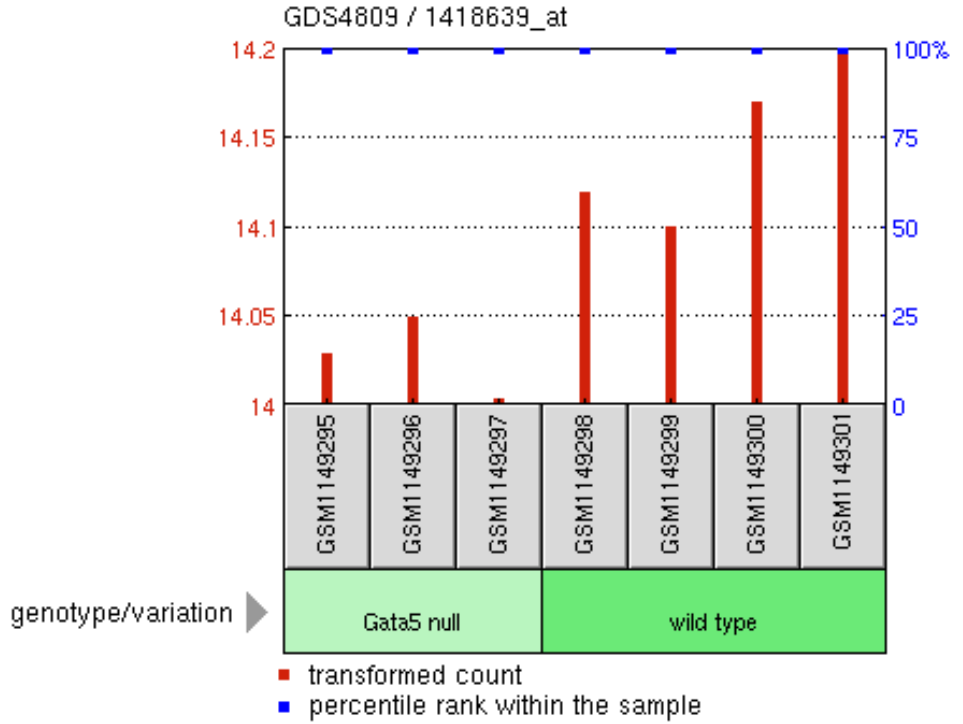

p = 0.005

GATA5: a candidate activator of the *SFTPC* expression

Sample	Title	Value
GSM1149295	KO618	14.03
GSM1149296	KO621	14.05
GSM1149297	KO624	14
GSM1149298	WT619	14.12
GSM1149299	WT623	14.1
GSM1149300	WT648	14.17
GSM1149301	WT659	14.2

Profile: GATA5 expression
GDS2708 / 15347
Title
Quercetin effect on cultured cardiomyocytes: time course
Organism
Rattus norvegicus

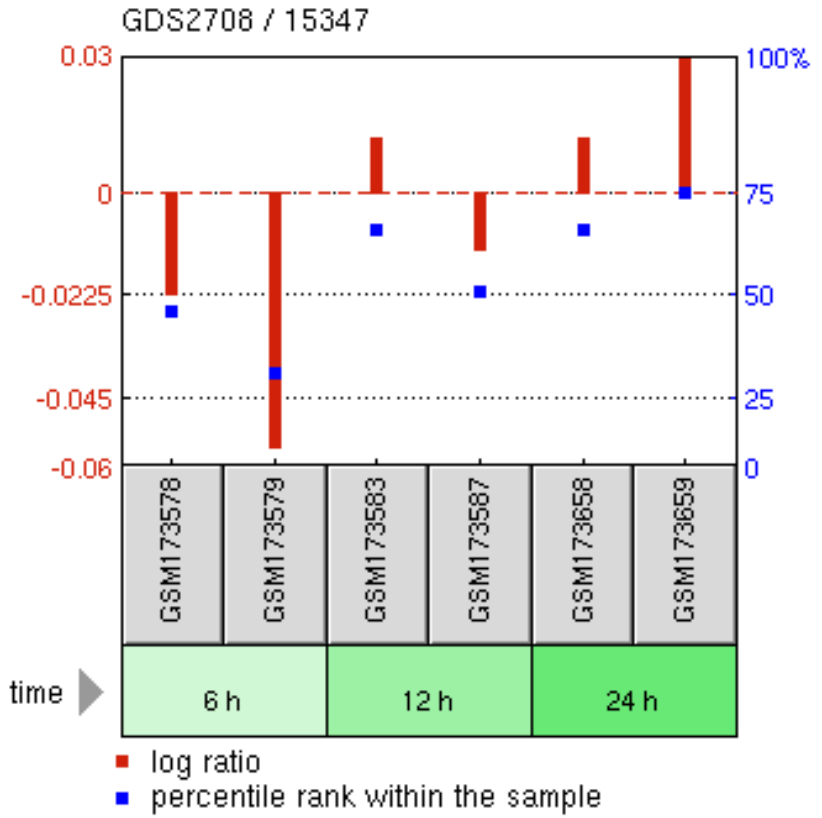

p = 0.043

Quercetin enhances the *GATA5* expression

Sample	Title	Value
GSM173578	Quercetin treated cardiomyocytes for 6 hours (Q6-A).	-0.0227201
GSM173579	Quercetin treated cardiomyocytes for 6 hours (Q6-B).	-0.0564461
GSM173583	Quercetin treated cardiomyocytes for 12 hours (Q12-A).	0.0121804
GSM173587	Quercetin treated cardiomyocytes for 12 hours (Q12-B).	-0.0128478
GSM173658	Quercetin treated cardiomyocytes for 24 hours (Q24-A).	0.0121804
GSM173659	Quercetin treated cardiomyocytes for 24 hours (Q24-B).	0.0297642

Profile: *GATA5* expression
GDS2628 / 238095_at
Title
Vitamin D effect on bronchial smooth muscle cells
Organism
Homo sapiens

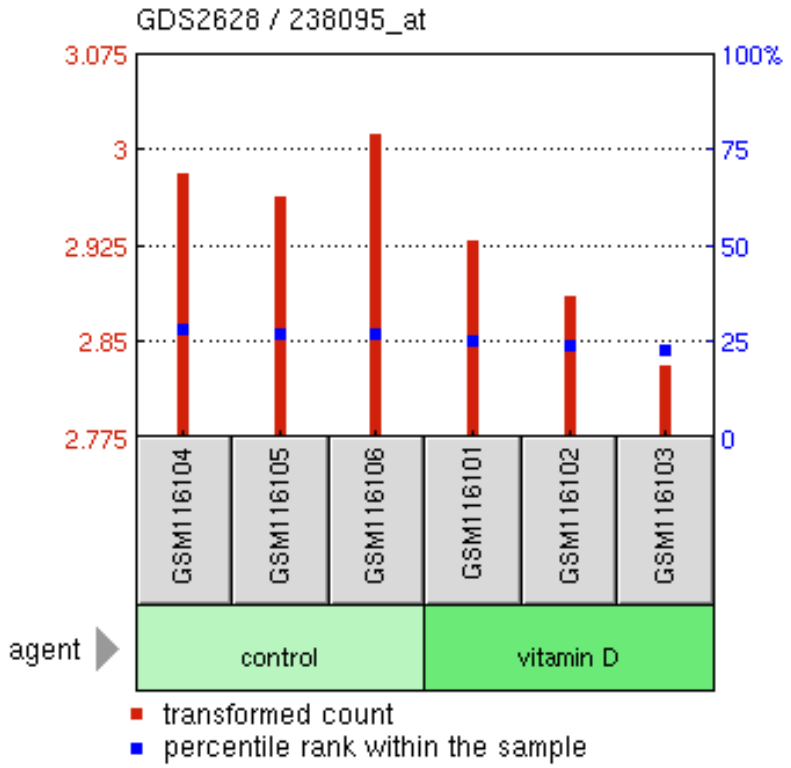

p = 0.015

Vitamin D inhibits the *GATA5* expression

Sample	Title	Value
GSM116104	hBSMC_control_rep1	2.98202
GSM116105	hBSMC_control_rep2	2.96376
GSM116106	hBSMC_control_rep3	3.01345
GSM116101	hBSMC_vitamin D_rep1	2.92934
GSM116102	hBSMC_vitamin D_rep2	2.88574
GSM116103	hBSMC_vitamin D_rep3	2.83171

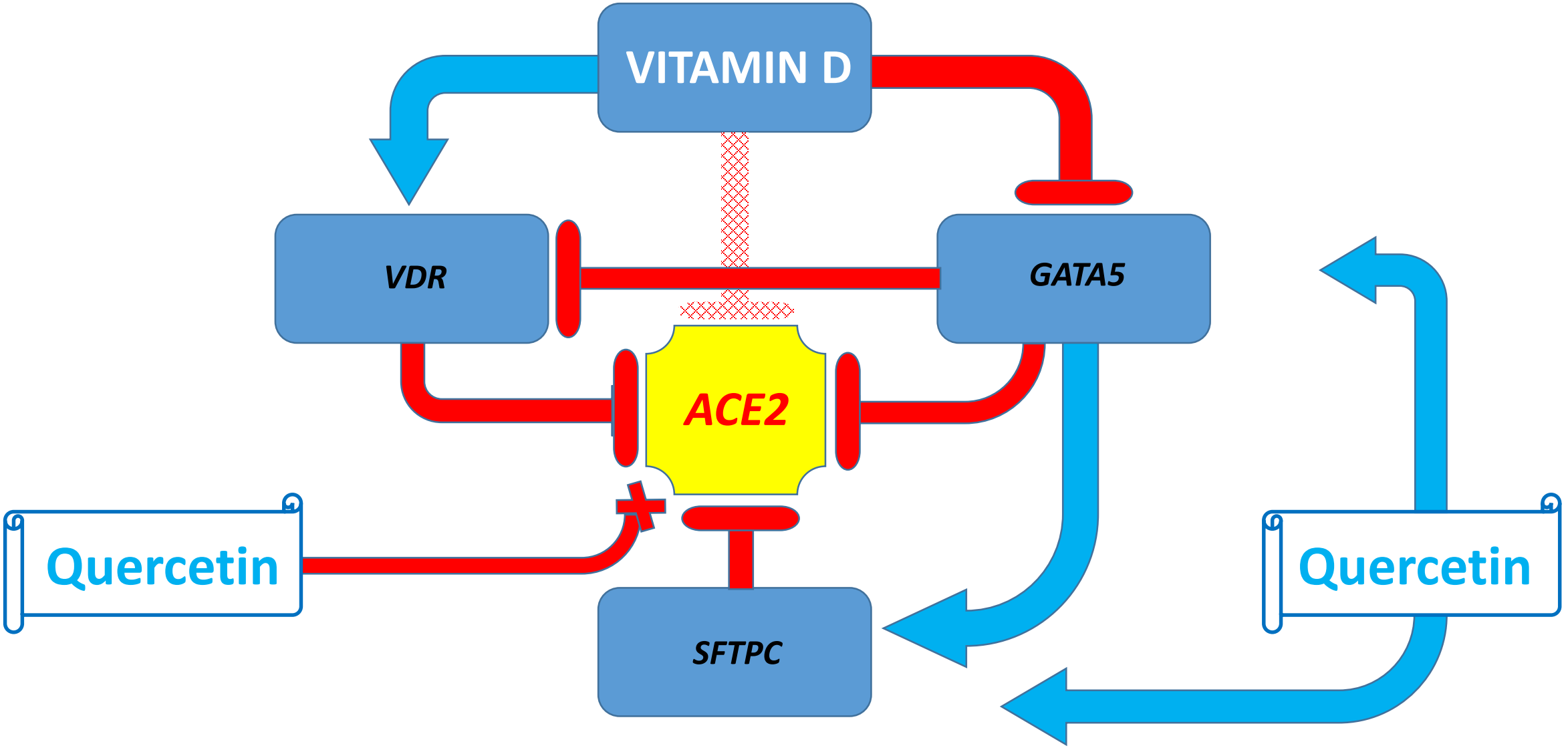
VITAMIN D
VDR
GATA5
ACE2
Quercetin
SFTPC
Quercetin

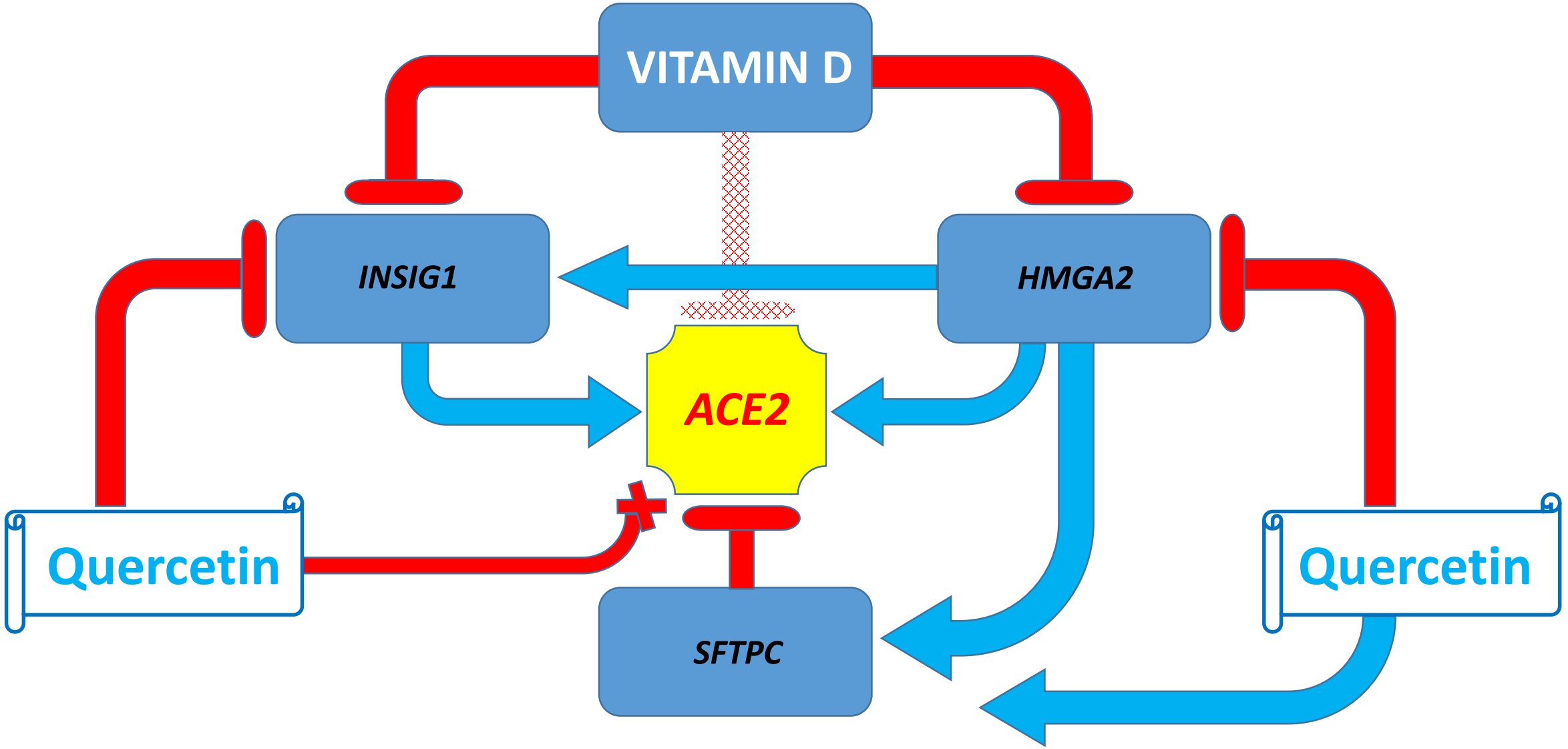
VITAMIN D
INSIG1
HMGA2
ACE2
Quercetin
Quercetin
SFTPC

Profile: *SFTPC* expression
GDS4809 / 1438290_x_at
Title
Gata5 deficiency effect on the lung
Organism
Mus musculus

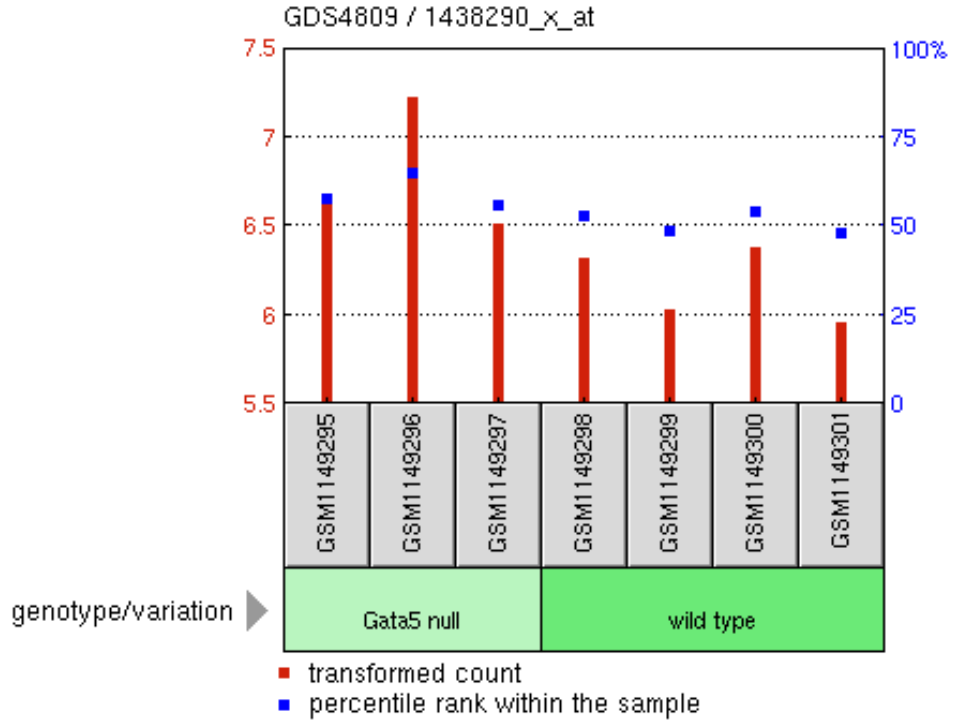

p = 0.019

GATA5: a candidate inhibitor of the *SFTPC* expression

Sample	Title	Value
GSM1149295	KO618	6.65
GSM1149296	KO621	7.23
GSM1149297	KO624	6.52
GSM1149298	WT619	6.32
GSM1149299	WT623	6.04
GSM1149300	WT648	6.39
GSM1149301	WT659	5.96

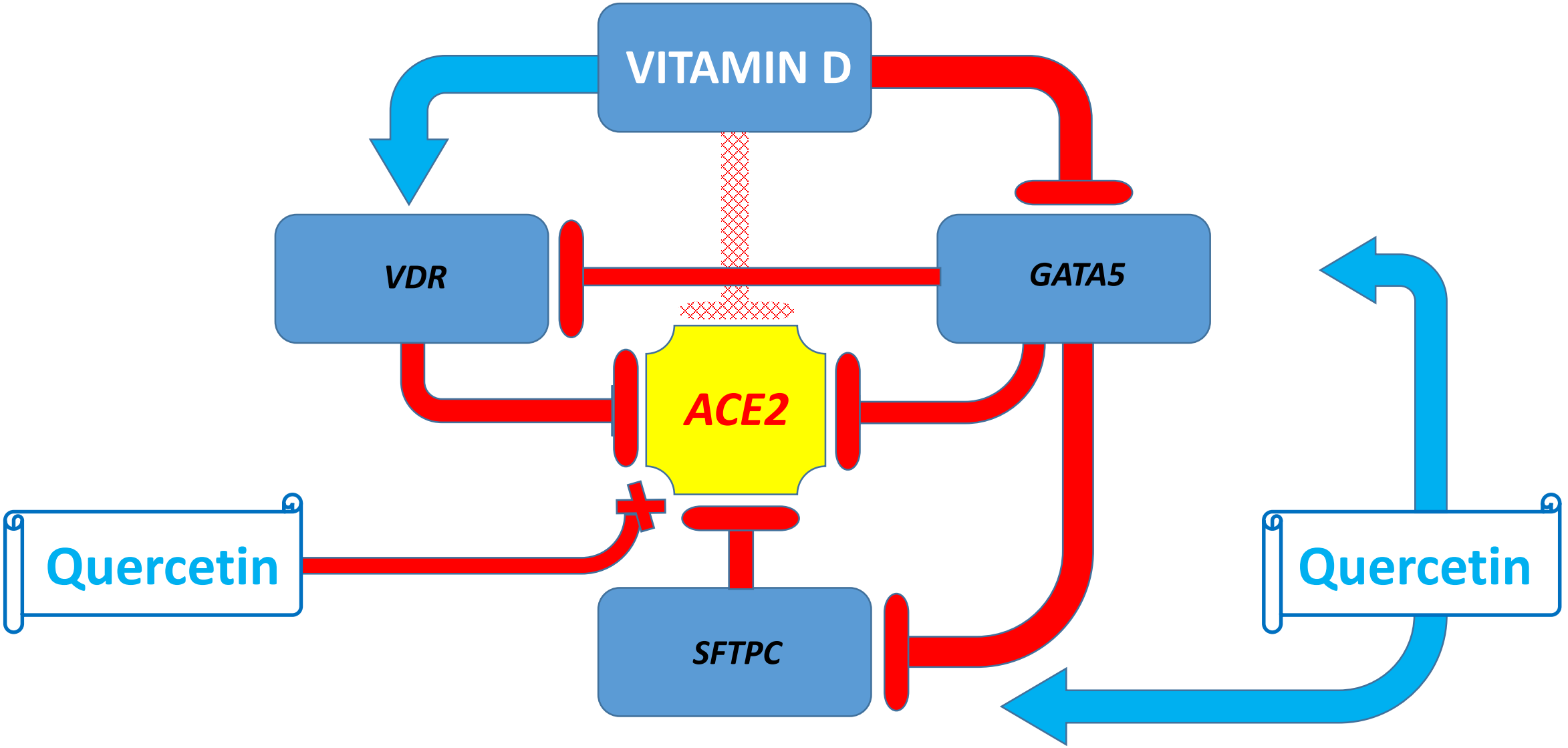
VITAMIN D
VDR
GATA5
ACE2
Quercetin
SFTPC
Quercetin

Examples of the potential negative effects of drugs on the ACE2 expression

Drug Perturbations from GEO up

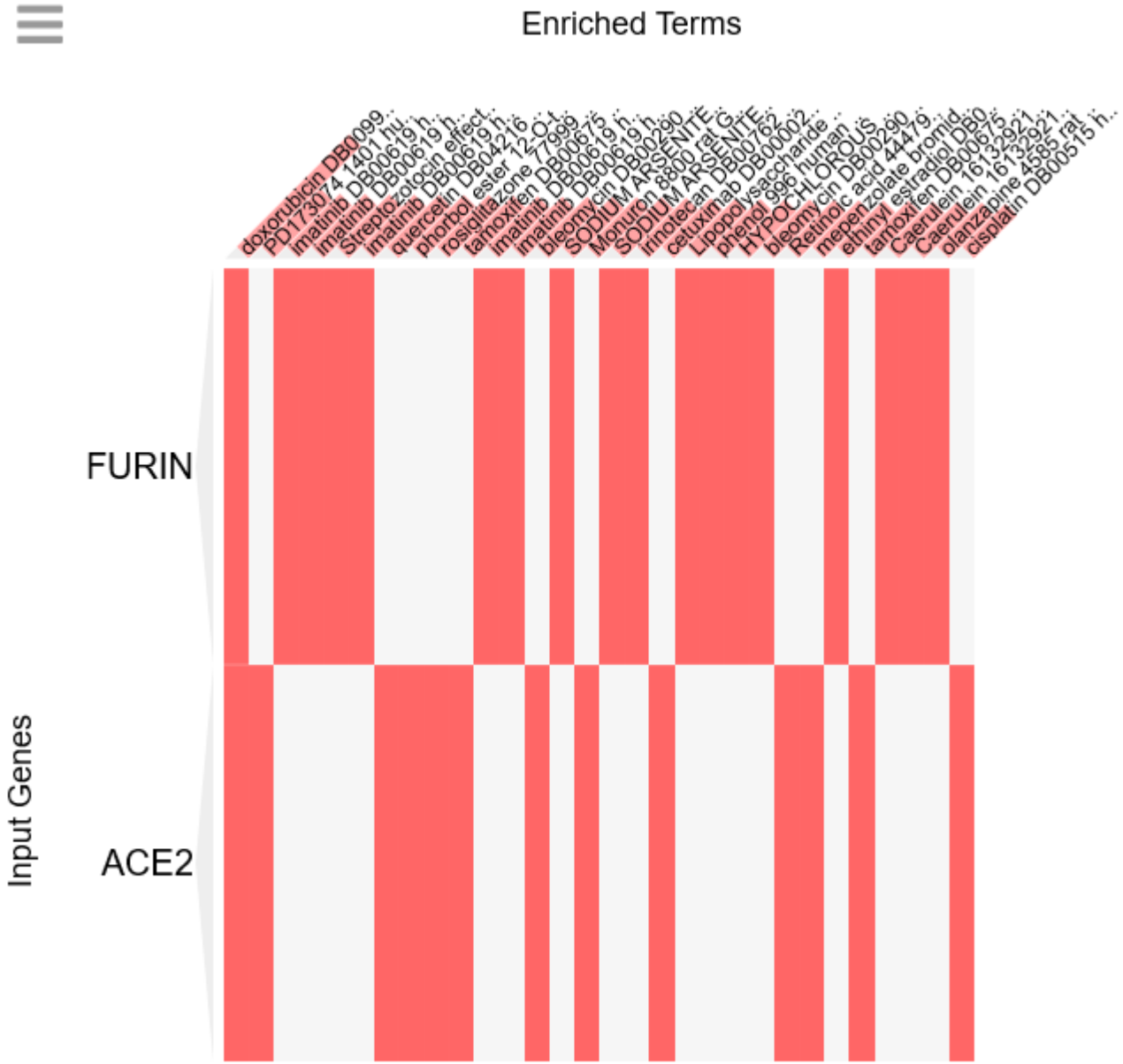

Profile *INSIG1* expression
GDS3032 / 201625_s_at
Title
Quercetin effect on intestinal cell differentiation in vitro: time course
Organism
Homo sapiens

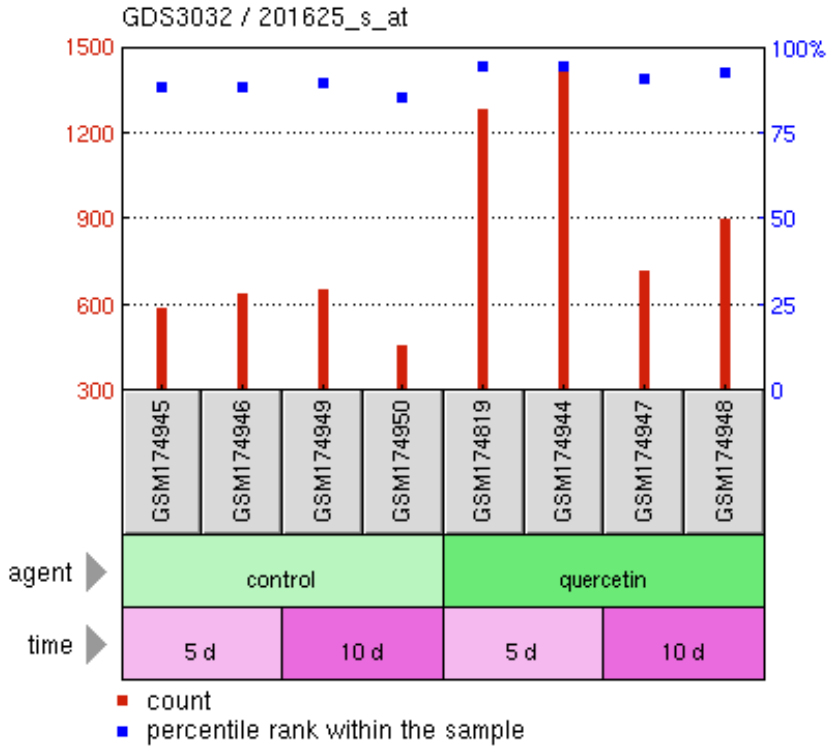

Quercetin enhances the *INSIG1* expression

Sample	Title	Value
GSM174945	Control day 05 sample 1	593.419
GSM174946	Control day 05 sample 2	640.636
GSM174949	Control day 10 sample 1	654.401
GSM174950	Control day 10 sample 2	465.967
GSM174819	Quercetin day 05 sample 1	1286.16
GSM174944	Quercetin day 05 sample 2	1420.46
GSM174947	Quercetin day 10 sample 1	722.644
GSM174948	Quercetin day 10 sample 2	905.527

Profile: *INSIG1* expression
GDS2628 / 201627_s_at
Title
Vitamin D effect on bronchial smooth muscle cells
Organism
Homo sapiens

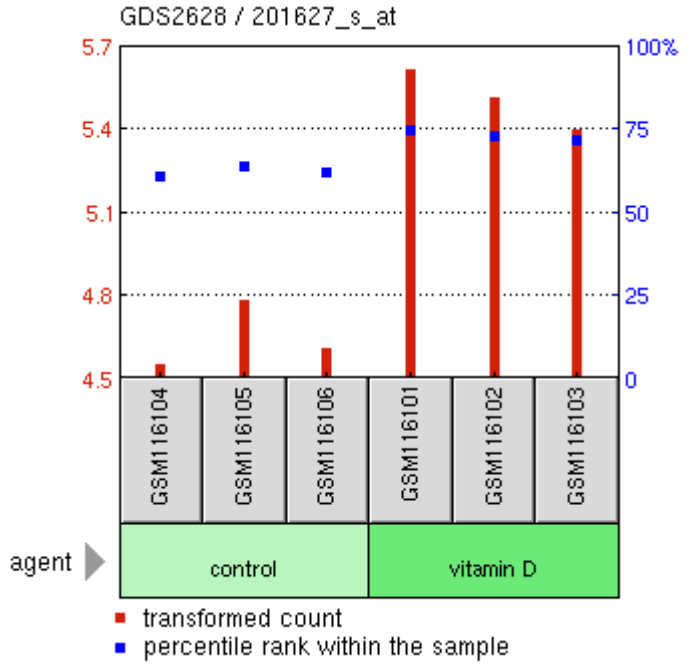

p = 0.0008

Vitamin D enhances the *INSIG1* expression

Sample	Title	Value
GSM116104	hBSMC_control_rep1	4.5524
GSM116105	hBSMC_control_rep2	4.78368
GSM116106	hBSMC_control_rep3	4.6123
GSM116101	hBSMC_vitamin D_rep1	5.61848
GSM116102	hBSMC_vitamin D_rep2	5.51657
GSM116103	hBSMC_vitamin D_rep3	5.40349

Profile: *INSIG1* expression
GDS2628 / 201625_s_at
Title
Vitamin D effect on bronchial smooth muscle cells
Organism
Homo sapiens

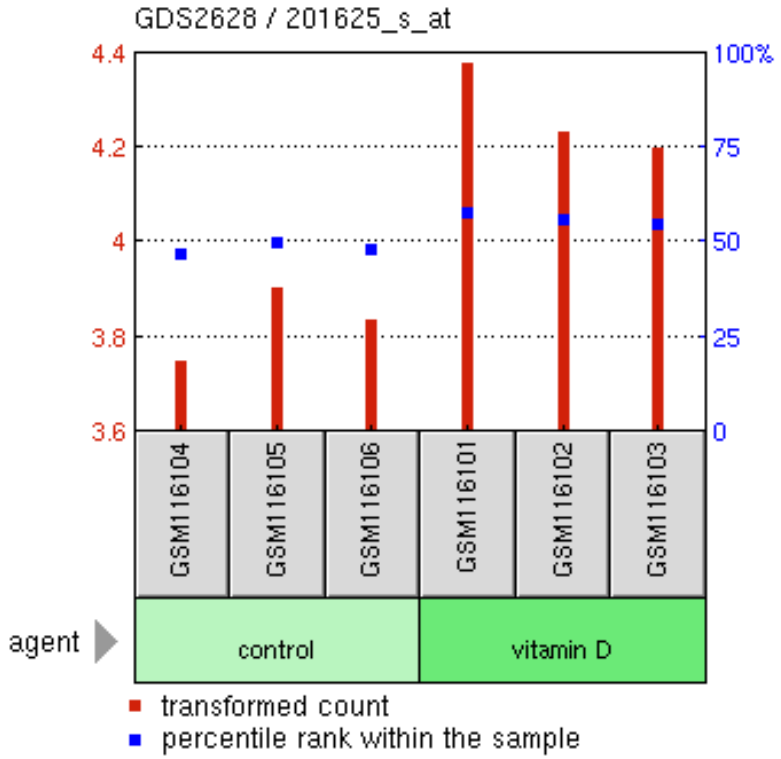

p = 0.0039

Vitamin D enhances the *INSIG1* expression

Sample	Title	Value
GSM116104	hBSMC_control_rep1	3.75107
GSM116105	hBSMC_control_rep2	3.90763
GSM116106	hBSMC_control_rep3	3.83897
GSM116101	hBSMC_vitamin D_rep1	4.37812
GSM116102	hBSMC_vitamin D_rep2	4.2358
GSM116103	hBSMC_vitamin D_rep3	4.19935

Profile: *INSIG1* expression
GDS2628 / 201626_at
Title
Vitamin D effect on bronchial smooth muscle cells
Organism
Homo sapiens

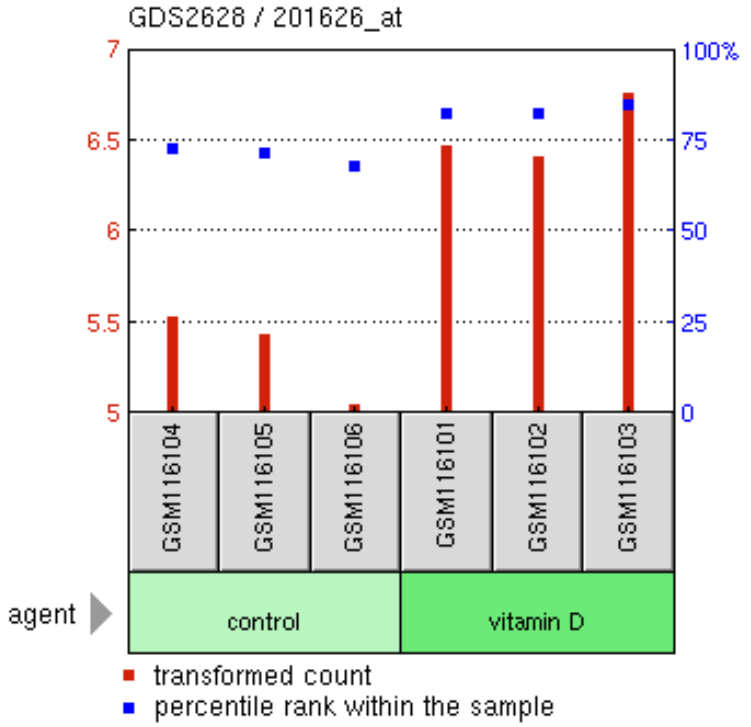

p = 0.0049

Vitamin D enhances the *INSIG1* expression

Sample	Title	Value
GSM116104	hBSMC_control_rep1	5.53893
GSM116105	hBSMC_control_rep2	5.43847
GSM116106	hBSMC_control_rep3	5.01659
GSM116101	hBSMC_vitamin D_rep1	6.47195
GSM116102	hBSMC_vitamin D_rep2	6.42131
GSM116103	hBSMC_vitamin D_rep3	6.76932

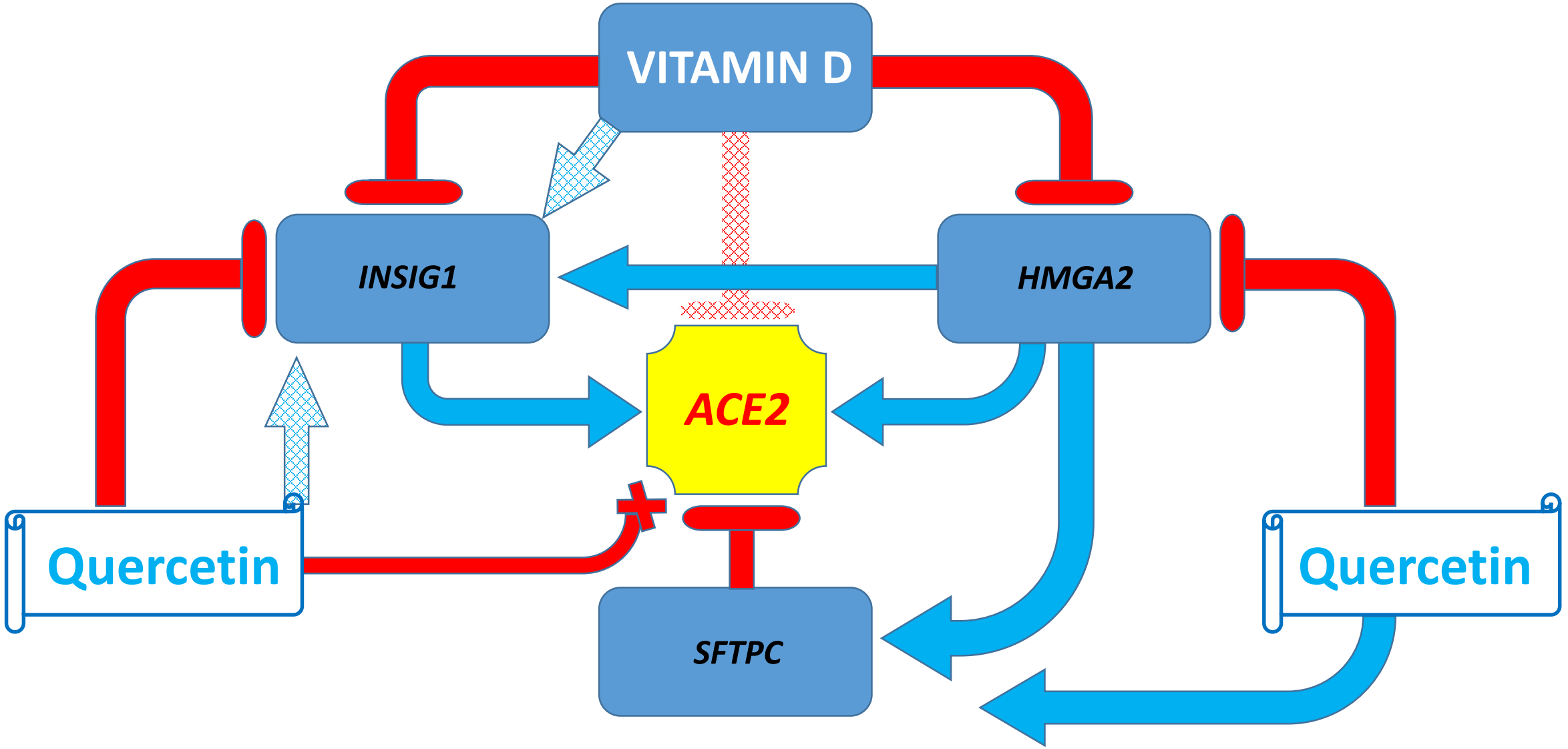
VITAMIN D
INSIG1
HMGA2
ACE2
Quercetin
Quercetin
SFTPC

Profile: ACE2 expression
GDS2314 / 1425102_a_at
Title
Antenatal steroid effect on the placenta
Organism
Mus musculus

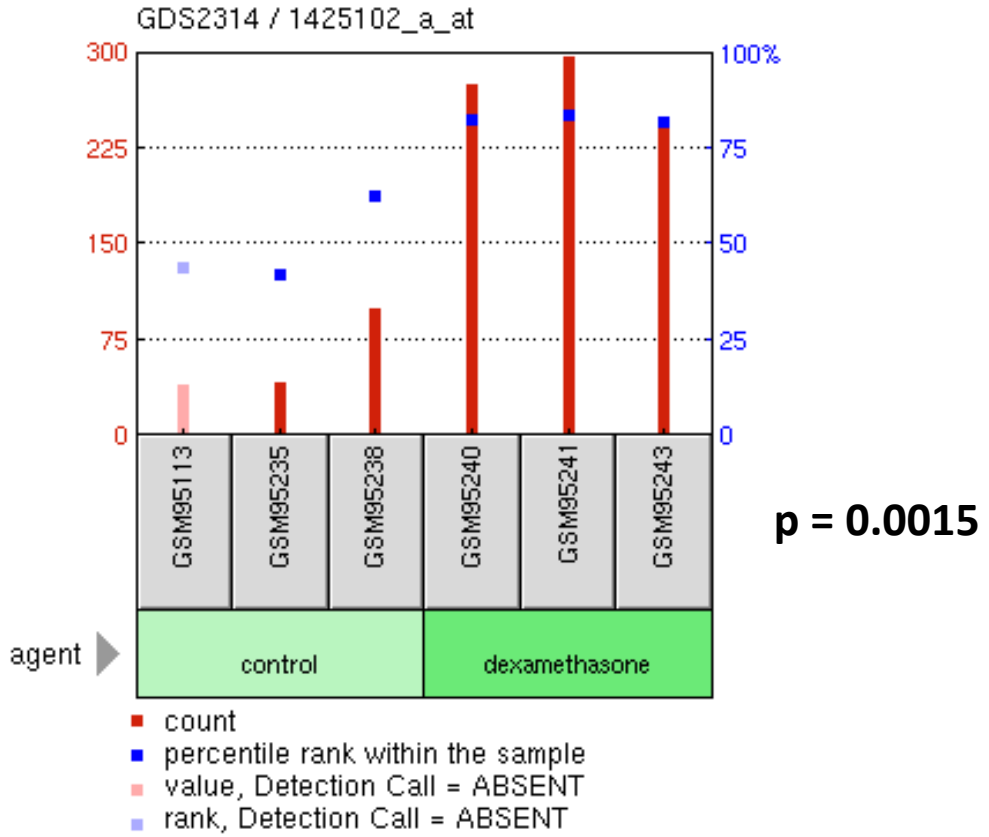

p = 0.0015

Dexamethasone enhances the *ACE2* expression

Sample	Title	Value
GSM95113	Control 1	40.6
GSM95235	Control 2	42
GSM95238	Control 3	100.9
GSM95240	Dexamethasone 1	275.7
GSM95241	Dexamethasone 2	298
GSM95243	Dexamethasone 3	249.5

Profile: ACE2 expression
GDS2314 / 1425103_at
Title
Antenatal steroid effect on the placenta
Organism
Mus musculus

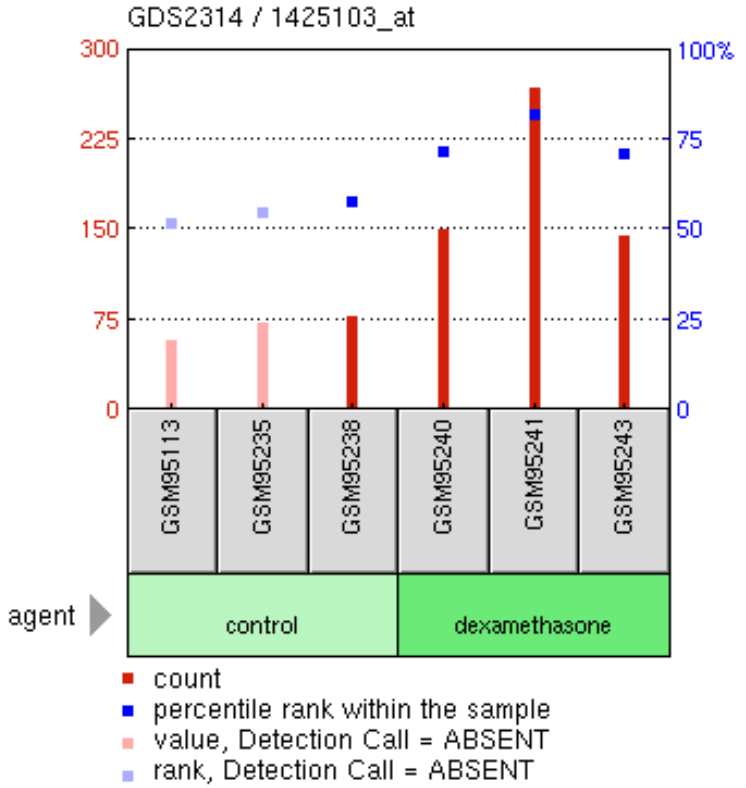

Dexamethasone enhances the *ACE2* expression

Sample	Title	Value	Rank
GSM95113	Control 1	58	52
GSM95235	Control 2	73.3	55
GSM95238	Control 3	79.1	58
GSM95240	Dexamethasone 1	151	72
GSM95241	Dexamethasone 2	268.3	82
GSM95243	Dexamethasone 3	145.8	71

Profile: ACE2 expression
GDS2314 / 1452138_a_at
Title
Antenatal steroid effect on the placenta
Organism
Mus musculus

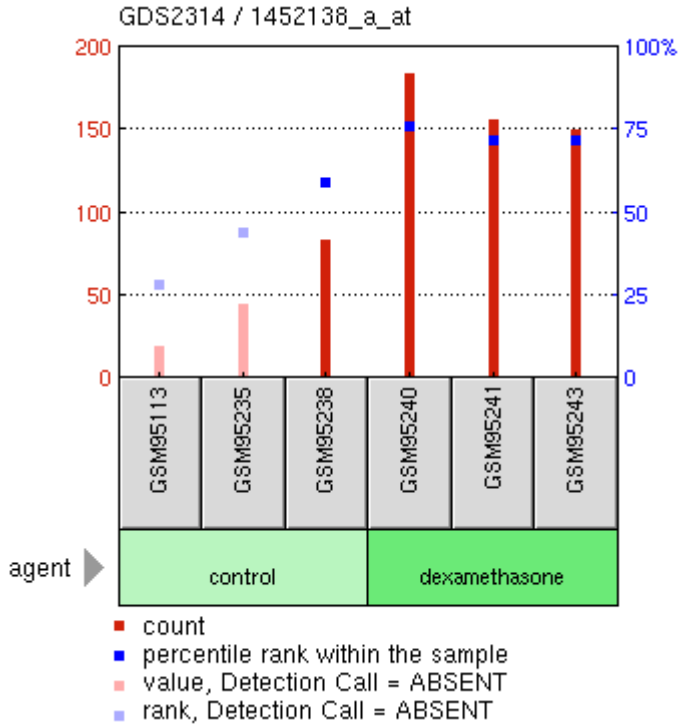

Dexamethasone enhances the *ACE2* expression

Sample	Title	Value	Rank
GSM95113	Control 1	19.6	28
GSM95235	Control 2	45.5	44
GSM95238	Control 3	83.4	59
GSM95240	Dexamethasone 1	183.3	76
GSM95241	Dexamethasone 2	155.8	72
GSM95243	Dexamethasone 3	150	72

Supplemental Table S13. Additional examples of the potential activators and repressors of the *ACE2* expression identified using transgenic mouse models

Additional examples of the potential activators of the *ACE2* expression identified using transgenic mouse models

Profile: ACE2 expression
GDS4384 / 222257_s_at
Title
p53 mutations in microsatellite-stable, stage III colorectal cancer
Organism
Homo sapiens

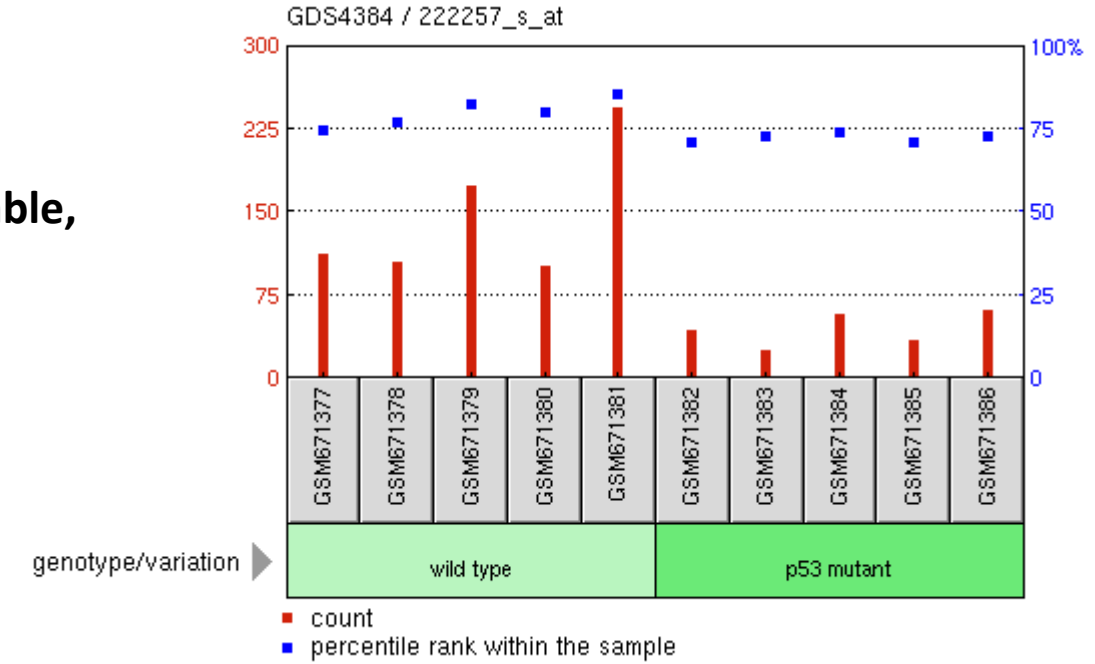

Sample	Title	Value
GSM671377	UM13_Wt_rep1	112.441
GSM671378	UM23_Wt_rep2	105.683
GSM671379	UM30_Wt_rep3	173.535
GSM671380	UM9_Wt_rep4	101.705
GSM671381	UM3_Wt_rep5	244.407
GSM671382	UM1_Mut_rep1	44.3901
GSM671383	UM15_Mtu_rep2	26.5371
GSM671384	UM17_Mtu_rep3	59.3536
GSM671385	UM2_Mtu_rep4	34.4729
GSM671386	UM25_Mtu_rep5	62.1878

Profile: ACE2 expression
GDS1434 / 160986_r_at
Title
Transcription factor p63 null mutation effect on skin (MG-U74A)
Organism
Mus musculus

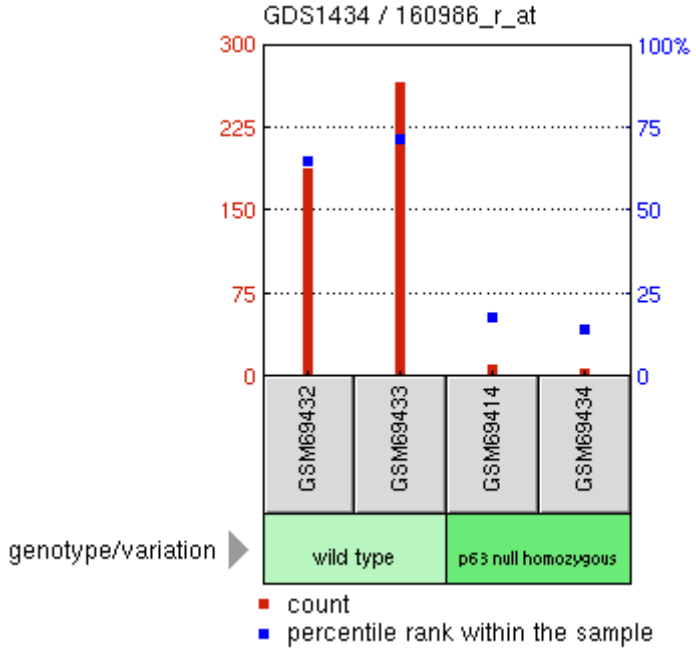

Sample	Title	Value
GSM69432	E18.5 p63 wt skin 1 A-chip	189.3
GSM69433	E18.5 p63 wt skin 2 A-chip	267.1
GSM69414	E18.5 p63 null skin 1 A-chip	11.5
GSM69434	E18.5 p63 null skin 2 A-chip	8.4

Profile: ACE2 expression
GDS1435 / 115071_at
Title
Transcription factor p63 null mutation effect on skin (MG-U74B)
Organism
Mus musculus

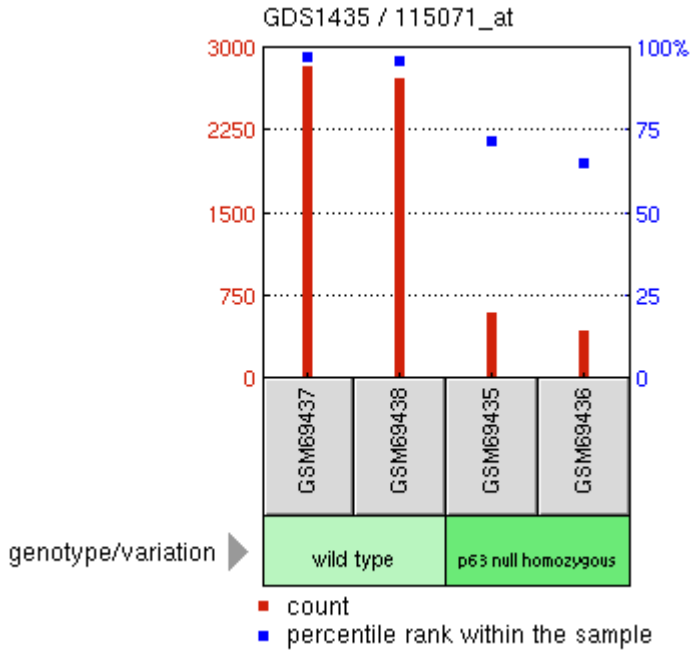

Sample	Title	Value
GSM69437	E18.5 wt skin 1 B-chip	2821.9
GSM69438	E18.5 wt skin 2 B-chip	2718.1
GSM69435	E18.5 p63 null skin 1 B-chip	602.2
GSM69436	E18.5 p63 null skin 2 B-chip	449.1

Profile: ACE2 expression
GDS4599 / 8171449
Title
ZNF750 silencing effect on differentiated keratinocytes
Organism
Homo sapiens

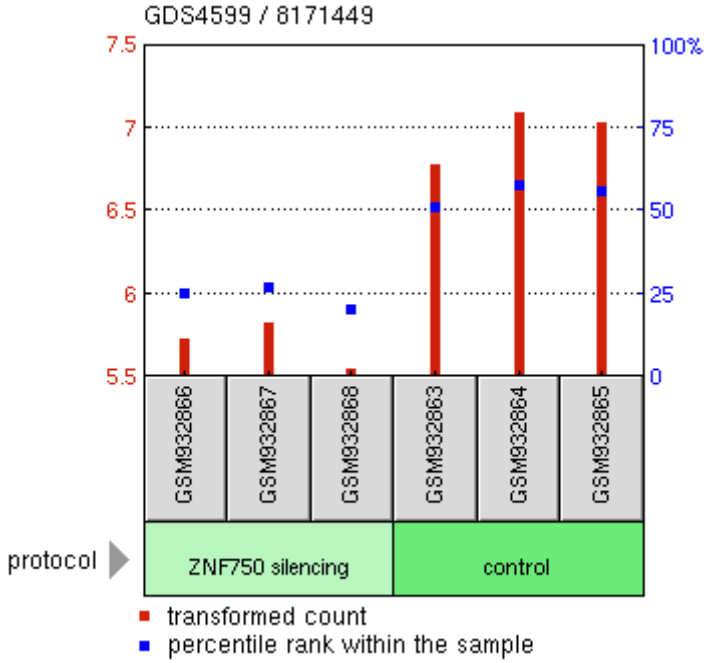

Sample	Title	Value
GSM932866	HaCaT_ZNF750i_ biological rep1	5.74045
GSM932867	HaCaT_ZNF750i_ biological rep2	5.82679
GSM932868	HaCaT_ZNF750i_ biological rep3	5.52392
GSM932863	HaCaT_Control_ biological rep1	6.78372
GSM932864	HaCaT_Control_ biological rep2	7.09307
GSM932865	HaCaT_Control_ biological rep3	7.03868

Profile: ACE2 expression
GDS4475 / 219962_at
Title
Extracellular matrix protein cysteine rich 61 (CCN1) effect on LN229 glioma cells
Organism
Homo sapiens

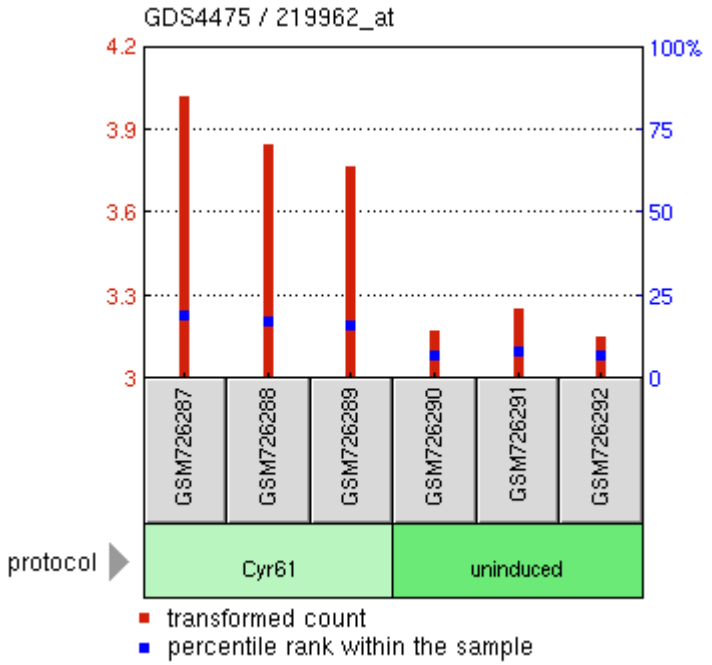

Sample	Title	Value
GSM726287	Tetracycline-inducible glioma cells dox 1	4.02176
GSM726288	Tetracycline-inducible glioma cells dox 2	3.85144
GSM726289	Tetracycline-inducible glioma cells dox 3	3.77096
GSM726290	Tetracycline-inducible glioma cells no dox 1	3.17831
GSM726291	Tetracycline-inducible glioma cells no dox 2	3.25989
GSM726292	Tetracycline-inducible glioma cells no dox 3	3.15658

Profile: ACE2 expression
GDS4061 / 222257_s_at
Title
Estrogen receptor alpha-silenced MCF7 breast cancer cells
Organism
Homo sapiens

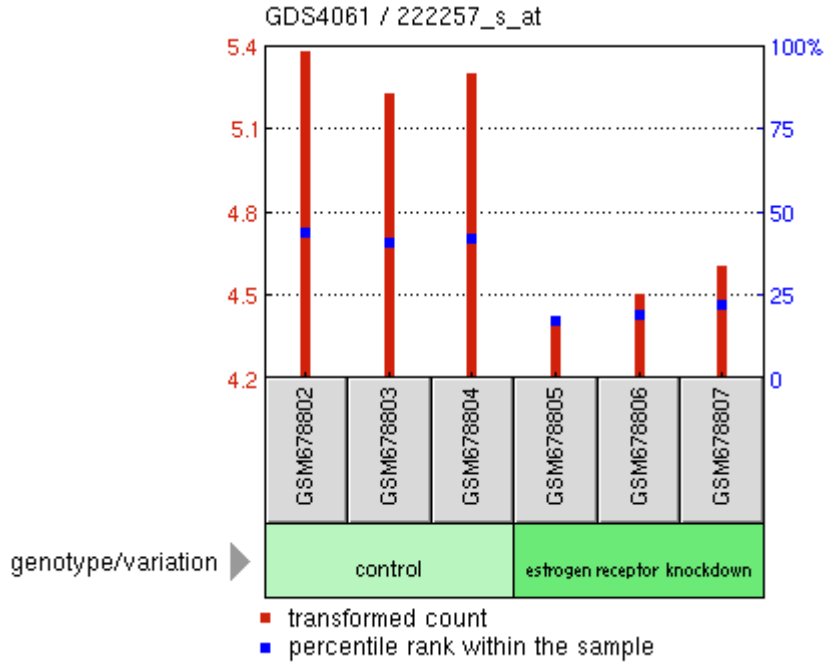

Sample	Title	Value
GSM678802	MCF7, biological rep1	5.37948
GSM678803	MCF7, biological rep2	5.23028
GSM678804	MCF7, biological rep3	5.30543
GSM678805	MCF7 silenced Estrogen receptor, biological rep1	4.40684
GSM678806	MCF7 silenced Estrogen receptor, biological rep2	4.50939
GSM678807	MCF7 silenced Estrogen receptor, biological rep3	4.609

Profile: ACE2 expression
GDS4061 / 219962_at
Title
Estrogen receptor alpha-silenced MCF7 breast cancer cells
Organism
Homo sapiens

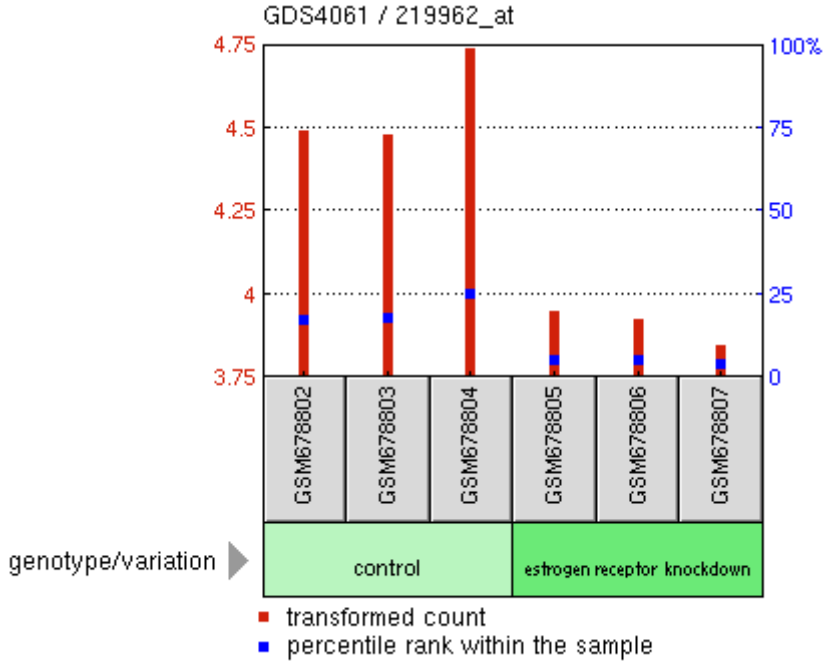

Sample	Title	Value
GSM678802	MCF7, biological rep1	4.49106
GSM678803	MCF7, biological rep2	4.48349
GSM678804	MCF7, biological rep3	4.73862
GSM678805	MCF7 silenced Estrogen receptor, biological rep1	3.94941
GSM678806	MCF7 silenced Estrogen receptor, biological rep2	3.9283
GSM678807	MCF7 silenced Estrogen receptor, biological rep3	3.84918

Profile: ACE2 expression
GDS4061 / 219962_at
Title
Estrogen receptor alpha-silenced MCF7 breast cancer cells
Organism
Homo sapiens

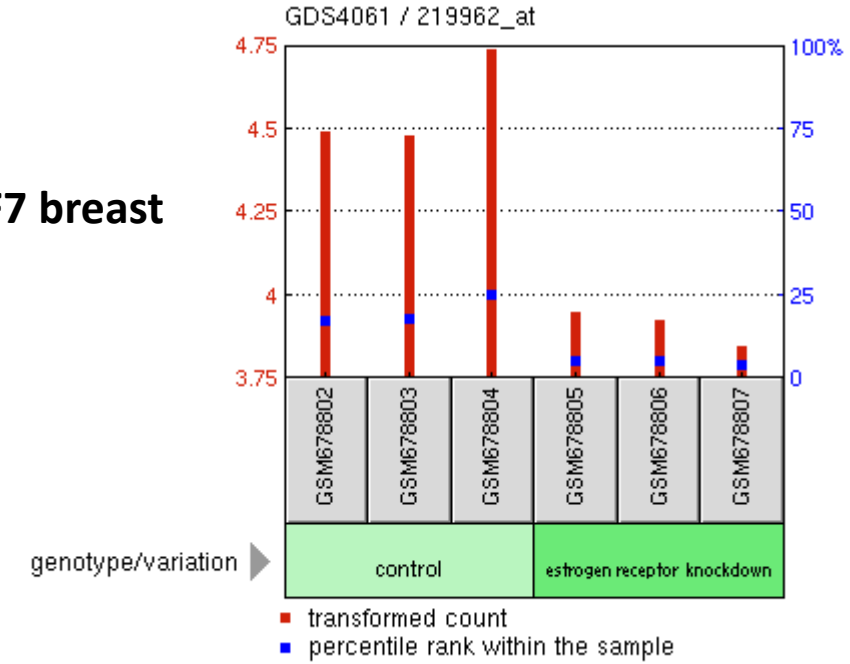

Sample	Title	Value
GSM678802	MCF7, biological rep1	4.49106
GSM678803	MCF7, biological rep2	4.48349
GSM678804	MCF7, biological rep3	4.73862
GSM678805	MCF7 silenced Estrogen receptor, biological rep1	3.94941
GSM678806	MCF7 silenced Estrogen receptor, biological rep2	3.9283
GSM678807	MCF7 silenced Estrogen receptor, biological rep3	3.84918

Profile: ACE2 expression
GDS1644 / 10205_at
Title
VTS1 deletion mutant
Organism
Saccharomyces cerevisiae

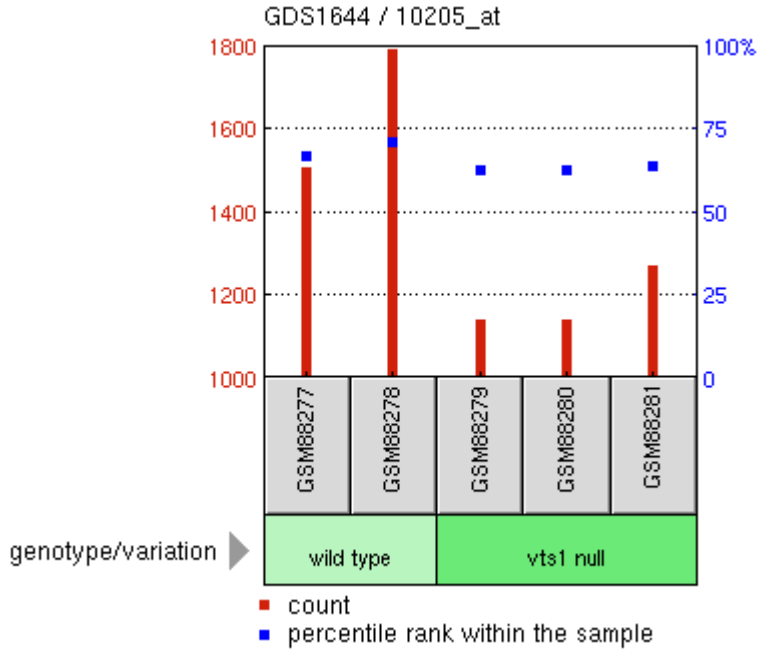

Sample	Title	Value
GSM88277	WT1	1506.8
GSM88278	WT2	1791
GSM88279	Exp Pt 1(dvts1-1 VTS1)	1141.9
GSM88280	Exp Pt 2(dvts1-2 VTS1)	1143.6
GSM88281	Exp Pt 3(VTS1)	1271.5

Profile: ACE2 expression
GDS3294 / 1425103_at
Title
CTCF depletion effect in oocytes
Organism
Mus musculus

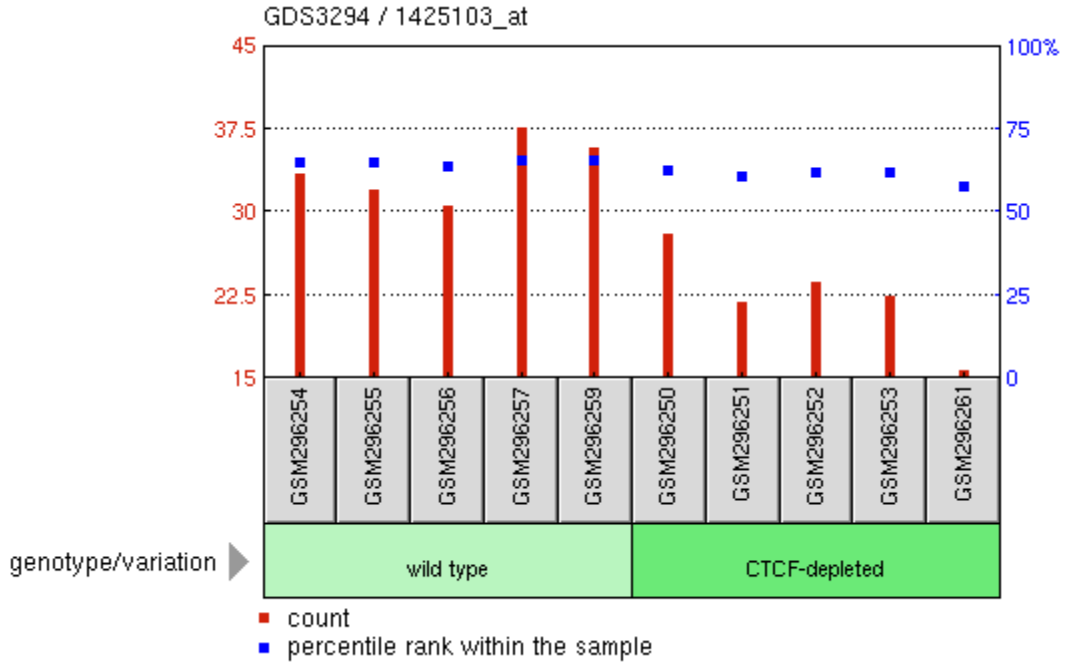

Sample	Title	Value
GSM296254	gene expression of wild type oocyte, replicate 1	33.5935
GSM296255	gene expression of wild type oocyte, replicate 2	32.1628
GSM296256	gene expression of wild type oocyte, replicate 3	30.5551
GSM296257	gene expression of wild type oocyte, replicate 4	37.7155
GSM296259	gene expression of wild type oocyte, replicate 5	35.8225
GSM296250	gene expression of CTCF-depleted oocyte, replicate 1	28.1471
GSM296251	gene expression of CTCF-depleted oocyte, replicate 3	21.9578
GSM296252	gene expression of CTCF-depleted oocyte, replicate 4	23.7345
GSM296253	gene expression of CTCF-depleted oocyte, replicate 5	22.4628
GSM296261	gene expression of CTCF-depleted oocyte, replicate 2	15.8604

Profile: ACE2 expression
GDS1555 / 1425103_at
Title
Glycerol kinase knockout effect on liver
Organism
Mus musculus

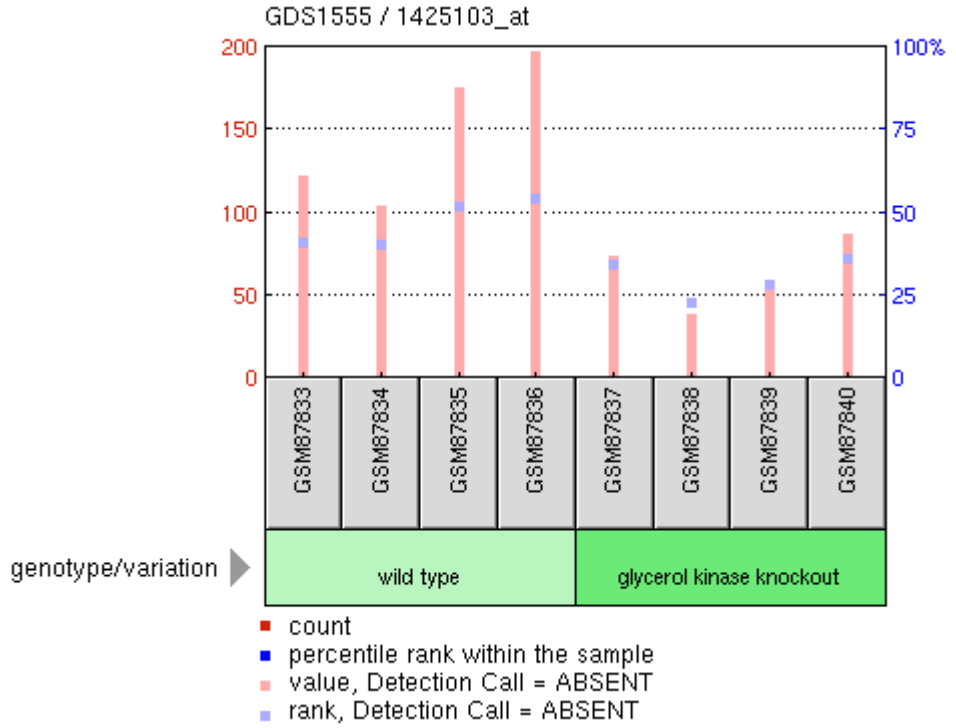

Sample	Title	Value
GSM87833	Liver_WildType_1	122.1
GSM87834	Liver_WildType_2	104.3
GSM87835	Liver_WildType_3	174.9
GSM87836	Liver_WildType_4	197.4
GSM87837	Liver_KnockOut_1	74
GSM87838	Liver_KnockOut_2	39.3
GSM87839	Liver_KnockOut_3	59.1
GSM87840	Liver_KnockOut_4	87.3

Profile: ACE2 expression
GDS4895 / 1425102_a_at
Title
SIRT1 deficiency effect on the brain
Organism
Mus musculus

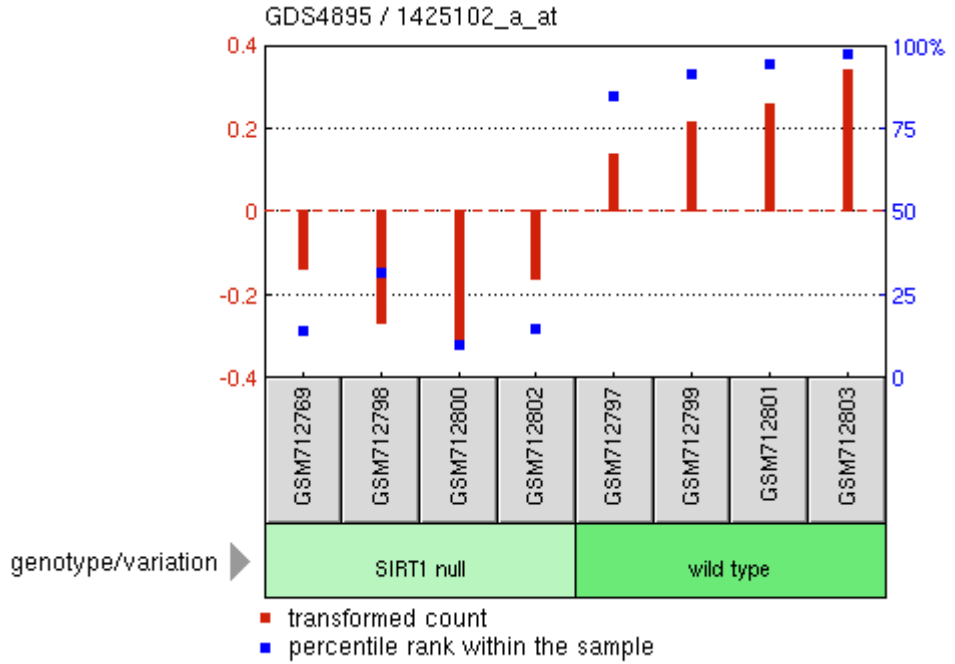

Sample	Title	Value
GSM712769	BSKO 1	-0.140546
GSM712798	BSKO 2	-0.27286
GSM712800	BSKO 3	-0.312008
GSM712802	BSKO 4	-0.167778
GSM712797	WT 1	0.140546
GSM712799	WT 2	0.221
GSM712801	WT 3	0.261022
GSM712803	WT 4	0.344256

Additional examples of the potential repressors of the *ACE2* expression identified using transgenic mouse models

Profile: ACE2 expression
GDS3361 / 160986_r_at
Title
Fibroblast growth factor-23 transgenic model
Organism
Mus musculus

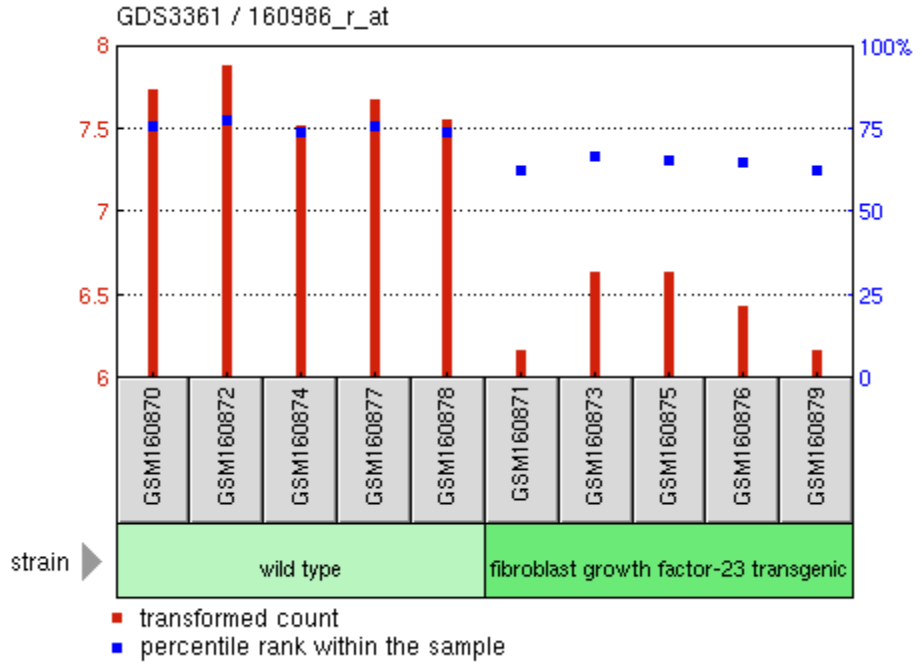

Sample	Title	Value
GSM160870	Wild Type 612	7.73651
GSM160872	Wild type 618	7.89066
GSM160874	Wild Type 650	7.5183
GSM160877	Wild Type nr 658	7.67757
GSM160878	Wild Type nr 663	7.55491
GSM160871	Transgenic nr 614	6.17722
GSM160873	Transgenic nr 619	6.64023
GSM160875	Transgenic nr 652	6.64915
GSM160876	Transgenic nr 657	6.44524
GSM160879	Transgenic nr 661	6.17914

Profile: ACE2 expression
GDS2359 / 1452138_a_at
Title
Interferon regulatory factor 6 null mutation effect on the skin
Organism
Mus musculus

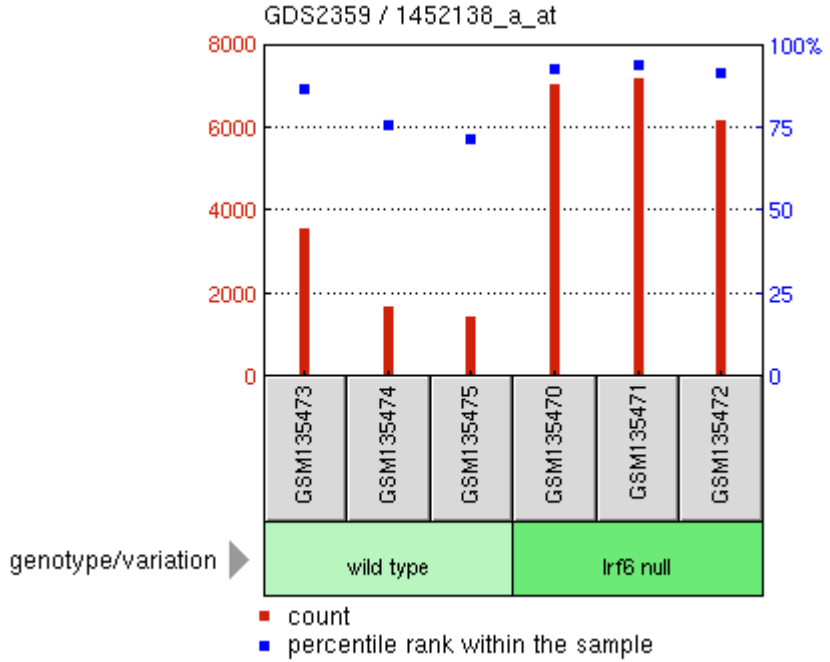

Sample	Title	Value
GSM135473	IRF6 wt, biological rep1	3607.2
GSM135474	IRF6 wt, biological rep2	1727.4
GSM135475	IRF6 wt, biological rep3	1461.4
GSM135470	IRF6 knockout, biological rep1	7077
GSM135471	IRF6 knockout, biological rep2	7212.6
GSM135472	IRF6 knockout, biological rep3	6184.5

Profile: ACE2 expression
GDS2359 / 1425103_at
Title
Interferon regulatory factor 6 null mutation effect on the skin
Organism
Mus musculus

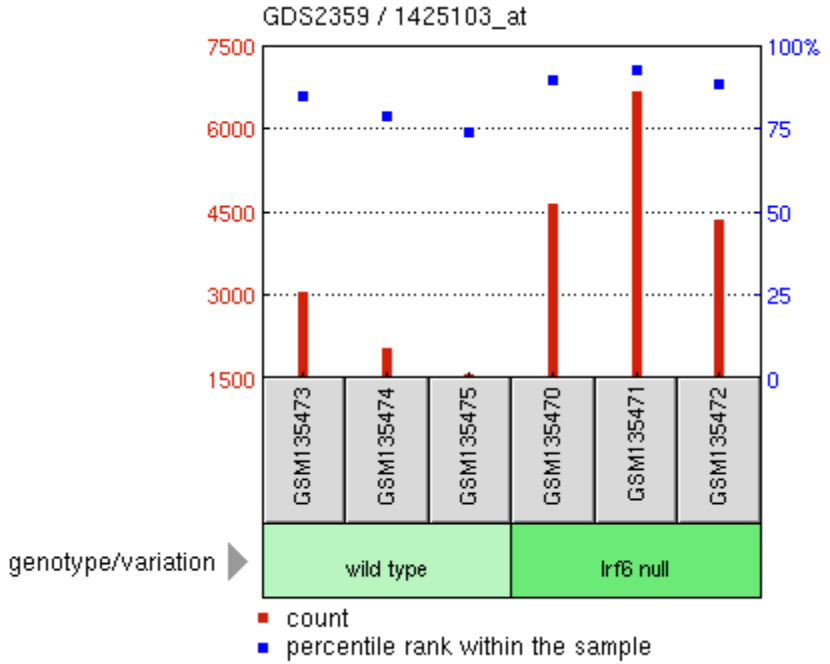

Sample	Title	Value
GSM135473	IRF6 wt, biological rep1	3067.9
GSM135474	IRF6 wt, biological rep2	2065.9
GSM135475	IRF6 wt, biological rep3	1589.4
GSM135470	IRF6 knockout, biological rep1	4678.8
GSM135471	IRF6 knockout, biological rep2	6695.8
GSM135472	IRF6 knockout, biological rep3	4381.7

Profile: ACE2 expression
GDS4498 / 1425102_a_at
Title
Transcription factor Nrf2 gain-of-function model: postnatal day 2.5 whole skin
Organism
Mus musculus

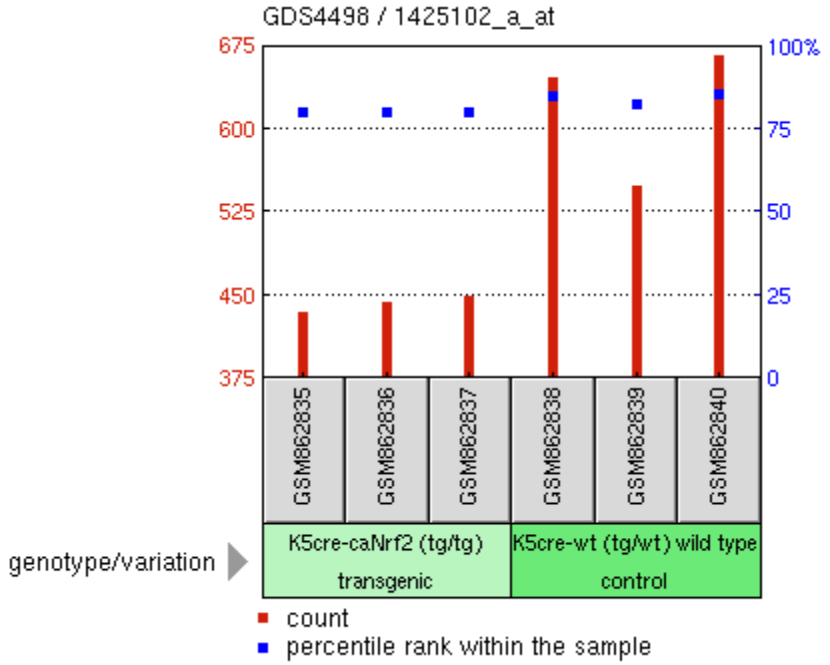

Sample	Title	Value
GSM862835	transgene strong 1	435.03
GSM862836	transgene strong 2	444.737
GSM862837	transgene strong 3	449.601
GSM862838	wildtype strong 1	647.134
GSM862839	wildtype strong 2	548.634
GSM862840	wildtype strong 3	667.753

Profile: ACE2 expression
GDS3397 / 1425102_a_at
Title
Dent disease model: renal proximal tubules
Organism
Mus musculus

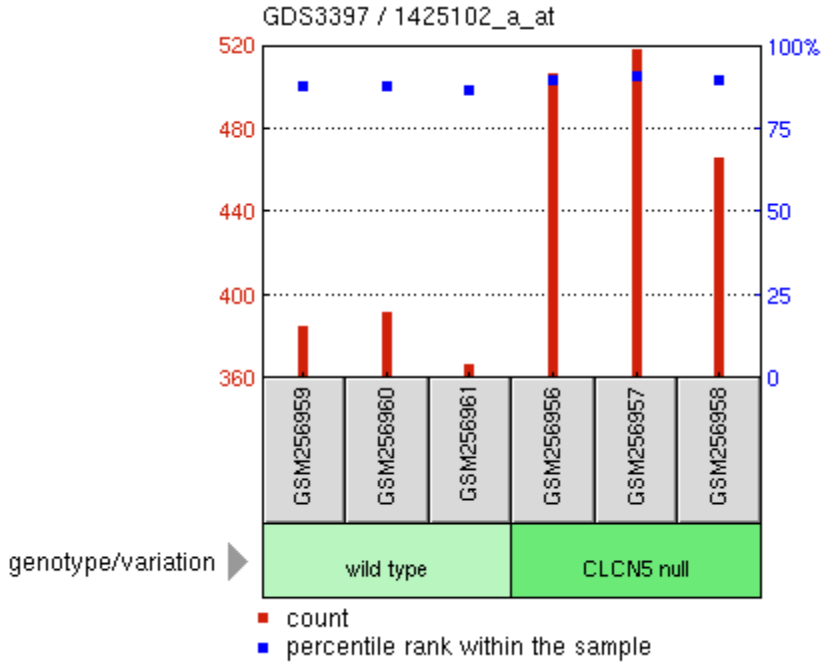

Sample	Title	Value
GSM256959	Wild type rep 1	385.878
GSM256960	Wild type rep 2	392.178
GSM256961	Wild type rep 3	367.379
GSM256956	CLC5 ko rep 1	507.455
GSM256957	CLC5 ko rep 2	518.388
GSM256958	CLC5 ko rep 3	466.324

Profile: ACE2 expression
GDS3323 / 1425103_at
Title
Na+/H+ exchanger 3 deficiency effect on the colon
Organism
Mus musculus

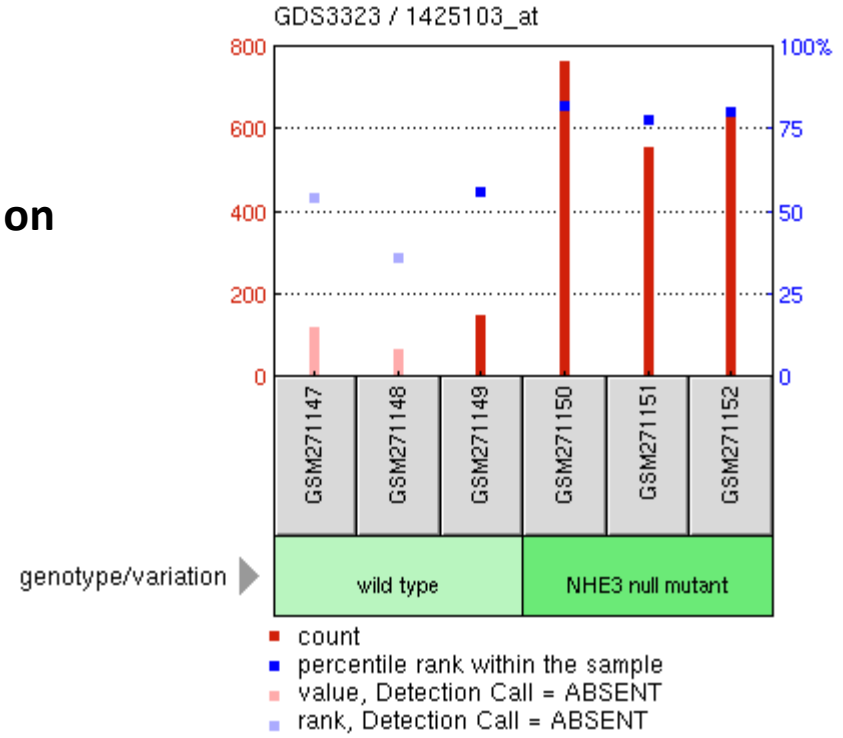

Sample	Title	Value
GSM271147	NHE3+/+ replicate 1	122.3
GSM271148	NHE3+/+ replicate 2	68.2
GSM271149	NHE3+/+ replicate 3	150.2
GSM271150	NHE3-/- replicate 1	762.3
GSM271151	NHE3-/- replicate 2	554.9
GSM271152	NHE3-/- replicate 3	634.3

Profile: ACE2 expression
GDS4910 / 1425103_at
Title
Stearoyl-CoA desaturase-1 deficiency effect on the skin
Organism
Mus musculus

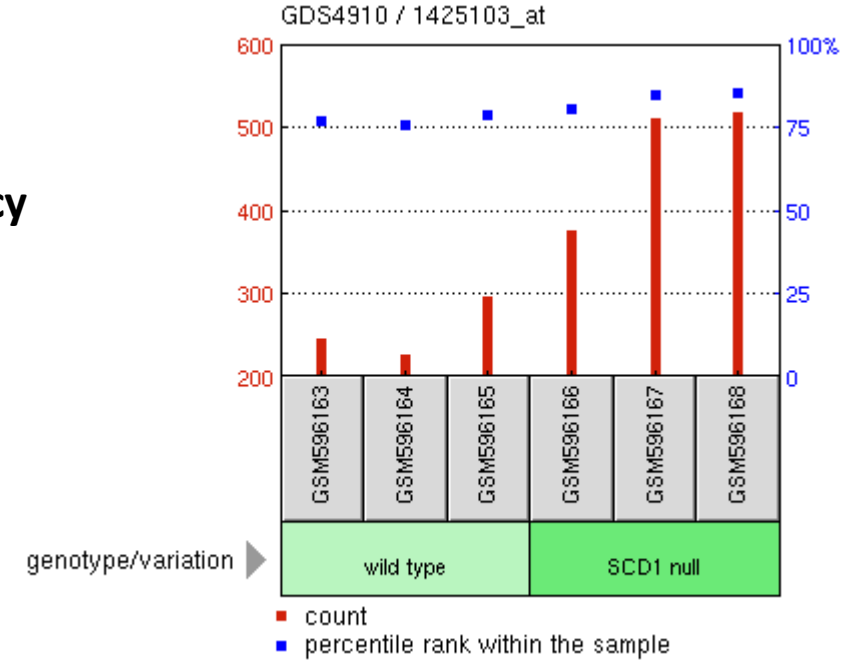

Sample	Title	Value
GSM596163	Skin_Lox_Control_Rep1	246.595
GSM596164	Skin_Lox_Control_Rep2	227.702
GSM596165	Skin_Lox_Control_Rep3	297.552
GSM596166	Skin_SKO_Rep1	377.151
GSM596167	Skin_SKO_Rep2	512
GSM596168	Skin_SKO_Rep3	519.147

Profile: ACE2 expression
GDS4910 / 1452138_a_at
Title
Stearoyl-CoA desaturase-1 deficiency effect on the skin
Organism
Mus musculus

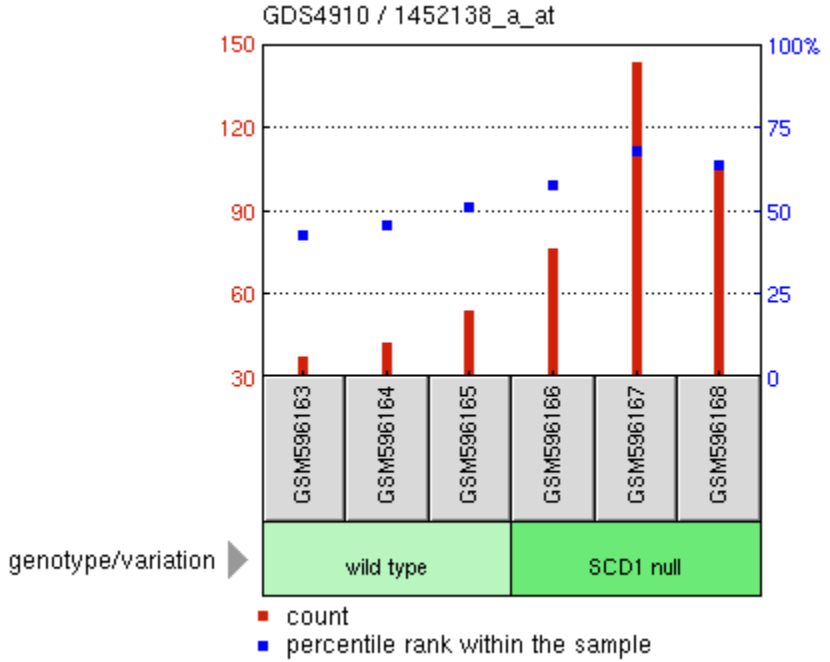

Sample	Title	Value
GSM596163	Skin_Lox_Control_Rep1	37.453
GSM596164	Skin_Lox_Control_Rep2	42.992
GSM596165	Skin_Lox_Control_Rep3	53.967
GSM596166	Skin_SKO_Rep1	76.692
GSM596167	Skin_SKO_Rep2	143.908
GSM596168	Skin_SKO_Rep3	105.639

Profile: ACE2 expression
GDS4910 / 1425102_a_at
Title
Stearoyl-CoA desaturase-1 deficiency effect on the skin
Organism
Mus musculus

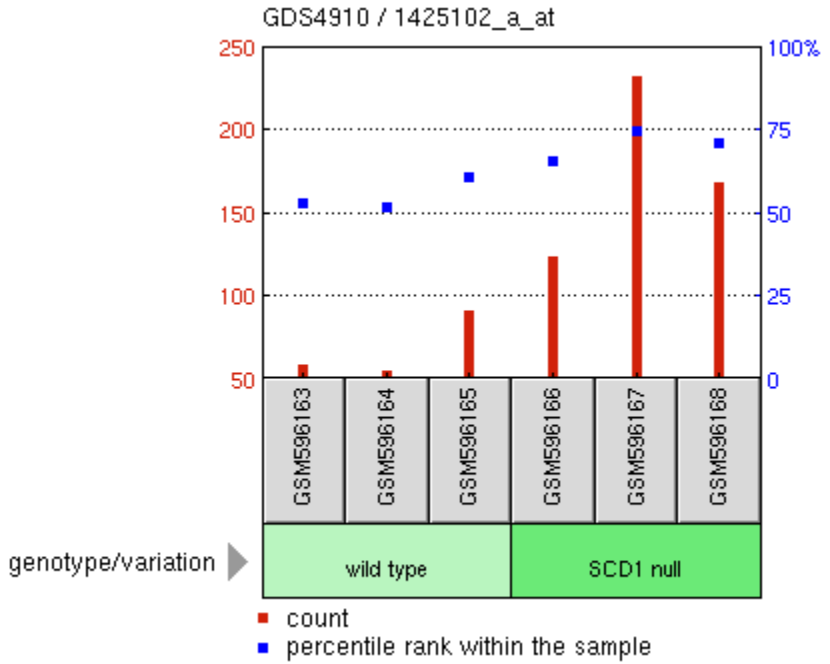

Sample	Title	Value
GSM596163	Skin_Lox_Control_Rep1	59.631
GSM596164	Skin_Lox_Control_Rep2	55.139
GSM596165	Skin_Lox_Control_Rep3	91.71
GSM596166	Skin_SKO_Rep1	123.983
GSM596167	Skin_SKO_Rep2	233.131
GSM596168	Skin_SKO_Rep3	168.429

Profile: ACE2 expression
GDS5087 / 1425102_a_at
Title
Transcriptional regulator steroid receptor coactivator-2 deficiency effect on the heart
Organism
Mus musculus

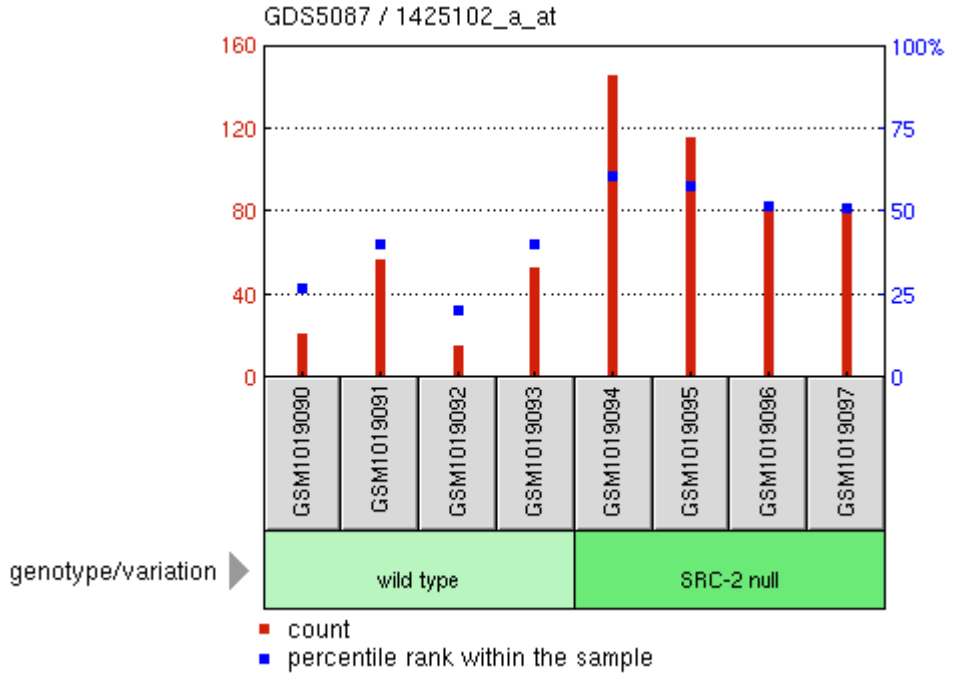

Sample	Title	Value
GSM1019090	Heart_WT_1	22.0184
GSM1019091	Heart_WT_2	57.5679
GSM1019092	Heart_WT_3	15.678
GSM1019093	Heart_WT_4	53.6421
GSM1019094	Heart_KO_1	145.776
GSM1019095	Heart_KO_2	116.278
GSM1019096	Heart_KO_3	85.0996
GSM1019097	Heart_KO_4	84.2244

Supplemenmtal Figure S1_S13. ACE2 and FURIN genes.... (3.95 MiB) view on ChemRxiv • download file